論文 / 著書情報
Article / Book Information

題目(和文)	
Title(English)	Integrable dynamics on intelacing arrays for $U_q(\widehat{ \mathfrak{sl₂}})$ stochastic vertex models
著者(和文)	ムッチコニ マッテオ
Author(English)	Matteo Mucciconi
出典(和文)	学位:博士(理学), 学位授与機関:東京工業大学, 報告番号:甲第11569号, 授与年月日:2020年9月25日, 学位の種別:課程博士, 審査員:笹本 智弘,齋藤 晋,村上 修一,古賀 昌久,利根川 吉廣
Citation(English)	Degree:Doctor (Science), Conferring organization: Tokyo Institute of Technology, Report number:甲第11569号, Conferred date:2020/9/25, Degree Type:Course doctor, Examiner:,,,,
学位種別(和文)	博士論文
Type(English)	Doctoral Thesis

Doctoral thesis

Integrable dynamics on intelacing arrays for $U_q(\widehat{\mathfrak{sl}_2})$ stochastic vertex models

Matteo Mucciconi

東京工業大学
Tokyo Institute of Technology

Abstract

In the context of randomly fluctuating interfaces in (1+1)-dimensions we consider the Kardar-Parisi-Zhang universality class. In the last 20 years integrable techniques were developed to study representative models in this class and mathematical predictions have been experimentally verified with extreme precision.

The most general integrable model available to study KPZ phenomena is the Higher Spin Vertex Model (HSVM) and in this thesis we extend the theory of its integrability. This is accomplished through the study of two families of special symmetric functions: the spin Hall-Littlewood (F) and the spin q-Whittaker ($\mathbb{F}$) functions. Yang-Baxter relations endow F and $\mathbb{F}$ of symmetries and in parallel offer them probabilistic meaning via bijectivization techniques. Random fields weighted by F and $\mathbb{F}$ possess Markov projections giving rise to the HSVM.

Novel eigenrelations for these special functions allow a systematic study of one point statistics of the fields. From these we recover the $1:2:3$ scaling and characteristic fluctuations for the HSVM and its various specializations.

Contents

Acknowledgements

I arrived in Japan in September 2016 and I have been in Tokyo Institute of Technology first as a Research Student and then as a PhD Student. In these four years I have conducted my research under the supervision of Tomohiro Sasamoto and he is the first person I would like to thank. He introduced me to the study of the wonderful theory of Integrable Probability, he thought me a method to understand and attack problems and he has constantly encouranged and fostered my ambition to produce valuable and original research. I will give my best to live up to these standards.

Soon after I arrived in Tokyo, Tomohiro Sasamoto introduced me to his collaborator and friend Takashi Imamura. Since then Imamura Sensei has been for me a second mentor and together we have been through countless many difficult calculations and puzzling problems, the solutions of which will find their way to the press in the coming years. I would like to thank him for his invaluable help and patience.

In January 2018, at a conference in Melbourne I met Leonid Petrov and since then we have been collaborators. My dearest thanks go to him too, for giving me the chance to work with him and for spending his time to teach me valuable lessons.

In Melbourne I also met Alexander Garbali and we have since then been friends. I would like to thank him for being an invaluable resource when in need of clarifications and discussions about special symmetric functions.

I would also like to express my gratitude towards all members of Sasamoto Sensei's laboratory. Especially I would like to thank Masato Usui, Rykuo Nagao and Hiroki Moriya for all the friendly conversations we have had and for helping me improve my japanese skills.

In December 2018 I became married to Natasha Ikhsan and my final thanks go to her. She is the strongest and smartest person I know and my highest source of inspiration and I feel priviledged to have the honor to spend the rest of my life with her. Thank to her for always chosing to be on my side.

About this thesis

In 2017 Sasamoto Sensei had showed me a recent discovery by him and Imamura Sensei, and that was an elegant computation producing exact formulas for a solvable model in the KPZ class. The model in case was the q-TASEP, a deformation of the classical Totally Asymmetric Simple Exclusion Process (TASEP). Two years earlier Corwin and Petrov had introduced a rich generalization of the q-TASEP, the higher spin vertex model, that as of today remains the most general exactly solvable model in the KPZ class. A natural question was whether it was possible to bring techniques invented by Imamura and Sasamoto at the level of the stochatic vertex models and this thesis contains results stemming from this investigation.

Publication List

[IMS20] *Stationary Stochastic Higher Spin Six Vertex Model and q-Whittaker measure.* T.Imamura, M. Mucciconi and T. Sasamoto. Probab. Theory Relat. Fields (2020).

[BMP19] *Yang-Baxter random fields and stochastic vertex models.* A.Bufetov, M.Mucciconi and L.Petrov. Advances in Mathematics (to appear).

[MP20] *Spin q-Whittaker polynomials and deformed quantum Toda.* M.Mucciconi and L.Petrov. arxiv:2003.14260 (submitted)

Chapter 1

Introduction and results

1.1 Background

1.1.1 Brief history of KPZ universality

Investigations around universality aspects of growing surfaces have been conducted by the statistical physics community since at least the early '80s. It was then known, thanks to numerical observations and renormalization group arguments, that certain models of random surfaces allowing lateral growth and possessing smoothening mechanisms exhibit non trivial relaxations patterns, resulting in the emergence of scaling exponents for correlations and fluctuations. The most eminent representative of such growth models became the KPZ stochastic partial differential equation, studied first by Kardar, Parisi and Zhang in 1986 [KPZ86]. For one spatial dimension it reads

$$\partial_t \mathcal{H} = \nu \partial_x^2 \mathcal{H} + \frac{\lambda}{2}(\partial_x \mathcal{H})^2 + \sqrt{D}\eta, \tag{1.1}$$

where $\mathcal{H}$ is the height profile, η is the space-time Gaussian white noise and $\nu > 0, D > 0, \lambda$ are non-zero constants[1]. In this particular case scaling exponents can be explicitly determined and predictions on the universal phenomena made more precise [KPZ86; HH85]: this is the case of the so called KPZ universality class, borrowing the name from the model that started the field. This class of systems includes directed polymers, random stirred fluids and many more processes along with growth phenomena, but in general each of them can be described by its own height function $h(x,t)$ depending on the time t and on one spatial coordinate x. In the large space-time limit the process h, under the $1:2:3$ characteristic scaling,

$$\epsilon h(\epsilon^{-2}x, \epsilon^{-3}t) \qquad \epsilon \to 0, \tag{1.2}$$

is expected to converge, after model dependent deterministic shifts, to a universal fluctuation field, today commonly known as *KPZ fixed point* [MQR17]. This the *strong KPZ universality conjecture*. In fig. 1.1 we compare the KPZ scaling theory with that of weakly

[1] A rescaling of height, space and time transforms (1.1) into the same equation with $\nu = \lambda = D = 1$.

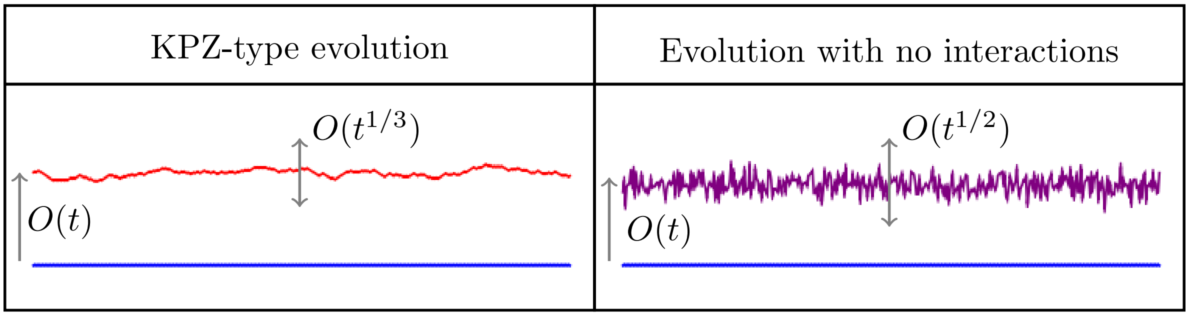

Figure 1.1: Comparison between two types of random evolution of a surface, both obtained as large scales of discrete systems. In the left panel the microscopic dynamics follows a corner growth model, defined in section 1.1.2. Fluctuations have size $t^{1/3}$ and since the initial profile is flat they obey GOE Tracy-Widom distribution when $t \gg 0$. Spatial correlations scale as $t^{2/3}$. In the right panel each point of the interface updates $f(x) \to f(x) + 1$ with rate 1. In this case one point fluctuations have size $t^{1/2}$ and they follow the gaussian distribution.

interacting systems (obeying the gaussian law) to give a taste of the non trivial implications of such predictions; for example one point fluctuations scale as $t^{1/3}$ and they are not in general governed by the gaussian distribution.

The pivotal realization that KPZ universal fluctuations admit an exact description came in 1999 from the work of Baik, Deift and Johansson on the Ulam problem [BDJ99]. This asks to characterize the statistics of the longest increasing subsequence in a random permutation, but it can rephrased as a problem of growth of random surfaces. The absolutely surprising finding is that the limiting law of the longest increasing subsequence is given by none other than the Tracy-Widom distribution F_2, that describes fluctuations of the largest eigenvalue in the Gaussian Unitary Ensemble (GUE) [TW94]. Tracy-Widom distributions were already known to be universal object in random matrices and more in general they were regarded as the analog of the gaussian bell curve for strongly interacting systems.

Stemming from these intriguing developments, the literature of the last twenty years has presented a constellation of spectacular progresses in characterizing KPZ phenomena. Further connections with random matrix models came from results of Baik and Rains [BR01] and Sasamoto [Sas05] that related asymptotic law of the Gaussian Orthogonal Ensemble (GOE) with that of a surface growing off a substrate, while Johansson [Joh00] studied first the so called droplet initial condition case and related the one point fluctuation with GUE statistics. Growth processes corresponding to other special classes of initial conditions were also considered. As an example the limiting process produced by the stationary evolution of a surface was characterized again by Baik and Rains [BR00], although this was not found to have connections with matrix models. More recently a full description of the KPZ fixed point for general classes of initial conditions became available thanks to Matetski, Quastel and Remenik [MQR17]. We will give a more thorough account of this list of progresses and what made them possible in the following sections, but we still like to suggest the interested reader to consult [Cor12], [QS15] and references therein for a detailed exposition on the topic.

The existence of exact methods to determine exponents and fluctuations for a general class of growth phenomena carries significant physical implications. The derivation of laws such as Tracy-Widom statistics is only possible while studying very special exactly solvable system, therefore experimental proofs of theoretical predictions are of crucial importance. Early attempts to detect universal scaling exponents were done in the late '90s studying growing interfaces of mutant bacteria colony [Wak+97] or slow combustion of paper [Myl+01]. In 2010 breakthrough results of Takeuchi and Sano gave the first precise experimental confirmation of KPZ universal phenomena [TS10], when they observed that the growing interface of topological-defect turbulence in liquid crystals possesses characteristic 1:2:3 scaling and GUE Tracy-Widom distribution. By properly triggering the liquid crystal with a laser beam they were also able to reproduce interfaces growing off a flat substrate [TS12] and off a brownian motion shaped profile [IFT20], confirming the emergence respectively of GOE and Baik-Rains statistics and therefore the geometry dependence of the universal fluctuation field. Additional experimental studies include cancer colony growth [Hue+12; Hue+10] and the deposition of colloid particles [Yun+11; Yun+13]; see [Tak14] for a review.

Despite the tremendous successes achieved in the difficult task of pinning down the universal scale invariant process describing out of equilibrium one dimensional fluctuating interfaces, our understanding of properties and boundaries of KPZ phenomena is far from satisfactory. Mathematically exact results such that of Baik-Deift-Johansson are only available for a handful of models and no technique at the moment has proven successful in rigorously extending universal laws to more general settings. A full comprehension of the range of systems encompassed by the theory of KPZ universality is also currently out of reach as literature keeps presenting surprises day after day; see [LŽP19] for a recent example and [Spo20] for a review.

1.1.2 Stochastic integrable systems and special functions

The major takeaway from the course of events leading to the discovery of Tracy-Widom laws in growth processes is that a full description of KPZ universal phenomena is accessible thanks to inexplicably nice and rich algebraic structures underlying some of its representative models. These are the so called stochastic integrable models and their systematic study has become known in literature as *integrable probability*.

The scope of this subsection is to provide the reader a glance at some tools and philosophy aspects driving the study of integrable probability, especially in the context of KPZ class. We will do this presenting simple examples with historical relevance, such as the corner growth model and the Schur processes and doing so we will stress the interplay between stochastic systems and special symmetric functions coming from representation theory and algebraic combinatorics.

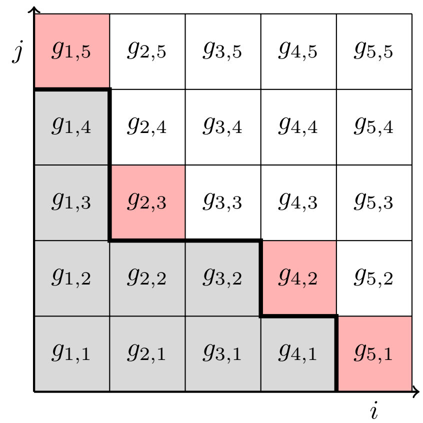

Figure 1.2: A realization of the corner growth model. Red cells lay at corners of the interface delimiting the gray area and they will be absorbed (become gray) after a waiting time given by the value of the respective $g_{i,j}$.

Corner growth model and Schur measure

Among the earliest and simplest models of random growth in one dimension we find the corner growth model [Ros81]. Decorate the cells of the lattice $\mathbb{Z}_{\geq 0} \times \mathbb{Z}_{\geq 0}$ with independent non-negative random variables $\{g_{i,j} : i, j \geq 1\}$, like in fig. 1.2. In the figure the set of gray cells represents the growth process, while the thick black down-right path π is the interface. White cells become active (red) once they are at a corner of the profile π and get absorbed after a waiting time given by the value of the respective $g_{i,j}$. A simple quantity we can consider is the first absorption time $T(i, j)$ of a cell (i, j) and this also turns out to have a simple characterization. Since the cell (i, j) can only be absorbed if both $(i-1, j)$ and $(i, j-1)$ are already in the gray area, the function T satisfies the recursion $T(i, j) = g_{i,j} + \max\{T(i-1, j), T(i, j-1)\}$ and more in general we have

$$T(i, j) = \max_{p:(1,1)\to(i,j)} \left\{ \sum_{(i',j')\in p} g_{i',j'} \right\}, \tag{1.3}$$

where $p : (1, 1) \to (i, j)$ indicates an up-right paths connecting cells $(1, 1)$ and (i, j). The quantity in the right hand side of (1.3) is known as last passage percolation time in the environment $G_{i,j} = \{g_{i',j'} : 1 \leq i' \leq i, 1 \leq j' \leq j\}$ and it is an object with deep meaning in combinatorics. The celebrated Robinson-Shensted-Knuth (RSK) correspondence [Sag01] provides a bijection between matrices of integers $G_{i,j}$ and pairs of semi-standard tableaux[2] (P, Q) of the same shape λ. A crucial feature of the RSK algorithm is that the shape λ is determined by the last passage percolation times of $G_{i,j}$ and in particular $\lambda_1 = T(i, j)$. Assuming that random variables $g_{i',j'}$ are geometrically distributed as $\mathrm{Geo}(x_{i'} y_{j'})$ for some

[2]Given a Young diagram $\lambda = (\lambda_1 \geq \lambda_2 \geq \cdots \geq \lambda_\ell > 0)$ a semi standard Young tableaux P is a $\mathbb{N}$-valued filling of cells $\{(i, j) : 1 \leq j \leq \lambda_i\}$ that is strictly increasing along columns and weakly increasing along rows. Here λ is the shape of P.

set of positive parameters $x_{i'}, y_{j'}$, a simple calculation and a careful use of the RSK show that

$$\begin{aligned} \text{Prob}\{T(i,j)=k\} &\propto \sum_{G_{i,j}:T(i,j)=k} \prod_{\alpha=1}^{i} x_\alpha^{\sum_\gamma g_{\alpha,\gamma}} \prod_{\beta=1}^{j} y_\beta^{\sum_\delta g_{\delta,\beta}} \\ &\overset{RSK}{=} \sum_{\lambda:\lambda_1=k} \left(\sum_{P:\text{sh}(P)=\lambda} x^P \right) \left(\sum_{P:\text{sh}(Q)=\lambda} y^Q \right) = \sum_{\lambda:\lambda_1=k} s_\lambda(x) s_\lambda(y), \end{aligned} \tag{1.4}$$

where the monomial $x^P = \prod_i x_i^{\#\{c:P(c)=i\}}$ and normalization factor in the right hand side is $\prod_{\alpha=1}^{i}\prod_{\beta=1}^{j}(1-x_\alpha y_\beta)$. Functions s_λ, defined by the sum over tableaux in the parentheses are the Schur symmetric polynomials and are fundamental objects in representation theory and algebraic combinatorics. They are basis of the space of symmetric functions and they possess a large number of properties and symmetries, including determinantal representations and summation identities. Their emergence in the study of corner growth model is evidence of its integrability. In particular (1.4) shows that the study of an abstract probability measure on Young diagrams weighted by Schur polynomials

$$S(\lambda) \propto s_\lambda(x) s_\lambda(y), \tag{1.5}$$

gives informations about a meaningful physical system once we consider the marginal projection $S(\lambda : \lambda_1 = k)$. The probability measure $S(\lambda)$ takes the name of *Schur measure* and was introduced in literature by Okounkov in 1999 [Oko01]. Among all its outstanding properties, the Schur measure is a determinantal point process and in fact it was employed by Okounkov in the study of a system of free fermions.

The connection with Schur measures is not the only way to "solve" the corner growth model. Other techniques involve connections with random matrices [Joh00], Gelfand-Tsetlin pattern representations [Sas05] and many more; see [Sep09] for a review. In particular an extensive study of this model led to the complete characterization of the KPZ fixed point [MQR17].

There also exists several other models that can be described in terms of Schur measures. These include exclusion processes [Joh00], polynuclear growth models [PS02; Fer04], random polymers at zero temperature in various geometries [BZ19]. Moreover a measure of the form (1.5) admits straightforward generalizations replacing Schur polynomials with more general symmetric functions, e.g. Macdonald polynomials [Mac95]. We will review such extensions below in section 1.1.3 and construct a new class of measures, based on spin q-Whittaker polynomials, in chapter 3.

Schur processes and TASEPs

The mapping contained in computation (1.4) is certainly not the only way to make physical sense of the Schur measure. A different idea, that we will largely explore in this thesis, allows to relate the Schur measure to Markov processes using certain summation identities.

To explain this we need to introduce skew variants of Schur polynomials. The *skew Schur polynomials* $s_{\lambda/\mu}$ [Mac95] can be defined as the coefficients of the branching expansion

$$s_\lambda(x_1,\dots,x_n) = \sum_\mu s_\mu(x_1,\dots,x_{n-1}) s_{\lambda/\mu}(x_n). \tag{1.6}$$

They are labeled by pairs of *interlacing* Young diagrams μ, λ, that is

$$\lambda_1 \geq \mu_1 \geq \lambda_2 \geq \mu_2 \geq \cdots \tag{1.7}$$

and most importantly they satisfy the *skew Cauchy identity*

$$\frac{1}{1-xy} \sum_\varkappa s_{\lambda/\varkappa}(y) s_{\mu/\varkappa}(x) = \sum_\nu s_{\nu/\lambda}(x) s_{\nu/\mu}(y). \tag{1.8}$$

Relation (1.8) is essential for probabilistic interpretation of skew polynomials and suggests the construction of transition probabilities bringing the configuration $\varkappa \subseteq \mu, \lambda \mapsto \mu, \lambda \subseteq \nu$ and viceversa. One example (but not the only one) of such transition probabilities can be obtained taking the independent coupling as

$$\mathsf{U}^{\mathrm{fwd}}_{x,y}(\varkappa \to \nu | \lambda, \mu) \propto s_{\nu/\lambda}(x) s_{\nu/\mu}(y), \qquad \mathsf{U}^{\mathrm{bwd}}_{x,y}(\nu \to \varkappa | \lambda, \mu) \propto s_{\lambda/\varkappa}(y) s_{\mu/\varkappa}(x) \tag{1.9}$$

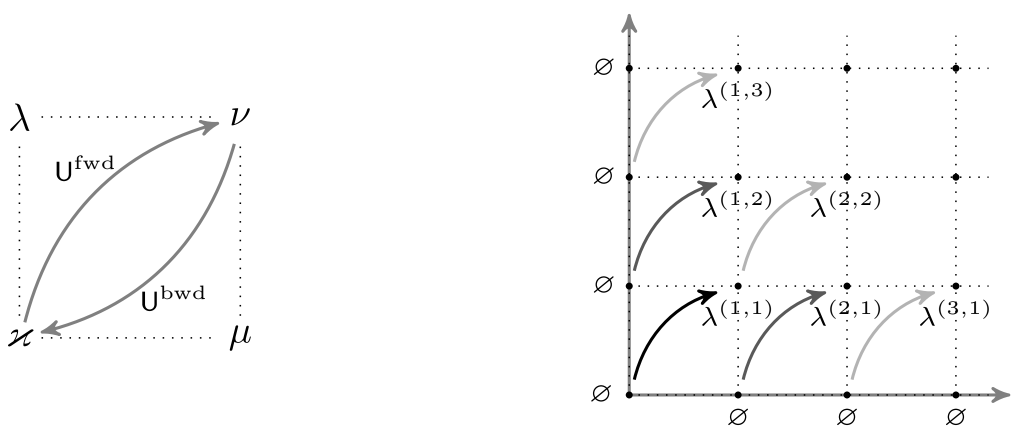

Figure 1.3: Left: Forward and backward transition operators. Right: Construction of a random field using $\mathsf{U}^{\mathrm{fwd}}$, where lighter arrows correspond to moves happening later in the update.

Performing moves weighted by $\mathsf{U}^{\mathrm{fwd}}$ we can construct recursively a full field of Young diagrams $\{\lambda^{(i,j)} : i,j \geq 0\}$, starting from initial conditions $\lambda^{(0,j)} = \lambda^{(i,0)} = \varnothing$ as done in fig. 1.3. We see that such random field describes a growth process of Young diagrams and as a result of branching rules its joint probability laws will be written in terms of products of skew Schur polynomials. In particular the single point law is the Schur measure

$$\mathrm{Prob}\{\lambda^{(i,j)} = \lambda\} \propto s_\lambda(x_1,\dots,x_i) s_\lambda(y_1,\dots,y_j). \tag{1.10}$$

and the joint law across a straight segment is the *Schur process* of Okounkov and Reshetikin [OR03]

$$\mathrm{Prob}\{\lambda^{(1,j)} = \mu^{(1)}, \dots, \lambda^{(i,j)} = \mu^{(i)}\} \propto s_{\mu^{(1)}}(x_1) s_{\mu^{(2)}/\mu^{(1)}}(x_2) \cdots s_{\mu^{(i)}/\mu^{(i-1)}}(x_i) s_{\mu^{(i)}}(y_1, \dots, y_j). \tag{1.11}$$

We can take a look at fig. 1.4 left panel to visualize a schematic example of a sequence of interlacing Young diagrams such as those weighted by the Schur process.

Random fields built following this recipe are certainly integrable, since nice properties of Schur polynomials allow exact computations for a multitude of observables: they are determinantal point processes [OR03] as a result of Jacobi-Trudi formulas, their correlations are given by integral formulas thanks to certain eigenrelation [Agg15] and so on. Nevertheless this abstract algebraic construction does not reveal much about the true physical meaning of the process. That is we do not know a priori if any reasonable stochastic process will be described by a measure of the form (1.11). This is a problem that needs to be addressed separately by carefully studying Markov maps $\mathsf{U}^{\mathrm{fwd}}, \mathsf{U}^{\mathrm{bwd}}$. For the case of fields built from Schur polynomials this sampling problem admits a number of different solutions, from which one deduces that marginals of the Schur process are sampled by very natural stochastic systems: the Totally Asymmetric Simple Exclusion Process (TASEP) and its push variant (pushTASEP); see fig. 1.4. This last result was found first by Borodin and Ferrari in [BF14], where this general construction was also introduced. Employing the RSK algorithm more refined constructions of Markov operator $\mathsf{U}^{\mathrm{fwd}}$ lead to analogous results with TASEP and pushTASEP replaced by their discrete time analogs [MP17]. In this thesis, we will construct generalizations of these arguments in the context of growth processes of Young diagrams weighted by other special function, namely the spin Hall-Littlewood and the spin q-Whittaker functions; see chapter 2 and chapter 3.

We close this short section stressing the fact that probability measures on interlacing arrays are not an unusual object. In fact they are rather common in random matrix theory, where eigenvalues of minors of symmetric and hermitian matrices arrange themselves in interlacing sequences[3]. Alternatively one can recall that Dyson's Brownian motion [Dys62] for GUE random matrices arises from ensembles of reflecting Brownian particles, condition that can be seen as a continuous analog of the interlacing. One can therefore think of the Schur process (1.11) as a discrete versions of these common constructions.

1.1.3 Beyond Schur processes

The blueprint described above to construct growth processes on Young diagrams starting for skew Cauchy identities (1.8) works in much higher generality. A truly successful application of this scheme comes replacing the Schur polynomials $s_{\lambda/\mu}$ with Macdonald polynomials $P_{\lambda/\mu}$ [Mac95]. The *Macdonald processes* are introduced by Borodin and Corwin in 2011 [BC14] and they sit on top of a vast hierarchy of integrable stochastic systems; see fig. 1.5. They simultaneously generalize particle processes, random polymers and last passage percolation models, ensembles of random matrices and also the KPZ

[3]this is the Cauchy interlacing theorem

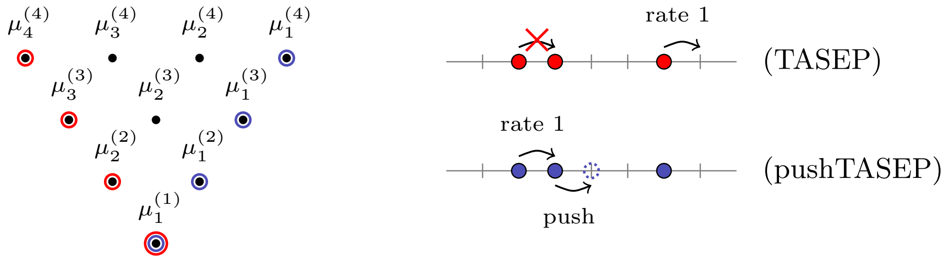

Figure 1.4: In the left panel we see an interlacing array $\mu^{(1)} \prec \cdots \prec \mu^{(4)}$. Under the Schur process, coordinates $\mu_1^{(i)}$ (circled in blue) and $\mu_i^{(i)}$ (circled in red) form autonomous Markov processes. They are equivalent to pushTASEP and TASEP, whose dynamic is sketched in the right panel. In the TASEP particles jump to their right neighboring site with rate 1 provided the site is empty. In the push-TASEP, in case the target site is occupied a deterministic push happens.

stochastic partial differential equation. Algebraic structures of Macdonald polynomials descending from representation theory survive in each of these systems and provide tools to analyze exactly a range of observables. In particular the theory of Macdonald processes offers a way to rigorously solve the KPZ equation under a class of initial conditions [BC14; Bor+15a; Bar+18]. Other techniques to solve the KPZ equation include duality arguments, moment expansion, Bethe Ansatz and so on; see [ACQ11; SS10; CLR10; Dot11; LC12; IS13].

In the case of Macdonald processes the problem of characterizing interesting marginal processes, like the corner growth model or the TASEPs in the Schur case, has attracted considerable attention in the last decade. A certain simplification of the general Macdonald processes, called q-Whittaker processes, was found to be sampled by randomized versions of the RSK algorithm [OP13; BP16; MP17], relating marginals to q deformations of TASEPs of fig. 1.4. Other uses of the RSK algorithm in Macdonald processes give also rise to the stochastic six vertex model [BM18] and to random polymers [Cor+14], [OSZ14], [OO15], [CSS15].

In parallel to developments strictly pertaining Macdonald processes in the last 10 years, different techniques and theories have emerged and attracted their own share of attention. The most remarkable of these is arguably related to Yang-Baxter integrability. The earliest and most fundamental example of such systems is the stochastic six vertex model dating back to 1992 [GS92] that was studied by Gwa and Spohn to confirm kinetic roughening exponent of KPZ models. More recently the stochastic six vertex model was resurrected [BCG16] and largely generalized using algebraic techniques of representation theoretic origin. This is the higher spin vertex model [CP16], which we will discuss more in detail in the next section. The higher spin vertex model is a rather general stochastic integrable system that possesses as particular case a number of other interesting models: these are exclusion processes like the q-Hahn TASEP [Pov13] and systems of random walkers in random environment like the Beta polymer model [BC16a].

Before the works [BMP19; MP20] reported in this thesis it was not known if a description of the higher spin vertex model in terms of dynamics of interlacing arrays was

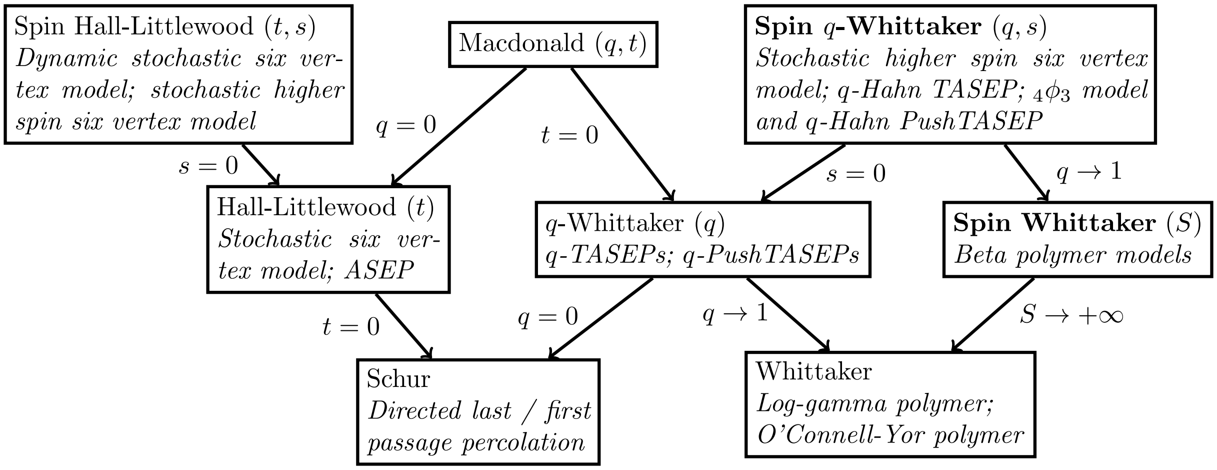

Figure 1.5: A scheme of various families of symmetric functions together with stochastic systems based on them. Arrows indicate degenerations or scaling limits. The two families which are our main focus are indicated in bold.

possible or not. Among the results we will see in chapter 3 we find a positive answer to this problem employing random fields with spin q-Whittaker symmetric functions [BW17; MP20]; see fig. 1.5. Consequences of this finding are algebraic derivations of formulas for observables of the higher spin vertex model or also more generally the possibility to employ line ensembles techniques as the one introduced in [CH14] for to study general stochastic integrable models. These will be object of future studies.

1.1.4 The higher spin vertex model

Let us now informally define the main character of this thesis, whose investigation drives the majority of results we present. The higher spin vertex model was introduced by Corwin and Petrov in 2015 [CP16] in an attempt to unify under the same umbrella the growing collection of different stochastic integrable models that had been studied in the previous years in the context of KPZ universal phenomena. These include a variety of exclusion processes, zero range processes and polymer models in continuous and discrete time.

The higher spin vertex model is a probability measure on ensembles of directed paths in the quadrant $\mathbb{Z}_{\geq 0} \times \mathbb{Z}_{\geq 0}$; see fig. 1.6, left. Paths emanate from boundary vertices and propagate through the lattice keeping up-right direction, where the propagation rules are given by vertex weights $\mathsf{L}^{\mathrm{ur}}_{x,v}$ of fig. 1.7. More precisely the process is constructed as follows:

- each vertex $(0, j)$ emanates b^{v}_j paths initially directed to the right;
- each vertex $(i, 0)$ emanates b^{h}_i paths initially directed upwards;
- the probability of observing a configuration $(\alpha_1, \beta_1; \alpha_2, \beta_2)$ at vertex (i, j), conditioned on the configuration at all vertices (i', j') with $i' + j' < i + j$, is given by

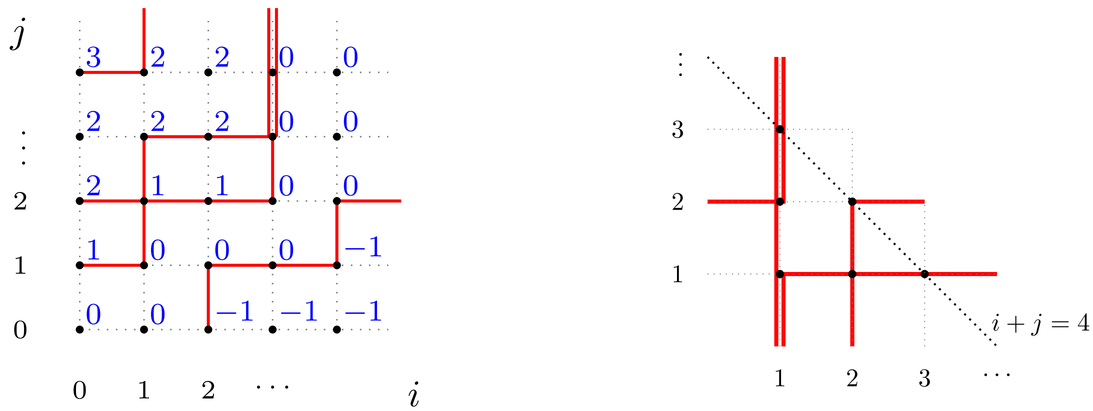

Figure 1.6: Left: a configuration of up-right paths. The numbers in blue are the values of the height function $\mathcal{H}_{\mathrm{HS}}$ at each vertex.
Right: a configuration of paths in the triangle $i + j \leq 4$. The probability to observe this specific arrangement is reported in (1.13).

$\mathsf{L}^{\mathrm{ur}}_{x_i,v_j}(\alpha_1, \beta_1; \alpha_2, \beta_2)$. Moreover, this event is independent of choosing arrow configurations at other vertices $\dots, (i-1, j+1), (i+1, j-1), \dots$ on the same diagonal.

Informally the probability of a configuration of paths $\mathcal{C}$ in the full lattice is given by

$$\mathrm{Prob}(\mathcal{C}) = \prod_{i \geq 1} \mathrm{Prob}(b^{\mathrm{h}}_i) \times \prod_{j \geq 1} \mathrm{Prob}(b^{\mathrm{v}}_j) \times \prod_{i,j \geq 1} \mathsf{L}^{\mathrm{ur}}_{x_i,v_j} \begin{pmatrix} \text{vertex config.} \\ \text{at } (i,j) \end{pmatrix}. \tag{1.12}$$

We notice that the system is completely inhomogeneous both in the i and j direction and this is due to the fact that weights $\mathsf{L}^{\mathrm{ur}}_{x_i,v_j}$ depend on sets of parameters x_i, v_j other than on global parameters s, q. We also will always assume that boundary paths $B^{\mathrm{h}} = (b^{\mathrm{h}}_1, b^{\mathrm{h}}_2, \dots)$, $B^{\mathrm{v}} = (b^{\mathrm{v}}_1, b^{\mathrm{v}}_2, \dots)$ are sampled independently from each other and from the bulk configuration. Since vertex weights L are assigned the measure on the path ensemble is determined only assigning boundary conditions $B^{\mathrm{h}}, B^{\mathrm{v}}$ and we denote it with $\mathcal{P}(B^{\mathrm{h}}, B^{\mathrm{v}})$.

To illustrate more clearly how the construction woks, we report here the explicit expression of the probability of observing, in the region $\{(i,j) \in \mathbb{Z}_{\geq 0} \times \mathbb{Z}_{\geq 0} : i + j \leq 4\}$, the configuration drawn in fig. 1.6 right panel. We have

$\mathrm{Prob}(\text{fig. 1.6 right}) = \mathrm{Prob}(b^{\mathrm{h}}_1 = 2, b^{\mathrm{h}}_2 = 1, b^{\mathrm{h}}_1 = 0) \times \mathrm{Prob}(b^{\mathrm{v}}_1 = 0, b^{\mathrm{v}}_2 = 1, b^{\mathrm{v}}_1 = 0)$

$\times \mathsf{L}^{\mathrm{ur}}_{x_1,v_1}$ 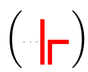 $\mathsf{L}^{\mathrm{ur}}_{x_2,v_1}$ 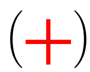 $\mathsf{L}^{\mathrm{ur}}_{x_3,v_1}$ 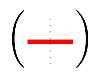 (1.13)

$\times \mathsf{L}^{\mathrm{ur}}_{x_1,v_2}$ 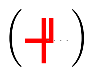 $\mathsf{L}^{\mathrm{ur}}_{x_2,v_2}$ 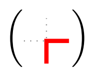 $\mathsf{L}^{\mathrm{ur}}_{x_1,v_3}$ 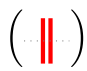 .

An equivalent description of the ensemble can be given defining a height function $\mathcal{H}_{\mathrm{HS}}$. Given a configuration of paths and a vertex (i,j) we set

$$\mathcal{H}_{\mathrm{HS}}(i,j) = \#\{\text{occupations at horizontal edges}\} - \#\{\text{occupations at vertical edges}\}, \tag{1.14}$$

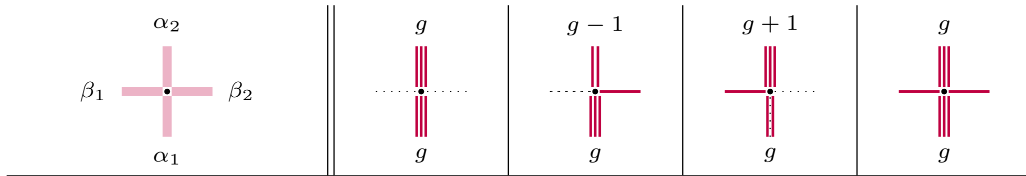

$\mathsf{L}^{\mathrm{ur}}_{x,v}(\alpha_1,\beta_1;\alpha_2,\beta_2)$	$\frac{1+q^g xv}{1+xv}$	$\frac{xv(1-q^g)}{1+xv}$	$\frac{1+q^g sx}{1+xv}$	$\frac{xv-q^g sx}{1+xv}$

Figure 1.7: The stochastic vertex weights $\mathsf{L}^{\mathrm{ur}}_{x,v}$ for the up-right stochastic higher spin six vertex model. Configurations that are not of the type reported in the table are assigned weight zero. The stochasticity condition means that fixed down and left edges occupation numbers α_1, β_1, the sum of weights $\mathsf{L}^{\mathrm{ur}}_{x,v}(\alpha_1,\beta_1;\alpha_2,\beta_2)$ over all possible α_2, β_2 is 1.

counted on the union of two segments $(\frac{1}{2},\frac{1}{2}) \to (i+\frac{1}{2},\frac{1}{2}) \to (i+\frac{1}{2}, j+\frac{1}{2})$; see fig. 1.6 for an example. The height function allows to relate the higher spin vertex model to exclusion processes interpreting the difference $\mathcal{H}(n,t) - \mathcal{H}(n+1,t)$ as the gap between consecutive particles and hence weights L^{ur} as jump rules.

The stationary higher spin vertex model has been studied in [IMS20]. The model is potentially fully inhomogeneous as weights L^{ur} can depend on both coordinates i, j, therefore a proper notion of translation invariant measures ought to be defined. For this consider random boundary conditions $B^{\mathrm{h}}, B^{\mathrm{v}}$ and their shifts $B^{\mathrm{h}}_{+i} = (b^{\mathrm{h}}_{i+1}, b^{\mathrm{h}}_{i+2}, \dots)$, $B^{\mathrm{v}}_{+j} = (b^{\mathrm{v}}_{j+1}, b^{\mathrm{v}}_{j+2}, \dots)$. We say that a measure $\mathcal{P}(B^{\mathrm{h}}, B^{\mathrm{v}})$ is translation invariant if the restriction of the ensemble to the quadrant $\mathbb{Z}_{\geq i} \times \mathbb{Z}_{\geq j}$ originating from a generic point (i,j) is equivalent in distribution to $\mathcal{P}(B^{\mathrm{h}}_{+i}, B^{\mathrm{v}}_{+j})$.

Translation invariant measures for the higher spin vertex model form a one parameter family. They are obtained fixing the law of boundary conditions as

$$b^{\mathrm{v}}_j \sim \mathrm{Ber}\left(\frac{\mathscr{d} v_j}{1+\mathscr{d} v_j}\right), \qquad b^{\mathrm{h}}_i \sim q\mathrm{NB}(-s x_i, \mathscr{d}/x_i), \tag{1.15}$$

where Ber indicates the Bernoulli distribution and qNB is the q-negative binomial distribution defined by

$$X \sim q\mathrm{NB}(b,p) \qquad \Longrightarrow \qquad \mathbb{P}(X=n) = p^n \frac{(b;q)_n}{(q;q)_n} \frac{(p;q)_\infty}{(pb;q)_\infty}, \qquad \text{for all } n \in \mathbb{Z}_{\geq 0}. \tag{1.16}$$

We used the notion of q-Pochhammer symbol $(a;q)_n$ (A.1). We refer to the model with boundary conditions (1.15) as the *stationary higher spin vertex model with density* $\mathscr{d}$. We will study its asymptotic properties and establish Baik-Rains characteristic fluctuations in chapter 4 based on results of [IMS20].

1.1.5 Spin Hall-Littlewood functions

The salient feature that makes the higher spin vertex model an integrable systems is the fact that stochastic weights $\mathsf{L}_{x,v}$ are in fact $U_q(\widehat{\mathfrak{sl}_2})$ R-matrices and they satisfy the Yang-Baxter equation. This equips the model with a large variety of symmetries that produce striking implications and whose investigation is at the moment still active; see [Pet19; BGW19] for very recent developments.

Coordinate Bethe Ansatz eigenfunctions of the transfer matrix of the higher spin vertex model are known as spin Hall-Littlewood functions. They were defined in [Bor17] and their main combinatorial and algebraic properties were studied in [Bor+15c; BP18a]. These include the symmetrization formula [BP18a]

$$\mathsf{F}_\lambda(u_1,\dots,u_n;\mathbf{s}) = \frac{(1-q)^n}{(q;q)_{n-\ell(\lambda)}} \sum_{\sigma\in\mathfrak{S}_n} \sigma\left\{ \prod_{1\le i<j\le n} \frac{u_i - q u_j}{u_i - u_j} \prod_{i=1}^{n}\prod_{j=1}^{\lambda_i} \left(\frac{u_i - s_j}{1 - s_j u_i}\right) \prod_{i=1}^{\ell(\lambda)} \frac{u_i}{u_i - s_{\lambda_i}} \right\}, \tag{1.17}$$

that we largely make use of in chapter 2. Specializing all spin parameters $s_j = 0$, functions F_λ reduce to the Hall-Littlewood polynomials and additionally setting $q = 0$ they become the Schur polynomials. Most remarkably spin Hall-Littlewood functions form a complete set as a result of orthogonality relations both in the λ and in the u variables.

In [BMP19; MP20] eigenrelations for them with respect to Macdonald type operators were first established. We will review these results in chapter 2.

1.2 Results

Before we enumerate the list of results presented in this thesis we like to dedicate a small subsection to stress motivations driving the author in the extensive study of stochastic integrable systems.

1.2.1 Motivations

In the last twenty years the study of stochastic integrable systems has brought significant advances to the understanding of properties and boundaries of KPZ universal phenomena. In the last decade in particular the understanding of algebraic and combinatorial structures underlying certain models of growth has allowed rigorous derivations of solutions of the KPZ equation [ACQ11; SS10] along with a full descriptions of conjectural universal limiting objects [MQR17].

Among the highest goals of the theory is to capture a general set of conditions that would automatically provide a physical process of KPZ behaviors and hence to establish a "central limit theorem" for strongly interacting systems. Nevertheless at the current state such general type of result appears to be out of hand: rigorous statements are proven only for a few toy models and the real breadth of the universality class is still object of active investigations.

We are then forced to develop a solid theory of the few models we are able to solve, possibly discovering new ones with the aim of expanding the scope of their associated universality. In doing so, in the last decade a number of models were defined. Starting from the classical Totally Asymmetric Simple Exclusion Process (TASEP) which we briefly touched upon in section 1.1.2, it was realized that its exact solvability does not break by adding additional parameters in specific ways. ASEP and q-TASEP are two such deformations (see also the q-boson of [SW98]): both systems depend, albeit in a different ways, on a quantization parameter q, governing the asymmetry of the transport. By taking scaling limits in q one discovers that integrability of discrete systems translates into solutions of otherwise intractable continuous models, like directed polymers in random media [OY01] or the KPZ equation.

More recently it was found that integrability survives the addition of a further parameter, which in this thesis we denote with s, leading to the introduction of the q-Hahn TASEP [Pov13] and of the higher spin vertex model [CP16], defined in section 1.1.4. The presence of two "quantization" parameters offers the possibility of richer scaling limits, that in the particular case of the q-Hahn TASEP led to the remarkable discovery that certain phenomena in diffusion in random media or certain statistics in extreme value theory of strongly correlated processes obey KPZ universal laws [BC16a].

The scope of this thesis is that of deepening the understanding of the stochastic integrable systems in the (1+1)-KPZ universality class. We do so by defining a general integrable system, which we call spin q-Whittaker process. The importance of this new model lays in the fact that it simultaneously generalizes all the models introduced above and a number of other ones, which we will discuss below. This solves a question that was asked several times in literature (eg. [Cor14]) and that is to inscribe integrable stochastic models in more general dynamics on interlacing arrays in the spirit of the *Macdonald Processes* [BC14]. Properties of the spin q-Whittaker processes are described by a family of special functions we study extensively: the spin q-Whittaker polynomials. Based on an idea of [BC14], we also propose a systematic scheme to recover formulas for observables of the various systems, that passes through the computation of eigenrelations for the spin q-Whittaker polynomials. This has also allowed to solve certain conjectures which had appeared in literature in recent years [CMP19] regarding the rigorous derivation of observables for models with diverging moments. We imagine that the simplicity of this procedure will find applications in establishing refined convergence results of the different systems to the universal object (eg. convergence of two-point distribution as in [Dim20]). From a more probabilistic standpoint one of the consequences of our constructions is that there exist Gibbsian line ensembles behind all of the integrable vertex models. These objects, considered first in [CH14], represent a powerful tool to show regularity of convergence of various models to universal objects and their analysis will be object of future works.

Along the way we study the stationary states of the higher spin vertex model, as a general model of KPZ growth, and establish the convergence of the one point function to the so-called Baik-Rains universal law. A brief discussion on experimental relevance of this last result is offered below.

We are now ready to explain in detail the results contained in this thesis.

1.2.2 Improving the theory of spin q-Whittaker polynomials

In [BW17], Borodin and Wheeler defined a family of symmetric functions that they called spin q-Whittaker polynomials. Their basic properties were studied from a combinatorial standpoint leveraging Yang-Baxter relations, but no result about their relations to probabilistic integrable systems or about their relevant algebraic properties was given. Our first stream of results is an attempt to resolve this issue.

We introduce modified versions of the spin q-Whittaker symmetric polynomials. Their expression can be given through a usual branching expansion

$$\mathbb{F}_\nu(x_1, \dots, x_N) = \sum_{\varnothing = \nu^0 \prec \nu^1 \prec \cdots \nu^n = \lambda} \prod_{i=1}^{n} \mathbb{F}_{\nu^i/\nu^{i-1}}(x_i), \tag{1.18}$$

where ν^i are non-negative signatures of i parts, $\prec$ is the interlacing condition (1.7) and the branching coefficients are

$$\mathbb{F}_{\lambda/\mu}(x) := x^{|\lambda|-|\mu|} \prod_{i=1}^{k} \frac{(-s/x;q)_{\lambda_i-\mu_i}(-sx;q)_{\mu_i-\lambda_{i+1}}(q;q)_{\lambda_i-\lambda_{i+1}}}{(q;q)_{\lambda_i-\mu_i}(q;q)_{\mu_i-\lambda_{i+i}}(s^2;q)_{\lambda_i-\lambda_{i+i}}}, \qquad \begin{matrix} \lambda = \lambda_1 \geq \cdots \geq \lambda_{k+1} \geq 0 \\ \mu = \mu_1 \geq \cdots \geq \mu_k \geq 0. \end{matrix} \tag{1.19}$$

We used again the notion of q-Pochhammer coefficient $(a;q)_n$ (A.1). Our polynomials are slightly more general than the Borodin–Wheeler's version $\mathbb{F}_\lambda^{BW}$ [BW17], since we have

$$\mathbb{F}_\lambda(x_1, x_2, \dots, x_n)\big|_{x_1=0} = \mathbb{F}_\lambda^{BW}(x_2, \dots, x_n),$$

but, rather surprisingly, this little improvement grants them of a number of additional properties, including shifting, summation identities and eigenrelations. We outline now a list of their features all of which are proven in chapter 2.

- The $\mathbb{F}_\lambda$ are symmetric with respect to exchange of the x variables. This property follows from a combination of two Yang-Baxter type relations. One is a classical Yang-Baxter equation for the fused $U_q(\widehat{\mathfrak{sl}_2})$ R-matrix [Man14]. The other is a new commutation relation between $U_q(\widehat{\mathfrak{sl}_2})$ R-matrix and a new "corner" weight we introduce; see fig. B.7 and proposition B.2.1.
- Under the degeneration $s = 0$, both families $\mathbb{F}_\lambda$ and $\mathbb{F}_\lambda^{BW}$ coincide and turn into the usual q-Whittaker polynomials. The different scaling $s \to 0, xs = \text{const.}$ produces the Grothendieck polynomials, a key object in algebraic combinatorics. This second fact was also not observed before in literature.
- They satisfy skew Cauchy identities as a result of Yang-Baxter equations for $U_q(\widehat{\mathfrak{sl}_2})$ R-matrices and corner weights.
- We present q-difference operators $\mathfrak{D}_1$, $\overline{\mathfrak{D}}_1$ which act on our new spin q-Whittaker polynomials diagonally as

  $$\mathfrak{D}_1 \mathbb{F}_\lambda = q^{\lambda_N} \mathbb{F}_\lambda \qquad \text{and} \qquad \overline{\mathfrak{D}}_1 \mathbb{F}_\lambda = q^{-\lambda_1} \mathbb{F}_\lambda.$$

  These represent one parameter generalizations of the first q-Whittaker operators (these are $t = 0$ degenerations of the Macdonald operators from [Mac95]). The emergence of a theory of operators is a strong hint of algebraic relevance of our spin q-Whittaker polynomials.

- We observe that the operators $\mathfrak{D}_1$, $\overline{\mathfrak{D}}_1$ can be represented as conjugations of the first q-Whittaker q-difference operators. From higher q-Whittaker operators we thus get higher order q-difference operators commuting with either $\mathfrak{D}_1$ or $\overline{\mathfrak{D}}_1$ (the conjugations leading to $\mathfrak{D}_1$ and $\overline{\mathfrak{D}}_1$ are different, even though these operators commute). The higher order operators coming from the q-Whittaker operators are not diagonal in the spin q-Whittaker polynomials.

Our modification of the spin q-Whittaker polynomials originates from computer experiments informed by the existing definition from [BW17] combined with the desire to have q-difference eigenoperators. A particular case of one of the eigenoperators appeared in [BMP19], while the $\mathfrak{D}_1, \overline{\mathfrak{D}}_1$ we present here were introduced in [MP20]. This led us to discover the existence of commutation relations involving corner vertex weights. It would be very interesting to connect our corner vertex weights and the corresponding Yang–Baxter equation with known integrable vertex model constructions.

The major unsolved problem in the theory of spin q-Whittaker polynomials, that we believe could uncover their true algebraic meaning, is represented by the conjectural orthogonality relation

$$\int_{\mathbb{T}^N} \mathbb{F}_\lambda(z_1,\dots,z_N)\,\mathbb{F}_\mu(1/z_1,\dots,1/z_N)\,m_{q,s}^N(z_1,\dots,z_N)\,dz_1\cdots dz_N \overset{?}{=} c_\lambda \mathbf{1}_{\lambda=\mu}; \tag{1.20}$$

see section 2.7 for precise definitions of quantities. This represents a natural generalization of the torus scalar product for Macdonald polynomials [Mac95]. In the Macdonald case the existence of families of commuting eigenoperators suffices to show the orthogonality, but in our case operators could only suggest us the exact form of the scalar product and are not enough to conclude. Our conjecture was tested numerically for small examples, a more thorough check was made under the assumption $q = 0$ and in the text we also provide a few arguments in support of it.

1.2.3 Characterizing marginals of random fields

We provide a detailed anaysis of random fields of Young diagrams weighted by spin Hall-Littlewood and spin q-Whittaker functions. Leveraging on their combinatorial and algebraic properties we identify two classes of Markov marginal projections and match their distribution with a number of general integrable stochastic systems. The theory of eigenrelations offers a systematic way to study multi point joint distribution of the processes, that in turn allows us to recover determinantal formulas for the one-point distrubutions of certain observables using a strategy introduced in [BC14]. The following is a list of main results contained in chapter 3.

- In section 3.1 we review a general scheme to construct integrable probability measures on fields of Young diagrams $\boldsymbol{\lambda} = \{\lambda^{(i,j)} : i, j \geq 1\}$ from pairing of symmetric functions satisfying skew Cauchy identities. In the case of spin Hall-Littlewood (sHL) and spin q-Whittaker (sqW) functions, leveraging on Yang-Baxter relations, we build up Markov processes with the remarkable property sampling the respective

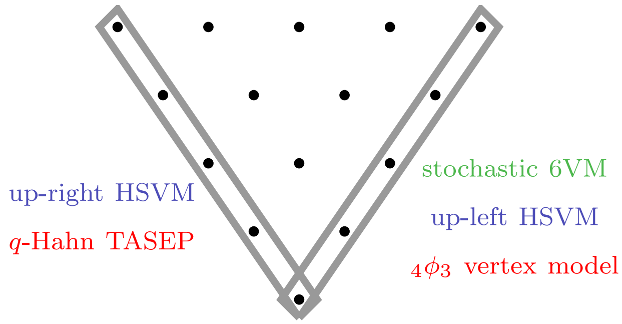

Figure 1.8: Schematic representation of marginals of fields studied in section 3.3. The first row of a sHL/sHL field is equivalent to the stochastic six vertex model (green). The first and the last row of a sqW/sHL field are equivalent respectively to the up-left and up-right directed higher spin vertex model (blue). Finally the first and the last row of a sqW/sHL field are equivalent respectively to the $_4\phi_3$ vertex model and to the q-Hahn TASEP (red).

fields. The construction of these Yang-Baxter fields uses a technique called bijectivization that was introduced in [BP19]. As a result of bijectivization certain classes of projections of the fields are found to be form autonomous Markov processes.

- Bijectivization of the $U_q(\widehat{\mathfrak{sl}_2})$ Yang-Baxter equation reduces, in the limit $q \to 0$ to local moves of the Robinson-Schensted-Knuth insertion algorithm. This reduction to the RSK is presented in section 3.2.

- We define the sHL/sHL field $\boldsymbol{\lambda}$, where joint law of partitions is given by products of skew sHL functions. For example the single point distribution is

$$\mathrm{Prob}(\lambda^{(i,j)} = \lambda) \propto \mathsf{F}_{\lambda'}(u_1, \dots, u_i)\mathsf{F}^*_{\lambda'}(v_1, \dots, v_j). \tag{1.21}$$

  The first row marginal of the field $\lambda_1^{(i,j)}$ forms an autonomous Markov process and it is equivalent in distribution with the height function of a stochastic six vertex model; see fig. 1.8. This result was obtained first in [BBW18; BP19]. Additionally, making use of scaled geometric specializations of sHL functions studied in section 2.5 we can produce fields of Young diagrams with gibbsian random boundary conditions. These, at the level of the $\lambda_1^{(i,j)}$ marginal produce the six vertex model with two sided Bernoulli boundary conditions studied in [Agg18].

- In the sqW/sHL field $\boldsymbol{\lambda}$ joint law of signatures is given by product of pairs of skew sqW and sHL functions; for example the single point distribution is

$$\mathrm{Prob}(\lambda^{(i,j)} = \lambda) \propto \mathbb{F}_{\lambda}(x_1, \dots, x_i)\mathsf{F}^\bullet_{\lambda'}(v_1, \dots, v_j). \tag{1.22}$$

  Using bijectivizations we characterize two autonomous Markov marginal projections. The first row marginal $\lambda_1^{(i,j)}$ is equivalent to the height function of a variant of the higher spin vertex model with up-left directed paths. On the other hand the last row marginal $\lambda_i^{(i,j)}$ is matched with the height function of a higher spin vertex model with up-right directed paths; see fig. 1.8. These results were obtained in [BMP19; MP20].

- We finally construct the sqW/sqW field $\boldsymbol{\lambda}$ and in it joint law of signatures is given by product of pairs of skew sqW and sqW functions; for example the single point distribution is

$$\mathrm{Prob}(\lambda^{(i,j)} = \lambda) \propto \mathbb{F}_\lambda(x_1, \dots, x_i)\mathbb{F}^*_\lambda(y_1, \dots, y_j). \tag{1.23}$$

The fields possess two natural Markov marginal projections. The first row marginal $\lambda_1^{(i,j)}$ is equivalent to the height function of a general exclusion process with pushing mechanism called ${}_4\phi_3$ vertex model with up-left directed path. This was introduced in [BMP19; CMP19]. The last row marginal $\lambda_i^{(i,j)}$ is matched with the position of a tagged particle in a q-Hahn TASEP; see fig. 1.8. These results were obtained in [BMP19; MP20].

- In a simplified "Plancherel" (or "Poisson-type") continuous time limit we construct a Markov dynamics on interlacing arrays under which the last rows marginally evolve as a continuous time version of the q-Hahn TASEP (appeared in [BC16b]). Our new two-dimensional continuous time dynamics is a model of 2d anysotropic growth and represents a one-parameter deformation of the q-Whittaker 2d-growth model introduced in [BC14, Definition 3.3.3]. The latter growth model has continuous time q-TASEP as the last row marginal dynamics.

- Eigenrelations for sHL and sqW functions provide nested integral formulas for joint q-moments of the fields. In particular the generating function of single point q-moments of coordinates $\lambda_1^{(i,j)}$ or $\lambda_i^{(i,j)}$ can be rearranged in a Fredholm determinant. In the simple case of the sHL/sHL field this gives a determinatal formula for the height function $\mathcal{H}_{6\mathrm{V}}$ of six vertex model with domain wall boundary conditions. We have

$$\mathbb{E}\left(\frac{1}{(\zeta q^{\mathcal{H}_{6\mathrm{V}}(i,j)}; q)_\infty}\right) = \det\left(Id + \mathsf{K}\right)_{L^2(\mathsf{C})}, \qquad \zeta \in \mathbb{C} \setminus \mathbb{R}_{>0}, \tag{1.24}$$

where the integral kernel K is given by

$$\mathsf{K}(w, w') = \frac{1}{2\mathrm{i}} \int_{d+\mathrm{i}\mathbb{R}} \frac{(-\zeta)^r}{\sin(\pi r)} \frac{\mathsf{f}(w)/\mathsf{f}(q^r w)}{q^r w - w'} dr, \qquad \text{with} \qquad \mathsf{f}(w) = \frac{\prod_{k=1}^{i}(w-u_k)}{\prod_{k=1}^{j}(w-v_k)}. \tag{1.25}$$

Formulas for models with random boundary conditions are also accessible thanks to analytic continuations and fusion techniques.

The main immediate consequence of the connection between random growth processes of Young diagrams weighted by our symmetric functions and stochastic integrable systems in the KPZ universality class is a fully algebraic unified theory of observables for these models. This was used in [BMP19] to prove conjectures about determinantal expressions for certain systems of particles and polymers formulated in [CMP19]. More in general our theory brings the realm of complicated integrable systems, like the higher spin vertex model, closer to that of determinantal point processes like the Schur processes. We envision that further studies might reveal additional connections extending our theories to the evaluations of more interesting observables, including multi point joint distributions. A possible strategy to describe multi point statistics would be to follow techniques introduced in the very recent work of Dimitrov [Dim20], where he characterized the two point correlations of the stochastic six vertex model using difference operators analogous to our $\overline{\mathfrak{D}}_1$. We leave these investigations for future works.

1.2.4 Asymptotic analysis for the stationary higher spin vertex model

In chapter 4 we establish KPZ fluctuations for the stationary higher spin vertex model. Our starting point is a Fredholm determinant expression for the q-Laplace transform of the height function that was obtained in [IMS20]. The derivation of the formula we use employs an elliptic generalization of the Cauchy determinant, following techniques invented by Imamura and Sasamoto in [IS19].

Stationary growth processes in the KPZ class exhibit typical fluctuations and characteristic 1:2:3 scaling only if we follow the evolution of the interface along a specific direction. To explain this phenomenon consider the KPZ equation. In the stationary evolution the height profile is a Brownian motions and we consider its displacement between two point in space and time that with no loss of generality we take as $(0, 0)$ and (x, t). Such height displacement possesses in the long space time limit two different regimes. Around the characteristic line of the Burgers equation associated with the dynamics, that one can understand as the direction of the growth, the height scales according to KPZ exponents and its one point distribution is governed by the Baik-Rains distribution F_0 (see Definition 4.2.3). Alternatively, when we move away from the characteristic line the size of fluctuations coming from the stationary initial data, the brownian motion, overwhelms any possible nontrivial behavior produced by the random dynamics and the height performs a gaussian process. The same is true for discrete models where instead of the brownian motion, the stationary profile of the height is given by a sequence of independent increments.

For the stationary higher spin vertex model we now want to give the exact expression of scaling parameters defining the characteristic line and the expected behavior of the height function $\mathcal{H}$. For simplicity in this case we suppress time inhomogeneities and we set $v_j = v$. We make use of q-polygamma type functions υ_k defined in chapter A. For non-negative integers k consider the functions

$$a_k(d) = \upsilon_k(qvd) - \upsilon_k(vd), \qquad h_k(d) = \frac{1}{n}\sum_{i=2}^{n} \left(\upsilon_k(d/x_i) - \upsilon_k(-ds)\right) \tag{1.26}$$

and, depending on the parameter $\mathscr{d}$, define the quantities

$$\kappa_0 = \frac{h_1(\mathscr{d})}{a_1(\mathscr{d})}, \qquad \eta_0 = \kappa_0 a_0(\mathscr{d}) - h_0(\mathscr{d}), \qquad \gamma = -\left(\frac{1}{2}(\kappa_0 a_2(\mathscr{d}) - h_2(\mathscr{d}))\right)^{1/3}. \tag{1.27}$$

We assume that the functions h_k always converge in the large n limit and we refer to the curve $(n, \kappa_0 n)$ as the *characteristic line* of the stationary higher spin vertex model. For random growth models usually the characteristic line is expressed as a function of the time t, rather than of the coordinate n, but in our case, since the system exhibits spatial inhomogeneities we find more natural to adopt the notation $(n, \kappa_0 n)$. The parameter η_0 multiplied by n is readily understood as the expectation $\mathbb{E}(\mathcal{H}(n, \kappa_0 n))$, whereas γ will be used to describe the size of the characteristic fluctuations of $\mathcal{H}$ around η_0. By slightly perturbing quantities κ_0, η_0 we can analyze the asymptotic behavior of $\mathcal{H}$ in a region of size $n^{2/3}$ around the characteristic line. For this we extend the definitions given in above setting

$$\kappa_\varpi = \kappa_0 + \frac{h_2 a_1 - h_1 a_2}{a_1^2} \frac{\varpi}{\gamma n^{1/3}} \tag{1.28}$$

$$\eta_\varpi = \eta_0 + \frac{a_0(h_2 a_1 - h_1 a_2)}{a_1^2} \frac{\varpi}{\gamma n^{1/3}} + \frac{h_2 a_1 - h_1 a_2}{a_1} \frac{\varpi^2}{\gamma^2 n^{2/3}}, \tag{1.29}$$

where ϖ is a real number parameterizing the displacement from the characteristic line and functions a_k, h_k are evaluated at $\mathscr{d}$. We come now to state our result.

Theorem 1.2.1. *Consider the stationary higher spin vertex model with density $\mathscr{d}$. Then, for any real numbers ϖ, r we have*

$$\lim_{n \to \infty} \mathbb{P}\left(\frac{\mathcal{H}(n, \kappa_\varpi n) - \eta_\varpi n}{\gamma n^{1/3}} > -r\right) = F_\varpi(r), \tag{1.30}$$

where $F_\varpi(r)$ is the Baik-Rains distribution presented in Definition 4.2.3.

For a more precise statement of this theorem we refer to chapter 4.

An alternative procedure we could have followed to establish Baik-Rains fluctuations for the height functions of the higher spin vertex model is by using Fredholm determinant formulas derived in chapter 3. These turn out to be different than those obtained through elliptic determinant calculations and their asymptotic analysis would have been more along the line of [Agg18] where Aggarwal studied the stationary six vertex model.

1.2.5 A new class of functions: the spin Whittaker functions

Our final series of results deals with the $q \to 1$ scaling limit of the spin q-Whittaker polynomials and of stochastic systems associated with them. This leads to the definition of a new class of functions that can be seen as one parameter deformation of Whittaker functions [Jac67; Kos78]: we call them the spin-Whittaker functions.

The spin Whittaker functions $\mathfrak{f}_{X_1,\dots,X_N}(L_1,\dots,L_N)$ depend on a global parameter $S > 0$, complex numbers $X_1, \dots X_N$, such that $|X_i| < S$ and a continuous signature $\underline{L}_N =$

$(L_1 \geq \ldots \geq L_N \geq 0)$. They may be defined via a recursive Givental-type integral representation. Let $\underline{L}'_{N-1}$ and $\underline{L}_N$ be interlacing sequences:

$$1 \leq L_N \leq L'_{N-1} \leq L_{N-1} \leq \ldots \leq L'_1 \leq L_1$$

(notation: $\underline{L}'_{N-1} \prec \underline{L}_N$) and define the branching functions

$$\begin{aligned}\mathfrak{f}_X(\underline{L}'_{N-1};\underline{L}_N) \coloneqq & \frac{1}{(\mathrm{B}(S+X,S-X))^{N-1}}\left(\frac{L_N\cdots L_1}{L'_{N-1}\cdots L'_1}\right)^{-X} \\ & \times \prod_{j=1}^{N-1}\left(1-\frac{L'_j}{L_j}\right)^{S-X-1}\left(1-\frac{L_{j+1}}{L'_j}\right)^{S+X-1}\left(1-\frac{L_{j+1}}{L_j}\right)^{1-2S},\end{aligned} \tag{1.31}$$

where $\mathrm{B}(S+X,S-X)$ is the Beta function. Set $\mathfrak{f}_{X_1}(L_1) \coloneqq L_1^{-X_1}$, and, inductively,

$$f_{X_1,\ldots,X_N}(\underline{L}_N) \coloneqq \int_{\underline{L}'_{N-1}:\,\underline{L}'_{N-1}\prec\underline{L}_N} \mathfrak{f}_{X_1,\ldots,X_{N-1}}(\underline{L}'_{N-1})\,\mathfrak{f}_{X_N}(\underline{L}'_{N-1};\underline{L}_N)\,\frac{d\underline{L}_{N-1}}{\underline{L}'_{N-1}}. \tag{1.32}$$

To familiarize the reader with the notion of spin Whittaker functions we report the simplest nontrivial case $N=2$ that takes the simple form

$$\mathfrak{f}_{X,Y}(u,z) = (z/u)^S u^{-X-Y}\,{}_2F_1\left(\begin{matrix}S+X, & S+Y\\ 2S, & -\end{matrix}\,\middle|\, 1-\frac{z}{u}\right), \qquad 1 \leq u \leq z,$$

where ${}_2F_1$ is the Gauss hypergeometric function (A.24).

We now give a list of results concerning spin Whittaker functions contained in chapter 5.

- After establishing regularity and well posedness of the Givental representation (1.32), we define a notion of dual spin Whittaker functions $\mathfrak{g}_{Y_1,\ldots,Y_M}(\underline{L}_N)$. The pair of functions $\mathfrak{f},\mathfrak{g}$ satisfies Cauchy identities an example of which reads

$$\int \mathfrak{f}_{X_1,\ldots,X_N}(\underline{L}_N)\,\mathfrak{g}_{Y_1,\ldots,Y_M}(\underline{L}_N)\,\frac{d\underline{L}_N}{\underline{L}_N} = \prod_{j=1}^{M}\frac{\Gamma(X_1+Y_j)}{\Gamma(S+X_1)}\left(\prod_{i=2}^{N}\frac{\Gamma(X_i+Y_j)\Gamma(2S)}{\Gamma(S+X_i)\Gamma(S+Y_j)}\right). \tag{1.33}$$

  For the usual Whittaker functions, the first Cauchy type identity with $M=N$ is due to Bump and Stade [Bum89], [Sta02], [GLO08], and was later generalized in [Cor+14, (1.2)], [BC14, Section 4.2.1].

- Consider the spin q-Whittaker polynomial $\mathbb{F}_\lambda(x_1,\ldots,x_N)$ and introduce the scaling

$$q \to 1, \qquad x_i = q^{X_i}, \qquad s = -q^S, \qquad q^{-\lambda_i} = L_i,$$

  where $S>0$, $|X_i|<S$, and $1 \leq L_N \leq \ldots \leq L_1$ are fixed real numbers. We show in Theorem 5.1.14 that under this scaling the convergence

$$\mathbb{F}_\lambda(x_1,\ldots,x_N) \longrightarrow \mathfrak{f}_{X_1,\ldots,X_N}(L_1,\ldots,L_N), \tag{1.34}$$

  holds uniformly on compacts. Similar results are also given for dual functions $\mathbb{F}^*$ and $\mathfrak{g}$.

- We also define spin Whittaker processes. These are probability measures on interlacing sequences of continuous signatures $\underline{L}_1 \prec \underline{L}_2 \prec \ldots \prec \underline{L}_N$, with probability weights expressed through the spin Whittaker functions. Cauchy type identity (1.33) provides an explicit normalizing constant for the spin Whittaker process. We match the distribution of the marginal process $L_{k,k}^{-1}$ to the strict-weak beta polymer model of [BC16a] (Theorem 5.2.6), and the distribution of the other marginal process $L_{k,1}$ to the other beta polymer like model which appeared in [CMP19] (Theorem 5.2.11).

- We show (Theorem 5.3.3) that the functions $\mathfrak{f}_{X_1,\ldots,X_N}(\underline{L}_N)$ are eigenfunctions of a deformation of the $\mathfrak{gl}_N$ quantum Toda Hamiltonian

$$\mathcal{H}_2 := -\frac{1}{2}\sum_{i=1}^{N}\partial_{u_i}^2 + \sum_{1\le i<j\le N} S^{-2(j-i)}e^{u_j-u_i}(S-\partial_{u_i})(S+\partial_{u_j}). \tag{1.35}$$

  Introduce a change of variables $L_j = S^{N+1-2j}e^{u_j}$. Then in these variables we have

$$\mathcal{H}_2\mathfrak{f}_{X_1,\ldots,X_N} = \left(-\frac{1}{2}\sum_{j=1}^{N}X_j^2\right)\mathfrak{f}_{X_1,\ldots,X_N}.$$

- As $S \to +\infty$ and under the scaling $L_j = S^{N+1-2j}e^{u_j}$, $X_j = -\mathrm{i}\lambda_j$, the operator $\mathcal{H}_2$ and the spin Whittaker functions $\mathfrak{f}_{X_1,\ldots,X_N}(\underline{L}_N)$ formally reduce to the usual quantum Toda hamiltonian Whittaker functions

$$\mathcal{H}_2^{\mathrm{Toda}} = -\frac{1}{2}\sum_{i=1}^{N}\frac{\partial^2}{\partial u_i^2} + \sum_{i=1}^{N-1}e^{u_{i+1}-u_i}, \qquad \mathcal{H}_2^{\mathrm{Toda}}\psi_{\underline{\lambda}}(\underline{u}_N) = \left(-\frac{1}{2}\sum_{i=1}^{N}\lambda_i^2\right)\psi_{\underline{\lambda}}(\underline{u}_N). \tag{1.36}$$

  A similar reduction brings spin Whittaker processes to Whittaker processes from [OCo12], [Cor+14], [BC14]. We do not fully justify these limit transitions, as this requires a much finer analysis and justification of the interchange of the $S \to +\infty$ limit with Givental-type representations. However, we note that at the level of marginals, the strict-weak beta polymer becomes the strict-weak log-gamma polymer [BC16a, Remark 1.5]. We also show (Proposition 5.2.13) that the other beta polymer type model turns into the log-gamma polymer from [Sep12].

The emergence of new classes of functions with a list of remarkable features is not a very common event. In this thesis we define the spin Whittaker function in full generality and establish some of they immediate properties. We do not consider the study of non trivial scaling limits, that could reveal additional hidden structures. For example we do not investigate to what extent such functions arise from different combinatorial constructions, like the classical Whittaker functions and their relation to tropical RSK [OSZ14]. We will explore these directions in further works.

1.2.6 Physical relevance of results

This thesis mainly focuses on mathematical properties of the stochastic integrable models in the KPZ class. Nevertheless, our results clearly have relevance also from the experimental standpoint. Here we will briefly discuss two examples.

Transport in inhomogeneous space

The higher spin vertex model can be seen as a model of transport in inhomogeneous space. To see this we naturally interpret the path ensemble as a collection of trajectories of particles forced to move in one spatial dimension (the i coordinate in fig. 1.6 left) over time (the j coordinate). A scaling of parameters $v = \varepsilon \sim 0, s = -1$ transforms the probability weights of fig. 1.7 into

$\mathsf{L}^{\mathrm{ur}}_{x_i,\varepsilon}\Bigg($ 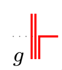 $\Bigg) \sim \varepsilon x_i(1-q^g) \qquad \mathsf{L}^{\mathrm{ur}}_{x_i,\varepsilon}\Bigg($ 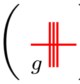 $\Bigg) \sim x_i q^g.$

This, following a time rescaling $j = t/\varepsilon$, translates the higher spin vertex model in a continuous time process of particles in the lattice obeying the following dynamics:

- particles are positioned at vertices of $\mathbb{Z}_{\geq 0}$, possibly sharing their location;
- if at time t, g_i particle are sitting at location i, with rate $x_i(1-q^{g_i})$ one of them activates and starts flying to its right. During this rightward motion the particle crosses each location $i' > i$ with probability $x_{i'}q^{g_{i'}}$ otherwise it stops there;
- with a fixed rate r a particle is injected at the leftmost location $i = 1$.

What we have just informally described is a model for a one dimensional fluid with viscosity (governed by the parameter q) and microscopic inhomogeneities (produced by the x_i). Result of theorem 1.2.1 establishes that, under certain conditions on the parameters x_i, the height function of this process, which is closely related to its cumulative current, in the stationary state follows typical $t^{1/3}$ KPZ asymptotic fluctuations distributed according to the Baik-Rains law. Conditions on the inhomogeneities do not forbid the presence of "slower regions", where the particles, in the long time tend to accumulate with higher density.

In mathematical and physical literature "slow bond" problems are of great interest since it is known that for one dimensional transport, the presence of even minimal microscopic defects has the effect of drastically changing hydrodynamic properties of the system [BSS14; BSS17]. In this sense we show that defects of the form described above (which are qualitatively different from those in [BSS14]) do not affect KPZ asymptotic limit of the process; see also [BP18b].

In recent years KPZ exponents and sometimes fluctuations have been observed directly in a number of remarkable experiments, involving liquid crystals [TS10], collidal suspensions [Yun+13], bacteria growth [Hue+10] and many more. In particular it became possible only very recently to directly detect KPZ universality and Baik-Rains universal law from systems in steady states [IFT20]. It would be very interesting to see whether a direct observation of KPZ exponents can be made also in more anthropological context. The model of viscous fluid we introduced above can be thought as a traffic model (for pedestrians more realistically) in an environment where overtaking is allowed and a few roadblocks are present. Steady states in such systems are reached at peak hours and predictions of theorem 1.2.1 imply that a certain linear combination of the initial state and the cumulative current through a location will exhibit $t^{1/3}$-sized fluctuations, when the time t is sufficiently large. The discussion in section 4.2.1 can then be used to express scaling parameters κ, η, γ appearing in theorem 1.2.1 in dependence only of physical observables of the macroscopic system; see also [Spo12]. We leave such interesting developments for future works.

Baik-Rains distribution in diffusion processes

Other new physical implications of our results can be argued considering the Beta polymer model; see definition 5.2.4. It was observed in [BC16a] that such model of polymers is equivalent to a simple model of diffusion: the Beta random walk in random environment (RWRE).

A particle $X(t)$ moves on the lattice $\mathbb{Z}$ jumping at each time step to its left (resp. right) neighboring site with probabilities p (resp. $1-p$), that are themselves i.i.d. random variables (the environment) with Beta distribution. It is clear that in the long time limit, the particle obeys the central limit theorem and the fluctuation of its endpoint are of size $\sqrt{t}$ and converge to the gaussian law. KPZ statistics enter the picture when conditioning the walker to have an anomalous speed. In this case the large deviations of the random walk endpoint are corrected at the second order by a random term which scales as $t^{1/3}$ and converges to the GUE Tracy-Widom distribution. More precisely [BC16a] proves that

$$\lim_{t\to\infty} \mathbb{P}\left(\frac{\log \mathsf{P}\{X(t) \geq t x_0\} + I(x_0) t}{C(x_0) t^{1/3}} \leq y \right) = F_{GUE}(y), \tag{1.37}$$

where P is the probability of the random walk, $\mathbb{P}$ is that of the random environment and $I(x_0), C(x_0)$ are constants.

A question raised by this result is how other KPZ universal statistics can describe properties of RWRE and our analysis of the stationary higher spin vertex model (which is a generalization of the Beta polymer and hence of the Beta RWRE) suggests the answer for the case of the Baik-Rains distribution. This is done by replacing the logarithm of the probability P with an appropriate expectation of statistics of walks with free endpoint; see also [BRS19] for a probabilistic approach to the topic. We will cover such interesting developments in a further work.

Chapter 2

Spin Hall-Littlewood and spin q-Whittaker functions

This chapter presents results contained in sections 3,4,5,8 of

[BMP19] A. Bufetov, M. Mucciconi, and L. Petrov. "Yang-Baxter random fields and stochastic vertex models". In: *arXiv preprint* (2019). arXiv:1905.06815 [math.PR]. To appear in Adv. Math.

and of sections 2,3 of

[MP20] M. Mucciconi and L. Petrov. "Spin q-Whitaker polynomials and deformed quantum Toda". In: *arXiv preprint* (2020). arXiv:2003.14260 [math.PR]

2.1 Basic notions

2.1.1 Partitions and Signatures

A *partition* is a sequence of nonnegative integers $\lambda = (\lambda_1 \geq \lambda_2 \geq \dots)$ such that $\lambda_i = 0$ eventually. The last positive entry of the sequence is denoted with $\lambda_{\ell(\lambda)}$ and $\ell(\lambda)$ is called the *length* of the partition λ while elements $\lambda_1, \lambda_2, \dots$ are its *parts*. Denote by $\mathbb{Y}$ the set of all partitions including the empty one $\lambda = \varnothing$ (by agreement, $\ell(\varnothing) = 0$). A partition λ is naturally represented by its Young diagram, obtained drawing on the plane $\mathbb{N} \times \mathbb{N}$ left justified sequences of λ_i boxes; the order we use is matrix-style with i growing downward. The use of a multiplicative notation is also common:

$$\lambda = 1^{m_1(\lambda)} 2^{m_2(\lambda)} \dots, \qquad \text{where} \qquad m_i(\lambda) = \#\{j \colon \lambda_j = i\}.$$

For a given λ its *transposed partition* λ' is given as

$$\lambda'_i \coloneqq \#\{j \colon \lambda_j \geq i\}, \qquad i = 1, 2 \dots.$$

We easily see that the Young diagrams of λ and λ' are related by reflection with respect to the main diagonal.

Given two partitions μ and λ we say that they *interlace* if

$$\lambda_1 \geq \mu_1 \geq \lambda_2 \geq \mu_2 \geq \cdots \geq \lambda_k \geq \mu_k \geq \lambda_{k+1} \geq \cdots . \tag{2.1}$$

We will use notation $\mu \prec \lambda$ for interlacing. When λ and μ are such that $\mu' \prec \lambda'$, we say that they are *transposed interlacing*, and use the notation $\mu \prec' \lambda$.

A *nonnegative signature* is a partition with a fixed finite number of parts N. We will drop the word "nonnegative", and refer to them simply as "signatures". Their set is denoted by

$$\mathrm{Sign}_N \coloneqq \{\lambda = (\lambda_1 \geq \cdots \geq \lambda_N \geq 0) \colon \lambda_i \in \mathbb{Z}_{\geq 0}\}, \qquad N \in \mathbb{Z}_{\geq 0}$$

and by agreement, $\mathrm{Sign}_0 = \{\varnothing\}$. To define the transposition in the context of signatures, introduce the set of *boxed signatures*

$$\mathrm{Sign}_M^{\leq N} \coloneqq \{\lambda = (\lambda_1 \geq \cdots \geq \lambda_M \geq 0) \colon 0 \leq \lambda_i \leq N\} \subset \mathrm{Sign}_M$$

and $\mathrm{Sign}^{\leq N} = \bigcup_{M \geq 0} \mathrm{Sign}_M^{\leq N}$ When $\lambda \in \mathrm{Sign}_M^{\leq N}$ we have $\lambda' \in \mathrm{Sign}_N^{\leq M}$. In this case, the Young diagram of λ fits inside the the box

$$\mathrm{Box}(N, M) = \{1, \ldots, N\} \times \{1, \ldots, M\},$$

while that of λ' fits inside $\mathrm{Box}(M, N)$; see Figure 2.1 for an illustration. For pairs of signatures λ, μ the notion of interlacing is defined dropping unnecessary inequalities in (2.1).

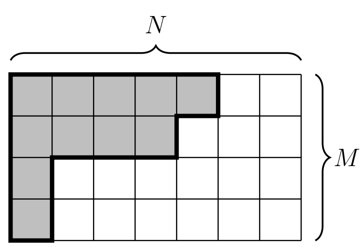

Figure 2.1: An example of a signature $\lambda = (5, 4, 1, 1) \in \mathrm{Sign}_4^{\leq 7}$. Its transposed signature is $\lambda' = (4, 2, 2, 2, 1, 0, 0) \in \mathrm{Sign}_7^{\leq 4}$.

2.1.2 Young diagrams as arrow configurations

Functions we introduce in this Chapter are labeled by (skew) Young diagrams which we represent as configurations of vertical arrows on $\mathbb{Z}_{\geq 0}$. Let λ be written in the multiplicative notation as $\lambda = 1^{l_1} 2^{l_2} \ldots$, where l_i is the number of parts of λ which are equal to i. By definition, the arrow configuration corresponding to λ, denoted by $|\lambda\rangle$, contains l_i vertical arrows at location i. The number of vertical arrows at 0 is assumed infinite which reflects the fact that one can append Young diagrams by zeros without changing them. See Figure 2.2, left, for an illustration. At times it will be convenient to work with the arrow configuration corresponding to the transposed of a specific Young diagram λ. In this case we observe that the number of arrow at position i in $|\lambda'\rangle$ is given by $\lambda_i - \lambda_{i+1}$ and we call this the *dual arrow representation of* λ.

We will use arrow configurations to construct our special functions following a simple recipe. Decorate each vertex x of the lattice $\mathbb{Z}_{\geq 0}$ with a function $w_x(u)$ that assigns a weight to arrows configurations around x. Assuming that the weights w are non-zero only at *up-right directed* arrow configurations and that they are 1 if no arrow crosses the vertex, we consider then the transfer matrix $\mathfrak{T}(u) = w_0(u)w_1(u)w_2(u)\cdots$ and its matrix elements

$$\mathfrak{F}_{\lambda/\mu}(u) = \langle \mu|\mathfrak{T}(u)|\lambda\rangle.$$

Then the functions $\mathfrak{F}$ are well defined and they admit multi-variable extensions stacking together multiple rows, as in Figure 2.4, left panel. This procedure guarantees that they also follow branching rules (e.g. (2.4) below). To impose symmetries we will request that the weights w will be solutions of Yang-Baxter equations, for example we easily see that the commutation of transfer matrices $\mathfrak{T}(u_1)$,$\mathfrak{T}(u_2)$ implies that the $\mathfrak{F}$'s are symmetric with respect to the permutation of variables. In the following sections we will need also families of dual functions $\mathfrak{G}$, that we will generally produce using *down-right* directed path ensembles; see Figure 2.4, right panel.

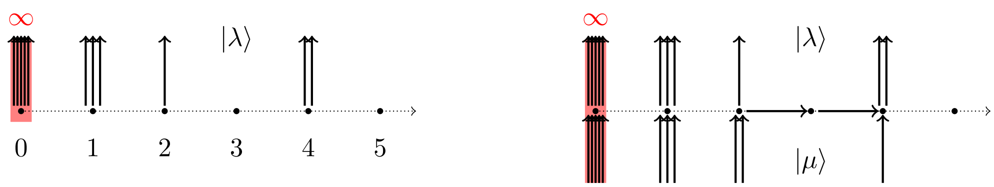

Figure 2.2: Left: Configuration $|\lambda\rangle$ of vertical arrows corresponding to the Young diagram $\lambda = (4, 4, 2, 1, 1, 1)$. Right: Interlacing of λ with $\mu = (4, 2, 2, 1, 1, 1)$.

2.2 Spin Hall-Littlewood functions

2.2.1 Stable spin Hall-Littlewood functions

The first collection of vertex weights we work with is given in Figure 2.3. Along with q, these weights depend on two quantities $u, s \in \mathbb{C}$, which are called the *spectral* and the *spin* parameters, respectively. The weights $w_{u,s}$ satisfy the Yang-Baxter equation, see (B.1).

For vertices at the left boundary we set

$$w_{u,s}\left(\begin{array}{c} \infty \\ \cdot\!\!-\!\!- \\ \infty \end{array} \right) = w_{u,s}(\infty, \varnothing; \infty, 1) = u, \qquad w_{u,s}\left(\begin{array}{c} \infty \\ \cdot\cdots \\ \infty \end{array} \right) = w_{u,s}(\infty, \varnothing; \infty, 0) = 1, \quad (2.2)$$

Both in Figure 2.3 and in (2.2), we attribute weight zero to all configurations which are not listed. In particular, the following *arrow conservation property* holds:

$$w_{u,s}(i_1, j_1; i_2, j_2) = 0 \qquad \text{unless } i_1 + j_1 = i_2 + j_2. \tag{2.3}$$

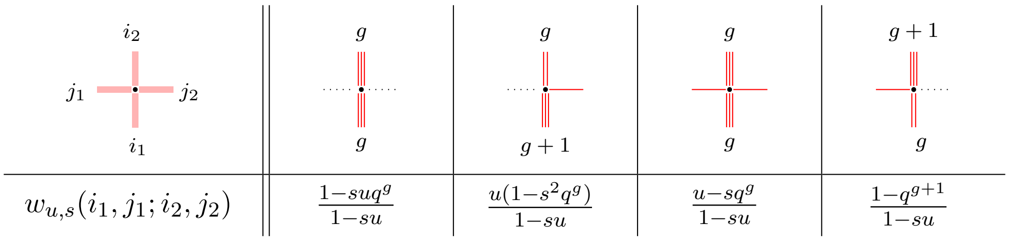

Figure 2.3: In the top row we see all acceptable configurations of arrows entering and exiting a vertex; below we reported the corresponding vertex weights $w_{u,s}(i_1, j_1; i_2, j_2)$.

Definition 2.2.1. Consider a sequence of spin parameters $\mathbf{s} = (s_1, s_2, \cdots)$ and a spectral parameter $u \neq 1/s_x$ for all x. For $\mu, \lambda \in \mathbb{Y}$ with $\mu \prec \lambda$, the *stable spin Hall-Littlewood function* in one variable, denoted by $\mathsf{F}_{\lambda/\mu}(u; \mathbf{s})$, is defined as the total weight (= product of individual vertex weights) of the unique configuration of arrows between $|\mu\rangle$ and $|\lambda\rangle$ as in Figure 2.2, right panel. Here the individual vertex weights are the w_{u,s_x}'s from Figure 2.3, and the left boundary weights are (2.2). If $\mu \not\prec \lambda$, we set $\mathsf{F}_{\lambda/\mu}(u; \mathbf{s}) = 0$. In case all spin parameters are equal $s_x = s$ we will drop the explicit dependence on $\mathbf{s}$ and write $\mathsf{F}_{\lambda/\mu}(u)$.

In the sequel we will mostly omit the word "stable" (cf. [BMP19, Section 3.3] on connections to the non-stable functions which were originally defined in [Bor17]), and will also abbreviate the name to simply the *sHL functions*.

Define the functions with multiple variables inductively via the branching rule:

$$\mathsf{F}_{\lambda/\mu}(u_1, \dots, u_k; \mathbf{s}) = \sum_{\nu} \mathsf{F}_{\lambda/\nu}(u_k; \mathbf{s})\, \mathsf{F}_{\nu/\mu}(u_1, \dots, u_{k-1}; \mathbf{s}). \tag{2.4}$$

That is, $\mathsf{F}_{\lambda/\mu}(u_1, \dots, u_k; \mathbf{s})$ is a partition function of ensembles of up-right paths as in Figure 2.4, left, with height k, spectral parameters $u_1, \dots, u_k$ corresponding to horizontal slices, and boundary conditions $|\mu\rangle$, 0^∞, $|\lambda\rangle$ and empty at the bottom, left, up, and right, respectively. The fact that the paths are directed up-right corresponds to the arrow conservation property (2.3). Note that $\mathsf{F}_{\lambda/\mu}(u_1, \dots, u_k; \mathbf{s})$ vanishes unless $0 \le \ell(\lambda) - \ell(\mu) \le k$, but this condition is not sufficient.

The Yang-Baxter equation implies that $\mathsf{F}_{\lambda/\mu}(u_1, \dots, u_k)$ is symmetric with respect to permutations of the u_i's, see, e.g., [Bor17, Theorem 3.6]. These functions also satisfy the *stability property*

$$\mathsf{F}_{\lambda/\mu}(u_1, \dots, u_k, 0; \mathbf{s}) = \mathsf{F}_{\lambda/\mu}(u_1, \dots, u_k; \mathbf{s}). \tag{2.5}$$

For $\mu = \varnothing$, the stable spin Hall-Littlewood functions admit an explicit symmetrization formula [BW17; BP18a] which we recall below. When all $s_x = 0$, the stable spin Hall-Littlewood functions become the usual Hall-Littlewood symmetric polynomials [Mac95, Chapter III].

Theorem 2.2.2. *For any Young diagram λ such that $n \ge \ell(\lambda)$, we have*

$$\mathsf{F}_{\lambda}(u_1, \dots, u_n; \mathbf{s}) = \frac{(1-q)^n}{(q;q)_{n-\ell(\lambda)}} \sum_{\sigma \in \mathfrak{S}_n} \sigma \Bigg\{ \prod_{1 \le i < j \le n} \frac{u_i - q u_j}{u_i - u_j} \prod_{i=1}^{n} \prod_{j=1}^{\lambda_i} \left(\frac{u_i - s_j}{1 - s_j u_i} \right) \prod_{i=1}^{\ell(\lambda)} \frac{u_i}{u_i - s_{\lambda_i}} \Bigg\}. \tag{2.6}$$

Here the symmetric group acts on the indices of the variables u_i, but not on λ_i.

Proof. This theorem is an easy corollary of [BP18a, Thm. 4.14], where a similar formula is stated for the non-stable spin Hall-Littlewood functions. To obtain (2.78) from equation (4.23) of [BP18a] all it takes is to set s_0=0. The denominator $(q;q)_{n-\ell(\lambda)}$ in the prefactor is a consequence of our choice of boundary weights (2.2). □

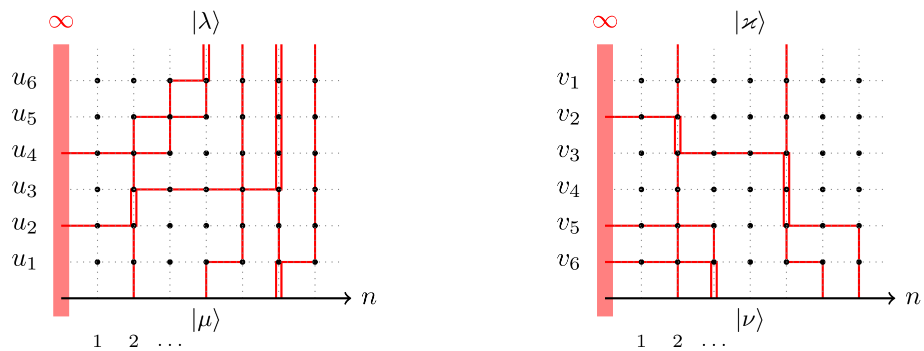

Figure 2.4: Examples of configurations of up-right and down-right paths used in the definitions of $\mathsf{F}_{\lambda/\mu}$ and $\mathsf{F}^*_{\nu/\varkappa}$, respectively.

We also report an additional remarkable property of the sHL functions usually called *spatial biorthogonality*. The following theorem was proven in [BP18a].

Proposition 2.2.3 (Corollary 7.5 [BP18a])**.** *For any Young diagrams λ, μ, we have*

$$\frac{\mathsf{c}_{\mathbf{s}}(\lambda)(q;q)_{n-\ell(\lambda)}}{(1-q)^n n!}\oint_\gamma \frac{dz_1}{2\pi \mathrm{i} z_1}\cdots\oint_\gamma \frac{dz_n}{2\pi \mathrm{i} z_n}\prod_{1\le i\neq j\le n}\frac{z_i-z_j}{z_i-qz_j}\,\mathsf{F}_\lambda(z_1,\dots,z_n;\mathbf{s})\mathsf{F}_\mu(1/z_1,\dots,1/z_n;\mathbf{s})=\mathbf{1}_{\lambda=\mu}, \tag{2.7}$$

where γ is a positively oriented contour encircling 0, $q^k s_x$ for all $k\ge 0, x\ge 0$, and the contour $q\gamma$ (its image under the multiplication by q), but not the points s_x^{-1}. Finally the coefficient $\mathsf{c}_{\mathbf{s}}(\lambda)$ is

$$\mathsf{c}_{\mathbf{s}}(\lambda)=\prod_{k\ge 1}\frac{(s_k^2;q)_{\ell_k}}{(q;q)_{\ell_k}}, \tag{2.8}$$

assuming $\lambda = 1^{\ell_1}2^{\ell_2}\cdots$.

We remark that for the statement of Proposition (2.2.3) we are tacitly assuming that the spin parameters allow the construction of the contour γ. Such assumption will always be satisfied for practical uses of the orthogonality throughout the thesis.

2.2.2 Dual stable spin Hall-Littlewood functions

Let us introduce the dual weights to $w_{u,s}$ from Figure 2.3 as follows:

$$w^*_{v,s}(i_1,j_1;i_2,j_2)=\frac{(s^2;q)_{i_1}(q;q)_{i_2}}{(q;q)_{i_1}(s^2;q)_{i_2}}\,w_{v,s}(i_2,j_1;i_1,j_2). \tag{2.9}$$

The arrow conservation law (2.3) implies that $w^*_{v,s}(i_1, j_1; i_2, j_2)$ vanishes unless $i_2 + j_1 = i_1 + j_2$, and as a result the corresponding vertex model produces configurations of directed down-right paths (see Figure 2.4, right). The explicit form of the weights $w^*_{v,s}$ is given in Figure 2.5. The weights $w^*_{v,s}$ at the left boundary are given by the same formulas as in

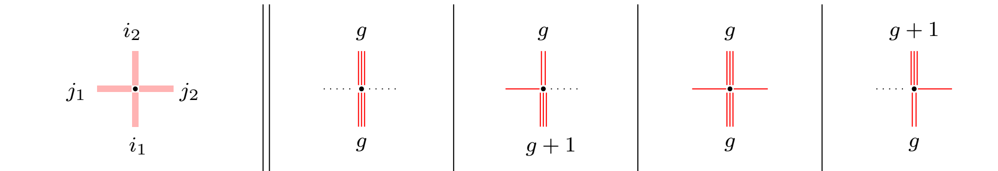

$w^*_{v,s}(i_1, j_1; i_2, j_2)$	$\frac{1-svq^g}{1-sv}$	$\frac{1-s^2q^g}{1-sv}$	$\frac{v-sq^g}{1-sv}$	$\frac{(1-q^{g+1})v}{1-sv}$

Figure 2.5: In the top row we see all acceptable configurations of paths entering and exiting a vertex; below we reported the corresponding vertex weights $w^*_{v,s}(i_1, j_1; i_2, j_2)$.

(2.2).

The weights $w^*_{v,s}$ can be obtained from $w_{u,s}$ by substituting u with $1/v$, swapping the values of both horizontal edge indices j_1 and j_2 (that is if $j_1 = 0$, then we change its value 1 and vice versa, and the same for j_2), and multiplying the result by $(v-s)/(1-vs)$. This swapping construction of the dual weights was instrumental in deriving Cauchy identities for the sHL functions from the Yang-Baxter equation [Bor17] (a bijectivization of this argument appeared in [BP19]). In the present thesis we employ a more direct approach with down-right paths which is better suited for the generalization to spin q-Whittaker functions. The Yang-Baxter equation connecting $w_{u,s}$ and $w^*_{v,s}$ is recorded in (B.2).

Definition 2.2.4. Consider a sequence of spin parameters $\mathbf{s} = (s_1, s_2, \cdots)$ and a spectral parameter $v \neq 1/s_x$ for all x. Fix $\varkappa, \nu \in \mathbb{Y}$ with $\varkappa \prec \nu$ and place the arrow configuration $|\nu\rangle$ *under* $|\varkappa\rangle$. Then there exists a unique configuration of horizontal arrows between $|\varkappa\rangle$ and $|\nu\rangle$. By definition, a *dual stable sHL function* in one variable, denoted by $\mathsf{F}^*_{\nu/\varkappa}(v; \mathbf{s})$, is the total weight of this horizontal arrow configuration, where the individual vertex weights are the w^*_{v,s_x}'s from Figure 2.5, and the left boundary weights are the same as in (2.2). If $\varkappa \not\prec \nu$, we set $\mathsf{F}^*_{\nu/\varkappa}(v; \mathbf{s}) = 0$. We will mainly work with two instances of dual sHL functions, depending on the choice of $\mathbf{s}$. When we take $s_x = s$ for all x we will use the notation $\mathsf{F}^*_{\nu/\varkappa}(v)$. When we take $s_1 = \cdots = s_{N-1} = s$ and $s_N = s_{N+1} = \cdots = 0$ for some N we will use the notation $\mathsf{F}^\bullet_{\nu/\varkappa}(v)$.

The multivariable generalization $\mathsf{F}^*_{\nu/\varkappa}(v_1, \ldots, v_k; \mathbf{s})$ is defined via the branching rule exactly as in (2.4). It is the partition function of ensembles of down-right paths as in Figure 2.4, right, of height k, spectral parameters $v_1, \ldots, v_k$ corresponding to horizontal slices, and boundary conditions $|\varkappa\rangle$, 0^∞, $|\nu\rangle$, and empty at the bottom, left, top, and right, respectively.

The relation (2.9) between $w^*_{v,s}$ and $w_{u,s}$ implies that

$$\frac{\mathsf{c}_\mathbf{s}(\lambda)}{\mathsf{c}_\mathbf{s}(\mu)} \mathsf{F}_{\lambda/\mu}(u_1, \ldots, u_k; \mathbf{s}) = \mathsf{F}^*_{\lambda/\mu}(u_1, \ldots, u_k; \mathbf{s}), \tag{2.10}$$

where the factor $\mathsf{c_s}$ was defined in (2.8).

The symmetry of $\mathsf{F}^*_{\lambda/\mu}(v_1,\dots,v_k;\mathbf{s}))$ in the $v_i's$ follows from the symmetry of $\mathsf{F}_{\lambda/\mu}$. The dual sHL function also satisfies the same stability property (2.5) as the non-dual one.

2.2.3 Skew Cauchy identities for sHL/sHL pair

In this section we consider the homogeneous versions of the sHL functions, obtained setting all spectral parameters $s_x = s$, for some $s \in \mathbb{C}$. Generalizations in non-homogeneous settings are straightforward and are contained in [BP18a].

One of the main consequences of the Yang-Baxter equation (either Proposition B.1.1 or Proposition B.1.2) is the skew Cauchy identity for the sHL functions:

Theorem 2.2.5 ([Bor17], [BP18a], [BW17, Section 7.4])**.** *For any two Young diagrams λ,μ and generic parameters $u,v\in\mathbb{C}$ such that $\big|(u-s)(v-s)\big| < \big|(1-su)(1-sv)\big|$, we have*

$$\sum_\nu \mathsf{F}^*_{\nu/\lambda}(v)\,\mathsf{F}_{\nu/\mu}(u) = \frac{1-quv}{1-uv}\sum_\varkappa \mathsf{F}_{\lambda/\varkappa}(u)\,\mathsf{F}^*_{\mu/\varkappa}(v). \tag{2.11}$$

A more refined proof of Theorem 2.2.5 can be given using bijectivization arguments described below following the approach of [BP19].

2.3 Spin q-Whittaker polynomials

2.3.1 Spin q-Whittaker polynomials

The spin q-Whittaker polynomials are partition functions of up-right path ensembles and they are labeled by signatures rather than partitions.

We consider up-right directed paths living in the half-quadrant $\{(i,j)\in\mathbb{Z}_{\geq 0}\times\mathbb{Z}_{\geq 1}\colon j\geq i\}$ and we assign weights to a generic vertex (i,j) as:

$$W^{\llcorner}_{x,s}(k) := x^k\,\frac{(-s/x;q)_k}{(q;q)_k}, \qquad \text{if } i=0; \tag{2.12}$$

$$W_{x,s}(i_1,j_1;i_2,j_2) := \mathbf{1}_{i_1+j_1=i_2+j_2}\,\mathbf{1}_{i_1\geq j_2}\,x^{j_2}\,\frac{(-s/x;q)_{j_2}(-sx;q)_{i_1-j_2}(q;q)_{i_2}}{(q;q)_{j_2}(q;q)_{i_1-j_2}(s^2;q)_{i_2}}, \qquad \text{if } 0<i<j; \tag{2.13}$$

$$W^{\lrcorner}_{x,s}(k) := \frac{(q;q)_k}{(-s/x;q)_k}, \qquad \text{if } i=j. \tag{2.14}$$

Here in (2.12) and (2.14), $k\in\mathbb{Z}_{\geq 0}$ denotes the number of paths going through the vertex, and in (2.13) the numbers $i_1,j_1,i_2,j_2\in\mathbb{Z}_{\geq 0}$ denote, respectively, the numbers of entering vertical, entering horizontal, exiting vertical, and exiting horizontal paths to/from the vertex.

Remark 2.3.1. One can readily check that the condition $i_1 \geq j_2$ in (2.13) implies that up-right path configurations with nonzero global weight are those associated with sequences of interlacing signatures $\lambda^1 \prec \lambda^2 \prec \ldots$. In particular, the configuration in Figure 2.6, left, has global weight zero.

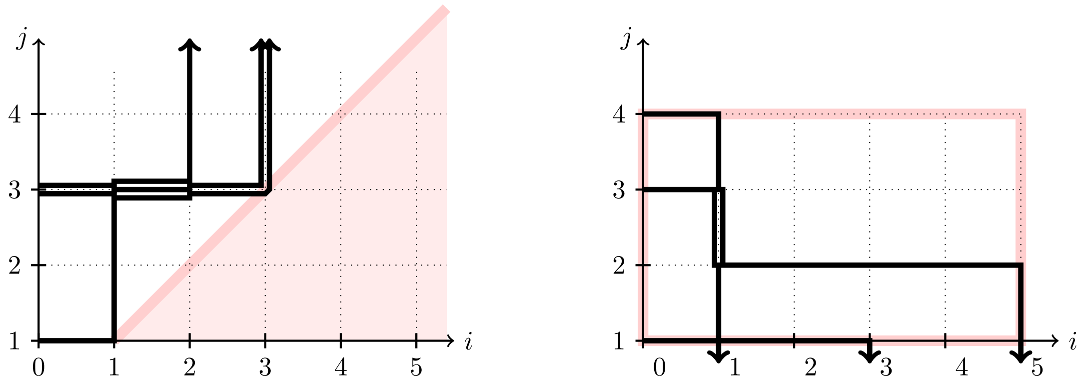

Figure 2.6: Left: Example of an up-right path ensemble. All paths must be above the main diagonal. Right: Example of a down-right path ensemble with $N = 5$ and $M = 4$. All paths must be inside the rectangle.

Remark 2.3.2. When $s = 0$, the bulk and the corner weights (2.13)-(2.14) coincide. More precisely, we have $W^{\lrcorner}_{x,s}(k) = W_{x,s}(0, k; k, 0) = (q; q)_k$.

Definition 2.3.3 (Spin q-Whittaker polynomials)**.** For given interlacing signatures $\mu \prec \lambda$ with $\mu \in \mathrm{Sign}_k$ and $\lambda \in \mathrm{Sign}_{k+1}$, the *skew spin q-Whittaker polynomial* in one variable is the weight of the unique path configuration between μ' and λ' at the k-th slice. It is given by

$$\mathbb{F}_{\lambda/\mu}(x) := x^{|\lambda|-|\mu|} \prod_{i=1}^{k} \frac{(-s/x; q)_{\lambda_i-\mu_i}(-sx; q)_{\mu_i-\lambda_{i+1}}(q; q)_{\lambda_i-\lambda_{i+1}}}{(q; q)_{\lambda_i-\mu_i}(q; q)_{\mu_i-\lambda_{i+i}}(s^2; q)_{\lambda_i-\lambda_{i+i}}}. \tag{2.15}$$

This is clearly a polynomial in x, even though the right corner weight (2.14) is not polynomial. We will often abbreviate the name "spin q-Whittaker" as *sqW*.

For $\mu \in \mathrm{Sign}_k$ and $\nu \in \mathrm{Sign}_{k+n}$, we also define n-variable polynomials in a standard way via *branching*:

$$\mathbb{F}_{\nu/\mu}(x_1, \ldots, x_n) = \sum_{\varkappa} \mathbb{F}_{\varkappa/\mu}(x_1, \ldots, x_{n-1})\, \mathbb{F}_{\nu/\varkappa}(x_n). \tag{2.16}$$

The polynomials $\mathbb{F}_{\nu/\mu}(x_1, \ldots, x_n)$ are partition functions of up-right path ensembles as in Figure 2.6, left, in a domain with the bottom and the top boundary conditions determined by $\mu \in \mathrm{Sign}_k$ and $\nu \in \mathrm{Sign}_{k+n}$, respectively.

We will use the shorthand notation $\mathbb{F}_\lambda(x_1, \ldots, x_n) \equiv \mathbb{F}_{\lambda/\varnothing}(x_1, \ldots, x_n)$, where $\lambda \in \mathrm{Sign}_n$.

Remark 2.3.4. It is important to notice that the number of variables in a sqW polynomial $\mathbb{F}_{\nu/\mu}$ is determined by the signatures ν, μ. If $\nu \in \mathrm{Sign}_{n+k}$ and $\mu \in \mathrm{Sign}_k$, then we can only evaluate $\mathbb{F}_{\nu/\mu}$ at n variables.

2.3.2 Comparison with Borodin–Wheeler's spin q-Whittaker polynomials

It is important to note that our version of the spin q-Whittaker polynomials is *different* from the original definition of Borodin and Wheeler [BW17]. Namely, the one-variable skew polynomials in [BW17] have the form

$$\mathbb{F}^{BW}_{\lambda/\mu}(x) = x^{|\lambda|-|\mu|} \prod_{i\ge 1} \frac{(-s/x;q)_{\lambda_i-\mu_i}(-sx;q)_{\mu_i-\lambda_{i+1}}(q;q)_{\lambda_i-\lambda_{i+1}}}{(q;q)_{\lambda_i-\mu_i}(q;q)_{\mu_i-\lambda_{i+i}}(s^2;q)_{\lambda_i-\lambda_{i+i}}}, \tag{2.17}$$

where $\mu \in \mathrm{Sign}_k$, $\lambda \in \mathrm{Sign}_{k+1}$, and the product over i extends to $i = k+1$ with the agreement that $\lambda_{k+2} = \mu_{k+1} = 0$. That is, our one-variable functions differ from (2.17) as

$$\mathbb{F}^{BW}_{\lambda/\mu}(x) = \frac{(-s/x;q)_{\lambda_{k+1}}}{(s^2;q)_{\lambda_{k+1}}} \mathbb{F}_{\lambda/\mu}(x). \tag{2.18}$$

The n-variable polynomials $\mathbb{F}^{BW}_{\nu/\mu}(x_1,\ldots,x_n)$ are defined from $\mathbb{F}^{BW}_{\lambda/\mu}(x)$ by branching as in (2.16). They admit a lattice path construction similarly to $\mathbb{F}_{\nu/\mu}$, but with the right corner weights $W^{\lrcorner}_{x,s}$ replaced by the bulk weights $W_{x,s}$.

The Borodin–Wheeler's spin q-Whittaker polynomials arise from our $\mathbb{F}_\lambda$ as a particular case:

Proposition 2.3.5. *For all* $\lambda \in \mathrm{Sign}_n$ *we have*

$$\mathbb{F}_\lambda(0,x_2,\ldots,x_n) = \mathbb{F}^{BW}_\lambda(x_2,\ldots,x_n). \tag{2.19}$$

Proof. The up-right paths that start at the left boundary at height 1 must immediately turn up at the right corner at $(1,1)$. If there are j such paths, their contribution to the global weight is $W^{\ulcorner}_{x_1,s}(j)W^{\lrcorner}_{x_1,s}(j) = x_1^j$. For $x_1 = 0$, this forces no paths to start at height 1. Next, due to the presence of $\mathbf{1}_{c_1\ge k_2}$ in the bulk weight $W_{x,s}$, we see that paths started at height $2,\ldots,n$ cannot reach the diagonal with the special right corner weights. Therefore, the partition function for $\mathbb{F}_\lambda(x_1,x_2,\ldots,x_n)$ with $x_1 = 0$ involves only left boundary and bulk weights, and is thus the same as the partition function for $\mathbb{F}^{BW}_\lambda(x_2,\ldots,x_n)$. □

Note that $\mathbb{F}^{BW}_\lambda(x_2,\ldots,x_n)$ is well-defined for any λ, and vanishes if $\ell(\lambda)$, the number of nonzero parts in λ, exceeds $n-1$. If $\ell(\lambda) \le n-1$, then we can treat λ as an element of Sign_n with $\lambda_n = 0$, and then (2.19) holds. Moreover, one readily sees that both sides of (2.19) vanish if $\lambda_n > 0$. Therefore, any polynomial $\mathbb{F}^{BW}_\lambda$ can be obtained from our polynomial $\mathbb{F}_\lambda$ by specializing one of the variables to zero. (By symmetry, see Section 2.3.3 below, we can specialize to zero any variable, and not necessarily the first one.)

2.3.3 Properties of the spin q-Whittaker polynomials

The fact that the Borodin–Wheeler's sqW polynomials are symmetric in their variables follows from the Yang–Baxter equation which we reproduce in (B.12). By looking at (2.18), it is not immediately clear why our version of the sqW polynomials should also be symmetric. We prove this next.

Proposition 2.3.6. *For any $\mu \in \mathrm{Sign}_k$, $\nu \in \mathrm{Sign}_{n+k}$ the polynomial $\mathbb{F}_{\nu/\mu}(x_1, \ldots, x_n)$ is symmetric with respect to permutations of its variables x_i.*

Proof. We use the Yang–Baxter equations (B.12) (B.25) and employ the standard "cross dragging" / commuting transfer matrices argument, cf. [Bor17, Theorem 3.6]. Using branching, it suffices to consider the two-variable case. The two-variable polynomial $\mathbb{F}_{\lambda/\mu}(x, y)$ is a partition function of up-right paths on two consecutive levels, with parameters x, y at the bottom and at the top, respectively, and boundary conditions determined by λ, μ.

First we use the new relation (B.25) that, as shown in Figure B.7 (a), implies that swapping the spectral parameters $x \leftrightarrow y$ at the right corners makes a cross appear at their left. Then we sequentially move the cross to the left while swapping the spectral parameters using the bulk Yang–Baxter equation (B.12), as shown by Figure B.5 (a). We proceed till the left boundary of the domain.

At the left boundary, we can swap the last two spectral parameters by noticing that

$$W^{\vdash}_{x,s}(j) = \frac{(s^2; q)_\infty}{(-sx; q)_\infty} W_{x,s}(\infty, l; \infty, j), \qquad \text{for any } l \in \mathbb{Z}_{\geq 0}. \tag{2.20}$$

This means that the left boundary weights $W^{\vdash}$ also satisfy the Yang–Baxter equation (B.12), and so we can take the cross out of the lattice. This completes the proof. □

Our sqW polynomials also satisfy an index shifting property which is the same as for the classical homogeneous Macdonald polynomials $P_\lambda(\cdot; q, t)$ [Mac95, VI(4.17)]:

Proposition 2.3.7. *For any signature $\lambda \in \mathrm{Sign}_N$ with $\lambda_N > 0$, we have*

$$\mathbb{F}_\lambda(x_1, \ldots, x_N) = x_1 \cdots x_N \, \mathbb{F}_{\lambda - 1^N}(x_1, \ldots, x_N), \qquad \lambda - 1^N = (\lambda_1 - 1, \ldots, \lambda_N - 1).$$

Proof. First, note that (2.15) implies that the one-variable skew polynomials satisfy the shifting property as

$$\mathbb{F}_{\nu/\mu}(x) = x \, \mathbb{F}_{(\nu - 1^{k+1})/(\mu - 1^k)}(x), \tag{2.21}$$

for any $\nu \in \mathrm{Sign}_{k+1}$ and $\mu \in \mathrm{Sign}_k$ with $\nu_{k+1} > 0$ (this also implies $\mu_k > 0$, since $\mu_k \geq \nu_{k+1}$). Next, we use the expansion

$$\mathbb{F}_\lambda(x_1, \ldots, x_N) = \sum_{\lambda^1 \prec \cdots \prec \lambda^{N-1} \prec \lambda} \mathbb{F}_{\lambda^1}(x_1) \, \mathbb{F}_{\lambda^2/\lambda^1}(x_2) \ldots \mathbb{F}_{\lambda^{N-1}/\lambda^{N-2}}(x_{N-1}) \, \mathbb{F}_{\lambda/\lambda^{N-1}}(x_N) \tag{2.22}$$

coming from iterating the branching rule, and apply the shifting property (2.21) to each of the terms to get the desired result. □

Remark 2.3.8. The polynomials $\mathbb{F}^{BW}_\lambda$ *do not* satisfy the index shifting property of Proposition 2.3.7, which can be seen from (2.18).

On the other hand, the polynomials $\mathbb{F}^{BW}_\lambda$ satisfy the stability property

$$\mathbb{F}^{BW}_\lambda(x_1, \ldots, x_{N-1}, -s) = \mathbb{F}^{BW}_\lambda(x_1, \ldots, x_{N-1}),$$

whereas the polynomials $\mathbb{F}_\lambda$ *do not*. More precisely, we have

$$\mathbb{F}_\lambda(x_1,\dots,x_{N-1},-s) = (-s)^{\lambda_N}\mathbb{F}_{\widetilde{\lambda}}(x_1,\dots,x_{N-1}),$$

where $\widetilde{\lambda} = (\lambda_1 \geq \cdots \geq \lambda_{N-1})$ and this is easily proven since the branching coefficient (2.15) evaluates as $\mathbb{F}_{\lambda/\mu}(-s) = (-s)^{\lambda_N}\prod_{i=1}^{N-1}\mathbf{1}_{\lambda_i=\mu_i}$.

In the following proposition we use the coefficient

$$\bar{\mathsf{c}}(\lambda) = \prod_{i=1}^{N-1}\frac{(s^2;q)_{\lambda_i-\lambda_{i+1}}}{(q;q)_{\lambda_i-\lambda_{i+1}}}, \qquad \lambda \in \mathrm{Sign}_N.$$

Proposition 2.3.9. *Let $|sx_i| < 1$ for $i = 1,\dots,N$. Then we have*

$$\sum_{\substack{\lambda\in\mathrm{Sign}_N\\ \lambda_N=0}} \bar{\mathsf{c}}(\lambda)\,(-s)^{|\lambda|}\mathbb{F}_\lambda(x_1,\dots,x_N) = \frac{((-s)^N x_1\dots x_N;q)_\infty (s^2;q)_\infty^{N-1}}{(-sx_1;q)_\infty\dots(-sx_N;q)_\infty}. \tag{2.23}$$

Proof. We will use the q-Gauss identity (A.8) that implies

$$\sum_{k=0}^{n} a^k \frac{(b;q)_k}{(q;q)_k}\frac{(a;q)_{n-k}}{(q;q)_{n-k}} = \frac{(ab;q)_n}{(q;q)_n}, \tag{2.24}$$

Expand the left-hand side of (2.23) as:

$$\begin{aligned}
&\sum_{\substack{\lambda=\lambda^N\in\mathrm{Sign}_N\\ \lambda^N_N=0}}\ \sum_{\lambda^{N-1}\in\mathrm{Sign}_{N-1}} (-sx_N)^{\lambda_1^N-\lambda_1^{N-1}}\frac{(-s/x_N;q)_{\lambda_1^N-\lambda_1^{N-1}}}{(q;q)_{\lambda_1^N-\lambda_1^{N-1}}}\\
&\qquad\times\prod_{k=2}^{N-1}\left((-sx_N)^{\lambda_k^N-\lambda_k^{N-1}}\frac{(-sx_N;q)_{\lambda_{k-1}^{N-1}-\lambda_k^N}}{(q;q)_{\lambda_{k-1}^{N-1}-\lambda_k^N}}\frac{(-s/x_N;q)_{\lambda_k^N-\lambda_k^{N-1}}}{(q;q)_{\lambda_k^N-\lambda_k^{N-1}}}\right)\\
&\qquad\times\frac{(-sx_N;q)_{\lambda_{N-1}^{N-1}}}{(q;q)_{\lambda_{N-1}^{N-1}}}\times(-s)^{|\lambda^{N-1}|}\mathbb{F}_{\lambda^{N-1}}(x_1,\dots,x_{N-1}).
\end{aligned}$$

Summing over λ_1^N by means of the q-binomial theorem gives us the factor $(s^2;q)_\infty/(-sx_N;q)_\infty$. We then sum sequentially over indices $\lambda_2^N,\dots,\lambda_{N-1}^N$ and using (2.24) we are left with

$$\frac{(s^2;q)_\infty}{(-sx_N;q)_\infty}\sum_{\lambda^{N-1}\in\mathrm{Sign}_{N-1}}\frac{(-sx_N;q)_{\lambda_{N-1}^{N-1}}}{(q;q)_{\lambda_{N-1}^{N-1}}}\bar{\mathsf{c}}(\lambda^{N-1})(-s)^{|\lambda^{N-1}|}\mathbb{F}_{\lambda^{N-1}}(x_1,\dots,x_{N-1}),$$

where $\bar{\mathsf{c}}(\lambda^{N-1})$ is the result of applying (2.24). Repeating the same procedure we can reduce the previous expression to

$$\begin{aligned}
&\frac{(s^2;q)_\infty^2}{(-sx_N;q)_\infty(-sx_{N-1};q)_\infty}\\
&\qquad\times\sum_{\lambda^{N-2}\in\mathrm{Sign}_{N-2}}\frac{((-s)^2x_{N-1}x_N;q)_{\lambda_{N-2}^{N-2}}}{(q;q)_{\lambda_{N-2}^{N-2}}}\bar{\mathsf{c}}(\lambda^{N-2})(-s)^{|\lambda^{N-2}|}\mathbb{F}_{\lambda^{N-2}}(x_1,\dots,x_{N-2}).
\end{aligned}$$

Here the reason for the appearance of the product $(-sx_N)(-sx_{N-1})$ in the q-Pochhammer symbol is again (2.24), where we also used that λ_{N-1}^{N-1} is not necessarily zero (in contrast with the first summation over λ_N^N). Continuing inductively, we exhaust all the summations down to the bottom one over λ_1^1, from which we recover the factor $((-sx_1)\cdots(-sx_N);q)_\infty/(-sx_1;q)_\infty$. This completes the proof. □

2.3.4 Skew Cauchy identities for sqW/sHL pair

The Yang-Baxter equations for the weights $w^*_{v,s}, W_{x,s}$ given in (B.26), (B.26) imply the following "dual" skew Cauchy identity for the sHL and sqW functions. We recall that the notation $\mathsf{F}^\bullet$ was introduced in 2.2.4

Theorem 2.3.10. *Fix $M \geq 1$. For $N > 0$, let $\mu \in \mathrm{Sign}_N^{\leq M}$ and $\lambda \in \mathrm{Sign}_{N+1}^{\leq M}$. Then, we have*

$$\sum_{\nu\in\mathrm{Sign}_{N+1}^{\leq M}} \mathbb{F}_{\nu/\mu}(x)\,\mathsf{F}^\bullet_{\nu'/\lambda'}(v) = \frac{1+vx}{1-sv}\sum_{\varkappa\in\mathrm{Sign}_N^{\leq M}} \mathbb{F}_{\lambda/\varkappa}(x)\,\mathsf{F}^\bullet_{\mu'/\varkappa'}(v). \tag{2.25}$$

For $N = 0$, we have

$$\sum_{\nu\in\mathrm{Sign}_1^{\leq M}} \mathbb{F}_{\nu}(x)\,\mathsf{F}^\bullet_{\nu'/\lambda'}(v) = (1+vx)\,\mathbb{F}_{\lambda}(x). \tag{2.26}$$

Note that all the sums in this proposition are over finite sets of signatures, so there are no convergence issues.

Proof of Theorem 2.3.10. The proof of (2.25) is similar to that of Proposition 2.3.6 as it also uses a "cross dragging" argument. The summation in the left-hand side of (2.25) is the partition function of path configurations across two rows of vertices glued together:

- the lower row has weights $W^{\llcorner}_{x,s}, W_{x,s}, W^{\lrcorner}_{x,s}$ and boundary condition μ at the bottom and ν at the top;
- the upper one has weights w^*_{v,s_i} with $s_i = 0$ for $i > N$, and boundary condition ν at the bottom and λ at the top.

Recall that the encoding of arrow configurations by signatures is described in detail in Section 2.1.2.

The Yang–Baxter equation (B.26) implies that the action of swapping weights at the rightmost pair of columns, makes a cross weight appear at their left, as shown in Figure B.5 (b). We then push the cross to the left one vertical step at a time, each time swapping the vertex weights and using the Yang–Baxter equation (B.11) as in Figure B.5 (b). This procedure sequentially turns the left-hand side of (2.25) into the right-hand side.

At the final step, we push the cross out of the lattice at the leftmost site. Using (2.20) and the left boundary weight (2.2)

$$w^*_v(j) = (1-sv)\,w^*_{v,s}(\infty, l; \infty, j), \qquad \text{for } l = 0, 1,$$

we obtain the combined contribution of the cross vertex weights $\mathcal{R}_{x,v,s}$ (defined in Figure B.4 in the Appendix) corresponding to the two cross configurations and . Their sum gives the factor $(1+vx)/(1-sv)$ in the right-hand side of (2.25), as desired.

The second identity (2.26) can be verified by simply using definition of functions. □

Combining the skew Cauchy identities of Theorem 2.3.10, we come to the following corollary for several variables:

Corollary 2.3.11. *For any positive integers N, M, m we have*

$$\sum_{\lambda \in \mathrm{Sign}_M^{\leq N}} \mathbb{F}_\lambda(x_1, \ldots, x_N)\, \mathsf{F}^{\bullet}_{\lambda'}(v_1, \ldots, v_m) = \prod_{j=1}^{m} \left(\frac{1}{1 - s v_j} \right)^{N-1} \prod_{i=1}^{N} \prod_{j=1}^{m} (1 + v_j x_i). \tag{2.27}$$

Proof. We use the branching expansion of functions $\mathbb{F}_\lambda, \mathsf{F}^{\bullet}_{\lambda'}$ and then apply the single-variable skew Cauchy identities (2.25) and (2.26). □

2.3.5 Dual spin q-Whittaker polynomials

Let us also define the dual versions of the sqW weights. These dual weights correspond to down-right lattice paths, and are given by (we use the notation (2.12)–(2.13)):

$$W^{*,\ulcorner}_{y,s}(j) := W^{\ulcorner}_{y,s}(j); \tag{2.28}$$

$$W^{*}_{y,s}(i_1, j_1; i_2, j_2) := \frac{(s^2;q)_{i_1}}{(q;q)_{i_1}} \frac{(q;q)_{i_2}}{(s^2;q)_{i_2}}\, W_{y,s}(i_2, j_1; i_1, j_2). \tag{2.29}$$

$$W^{*,\urcorner}(i_1, j_1; i_2) := \mathbf{1}_{i_2 + j_1 = i_1} \tag{2.30}$$

This choice of vertex weights implies that nonzero global weights are assigned to configurations of down-right paths in the grid $\{0, \ldots, N\} \times \{0, \ldots, k\}$ which are encoded by sequences of interlacing signatures $\lambda^1 \prec \cdots \prec \lambda^k$. (Compare this with the transposed interlacing property for the sHL functions.)

Definition 2.3.12. For given interlacing signatures $\lambda, \mu \in \mathrm{Sign}_N$, the *skew dual spin q-Whittaker polynomial* in one variable $\mathbb{F}^*_{\lambda/\mu}(y)$ is the weight of the unique down-right path configuration between μ' and λ' at a single row of vertices, with the weights (2.29), (2.28) and (2.30). Recall that the encoding of arrow configurations by signatures is described in Section 2.1.2.

An explicit expression for the skew dual sqW polynomial is

$$\mathbb{F}^*_{\lambda/\mu}(y) := y^{|\lambda| - |\mu|} \frac{(-s/y;q)_{\lambda_N - \mu_N}}{(q;q)_{\lambda_N - \mu_N}} \prod_{i=1}^{N-1} \frac{(-s/y;q)_{\lambda_i - \mu_i} (-sy;q)_{\mu_i - \lambda_{i+1}} (q;q)_{\mu_i - \mu_{i+1}}}{(q;q)_{\lambda_i - \mu_i} (q;q)_{\mu_i - \lambda_{i+i}} (s^2;q)_{\mu_i - \mu_{i+i}}}. \tag{2.31}$$

Observe that $\mathbb{F}^*_{\lambda/\mu}(y)$ is a polynomial in y.

Multi-variable extensions $\mathbb{F}^*_{\lambda/\mu}(y_1, \ldots, y_k)$, where $\lambda, \mu \in \mathrm{Sign}_N$ are arbitrary, are defined via branching in the same say as in (2.16). The non-skew functions are $\mathbb{F}^*_\nu \equiv \mathbb{F}^*_{\nu/0^N}$, where $\nu \in \mathrm{Sign}_N$, and $0^N \in \mathrm{Sign}_N$ is the signature with all parts equal to zero.

Remark 2.3.13. Like the dual sHL functions and unlike the usual sqW polynomials (cf. Remark 2.3.4), the dual sqW polynomials $\mathbb{F}^*_{\lambda/\mu}(y_1,\ldots,y_k)$ make sense for any number of variables k, regardless of the signatures λ,μ.

Proposition 2.3.14. *The polynomials $\mathbb{F}^*_{\lambda/\mu}(y_1,\ldots,y_k)$ are symmetric.*

Proof. This follows from the Yang–Baxter equation (B.12) and the sum-to-one property of the R-matrix (B.14). It suffices to consider swapping two variables. We apply the usual "cross-dragging" argument to exchange spectral parameters of two consecutive rows of vertices. Similarly to the proof of Proposition 2.3.6, identity (B.12) suffices to swap spectral parameters from the leftmost column up until the rightmost one. Since the right boundary weights $W^{*,\dashv}$ differ from the bulk weights W^*, we have to prove that we can drag the cross one more step to the right. We have using the definition of $W^{*,\dashv}$ that the partition function near the right wall with the cross vertex is equal to

$$\sum_{k_1,k_2,k_3} R_{x,y}(i_1,i_2;k_1,k_2)W^{*,\dashv}(k_3,k_2;j_3)W^{*,\dashv}(i_3,k_1;k_3) = \sum_{k} R_{x,y}(i_1,i_2;i_1{+}i_2{-}j_3{-}k,k{-}j_3).$$

(We used the arrow preservation property $i_1+i_2+j_3=i_3$.) The right-hand side is equal to one. Indeed, this sum-to-one property readily follows from identity (2.24). On the other hand, without the cross vertex, the partition function near the right wall is equal to $\sum_k W^{*,\dashv}(i_3,i_2;k)W^{*,\dashv}(k,i_1;j_3)$. This is also equal to 1, because only the summand with $k=i_1+j_3$ is nonzero. This completes the proof. □

2.3.6 Skew Cauchy identities for sqW/sqW pair

The spin q-Whittaker polynomials also satisfy the following skew Cauchy identity which follows from the Yang-Baxter equations (B.12), (B.27):

Theorem 2.3.15. *For $N>0$, let $\mu\in\mathrm{Sign}_N$ and $\lambda\in\mathrm{Sign}_{N+1}$. Then, for $|xy|<1$, we have*

$$\sum_{\nu\in\mathrm{Sign}_{N+1}} \mathbb{F}_{\nu/\mu}(x)\,\mathbb{F}^*_{\nu/\lambda}(y) = \frac{(-sx;q)_\infty(-sy;q)_\infty}{(s^2;q)_\infty(xy;q)_\infty} \sum_{\varkappa\in\mathrm{Sign}_N} \mathbb{F}_{\lambda/\varkappa}(x)\,\mathbb{F}^*_{\mu/\varkappa}(y). \tag{2.32}$$

For $N=0$, we have

$$\sum_{\nu\in\mathrm{Sign}_{N+1}} \mathbb{F}_{\nu}(x)\,\mathbb{F}^*_{\nu/\lambda}(y) = \frac{(-sx;q)_\infty}{(xy;q)_\infty}\,\mathbb{F}_{\lambda}(x). \tag{2.33}$$

Proof. For $N>0$ this is proven using the same method explained in Theorem 2.3.10 with the help of identity (B.10) (with $q^J\to -x/s$, $q^I\to -y/s$) when extracting the cross vertex weight from the rightmost column. For $N=0$ the statement is simply the q-binomial theorem. □

Corollary 2.3.16. *Let $|x_iy_j|<1$ for all $i=1,\ldots,N$, $j=1,\ldots,k$. Then, we have*

$$\sum_{\lambda\in\mathrm{Sign}_N} \mathbb{F}_{\lambda}(x_1,\ldots,x_N)\,\mathbb{F}^*_{\lambda}(y_1,\ldots,y_k) = \prod_{j=1}^{k}\left(\frac{(-sy_j;q)_\infty}{(s^2;q)_\infty}\right)^{N-1} \prod_{i=1}^{N}\prod_{j=1}^{k} \frac{(-sx_i;q)_\infty}{(x_iy_j;q)_\infty}. \tag{2.34}$$

2.3.7 Pieri rules

Pieri type rules for the Borodin–Wheeler spin q-Whittaker polynomials $\mathbb{F}_\lambda^{BW}$ are given in [BW17]. These are analogs of the classical Pieri type rules for Macdonald polynomials. The Pieri type rules follow from skew Cauchy identities, and here we present these rules for our version of the spin q-Whittaker polynomials.

Proposition 2.3.17. *Let $|x_i y| < 1$ for all $i = 1, \ldots, N$. Then we have*

$$\sum_{\lambda \in \mathrm{Sign}_N} \mathbb{F}_\lambda(x_1, \ldots x_N)\, \mathbb{F}^*_{\lambda/\mu}(y) = \left(\sum_{i \geq 0} y^i \frac{(-s/y; q)_i}{(q; q)_i} \mathbb{F}_{(i)}(x_1, \ldots, x_N) \right) \mathbb{F}_\mu(x_1, \ldots, x_N).$$

Proof. By the skew Cauchy identities of Theorem 2.3.15, we can write

$$\sum_{\lambda \in \mathrm{Sign}_N} \mathbb{F}_\lambda(x_1, \ldots x_N)\, \mathbb{F}^*_{\lambda/\mu}(y) = \left(\frac{(-sy; q)_\infty}{(s^2; q)_\infty} \right)^{N-1} \prod_{i=1}^{N} \frac{(-sx_i; q)_\infty}{(x_i y; q)_\infty} \mathbb{F}_\mu(x_1, \ldots, x_N), \quad (2.35)$$

and the claim follows by expanding $\left(\frac{(-sy;q)_\infty}{(s^2;q)_\infty}\right)^{N-1} \prod_{i=1}^N \frac{(-sx_i;q)_\infty}{(x_i y;q)_\infty}$ using (2.34). □

Proposition 2.3.18. *We have*

$$\sum_{\lambda} \mathbb{F}_\lambda(x_1, \ldots x_N)\, \mathsf{F}^\bullet_{\lambda'/\mu'}(v) = \left(\sum_{i=0}^{N} \mathsf{F}^\bullet_{(i)}(v)\, \mathbb{F}_{1^i}(x_1, \ldots x_N) \right) \mathbb{F}_\mu(x_1, \ldots, x_N)$$

Proof. By the skew Cauchy identities of Theorem 2.3.10, we have

$$\sum_{\lambda \in \mathrm{Sign}_N} \mathbb{F}_\lambda(x_1, \ldots x_N)\, \mathsf{F}^\bullet_{\lambda/\mu}(v) = \left(\frac{1}{1 - sv} \right)^{N-1} \prod_{i=i}^{N} (1 + x_i v)\, \mathbb{F}_\mu(x_1, \ldots, x_N), \quad (2.36)$$

and the claim follows by expanding $\left(\frac{1}{1-sv}\right)^{N-1} \prod_{i=i}^N (1 + x_i v)$ using (2.27). □

Pieri type rules of Propositions 2.3.17 and 2.3.18 are eigenrelations on the spin q-Whittaker polynomials in the *label* variable. Indeed, define operators $\mathfrak{H}^{\mathrm{sqW}}, \mathfrak{H}^{\mathrm{sHL}}$ as

$$(\mathfrak{H}^{\mathrm{sqW}} f)(\mu) = \sum_\lambda f(\lambda)\, \mathbb{F}^*_{\lambda/\mu}(y), \qquad (\mathfrak{H}^{\mathrm{sHL}} f)(\mu) = \sum_\lambda f(\lambda)\, \mathsf{F}^\bullet_{\lambda'/\mu'}(v). \quad (2.37)$$

Then these operators act diagonally on spin q-Whittaker functions $f(\lambda) = \mathbb{F}_\lambda(x_1, \ldots, x_N)$, with respective eigenvalues

$$\sum_{i \geq 0} y^i \frac{(-s/y; q)_i}{(q; q)_i} \mathbb{F}_{(i)}(x_1, \ldots, x_N) \quad \text{and} \quad \sum_{i=0}^{N} \mathsf{F}^\bullet_{(i)}(v)\, \mathbb{F}_{1^i}(x_1, \ldots x_N).$$

2.4 Analytic continuation

2.4.1 A common generalization of skew Cauchy identities

The skew Cauchy identities given in the previous sections admit a (partial) common generalization which can be viewed as an analytic continuation. In [Bor17], [BP18a], *principal specializations* of non-stable spin Hall-Littlewood functions were considered. They are obtained by setting spectral parameters to finite geometric progressions of ratio q. In our context, define

$$\mathfrak{F}^{(J_1,\dots J_n)}_{\lambda/\mu}(u_1,\dots,u_n) = \mathsf{F}_{\lambda/\mu}(u_1, qu_1,\dots,q^{J_1-1}u_1,\dots,u_n,qu_n,\dots,q^{J_n-1}u_n;\mathbf{s}) \tag{2.38}$$

$$\mathfrak{G}^{(I_1,\dots I_m)}_{\lambda/\mu}(v_1,\dots,v_m) = \mathsf{F}^*_{\lambda/\mu}(v_1, qv_1,\dots,q^{I_1-1}v_1,\dots,v_m,qv_m,\dots,q^{I_m-1}v_m;\mathbf{s}). \tag{2.39}$$

It is a consequence of the fusion procedure (dating back to [KRS81] and briefly recalled in Appendix B.1.2), that we can view $\mathfrak{F}^{(J_1,\dots J_n)}_{\lambda/\mu}(u_1,\dots,u_n)$ as a partition function in a "smaller" vertex model obtained by attaching together n (instead of $J_1+\ldots+J_n$) rows with fused weights $w^{(J_k)}_{u_k,s}$, (B.3) where $k=1,\dots,n$. Analogously $\mathfrak{G}^{(I_1,\dots I_m)}_{\lambda/\mu}(v_1,\dots,v_m)$ are partition functions of a vertex model with fused weights $w^{*,(I_k)}_{v_k,s}$ (B.6). As usual, at the leftmost column of these lattices we place infinitely many vertical paths.

As a result of the vertex model constructions and of the fact that the weights $w^{(J)}$, $w^{*,(I)}$ degenerate both to w, w^* and W, W^* (see Appendix B.1.3), we see that (2.38), (2.39) interpolate between the spin Hall-Littlewood functions and the Borodin-Wheeler's spin q-Whittaker functions. These functions (2.38)–(2.39) satisfy the following general skew Cauchy identity which we state for an appropriate "analytic" range of parameters:

Theorem 2.4.1. *Fix $m,n\in\mathbb{Z}_{\geq 0}$. Take $q\in(0,1)$, and let $s_i\neq 0, u_i, q^{J_i}, v_j, q^{I_j}$ be complex parameters satisfying*

$$|s_j|, |u_k|, |v_l|, |q^{J_k}u_k|, |q^{I_l}v_l|, \left|\frac{q^iu_k-s_j}{1-q^is_ju_k}\right|, \left|\frac{q^iv_l-s_j}{1-q^isv_l}\right| < \delta \qquad \text{for all } k,l,i,j, \tag{2.40}$$

for sufficiently small $\delta>0$ which might depend on m,n, but not on the other parameters of the functions.[1] *Then we have*

$$\sum_\nu \mathfrak{F}^{(J_1,\dots J_n)}_{\nu/\mu}(u_1,\dots,u_n)\mathfrak{G}^{(I_1,\dots I_m)}_{\nu/\lambda}(v_1,\dots,v_m)$$
$$= \prod_{k=1}^n\prod_{l=1}^m \frac{(u_kv_lq^{I_l};q)_\infty(u_kv_lq^{J_k};q)_\infty}{(u_kv_l;q)_\infty(u_kv_lq^{I_l+J_k};q)_\infty}\sum_\varkappa \mathfrak{F}^{(J_1,\dots,J_n)}_{\lambda/\varkappa}(u_1,\dots,u_n)\mathfrak{G}^{(I_1,\dots,I_m)}_{\mu/\varkappa}(v_1,\dots,v_m). \tag{2.41}$$

Remark 2.4.2. This identity immediately degenerates to the skew Cauchy identities for spin Hall-Littlewood and Borodin-Wheeler's spin q-Whittaker polynomials after appropriately specializing the parameters u_k, v_l and q^{J_k}, q^{I_l}.

[1]Here and below in this section we treat q^{J_k} and q^{I_l} as separate symbols independent of q. At the same time, for J_k a positive integer, q^{J_k} means the corresponding power of q, and same for q^{I_l}.

Remark 2.4.3. It is not true that the principal specializations of the spin Hall-Littlewood functions degenerate to our version of the spin q-Whittaker polynomials and this is because it does not seem possible to construct the corner weights $W^{\lrcorner}$ via fusion. Nevertheless, since most of our arguments and construction work the same for both cases, in order to keep the notation compact, we will sometime refer to the sqW polynomials as a specialization of the functions $\mathfrak{F}_{\lambda/\mu}^{(J_1,\dots,J_n)}$.

The proof of Theorem 2.4.1 requires an absolute convergence result for spin Hall-Littlewood functions with principal specializations:

Proposition 2.4.4. *Fix $n \in \mathbb{Z}_{\geq 1}$. Let $q \in (0,1)$. Take $s \neq 0, u_i, q^{J_i}$ to be complex parameters satisfying*

$$|s_j|, |u_k|, |q^{J_k} u_k|, \left| \frac{q^i u_k - s_j}{1 - q^i s_j u_k} \right| < \delta \qquad \textit{for all } k, i, \tag{2.42}$$

for some $\delta = \delta_n > 0$ (which might depend on n). Then for all Young diagrams μ we have

$$\sum_{\lambda:\ \mu \subseteq \lambda} \left| \mathfrak{F}_{\lambda/\mu}^{(J_1,\dots J_n)}(u_1,\dots,u_n) \right| < \infty. \tag{2.43}$$

The proof of Proposition 2.4.4 will be given later in Section 2.4.2. First we use its result to justify the general Cauchy identity (2.41):

Proof of Theorem 2.4.1 modulo Proposition 2.4.4. By Theorem 2.2.5, identity (2.41) holds in case $J_1,\dots,J_n$, $I_1,\dots,I_m$ are positive integers. Functions $\mathfrak{F}_{\lambda/\mu}^{(J_1,\dots,J_n)}, \mathfrak{G}_{\lambda/\mu}^{(I_1,\dots,I_m)}$ are finite sums of finite products of weights $w_{u_k,s}^{(J_k)}, w_{v_l,s}^{*,(I_l)}$ which are rational functions of q^{J_k}, q^{I_l}. Therefore, $\mathfrak{F}_{\lambda/\mu}^{(J_1,\dots,J_n)}, \mathfrak{G}_{\lambda/\mu}^{(I_1,\dots,I_m)}$ admit an extension to generic complex numbers q^{J_k}, q^{I_l}. This implies that the right-hand side of (2.41) extends to q^{J_k}, q^{I_l} in a complex region, too, since the sum over $\varkappa$ is finite (it ranges over $\varkappa \subseteq \mu, \lambda$).

The summation in the left-hand side of (2.41) has infinitely many terms as the only condition on ν is that $\mu, \lambda \subseteq \nu$. Therefore, to show that it can be extended to parameters q^{J_k}, q^{I_l} in a complex region we need a result of absolute convergence of the sum over ν. Under assumptions (2.40), this is a consequence of Proposition 2.4.4. Therefore, the left-hand side of (2.41) can be extended, too.

The equality between the two sides of (2.41) in a wider region (2.40) follows because these expressions agree for infinitely many values of J_k, I_l, namely, positive integers: if $|u_k| < \delta$, then $|u_k q^{J_k}| < \delta$ for all $J_k \in \mathbb{Z}_{\geq 1}$. This completes the proof. □

Despite the fact that the general skew Cauchy identity (Theorem 2.4.1) offers a unified description of all skew Cauchy structures we study, throughout the text we still consider possible degenerations separately. There are several reasons for this. First, the spin Hall-Littlewood and the spin q-Whittaker functions are more basic from an algebraic standpoint (see, e.g., Section 2.6 where we describe difference operators diagonalized by these functions). Second, when u, q^J, v, q^I are general parameters, it is difficult to give a probabilistic interpretation of the random fields — the positivity of the measure obtained by multiplying $\mathfrak{F}$ and $\mathfrak{G}$ is in general not guaranteed.

2.4.2 Absolute summability

We now turn to the proof of the absolute summability result of Proposition 2.4.4. This proof requires explicit expressions for the fused weights which can be found in Chapter B. We begin with a number of preliminary estimates, and assume that $q \in (0,1)$ throughout the subsection.

Lemma 2.4.5. *Consider the fused weights $w_{u,s}^{(J)}(i_1, j_1; i_2, j_2)$ defined in (B.3), with $\gamma = q^J \in \mathbb{C}$ and $i_1, j_1, i_2, j_2 \in \mathbb{Z}_{\geq 0}$. Let $s \neq 0$ and $\delta = \max\{|s|, |u|, |\gamma u|\} < 1$. Then*

$$\left|w_{u,s}^{(J)}(i_1, j_1; i_2, j_2)\right| \leq (\min\{i_1, j_2\} + 1)\, C\delta^{j_2}, \tag{2.44}$$

where C is a positive constant independent of the vertex configuration $(i_1, j_1; i_2, j_2)$.

Proof. Expand $w^{(J)}$ combining (B.3) and (A.9) as

$$\begin{aligned} &\frac{(-1)^{i_1+j_2} q^{\frac{1}{2}i_1(i_1-1+2j_1)} s^{j_2-i_1} u^{i_1} (u/s;q)_{j_1-i_2} (q;q)_{j_1}}{(q;q)_{i_1}(q;q)_{j_2}(su;q)_{j_1+i_1}} \\ &\quad \times \sum_{k=0}^{i_1} \frac{q^k}{(q;q)_k} (q^{-i_1};q)_k (q^{-i_2};q)_k (su\gamma;q)_k (qs/u;q)_k \\ &\qquad\qquad \times (q^k s^2;q)_{i_1-k} (q^{1+j_2-i_1+k};q)_{i_1-k} (\gamma q^{1-i_2-j_2+k};q)_{i_1-k}. \end{aligned} \tag{2.45}$$

First, the factor

$$\frac{(-1)^{i_1+j_2}(q;q)_{j_1}(su\gamma;q)_k(q^k s^2;q)_{i_1-k}}{(q;q)_{i_1}(q;q)_{j_2}(su;q)_{j_1+i_1}(q;q)_k}$$

is bounded in absolute value by a constant independent of i_1, j_1, i_2, j_2. The q-Pochhammer symbol $(q^{1+j_2-i_1+k};q)_{i_1-k}$ vanishes unless $k \geq i_1 - j_2$ and its contribution is bounded in absolute value by 1. The remaining factors are

$$q^{\frac{1}{2}i_1(i_1-1+2j_1)} s^{j_2-i_1} u^{i_1} (u/s;q)_{j_1-i_2} q^k (q^{-i_1};q)_k (q^{-i_2};q)_k (qs/u;q)_k (\gamma q^{1-i_2-j_2+k};q)_{i_1-k}.$$

Rewrite

$$q^{i_1 j_1}(q^{-i_2};q)_k(\gamma q^{1-i_2-j_2+k};q)_{i_1-k} = \prod_{l=0}^{k-1}(q^{j_1} - q^{-i_1+j_2+l}) \prod_{l=0}^{i_1-k-1}(q^{j_1} - \gamma q^{-l}), \tag{2.46}$$

where we used the arrow conservation property, and

$$q^{i_1(i_1-1)/2+k}(q^{-i_1};q)_k \prod_{l=0}^{i_1-k-1}(q^{j_1} - \gamma q^{-l}) = (-1)^{i_1}\gamma^{i_1-k}(q^{i_1-k+1};q)_k (q^{j_1}/\gamma;q)_{i_1-k}. \tag{2.47}$$

The factors $(-1)^{i_1}(q^{i_1-k+1};q)_k$ are bounded in the absolute value. By substituting (2.46), (2.47) into (2.45), we see that it remains to address the term

$$s^{j_2-i_1}u^{i_1}(u/s;q)_{j_2-i_1}(qs/u;q)_k\gamma^{i_1-k}(q^{j_1}/\gamma;q)_{i_1-k}\prod_{l=0}^{k-1}(q^{j_1} - q^{j_2-i_1+l}). \tag{2.48}$$

We consider two cases based on the sign of $j_2 - i_1$.

Case $j_2 \geq i_1$**.** The factor $\prod_{l=0}^{k-1}(q^{j_1} - q^{j_2-i_1+l})$ in (2.48) is bounded by a constant independent of the vertex configuration. The remaining terms are

$$s^{j_2-i_1}(u/s;q)_{j_2-i_1} \cdot u^{i_1}(qs/u;q)_k \cdot \gamma^{i_1-k}(q^{j_1}/\gamma;q)_{i_1-k}.$$

Distributing the factors s, u, and γ into the q-Pochhammer symbols, we can bound the above expression by const $\cdot\, \delta^{j_2}$, where j_2 is the total number of terms in the product. Note that the estimate works uniformly for small s, u, γ, too.

Case $i_1 > j_2$**.** Rewriting the q-Pochhammer symbol with the negative index (cf. (A.1)) and using the fact that $i_1 - j_2 \leq k \leq i_1$, we have

$$(2.48) = (-1)^{i_1-j_2}u^{j_2}(q^{i_1-j_2+1}s/u;q)_{k-i_1+j_2}\gamma^{i_1-k}(q^{j_1}/\gamma;q)_{i_1-k}\, q^{\binom{i_1-j_2+1}{2}}\prod_{l=0}^{k-1}(q^{j_1} - q^{j_2-i_1+l}).$$

The term $(-1)^{i_1-j_2}q^{\binom{i_1-j_2+1}{2}}\prod_{l=0}^{k-1}(q^{j_1} - q^{j_2-i_1+l})$ is bounded. The contribution of the term

$$u^{j_2}(q^{i_1-j_2+1}s/u;q)_{k-i_1+j_2}\gamma^{i_1-k}(q^{j_1}/\gamma;q)_{i_1-k}$$

is bounded by const $\cdot\, \delta^{j_2}$ similarly to the previous case.

We see that (2.45) can be written as a sum of terms bounded by const $\cdot\, \delta^{j_2}$. Because the number of terms is

$$\leq \min\{i_1, i_2\} + 1 - \max\{0, i_1 - j_2\} \leq \min\{i_1, j_2\} + 1,$$

we get the desired bound. □

Lemma 2.4.6. *Let*

$$\sup_{n\in\mathbb{Z}_{\geq 0}}\left|\frac{q^n u - s}{1 - q^n su}\right| < \delta < 1. \tag{2.49}$$

Then

$$|w_{u,s}^{(J)}(0, j_1; i_2, j_2)| \leq C(i_2)\, \delta^{j_2}, \tag{2.50}$$

where $C(0) = 1$ *and* $C = \sup_k\{C(k)\} < \infty$*.*

Proof. This bound follows from (B.3): after setting $i_1 = 0$, the q-hypergeometric series disappears, and we use the definition of δ to estimate the prefactor. □

For a Young diagram λ, let $m_i(\lambda)$ be the number of parts in λ which are equal to i.

Lemma 2.4.7. *Let* $s_j \neq 0, u, q^J$ *be complex parameters such that*

$$|s_j|, |u|, |q^J u|, \left|\frac{q^i u - s_j}{1 - q^i s_j u}\right| < \delta, \qquad \text{for all } i, j, \tag{2.51}$$

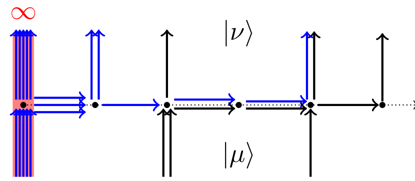

Figure 2.7: The decomposition of the Young diagram ν as a free superposition of η (black paths) and $\varkappa$ (blue paths) used in the proof of Lemma 2.4.8.

for some $\delta \in (0,1)$. Then there exists $C \geq 1$ such that for any two Young diagrams μ, λ we have

$$\left|\mathfrak{F}^{(J)}_{\lambda/\mu}(u)\right| \leq C^{M(\lambda,\mu)} \prod_{i\geq 1}(m_i(\mu)+1)\delta^{|\lambda|-|\mu|}, \tag{2.52}$$

where

$$M(\lambda,\mu) = 1 + \#\{i \colon m_i(\mu) \neq 0 \text{ or } m_i(\lambda) \neq 0\}. \tag{2.53}$$

Proof. It suffices to assume that $\mu \subseteq \lambda$ (i.e., $\mu_i \leq \lambda_i$ for all i), otherwise the skew function vanishes. We have

$$\mathfrak{F}^{(J)}_{\lambda/\mu}(u) = \sum_{j_0, j_1, \dots \geq 0} w^{(J)}_{u,s}\left(\begin{matrix} \infty \\ \cdot\!\equiv\; j_0 \\ \infty \end{matrix} \right) \prod_{l \geq 1} w^{(J)}_{u,s_l}(m_l(\mu), j_{l-1}; m_l(\lambda), j_l), \tag{2.54}$$

where the infinite sum has only one nonzero term due to arrow preservation. From (B.5) we have for the leftmost vertex

$$\left| w^{(J)}_{u,s}\left(\begin{matrix} \infty \\ \cdot\!\equiv\; j \\ \infty \end{matrix} \right) \right| \leq C\delta^{j}. \tag{2.55}$$

Lemmas 2.4.5 and 2.4.6 provide estimates for the remaining vertex weights: they are all bounded by $C\delta^{j_l}$, except if both $m_l(\mu) = m_l(\lambda) = 0$ when the bound is given by δ^{j_l}. □

Lemma 2.4.8. *Let $0 < \delta < 1$, $C \geq 1$, $1 \leq A < \delta^{-1}$, and $M(\lambda,\mu)$ be as in Lemma 2.4.7. Then for any Young diagram μ we have*

$$\sum_{\nu \colon \mu \subseteq \nu} C^{M(\nu,\mu)} \delta^{|\nu|-|\mu|} A^{\ell(\nu)} \prod_{i \geq 1}(m_i(\nu)+1) \leq C_1 A_1^{\ell(\mu)}, \tag{2.56}$$

where $C_1, A_1 \geq 1$ are constants.

Proof. The sum over ν can be visualized as a sum over path configurations in a row of vertices as in Figure 2.7. We distinguish the paths coming from the configuration μ (black dashed in Figure 2.7) and when they originate at the leftmost vertex (blue solid in Figure 2.7). Calling $\varkappa$ the Young diagram generated by the blue paths and η the Young diagram generated by the black paths we can write $\nu = \varkappa \cup \eta$ (this decomposition is not unique). The sum in the left-hand side of (2.56) is dominated by a sum where $\varkappa$ and η vary independently, and therefore we have

$$\begin{aligned}\text{lhs}\,(2.56) \le &\Bigg(\sum_{\varkappa} C^{M(\varkappa,\varnothing)}\delta^{|\varkappa|}A^{\ell(\varkappa)}\prod_{i\ge 1}(m_i(\varkappa)+1)\Bigg)\\ &\qquad\times\Bigg(\sum_{\substack{\eta:\ \mu\subseteq\eta\\ \ell(\eta)=\ell(\mu)}} C^{M(\eta,\mu)}\delta^{|\eta|-|\mu|}A^{\ell(\mu)}\prod_{i\ge 1}(m_i(\eta)+1)\Bigg).\end{aligned} \tag{2.57}$$

We estimate separately the two factors in (2.57), starting with the first one. Since $\ell(\varkappa) = \sum_i m_i(\varkappa)$ and $|\varkappa| = \sum_{i\ge 1} i\, m_i(\varkappa)$, the summation over $\varkappa$ can be rewritten as follows. Separate the term $\varkappa = \varnothing$. In the remaining sum, first select $\varkappa_1 \ge 1$ and its multiplicity $r \ge 1$; then for each $i = 1, \ldots, \varkappa_1 - 1$, select a multiplicity $m_i \ge 0$. Summing over all these possibilities, we have

$$C + \sum_{\varkappa_1\ge 1} C \sum_{r\ge 1} \delta^{r\varkappa_1} C(r+1)A^r \prod_{i=1}^{\varkappa_1-1}\Bigg(\sum_{m_i\ge 0} C^{\mathbf{1}_{m_i>0}}(m_i+1)\delta^{i m_i}A^{m_i}\Bigg).$$

Simplifying the geometric summations and using the fact that $A\delta < 1$, we can reduce the above sum to

$$C + C\sum_{\varkappa_1\ge 1}\frac{AC\delta^{\varkappa_1}(2-A\delta^{\varkappa_1})}{(1-A\delta^{\varkappa_1})^2}\prod_{i=1}^{\varkappa_1-1}\left(1 - C\left(1-\frac{1}{(1-A\delta^i)^2}\right)\right)$$

For all $i \ge i_0$, where i_0 depends on C, A, δ the i-th term in the product is less than δ^{-1} (because $\delta < 1$ and the term goes to 1 as $i \to \infty$). This implies that the above sum is convergent and thus is estimated from above by a constant.

We now address the second factor in the right-hand side of (2.57). We can again bound the sum over η by a superposition of $\ell(\mu)$ noninteracting paths starting at μ_i. This implies that the sum over η in (2.57) is dominated by

$$\prod_{i=1}^{\ell(\mu)}\sum_{k_i\ge\mu_i} C^{M(k_i,\mu_i)}2A\delta^{k_i-\mu_i} = \left[2C^2A\left(1 + C\frac{\delta}{1-\delta}\right)\right]^{\ell(\mu)}.$$

This completes the proof. □

Proof of Proposition 2.4.4. We first expand $\mathfrak{F}^{(J_1,\ldots J_n)}_{\lambda/\mu}(u_1,\ldots,u_n)$ in (2.43). Utilizing the branching rule and the triangle inequality, we can estimate

$$\text{lhs}\,(2.43) \le \sum_{\substack{\lambda^1,\ldots\lambda^n:\\ \mu\subseteq\lambda^1\subseteq\cdots\subseteq\lambda^n}}\prod_{i=1}^{n}\left|\mathfrak{F}^{(J_i)}_{\lambda^i/\lambda^{i-1}}(u_i)\right|. \tag{2.58}$$

In order to evaluate the previous nested summation we start from the most external term. For fixed λ^{n-1} we have

$$\sum_{\lambda^n:\ \lambda^{n-1}\subseteq\lambda^n}\left|\mathfrak{F}^{(J_n)}_{\lambda^n/\lambda^{n-1}}(u_n)\right| \le \prod_{i\ge 1}(m_i(\lambda^{n-1})+1)\sum_{\lambda^n:\ \lambda^{n-1}\subseteq\lambda^n} C^{M(\lambda^n,\lambda^{n-1})}\delta_1^{|\lambda^n|-|\lambda^{n-1}|},$$

where we used bound of Lemma 2.4.7 for some $\delta_1 \in (0,1)$. We can further estimate the sum over λ^n with the help of Lemma 2.4.8, and obtain the bound $\prod_{i\geq 1}(m_i(\lambda^{n-1})+1)C_1 A_1^{\ell(\lambda^{n-1})}$. Replacing δ_1 by a smaller value $0 < \delta_2 < A_1^{-1}$ if needed and multiplying this bound by the next term $\mathfrak{F}^{(J_{n-1})}_{\lambda^{n-1}/\lambda^{n-2}}(u_{n-1})$ in (2.58), we can apply Lemma 2.4.7 and then sum over λ^{n-1} with the help of Lemma 2.4.8. Iterating this procedure finitely many times, we get the desired statement with a sufficiently small $\delta_n > 0$. □

2.5 Scaled geometric specializations

In this section we introduce a third specialization — the scaled geometric one — of the general fused functions from the previous section. This specialization allows to include into our analysis stochastic particle systems with more general initial configurations.

2.5.1 Definition of scaled geometric specializations

We now introduce yet another specialization of (2.38), (2.39) which admits a meaningful probabilistic interpretation — it corresponds to two-sided stationary initial conditions for stochastic particle systems on the line arising as marginals of our Yang-Baxter fields.

Definition 2.5.1 ([BP18a])**.** The *scaled geometric* specialization with parameter α of the spin Hall-Littlewood function is given by

$$\mathsf{F}_{\lambda/\mu}(\breve{\alpha};\mathbf{s}) := \lim_{\epsilon\to 0} \mathsf{F}_{\lambda/\mu}(-\alpha\epsilon, -\alpha\epsilon q, \dots, -\alpha\epsilon q^{J-1}; \mathbf{s})\Big|_{q^J=1/\epsilon}. \tag{2.59}$$

The dual analog of $\mathsf{F}(\breve{\alpha};\mathbf{s})$ is given by the conjugation $\mathsf{F}^*_{\lambda/\mu}(\breve{\alpha};\mathbf{s}) = \frac{\mathsf{c}(\lambda)}{\mathsf{c}(\mu)}\mathsf{F}_{\lambda/\mu}(\breve{\alpha};\mathbf{s})$ as in (2.10). The skew functions in multiple variables $\mathsf{F}_{\lambda/\mu}(\breve{\alpha}_1,\dots,\breve{\alpha}_N;\mathbf{s})$ are defined in a standard way using the branching rules as in (2.4), and similarly for dual functions.

The functions $\mathsf{F}_{\lambda/\mu}(\breve{\alpha};\mathbf{s}), \mathsf{F}^*_{\lambda/\mu}(\breve{\beta};\mathbf{s})$ also admit a lattice construction with the vertex weights

$$\breve{w}_{\alpha,s} := \lim_{\epsilon\to 0} w^{(J)}_{-\alpha\epsilon,s}\Big|_{q^J=1/\epsilon}, \qquad \breve{w}^*_{\beta,s} := \lim_{\epsilon\to 0} w^{*,(I)}_{-\beta\epsilon,s}\Big|_{q^I=1/\epsilon}.$$

The expressions for these weights are given in Section B.1.4. The functions $\mathsf{F}_{\lambda/\mu}(\breve{\alpha};\mathbf{s}), \mathsf{F}^*_{\lambda/\mu}(\breve{\beta};\mathbf{s})$ vanish unless $\mu \subseteq \lambda$ (which means that $\mu_i \leq \lambda_i$ for all i).

By adding the scaled geometric specialization to our symmetric functions, we can define *mixed specializations* $\mathsf{F}_{\lambda/\mu}(u_1,\dots,u_n,\breve{\alpha}_1,\dots,\breve{\alpha}_N)$. They are obtained through the branching rules as

$$\mathsf{F}_{\lambda/\mu}(u_1,\dots,u_n,\breve{\alpha}_1,\dots,\breve{\alpha}_N;\mathbf{s}) = \sum_{\varkappa} \mathsf{F}_{\lambda/\varkappa}(\breve{\alpha}_1,\dots,\breve{\alpha}_N;\mathbf{s})\,\mathsf{F}_{\varkappa/\mu}(u_1,\dots,u_n;\mathbf{s}),$$

and similarly for the dual functions. By the Yang-Baxter equations (Section B.1.4), these functions are symmetric in all the $N+n$ variables. We will also sometimes use the notation sHL(u) and sg(α) to denote the two types of specializations of the general symmetric functions (2.38), (2.39). Similarly we will at times say that $w_{u,s}$ and $\breve{\alpha}_{\alpha,s}$ are respectively the sHL(u) and sg(α) specializations of the weight $w^{(J)}_{u,s}$.

Since the dual spin q-Whittaker functions can be obtained from F^* from fusion (unlike the non-dual $\mathbb{F}$), we can define their version with mixed specializations as

$$\mathbb{F}^*_{\lambda/\mu}(y_1,\dots,y_n,\breve{\alpha}_1,\dots,\breve{\alpha}_N)=\sum_{\varkappa}\mathsf{F}^{\bullet}_{\lambda/\varkappa}(\breve{\alpha}_1,\dots,\breve{\alpha}_N)\,\mathbb{F}_{\varkappa/\mu}(y_1,\dots,y_n), \tag{2.60}$$

where $\lambda\in\mathrm{Sign}_k$ and by agreement $\mathsf{F}^{\bullet}_{\lambda/\varkappa}(\breve{\alpha}_1,\dots,\breve{\alpha}_N)$ is equal to $\mathsf{F}^*_{\lambda/\varkappa}(\breve{\alpha}_1,\dots,\breve{\alpha}_N;\mathbf{s})$, with spin parameters $s_1=\dots=s_{k-1}=s$, $s_k=s_{k+1}=\dots=0$

2.5.2 Mixed Skew Cauchy identities

The scaled geometric specializations allow to extend the skew Cauchy identities considered in previous sections. We will list the results without going into the proofs, that in all cases follow arguments seen in the sections above.

In the following statements we will assume that $q\in(0,1)$, $s\in(-1,0]$.

Proposition 2.5.2. *Take $u\in\mathbb{C}$ such that $|s(s-u)|<|1-su|$. Then for all α we have*

$$\sum_{\nu}\mathsf{F}_{\nu/\mu}(u)\mathsf{F}^*_{\nu/\lambda}(\breve{\alpha})=(1+\alpha u)\sum_{\varkappa}\mathsf{F}_{\lambda/\varkappa}(u)\mathsf{F}^*_{\mu/\varkappa}(\breve{\alpha}). \tag{2.61}$$

Proposition 2.5.3. *Take α,x such that $|\alpha x|<1$. Then, for all $\mu,\lambda\in\mathrm{Sign}_N$, we have*

$$\sum_{\nu\in\mathrm{Sign}_{N+1}}\mathbb{F}_{\nu/\mu}(x)\mathsf{F}^{\bullet}_{\nu/\lambda}(\breve{\alpha})=\frac{(-s\alpha;q)_\infty}{(\alpha x;q)_\infty}\sum_{\varkappa\in\mathrm{Sign}_{N-1}}\mathbb{F}_{\lambda/\varkappa}(x)\mathsf{F}^{\bullet}_{\mu/\varkappa}(\breve{\alpha}), \tag{2.62}$$

if $N>1$. When $N=1$ we have

$$\sum_{\nu\in\mathrm{Sign}_{N+1}}\mathbb{F}_{\nu/\mu}(x)\mathsf{F}^{\bullet}_{\nu/\lambda}(\breve{\alpha})=\frac{1}{(\alpha x;q)_\infty}\mathbb{F}_{\lambda/\varkappa}(x). \tag{2.63}$$

We finally report the skew Cauchy identitiy for pairs of scaled geometric specializations.

Proposition 2.5.4. *Take α,β such that $|\alpha\beta|<1$. Then, for all μ,λ, we have*

$$\sum_{\nu}\mathsf{F}_{\nu/\mu}(\breve{\alpha})\mathsf{F}^*_{\nu/\lambda}(\breve{\beta})=\frac{1}{(\alpha\beta;q)_\infty}\sum_{\varkappa}\mathsf{F}_{\lambda/\varkappa}(\breve{\alpha})\mathsf{F}^*_{\mu/\varkappa}(\breve{\beta}). \tag{2.64}$$

2.6 Difference operators

In this Section we prove that the (stable) spin Hall-Littlewood and the spin q-Whittaker functions are eigenfunctions of certain (q-)difference operators acting on symmetric functions. In this section we denote the quantization parameter in the sHL functions by t instead of q because the sHL eigenoperators are the same as in the Macdonald case (recall that for $s=0$, the sHL functions become the usual Hall-Littlewood symmetric polynomials, which are the $q=0$ degenerations of the Macdonald symmetric polynomials).

2.6.1 Eigenrelations for the spin Hall-Littlewood functions

Consider the space of symmetric rational functions in $u_1, \ldots, u_n$. Let the operator T_{q,u_i} on this space be

$$T_{q,u_i} f(u_1, \ldots, u_n) = f(u_1, \ldots, u_{i-1}, qu_i, u_{i+1}, \ldots u_n), \tag{2.65}$$

that is, it acts by multiplying the variable u_i by q. In this subsection we will use the $q = 0$ version, T_{0,u_i}. Note that this operator acts only on rational functions whose denominators do not contain positive powers of u_i.

Definition 2.6.1 (Hall-Littlewood difference operators)**.** For $1 \leq r \leq n$, let the r-th Hall-Littlewood difference operator be

$$\overline{\mathfrak{D}}_r^* := \sum_{\substack{I \subset \{1,\ldots,n\} \\ |I|=r}} \Bigg(\prod_{\substack{i \in I \\ j \in \{1,\ldots,n\} \setminus I}} \frac{tu_i - u_j}{u_i - u_j} \Bigg) T_{0,I}, \tag{2.66}$$

with $T_{0,I} = \prod_{i \in I} T_{0,u_i}$.

The Hall-Littlewood operators are the $q = 0$ cases of the Macdonald difference operators [Mac95, Chapter VI.3] (the latter are obtained by taking T_{q,u_i} in (2.66) instead of T_{0,u_i}). The operators $\mathfrak{D}_r$ are diagonal in the Hall-Littlewood symmetric polynomials $\mathsf{F}_\lambda|_{\mathsf{s}=0}$:[2]

$$\overline{\mathfrak{D}}_r^* \mathsf{F}_\lambda(u_1, \ldots, u_n)|_{\mathsf{s}=0} = e_r(1, t, \ldots, t^{n-\ell(\lambda)-1})\, \mathsf{F}_\lambda(u_1, \ldots, u_n)|_{\mathsf{s}=0}, \tag{2.67}$$

where the eigenvalues are given in terms of $e_r(u_1, \ldots u_n)$, the r-th elementary symmetric polynomial:

$$e_r(z_1, \ldots, z_N) = \sum_{1 \leq i_1 < \cdots < i_r \leq N} z_{i_1} \cdots z_{i_r}. \tag{2.68}$$

In particular, $e_r(z_1, \ldots, z_N) = 0$ if $r > N$.

In the following Theorem we extend (2.67) to the spin Hall-Littlewood symmetric functions:

Theorem 2.6.2. *For all Young diagrams λ and $n \in \mathbb{Z}_{\geq 1}$ we have*

$$\overline{\mathfrak{D}}_r^* \mathsf{F}_\lambda(u_1, \ldots, u_n; \mathsf{s}) = e_r(1, t, \ldots, t^{n-\ell(\lambda)-1})\, \mathsf{F}_\lambda(u_1, \ldots, u_n; \mathsf{s}). \tag{2.69}$$

Remark 2.6.3. Certain difference operators acting diagonally on the non-stable spin Hall-Littlewood symmetric functions were considered in [Dim18].

In order to prove Theorem 2.6.2 we make use of a preliminary lemma.

Lemma 2.6.4. *We have*

$$\overline{\mathfrak{D}}_r^* \Bigg(\sum_{\sigma \in \mathfrak{S}_n} \sigma \Bigg\{ \prod_{1 \leq i < j \leq n} \frac{u_i - tu_j}{u_i - u_j} \Bigg\} \Bigg) = e_r(1, \ldots, t^{n-1}) \sum_{\sigma \in \mathfrak{S}_n} \sigma \Bigg\{ \prod_{1 \leq i < j \leq n} \frac{u_i - tu_j}{u_i - u_j} \Bigg\}. \tag{2.70}$$

[2] We have $\mathsf{F}_\lambda(u_1, \ldots, u_n)|_{\mathsf{s}=0} = Q_\lambda(u_1, \ldots, u_n; t)$ in the standard notation of [Mac95, Chapter III].

Proof. This is the $\lambda = \varnothing$ case of the known Hall-Littlewood relation (2.67). Notice that the symmetrized sum in fact does not depend on the variables $u_1, \dots, u_n$:

$$\sum_{\sigma \in \mathfrak{S}_n} \sigma \left\{ \prod_{1 \le i < j \le n} \frac{u_i - t u_j}{u_i - u_j} \right\} = \frac{(t;t)_n}{(1-t)^n},$$

see [Mac95, Chapter III.1, formula (1.4)]. □

Proof of Theorem 2.6.2. For a fixed Young diagram λ we define

$$A = \prod_{1 \le i < j \le n} \frac{u_i - t u_j}{u_i - u_j}, \qquad B = \prod_{i=1}^{n} \prod_{j=1}^{\lambda_i} \left(\frac{u_i - s_j}{1 - s_j u_i} \right), \qquad C = \prod_{i=1}^{\ell(\lambda)} \frac{u_i}{u_i - s_{\lambda_i}}.$$

With this notation, using (2.6), the left-hand side of (2.69) can be written as

$$c_\lambda \sum_{\substack{I \subset \{1,\dots,n\} \\ |I| = r}} \prod_{\substack{i \in I \\ j \in \{1,\dots,n\} \setminus I}} \frac{t u_i - u_j}{u_i - u_j} T_{0,I} \sum_{\sigma \in \mathfrak{S}_n} \sigma \left\{ ABC \right\}, \tag{2.71}$$

where $c_\lambda = (1-t)^n / (t;t)_{n-\ell(\lambda)}$. We first observe that

$$T_{0,I} \sigma\{C\} = \begin{cases} \sigma\{C\} & \text{if } I \subseteq \{\sigma_{\ell(\lambda)+1}, \dots, \sigma_n\}, \\ 0 & \text{otherwise.} \end{cases}$$

Therefore, we can reduce the sum over the symmetric group in (2.71) to permutations σ such that $I \subseteq \sigma(\{\ell(\lambda)+1, \dots, n\})$. Moreover, we see that the claim of Theorem 2.6.2 follows for $r > n - \ell(\lambda)$ since both sides of (2.69) vanish. Thus we will now assume that $r \le n - \ell(\lambda)$.

For a given permutation σ define the ordered sets V_σ, W_σ as

$$\begin{aligned} V_\sigma &= \sigma(\{1, \dots, \ell(\lambda)\}) = \left\{ v_1, \dots, v_{\ell(\lambda)} \right\}, \\ W_\sigma &= \sigma(\{\ell(\lambda)+1, \dots, n\}) = \{ w_1, \dots, w_{n-\ell(\lambda)} \} = I \cup K, \end{aligned}$$

and rewrite (2.71) as

$$c_\lambda \sum_{\substack{I \subset \{1,\dots,n\} \\ |I| = r}} \sum_{\substack{\sigma \in \mathfrak{S}_n \\ I \subseteq W_\sigma}} \sigma \left\{ BC \right\} \prod_{\substack{i \in I \\ j \in \{1,\dots,n\} \setminus I}} \frac{t u_i - u_j}{u_i - u_j} T_{0,I} \sigma \left\{ A \right\}, \tag{2.72}$$

where we used the fact that $\sigma\{BC\}$ only depends on variables u_j for $j \in V_\sigma$. We now focus on the remaining factors. For two disjoint or coinciding ordered sets S_1, S_2 denote

$P(S_1,S_2) := \prod_{i\in S_1,\, j\in S_2} \frac{u_i - tu_j}{u_i-u_j}$. When $S_1 = S_2$, the product is only over $i<j$. We have

$$\prod_{\substack{i\in I\\ j\in\{1,\dots,n\}\setminus I}} \frac{tu_i-u_j}{u_i-u_j}\, T_{0,I}\sigma\left\{A\right\} = P(I^c,I)P(V_\sigma,V_\sigma)P(V_\sigma,K)$$

$$\times\, T_{0,I}\Big(P(I,K)P(I,I)P(V_\sigma,I)P(K,I)P(K,K)\Big)$$

$$= P(V_\sigma,V_\sigma)P(V_\sigma,W_\sigma)P(K,I)\, T_{0,I}\Big(P(I,K)P(I,I)P(K,K)\Big)$$

$$= \prod_{1\le i<j\le \ell(\lambda)} \frac{u_{v_i}-tu_{v_j}}{u_{v_i}-u_{v_j}} \prod_{i\in V_\sigma,\, j\in W_\sigma} \frac{u_i-tu_j}{u_i-u_j} \prod_{i\in W_\sigma\setminus I,\, j\in I} \frac{u_i-tu_j}{u_i-u_j}\, T_{0,I} \prod_{1\le i<j\le n-\ell(\lambda)} \frac{u_{w_i}-tu_{w_j}}{u_{w_i}-u_{w_j}}.$$

In the above calculation we used the fact that $T_{0,I}$ acts on $P(S,I)$, $S\ne I$, by turning it into one. The action $T_{0,I}P(I,I)$ does not make sense before the symmetrization (i.e., summation over σ), and so we do not apply $T_{0,I}$ to this expression just yet. In the last line, the first two products are independent of I and of the ordering of W_σ, and the last two products are independent of the ordering of V_σ. Therefore, we can rearrange the two summations in (2.72) as

$$\begin{aligned} c_\lambda \sum_{\substack{V\subseteq\{1,\dots,n\}\\ |V|=\ell(\lambda),\, W=V^c}} \sum_{\tau\in\mathfrak{S}_{\ell(\lambda)}} \prod_{\substack{v\in V\\ w\in W}} \frac{u_v-tu_w}{u_v-u_w}\, \tau\Bigg\{ \prod_{1\le i<j\le\ell(\lambda)} \frac{u_{v_i}-tu_{v_j}}{u_{v_i}-u_{v_j}} BC\Bigg\} \\ \times \sum_{\substack{I\subset W\\ |I|=r}} \prod_{\substack{i\in I\\ w\in W\setminus I}} \frac{tu_i-u_w}{u_i-u_w}\, T_{0,I} \sum_{\sigma\in\mathfrak{S}_{n-\ell(\lambda)}} \sigma\Bigg\{ \prod_{1\le i<j\le n-\ell(\lambda)} \frac{u_{w_i}-tu_{w_j}}{u_{w_i}-u_{w_j}}\Bigg\}. \end{aligned} \tag{2.73}$$

The permutations τ,σ permute the variables u_{v_i}, u_{w_j}, $v_i\in V$, $w_j\in W$, acting respectively on indices i and j. We can now employ Lemma 2.6.4 to transform the second line of (2.73) into

$$e_r(1,t,\dots,t^{n-\ell(\lambda)-1}) \sum_{\sigma\in\mathfrak{S}_{n-\ell(\lambda)}} \sigma\Bigg\{ \prod_{1\le i<j\le n-\ell(\lambda)} \frac{u_{w_i}-tu_{w_j}}{u_{w_i}-u_{w_j}}\Bigg\}. \tag{2.74}$$

Therefore,

$$\begin{aligned} \text{lhs (2.69)} &= e_r(1,t,\dots,t^{n-\ell(\lambda)-1})\, c_\lambda \sum_{\substack{V\subseteq\{1,\dots,n\}\\ |V|=\ell(\lambda),\, W=V^c}} \sum_{\substack{\tau\in\mathfrak{S}_{\ell(\lambda)}\\ \sigma\in\mathfrak{S}_{n-\ell(\lambda)}}} \prod_{\substack{v\in V\\ w\in W}} \frac{u_v-tu_w}{u_v-u_w} \\ &\quad\times \sigma\Bigg\{ \prod_{1\le i<j\le n-\ell(\lambda)} \frac{u_{w_i}-tu_{w_j}}{u_{w_i}-u_{w_j}}\Bigg\}\, \tau\Bigg\{ \prod_{1\le i<j\le\ell(\lambda)} \frac{u_{v_i}-tu_{v_j}}{u_{v_i}-u_{v_j}} BC\Bigg\}. \end{aligned} \tag{2.75}$$

The summations in the right-hand side of this last expression (along with the factor c_λ) are easily rearranged into the symmetrized sum (2.6) producing the spin Hall Littlewood function F_λ. □

2.6.2 Eigenrelations for $\mathsf{F}^\bullet_\lambda$

The operator we introduce next depends on the number of variables M and on an additional positive integer N. Moreover, this operator acts only on a certain subspace of rational functions. Namely, let $\mathbf{V}(M)$ be the space of symmetric rational functions in M variables $v_1, \ldots, v_M$ of degree ≤ 1 in each variable. That is, its elements are functions $f(v_1, \ldots, v_M) = a(v_1, \ldots, v_M)/b(v_1, \ldots, v_M)$, where a and b are polynomials such that $\deg_{v_i}(a) - \deg_{v_i}(b) \le 1$ for all $i = 1, \ldots, M$. One readily sees that $\mathbf{V}(M)$ is a linear space. The dual sHL functions $\mathsf{F}^\bullet_\nu(v_1, \ldots, v_M)$ belong to $\mathbf{V}(M)$, see (2.78).

Definition 2.6.5. For positive integers M, N define the *dual s-deformed Macdonald operator* by

$$\mathfrak{D}^\bullet_{1,N} := \sum_{j=1}^{M} \prod_{\substack{l=1 \\ l \neq j}}^{M} \frac{v_j - t v_l}{v_j - v_l} \, \mathfrak{C}_{j,N}, \tag{2.76}$$

where

$$\mathfrak{C}_{j,N} := v_j \left(\frac{v_j - s}{1 - s v_j} \right)^{N-1} (-s)^{N-1} \lim_{\varepsilon \to 0} \varepsilon \, T_{\varepsilon^{-1}, v_j}.$$

The limit $\lim_{\varepsilon \to 0} \varepsilon \, T_{\varepsilon^{-1}, v_j}$ is well-defined on $\mathbf{V}(M)$, so $\mathfrak{D}^\bullet_{1,N}$ acts in the space $\mathbf{V}(M)$.

Theorem 2.6.6. *For any boxed signature $\lambda \subseteq \mathrm{Box}(N, M)$ (recall that this is $\mathrm{Sign}_M^{\le N}$), we have*

$$\mathfrak{D}^\bullet_{1,N} \mathsf{F}^\bullet_\lambda = e_1(1, t, \ldots, t^{\lambda'_N - 1}) \, \mathsf{F}^\bullet_\lambda, \tag{2.77}$$

where λ' is the transposed signature. In particular, $\lambda'_N = \#\{i \colon \lambda_i = N\}$.

For the proof it is useful to specialize symmetrization formula (2.6) to the case of functions $\mathsf{F}^\bullet$.

Proposition 2.6.7. *Let $\lambda \in \mathrm{Sign}_M^{\le N}$, then for all $k \ge M$ we have*

$$\mathsf{F}^\bullet_\lambda(v_1, \ldots, v_k) = \mathcal{C}(\lambda) \sum_{\sigma \in \mathfrak{S}_k} \sigma \left\{ \prod_{1 \le i < j \le k} \frac{v_i - q v_j}{v_i - v_j} \prod_{i=1}^{\ell(\lambda)} v_i \left(\frac{v_i - s}{1 - s v_i} \right)^{\lambda_i - 1} \left(\frac{1}{1 - s v_i} \right)^{\mathbf{1}_{\lambda_i < N}} \right\}, \tag{2.78}$$

where the symmetric group $\mathfrak{S}_k$ acts on the variables v_i but not on elements of the signature λ_i, and the constant prefactor has the form

$$\mathcal{C}(\lambda) = \frac{(1-q)^k}{(q;q)_{k - \ell(\lambda)}} \prod_{i=1}^{N} \frac{(s^2; q)_{m_i(\lambda)}}{(q;q)_{m_i(\lambda)}}. \tag{2.79}$$

Proof of theorem 2.6.6. We make use of the symmetrization formula (2.78) (recall that we have replaced the parameter q by t throughout this subsection). We use the notation

$$A = \prod_{1 \le l < r \le M} \frac{v_l - t v_r}{v_l - v_r} \qquad \text{and} \qquad B = \prod_{r=1}^{\ell(\lambda)} v_r \left(\frac{v_r - s}{1 - s v_r} \right)^{\lambda_r - 1} \left(\frac{1}{1 - s v_r} \right)^{\mathbf{1}_{\lambda_r < N}},$$

so that $\mathsf{F}^\bullet_\lambda = \mathcal{C}(\lambda)\sum_{\sigma\in\mathfrak{S}_M}\sigma\{AB\}$. The operator $\mathfrak{D}^*_{1,N}$ acts as

$$\mathfrak{D}^\bullet_{1,N}\mathsf{F}^\bullet_\lambda = \mathcal{C}(\lambda)\sum_{i=1}^{M}\prod_{\substack{j=1\\ j\neq i}}^{M}\frac{v_i - tv_j}{v_i - v_j}\sum_{\sigma\in\mathfrak{S}_M}\mathfrak{C}_{i,N}(\sigma\{AB\}).$$

The action of $\mathfrak{C}_{i,N}$ on the product $\sigma\{AB\}$ can be split as

$$\mathfrak{C}_{i,N}(\sigma\{AB\}) = \lim_{\varepsilon\to 0}\sigma\{A\}\Big|_{v_i=1/\varepsilon} \times \mathfrak{C}_{i,N}(\sigma\{B\}). \tag{2.80}$$

Assume now that $\lambda'_N = L$, that is $\lambda_1 = \cdots = \lambda_L = N$ and $\lambda_{L+1} < N$, for some $L \in \{0,\dots,M\}$. We focus on the second factor of (2.80). A simple computation shows that

$$\mathfrak{C}_{i,N}(\sigma\{B\}) = \begin{cases}\sigma\{B\} & \text{if } i \in \sigma(\{1,\dots,L\}),\\ 0 & \text{else,}\end{cases} \tag{2.81}$$

that in particular, implies that $\mathfrak{C}_{i,N}\sigma\{B\} = 0$ when $L = 0$, confirming (2.77) in this specific case.

For $L > 0$ and a permutation σ such that $i \in \sigma(\{1,\dots,L\})$, call $\bar{k}$ the element such that $\sigma(\bar{k}) = i$. We rewrite A into a product of factors $A = A_1A_2A_3$, obtained dividing the triangular product as

$$A_1 = \prod_{1\le l<r<\bar{k}}\frac{v_l - tv_r}{v_l - v_r}, \qquad A_2 = \prod_{1\le l<\bar{k}}\frac{v_l - tv_{\bar{k}}}{v_l - v_{\bar{k}}}, \qquad A_3 = \prod_{\substack{1\le l<M\\ \max(l,\bar{k})<r\le M}}\frac{v_l - tv_r}{v_l - v_r}.$$

We can evaluate the first factor in the right-hand site of (2.80) as

$$\prod_{\substack{j=1\\ j\neq i}}^{M}\frac{v_i - tv_j}{v_i - v_j}\lim_{\varepsilon\to 0}\sigma\{A\}\Big|_{v_i=1/\varepsilon} = t^{\bar{k}-1}\sigma\{A_1\widetilde{A}_2A_3\},$$

where

$$\widetilde{A}_2 \coloneqq \prod_{1\le l<\bar{k}}\frac{v_{\bar{k}} - tv_l}{v_{\bar{k}} - v_l}.$$

The action of $\mathfrak{D}^*_{1,N}$ on the sHL function can be therefore expressed (ignoring $\mathcal{C}(\lambda)$) as

$$\sum_{\bar{k}=1}^{L}t^{\bar{k}-1}\sum_{i=1}^{M}\sum_{\substack{\sigma\in\mathfrak{S}_M\\ \sigma(\bar{k})=i}}\sigma\{A_1\widetilde{A}_2A_3B\} = \sum_{\bar{k}=1}^{L}t^{\bar{k}-1}\sum_{\sigma\in\mathfrak{S}_M}\sigma\{A_1\widetilde{A}_2A_3B\}. \tag{2.82}$$

To prove relation (2.77) we show that each term $\sigma\{A_1\widetilde{A}_2A_3B\}$ is equal to one of the terms $\tau\{A_1A_2A_3B\}$ in the expansion of the original sHL function. For each permutation $\tau \in \mathfrak{S}_M$ and each $\bar{k}$ define the permutation σ as

$$\sigma(j) = \begin{cases}\tau(j+1) & \text{if } j = 1,\dots,\bar{k}-1,\\ \tau(1) & \text{if } j = \bar{k},\\ \tau(j) & \text{if } j = \bar{k}+1,\dots M.\end{cases}$$

With this choice we can easily check that $\sigma\{A_3B\} = \tau\{A_3B\}$ and more crucially that $\sigma\{A_1\widetilde{A}_2\} = \tau\{A_1A_2\}$ since the cyclic shift in the first $\bar{k}$ terms of σ makes up for the exchange of $\widetilde{A}_2$ and A_2. This in particular shows that the symmetric sum in the right-hand side of (2.82) is independent of $\bar{k}$ and it is equal, up to a factor $\mathcal{C}(\lambda)$ that we omitted, to $\mathsf{F}^{\bullet}_{\lambda}(v_1,\ldots,v_M)$. The sum $\sum_{\bar{k}=1}^{L} t^{\bar{k}-1}$ is the desired eigenvalue $e_1(1,t,\ldots,t^{\lambda'_N-1})$. This completes the proof. □

Remark 2.6.8 (Limit to the Hall–Littlewood case)**.** In the limit $s\to 0$, the new operator $\mathfrak{D}^{\bullet}_{1,N}$ (2.76) acting on the dual sHL functions should be replaced by

$$D^{*}_{1,N} = \sum_{j=1}^{M}\prod_{\substack{l=1\\ l\neq j}}^{M}\frac{v_j - tv_l}{v_j - v_l}\, v_j^N \lim_{\varepsilon\to 0}\varepsilon^N\, T_{\varepsilon^{-1},v_j}, \tag{2.83}$$

by mimicking the action (2.81). Similarly to Theorem 2.6.6, one can show that $D^{*}_{1,N}$ acts diagonally on the Hall–Littlewood polynomials $P_\lambda(\cdot;0,t)$.

The same operator (2.83) can be also obtained as a $q\to 0$ limit of a certain operator diagonal in the Macdonald polynomials $P_\lambda(\cdot;q,t)$. Take the first Macdonald q^{-1}-difference operator

$$M_1 = \sum_{j=1}^{M}\prod_{\substack{i=1\\ i\neq j}}^{M}\frac{tx_i - x_j}{x_i - x_j}\, T_{q^{-1},x_j}. \tag{2.84}$$

It acts on the Macdonald polynomials $P_\lambda(x_1,\ldots,x_M;q,t)$ with eigenvalues $\sum_{i=1}^{M} q^{-\lambda_i}t^{i-1}$ (this follows from, e.g., [BC14, Section 2.2.3]). Denote by $\mathbf{P}_N$ the subspace of polynomials in $x_1,\ldots,x_M$ which have degree $\le N$ in each of the variables x_i. It is spanned by the Macdonald polynomials $P_\lambda(x_1,\ldots,x_M;q,t)$ with $\lambda_1\le N$, i.e., $\lambda\subseteq \mathrm{Box}(N,M)$. On $\mathbf{P}_N$ consider the operator $q^N M_1$. Its limit as $q\to 0$ is well-defined. By looking at eigenvalues on Hall–Littlewood polynomials $P_\lambda(x_1,\ldots,x_M;0,t)$ with $\lambda_1\le N$, one readily sees that this limit coincides with $D^{*}_{1,N}$.

2.6.3 Eigenrelations for the spin q-Whittaker polynomials

The duality between sHL functions and sqW polynomials (Corollary 2.3.11 and Proposition 2.2.3) allows to pass from the eigenoperators for the sHL functions to the ones for the sqW polynomials.

Definition 2.6.9 (Spin q-Whittaker difference operators)**.** Fix a positive integer N, and define the *s-deformed q-Whittaker operators*

$$\mathfrak{D}_1 \coloneqq \sum_{i=1}^{N}\prod_{\substack{j=1\\ j\neq i}}^{N}\frac{(1+sx_i)}{1-x_i/x_j}\, T_{q,x_i}, \tag{2.85}$$

and

$$\overline{\mathfrak{D}}_1 \coloneqq \sum_{i=1}^{N}\prod_{\substack{j=1\\ j\neq i}}^{N}\frac{(1+s/x_i)}{1-x_j/x_i}\, T_{q^{-1},x_i}. \tag{2.86}$$

Let us make a remarks after this definition.

Remark 2.6.10. The operators $\mathfrak{D}_1$ and $\overline{\mathfrak{D}}_1$ reduce for $s=0$ to the $t=0$ specializations of the two Macdonald q-difference operators. The first one is the standard first order Macdonald operator $\sum_{i=1}^N \prod_{j\neq i} \frac{tx_i - x_j}{x_i - x_j} T_{q,x_i}$ (denoted by D_N^1 in [Mac95, Ch. VI]), and the second one is $\sum_{i=1}^N \prod_{j\neq i} \frac{x_i - tx_j}{x_i - x_j} T_{q^{-1},x_i}$ (denoted by $\tilde{D}_N^1$ in [BC14, Section 2.2.3]).

We establish two eigenrelations for the sqW polynomials in the next two theorems.

Theorem 2.6.11. *For all signatures $\lambda \in \mathrm{Sign}_N$ we have*

$$\mathfrak{D}_1 \mathbb{F}_\lambda(x_1,\ldots,x_N) = q^{\lambda_N} \mathbb{F}_\lambda(x_1,\ldots,x_N). \tag{2.87}$$

Proof. We will prove the identity

$$\left(1-(1-q)\mathfrak{D}^*_{1,N}\right)\Pi(x;v) = \mathfrak{D}_1 \Pi(x;v), \tag{2.88}$$

where

$$\Pi(x;v) = \prod_{j=1}^M \left(\frac{1}{1-sv_j}\right)^{N-1} \times \prod_{i=1}^N \prod_{j=1}^M (1+v_j x_i). \tag{2.89}$$

Indeed, modulo (2.88), the Cauchy Identity (2.27) and the eigenrelations (2.77) imply

$$\sum_{\lambda \subseteq \mathrm{Box}(N,M)} q^{\lambda_N} \mathbb{F}_\lambda(x_1,\ldots,x_N) \mathsf{F}^\bullet_{\lambda'}(v_1,\ldots,v_M) = \sum_{\lambda \subseteq \mathrm{Box}(N,M)} \mathfrak{D}_1 \mathbb{F}_\lambda(x_1,\ldots,x_N) \mathsf{F}^\bullet_{\lambda'}(v_1,\ldots,v_M),$$

and hence (2.87) follows by orthogonality of the sHL functions (Proposition 2.2.3).

It thus suffices to establish (2.88). Define

$$h(z) := \prod_{j=1}^M (1+v_j z).$$

We have

$$\frac{\mathfrak{D}_1 \Pi(x;v)}{\Pi(x;v)} = \frac{\mathfrak{D}_1 h(x_1)\cdots h(x_N)}{h(x_1)\cdots h(x_N)} = -\oint_{x_1,\ldots,x_N} \prod_{i=1}^N \frac{x_i(1+sz)}{x_i - z} \frac{h(qz)}{h(z)} \frac{dz}{z(1+sz)},$$

where in the second equality we used the residue expansion of the complex integral and the contour encircles only the poles $x_1,\ldots,x_N$. By subtracting 1 from both sides, we can enlarge the complex contour to also include the pole at $z=0$ (note that $h(z)$ is nonsingular at $z=0$). After a change of variable $z=-1/w$, we get

$$\frac{(-1+\mathfrak{D}_1)\Pi(x;v)}{\Pi(x;v)} = -\oint_{v_1,\ldots,v_M} \prod_{k=1}^M \frac{w-qv_k}{w-v_k} (w-s)^{N-1} \prod_{j=1}^N \frac{x_j}{1+x_j w} dw. \tag{2.90}$$

In the right-hand side of (2.90), after the change of variable, we switched the contour to a positively oriented curve around $v_1, \ldots, v_M$, which yielded the negative sign in front. Using

$$\lim_{\varepsilon \to 0} \varepsilon \left(\frac{1}{(1 - s/\varepsilon)^{N-1}} \prod_{j=1}^{N} (1 + x_j/\varepsilon) \right) = \frac{x_1 \cdots x_N}{(-s)^{N-1}}$$

and expanding the right-hand side of (2.90) as a sum of residues, we can rewrite it as

$$-\frac{(1-q)\mathfrak{D}^*_{1,N}\Pi(x;v)}{\Pi(x;v)}.$$

This proves (2.88), and hence the desired eigenrelation (2.87). □

Theorem 2.6.12. *For all signatures $\lambda \in \mathrm{Sign}_N$ we have*

$$\overline{\mathfrak{D}}_1 \mathbb{F}_\lambda = q^{-\lambda_1} \mathbb{F}_\lambda. \tag{2.91}$$

Proof. The proof of this eigenrelation is identical to that of theorem 2.6.11. And it uses the fact that

$$q^{-M} \left(1 - (1-q)\overline{\mathfrak{D}}_1^*\right) \Pi(x;v) = \overline{\mathfrak{D}}_1 \Pi(x;v),$$

where $\Pi(x;v)$ is given by (2.89). We will not repeat the detailed argument here. □

2.6.4 Commutation and conjugation

The q-difference operators $\mathfrak{D}_1$ (2.85) and $\overline{\mathfrak{D}}_1$ (2.86) commute. For this statement we cannot appeal to the eigenrelations of Theorems 2.6.11 and 2.6.12 since we did not prove that the sqW polynomials form a basis for the ring of symmetric polynomials in N variables. Nevertheless, the commutation can be checked independently:

Proposition 2.6.13. *We have $\mathfrak{D}_1\overline{\mathfrak{D}}_1 F = \overline{\mathfrak{D}}_1\mathfrak{D}_1 F$ for all symmetric polynomials F in N variables.*

Proof. By polarization, it suffices to check the action on product form functions $F(x_1, \ldots, x_N) = f(x_1) \ldots f(x_N)$, where $f(x)$ is an arbitrary polynomial.

The action of each operator can we written as a contour integral:

$$\mathfrak{D}_1 F = -\frac{1}{2\pi \mathrm{i}} \oint \prod_{i=1}^{N} \left(f(x_i) \frac{x_i(1+sz)}{x_i - z} \right) \frac{f(qz)}{f(z)} \frac{dz}{z(1+sz)},$$

$$\overline{\mathfrak{D}}_1 F = \frac{1}{2\pi \mathrm{i}} \oint \prod_{i=1}^{N} \left(f(x_i) \frac{w+s}{w - x_i} \right) \frac{f(q^{-1}w)}{f(w)} \frac{dw}{w+s},$$

where both integrals are over a contour containing $x_1, \ldots, x_N$ and no other poles of the integrand. Throughout the proof we assume that all contours exist, which might impose some restrictions on the x_i's. After checking the commutation under the restrictions, we can lift these restrictions by an analytic continuation.

We have

$$\mathfrak{D}_1\overline{\mathfrak{D}}_1 F = -\frac{1}{(2\pi\mathrm{i})^2}\oint_{\gamma_z^1}\oint_{\gamma_w^1}\prod_{i=1}^{N}\left(f(x_i)\,\frac{w+s}{w-x_i}\,\frac{x_i(1+sz)}{x_i-z}\right)\frac{w-z}{w-qz}\,\frac{f(qz)f(q^{-1}w)}{f(z)f(w)}\,\frac{dw}{w+s}\,\frac{dz}{z(1+sz)},$$

where γ_z^1 contains both γ_w^1 and $q^{-1}\gamma_w^1$, while γ_w^1 is around $x_1,\ldots,x_N$ and no other poles. In the other order, we have

$$\overline{\mathfrak{D}}_1\mathfrak{D}_1 F = -\frac{1}{(2\pi\mathrm{i})^2}\oint_{\gamma_w^2}\oint_{\gamma_z^2}\prod_{i=1}^{N}\left(f(x_i)\,\frac{x_i(1+sz)}{x_i-z}\,\frac{w+s}{w-x_i}\right)\frac{q^{-1}(w-z)}{q^{-1}w-z}\,\frac{f(q^{-1}w)f(qz)}{f(w)f(z)}\,\frac{dz}{z(1+sz)}\,\frac{dw}{w+s},$$

but now γ_w^2 contains both γ_z^2 and $q\gamma_z^2$, while γ_z^2 is around $x_1,\ldots,x_N$ and no other poles. Note that the integrands in both formulas coincide.

In the first expression, deform the integration contour γ_z^1 to coincide with γ_w^1, which picks up the residue at $z=q^{-1}w$. In the second expression, deform the contour γ_w^2 to coincide with γ_z^2, which picks up the residue at $w=qz$. The resulting double contour integrals are over the same contours and are thus equal. It remains to check the equality of the single integrals of the residues. We have

$$\operatorname*{Res}_{z=q^{-1}w}(\text{integrand in }\mathfrak{D}_1\overline{\mathfrak{D}}_1) = -(-1)^N(1-q)(s+w)^{N-1}(q+sw)^{N-1}\prod_{i=1}^{N}\frac{x_if(x_i)}{(w-x_i)(w-qx_i)},$$

$$\operatorname*{Res}_{w=qz}(\text{integrand in }\overline{\mathfrak{D}}_1\mathfrak{D}_1) = (-1)^N(1-q)(1+sz)^{N-1}(s+qz)^{N-1}\prod_{i=1}^{N}\frac{x_if(x_i)}{(z-x_i)(qz-x_i)}$$

We must show that the integral of the first expression over γ_w^1 is the same as the integral of the second expression over γ_z^2. Noting that both expressions have zero residue at infinity due to quadratic decay, we can compute the first integral as a sum of minus residues at $w=qx_i$. Then one readily sees that each minus residue at $w=qx_i$ is the same as the residue of the second expression at $z=x_i$. This shows the desired commutation. $\square$

The discussion in the rest of this subsection aims in part to demonstrate why the result of Proposition 2.6.13 is a rather unexpected one.

Both operators $\mathfrak{D}_1$ (2.85) and $\overline{\mathfrak{D}}_1$ (2.86) are related via conjugation to q-Whittaker difference operators. The latter are $t=0$ degenerations of the Macdonald q-difference operators from [Mac95]. Denote for $r=1,\ldots,N$:

$$W_N^r \coloneqq \sum_{|I|=r}\prod_{i\in I,\,j\notin I}\frac{1}{1-x_i/x_j}\prod_{i\in I}T_{q,x_i},\qquad \tilde W_N^r \coloneqq \sum_{I}\prod_{i\in I,\,j\notin I}\frac{1}{1-x_j/x_i}\prod_{i\in I}T_{q^{-1},x_i},\quad (2.92)$$

where the sums are over subsets of $\{1,\ldots,N\}$ of cardinality r. These operators are diagonal in the usual q-Whittaker polynomials (which are $t=0$ versions of the Macdonald polynomials). In particular, W_N^1 and $\tilde W_N^1$ have eigenvalues q^{λ_N} and $q^{-\lambda_1}$, respectively, on

q-Whittaker polynomials. All the operators $W_N^r, \tilde{W}_N^r$, $r = 1, \ldots, N$, commute. We refer to Sections 2.2.2 and 3.1.3 in [BC14] for details. Let

$$\mathbb{U}_N := \prod_{i=1}^{N} \frac{1}{(-sx_i; q)_\infty^{N-1}}, \qquad \mathbb{V}_N := \prod_{i=1}^{N} \frac{1}{(-s/x_i; q)_\infty^{N-1}}.$$

A straightforward computation shows:

Proposition 2.6.14. *The spin q-Whittaker operators* (2.85), (2.86) *are conjugates of the first q-Whittaker operators* (2.92)*:*

$$\mathfrak{D}_1 = \mathbb{U}_N^{-1} W_N^1 \mathbb{U}_N, \qquad \overline{\mathfrak{D}}_1 = \mathbb{V}_N^{-1} \tilde{W}_N^1 \mathbb{V}_N,$$

where $\mathbb{U}_N$*, etc., mean multiplication operators.*

Because the q-Whittaker operators (2.92) commute, we get many operators commuting with either $\mathfrak{D}_1$ or $\overline{\mathfrak{D}}_1$. That is, for $r = 1, \ldots, N$ we have:

$$\left[\mathfrak{D}_1, \mathbb{U}_N^{-1} W_N^r \mathbb{U}_N\right] = 0, \qquad \left[\overline{\mathfrak{D}}_1, \mathbb{V}_N^{-1} \tilde{W}_N^r \mathbb{V}_N\right] = 0. \tag{2.93}$$

For example,

$$\mathbb{U}_N^{-1} W_N^2 \mathbb{U}_N = \sum_{i,k \colon i \neq k} (1 + sx_i)^{N-1} (1 + sx_k)^{N-1} \prod_{j \colon j \neq i,k} \frac{1}{(1 - x_i/x_j)(1 - x_k/x_j)} T_{q,x_i} T_{q,x_k}. \tag{2.94}$$

However, one can directly check that the operator $\mathbb{U}_N^{-1} W_N^2 \mathbb{U}_N$ *does not commute* with $\overline{\mathfrak{D}}_1$. This suggests that the operators $\mathbb{U}_N^{-1} W_N^r \mathbb{U}_N$ or $\mathbb{V}_N^{-1} \tilde{W}_N^r \mathbb{V}_N$, $r \geq 2$, *should not be diagonal* in the spin q-Whittaker polynomials $\mathbb{F}_\lambda$. The following example shows that this is indeed the case:

Example 2.6.15. Take $N = 2$, then $(1 - s^2)\mathbb{F}_{(1,0)}(x_1, x_2) = s + x_1 + x_2 + sx_1x_2$. Applying (2.94) to this function, we obtain $(1 + sx_1)(1 + sx_2)(s + qx_1 + qx_2 + sq^2x_1x_2)$, which is not proportional to $\mathbb{F}_{(1,0)}(x_1, x_2)$ unless $s = 0$. Note that for $s = 0$ both $\mathbb{U}_N$ and $\mathbb{V}_N$ are the same (and are equal to the identity), and $\mathfrak{D}_1, \overline{\mathfrak{D}}_1$ are the usual q-Whittaker difference operators.

We also observe that by (2.93), polynomials of the form $\mathbb{U}_N^{-1} W_N^r \mathbb{U}_N \mathbb{F}_\lambda$, $r = 2, \ldots, N$, are eigenfunctions of the operator $\mathfrak{D}_1$ with eigenvalues q^{λ_N}. Similarly, $\mathbb{V}_N^{-1} \tilde{W}_N^r \mathbb{V}_N \mathbb{F}_\lambda$ are eigenfunctions of $\overline{\mathfrak{D}}_1$ with eigenvalues $q^{-\lambda_1}$. However, one can check that $\overline{\mathfrak{D}}_1$ does not act diagonally on, say, the polynomial $\mathbb{U}_N^{-1} W_N^2 \mathbb{U}_N \mathbb{F}_{(1,0)}$.

It remains unclear how to construct higher order q-difference operators which would be diagonal in the sqW polynomials (and whether such operators exist at all).

2.7 Open problems

2.7.1 Orthogonality and spectral theory for spin q-Whittaker polynomials

The q-Whittaker polynomials satisfy orthogonality relations coming from (the $t = 0$ degeneration of) the Macdonald torus scalar product [Mac95, Ch. VI.9]. This relation states that the $s = 0$ versions of $\mathbb{F}_\lambda(z_1, \ldots, z_N)$ and $\mathbb{F}_\mu(1/z_1, \ldots, 1/z_N)$ are orthogonal to each other when $\mu \neq \lambda$ with respect to a certain weight on the N-dimensional torus $\mathbb{T}^N = \{|z_i| = 1, i = 1, \ldots, N\}$.

Remark 2.7.1. Under the generalization with a spin parameter, the spin Hall–Littlewood polynomials also satisfy a version of the torus orthogonality (called spatial orthogonality in [Bor+15b, Corollary 3.10], see also [Bor17], [BMP19, Proposition 8.6]), as well as another biorthogonality involving the summation of over λ instead of integration over z. Here we discuss only the former conjectural orthogonality of the spin q-Whittaker polynomials.

Define

$$m_{q,s}^N(z_1, \ldots, z_N) \coloneqq \frac{1}{N!} \prod_{1 \le i \neq j \le N} \frac{(s^2, z_i/z_j; q)_\infty}{(-sz_i, -s/z_i; q)_\infty} \prod_{i=1}^{N} \frac{1}{2\pi \mathrm{i} z_i}, \qquad (z_1, \ldots, z_N) \in \mathbb{T}^N.$$

When $s = 0$, $m_{q,s}^N$ reduces to the orthogonality measure of the q-Whittaker polynomials on $\mathbb{T}^N$, which is a $t = 0$ degeneration of the Macdonald's torus scalar product $\Delta(z_1, \ldots, z_N; q, t)$, cf. [Mac95, VI.(9.2)].

Lemma 2.7.2. *Both eigenoperators $\mathfrak{D}_1$, $\overline{\mathfrak{D}}_1$ (2.85), (2.86) for the spin q-Whittaker polynomials are self-adjoint with respect to the scalar product*

$$\langle f, g \rangle_{q,s} \coloneqq \int_{\mathbb{T}^N} f(z_1, \ldots, z_N) \, \overline{g(z_1, \ldots, z_N)} \, m_{q,s}^N(z_1, \ldots, z_N) \, dz_1 \ldots dz_N,$$

where f, g are Laurent polynomials with coefficients in $\mathbb{R}(q, s)$.

Proof. A direct verification. □

Conjecture 2.7.3. *We have for all signatures λ, μ:*

$$\int_{\mathbb{T}^N} \mathbb{F}_\lambda(z_1, \ldots, z_N) \, \mathbb{F}_\mu(1/z_1, \ldots, 1/z_N) \, m_{q,s}^N(z_1, \ldots, z_N) \, dz_1 \cdots dz_N = c_\lambda \mathbf{1}_{\lambda=\mu}, \tag{2.95}$$

where

$$c_\lambda = \prod_{i=1}^{N-1} \frac{(s^2; q)_\infty}{(q; q)_\infty} \frac{(q; q)_{\lambda_i - \lambda_{i+1}}}{(s^2; q)_{\lambda_i - \lambda_{i+1}}}. \tag{2.96}$$

Note that for $N \le 2$ the statement (up to the concrete formula for the norm c_λ) follows from Lemma 2.7.2 and the eigenrelations of Theorems 2.6.11 and 2.6.12. However, for $N \ge 3$ the two operators $\mathfrak{D}_1$, $\overline{\mathfrak{D}}_1$ are not sufficient to conclude orthogonality.

Remark 2.7.4. When $s = 0$, the constant c_λ (2.96) coincides with the $t = 0$ degeneration of the torus scalar product norm of a Macdonald polynomial [Mac95, Ch. VI.9, Example 1].

Let us present one further argument in favor of Conjecture 2.7.3. It was proven in [IMS20, Proposition 4.10] that the probability mass function of a tagged particle in the homogeneous q-Hahn Tasep with parameters $\nu = s^2$ and $\mu = -ys$ is

$$\mathbb{P}(\mathcal{H}(N,t) = \ell) = \left(\frac{(q;q)_\infty}{(s^2;q)_\infty}\right)^{N-1} \int_{\mathbb{T}^N} m_{q,s}^N(z_1,\dots,z_N) \prod_{j=1}^N \left(\frac{\Pi(z_j;y)}{\Pi(-s;y)}\right)^t \times \left(\frac{(-s)^N}{z_1\cdots z_N}\right)^\ell \frac{(\frac{(-s)^N}{z_1\cdots z_N};q)_\infty (s^2;q)_\infty^{N-1}}{(-sz_1,\dots,-sz_N;q)_\infty} dz_1\cdots dz_N, \tag{2.97}$$

where $\Pi(z;y) = \dfrac{(-sz;q)_\infty}{(-sy;q)_\infty}$. The same probability can be expressed as

$$\sum_{\substack{\lambda\in\mathrm{Sign}_N\\ \lambda_N=\ell}} \mathbb{F}_\lambda(-s,\dots,-s)\, \frac{\mathbb{F}^*_\lambda(y,\dots,y)}{\Pi(-s;y)},$$

Assuming Conjecture 2.7.3, this sum becomes

$$\int_{\mathbb{T}^N} m_{q,s}^N(z_1,\dots,z_N) \prod_{j=1}^N \left(\frac{\Pi(z_j;y)}{\Pi(-s;y)}\right)^t \left(\frac{(-s)^N}{z_1\cdots z_N}\right)^\ell \sum_{\substack{\lambda\in\mathrm{Sign}_N\\ \lambda_N=0}} \frac{(-s)^{|\lambda|}}{c_\lambda} \mathbb{F}_\lambda(1/z_1,\dots,1/z_N)\, dz_1\cdots dz_N.$$

Here we used the Cauchy Identity and the torus scalar product to express the dual function $\mathbb{F}^*_\lambda$, and the shifting rule of Proposition 2.3.7 to take out the monomial of degree ℓ. Evaluating the sum inside the integral as in (2.23), we recover exactly (2.97).

2.7.2 Accessing spin q-Whittaker polynomials via free field

In this thesis we did not focus on Fredholm determinantal structures for marginals of spin q-Whittaker processes. These aspects have been covered quite extensively in literature for specific models in the last few years [Cor14], [CP16], [IS19], [IMS20], [BMP19]. Techniques to access such Fredholm determinantal formulas usually rely on manipulations with integral representations of q-moments (as in [BC14], [BCS14]).

In the realm of Macdonald processes there exists an alternative approach to expose the determinantal nature of specific observables. This is done via a free field realization of Macdonald functions and Macdonald operators [Fei+09], [Kos19], see also [Bor+16] and, e.g., [FW09] for the Hall–Littlewood case. In the yet simpler case of the Schur processes this reduces to the infinite wedge representation of Schur functions [Oko01], [OR03]. It would be of great interest to understand to what extent our spin q-Whittaker functions, operators, and processes admit a description in terms of Fock type representations of a hypothetical (q,s)-deformed Heisenberg algebra.

Chapter 3

Integrable random fields of Young diagrams

This chapter presents results contained in sections 6,7,9 of

[BMP19] A. Bufetov, M. Mucciconi, and L. Petrov. "Yang-Baxter random fields and stochastic vertex models". In: *arXiv preprint* (2019). arXiv:1905.06815 [math.PR]. To appear in Adv. Math.

and of sections 4,5,6 of

[MP20] M. Mucciconi and L. Petrov. "Spin q-Whitaker polynomials and deformed quantum Toda". In: *arXiv preprint* (2020). arXiv:2003.14260 [math.PR]

3.1 Integrable stochastic dynamics on interlacing arrays

In this section we implement the general scheme of passing from symmetric functions satisfying Cauchy type summation identities to probability measures. This approach closely follows the ideas of Schur / Macdonald processes [OR03], [BC14]. We use the framework of *skew Cauchy structures* which is explained in detail in [BMP19, Section 2].

3.1.1 Skew Cauchy structures and random fields

We say that two families of functions $\mathfrak{F}, \mathfrak{G}$ form a *skew Cauchy structure* if they satisfy the following properties:

1. $\mathfrak{F}_{\lambda/\mu}, \mathfrak{G}_{\lambda/\mu}$ are symmetric rational functions in their respective variables, parametrized by pairs of Young diagrams λ/μ (or signatures with appropriate numbers of parts). In particular, $\mathfrak{F}_{\lambda/\mu}, \mathfrak{G}_{\lambda/\mu}$ are nonzero only if $\mu \subseteq \lambda$.

2. Branching rules: for all μ, λ we have

$$\mathfrak{F}_{\nu/\lambda}(u_1, \dots, u_n) = \sum_{\mu} \mathfrak{F}_{\mu/\lambda}(u_1, \dots, u_{n-1}) \mathfrak{F}_{\nu/\mu}(u_n)$$

for any n and any set of variables $u_1, \dots, u_n$, and analogously for $\mathfrak{G}$.

3. There exists a function Π and a set $\mathsf{Adm} \subseteq \mathbb{C}^2$ such that the skew Cauchy identity

$$\Pi(u; v) \sum_{\varkappa} \mathfrak{F}_{\mu/\varkappa}(u) \mathfrak{G}_{\lambda/\varkappa}(v) = \sum_{\nu} \mathfrak{F}_{\nu/\lambda}(u)\, \mathfrak{G}_{\nu/\mu}(v) \tag{3.1}$$

holds numerically for all $(u, v) \in \mathsf{Adm}$. Note that u, v stand for single variables, as in Theorems 2.2.5, 2.3.10 and 2.3.15.

4. There exist two sets $\mathsf{P}, \dot{\mathsf{P}} \subseteq \mathbb{C}$, with $\mathsf{P} \times \dot{\mathsf{P}} \subseteq \mathsf{Adm}$, such that for any choice of $u \in \mathsf{P}$ and $v \in \dot{\mathsf{P}}$ the functions $\mathfrak{F}_{\lambda/\mu}(u), \mathfrak{G}_{\lambda/\mu}(v)$ are non negative for all λ, μ. In this case we say that u, v are *positive specializations*. (Nonnegativity of single-variable functions together with branching implies nonnegativity of multi-variable versions of the functions.)

Consider now two sequences of Young diagrams (or signatures) $\vec{\lambda} = (\lambda^1, \dots, \lambda^n)$ and $\vec{\mu} = (\mu^1, \dots, \mu^{n-1})$ with

$$\lambda^1 \supseteq \mu^1 \subseteq \lambda^2 \supseteq \mu^2 \subseteq \cdots \mu^{n-1} \subseteq \lambda^n,$$

and sequences of positive specializations $u_1, \dots, u_n$ and $v_1, \dots, v_n$ respectively of $\mathfrak{F}$ and $\mathfrak{G}$. The $\mathfrak{F}/\mathfrak{G}$ *process* is the probability measure

$$\mathrm{Prob}(\vec{\lambda}, \vec{\mu}) = \frac{1}{Z} \mathfrak{F}_{\lambda^1}(u_1) \left(\prod_{i=1}^{n-1} \mathfrak{G}_{\lambda^i/\mu^i}(v_i) \mathfrak{F}_{\lambda^{i+1}/\mu^i}(u_{i+1}) \right) \mathfrak{G}_{\lambda^n}(v_n), \tag{3.2}$$

where the normalization constant is $Z = \prod_{i,j} \Pi(u_i; v_j)$.

For applications to stochastic dynamics, it is of interest to consider *random fields* $\{\lambda^{(i,j)}\}$ of Young diagrams indexed by $\mathbb{Z}^2_{\geq 0}$, whose marginal distributions along down-right paths are given by suitable $\mathfrak{F}/\mathfrak{G}$ processes. A *down-right path* is

$$\varpi = \{\varpi_k = (i_k, j_k) \colon 0 \leq k \leq L\}, \quad \text{where} \quad i_0 = j_L = 0 \quad \text{and} \quad \varpi_{k+1} - \varpi_k \in \{\mathbf{e}_1, -\mathbf{e}_2\}.$$

Here L is arbitrary and depends on ϖ, and $\mathbf{e}_1, \mathbf{e}_2$ are the standard basis vectors $(1, 0), (0, 1)$.

Definition 3.1.1. Consider positive specializations $u_1, u_2, \dots$ and $v_1, v_2, \dots$ respectively of functions $\mathfrak{F}$ and $\mathfrak{G}$. An $\mathfrak{F}/\mathfrak{G}$ *field* is a probability measure on the set $\{\lambda^{(i,j)} \colon i, j \in \mathbb{Z}_{\geq 0}\}$ that associates the probability

$$\frac{1}{Z_\varpi} \prod_{k \colon \varpi_{k+1} = \varpi_k + \mathbf{e}_1} \mathfrak{F}_{\lambda^{\varpi_{k+1}}/\lambda^{\varpi_k}}(u_{i_{k+1}}) \prod_{k \colon \varpi_{k+1} = \varpi_k - \mathbf{e}_2} \mathfrak{G}_{\lambda^{\varpi_k}/\lambda^{\varpi_{k+1}}}(v_{j_k}). \tag{3.3}$$

to the event of finding Young diagrams $\lambda^{\varpi_1}, \dots, \lambda^{\varpi_{L-1}}$ along an down-right path ϖ. Here the normalization constant is $Z_\varpi = \prod_{(i,j) \text{ below } \varpi} \Pi(u_i; v_j)$, and at the boundary we fix $\lambda^{(0,j)} = \lambda^{(i,0)} = \varnothing$ with probability one.

Remark 3.1.2. While the $\mathfrak{F}/\mathfrak{G}$ process is defined uniquely by (3.2), it is not determined uniquely by Definition 3.1.1. Below in this section we outline two different constructions of a field in our particular cases. See also the discussion in [BMP19, Section 2.6] for more details and additional references.

To visualize an $\mathfrak{F}/\mathfrak{G}$ field, decorate edges $(i-1,j) \to (i,j)$ of the first quadrant with specializations u_i, and edges $(i,j-1) \to (i,j)$ with v_j. Then for each down-right path ϖ, the probability of finding the sequence λ^{ϖ_k} is computed by climbing down ϖ and picking up skew functions $\mathfrak{F}(u_{i_k})$ along horizontal edges, and $\mathfrak{G}(v_{j_k})$ along vertical edges. See Figure 3.1 for an illustration.

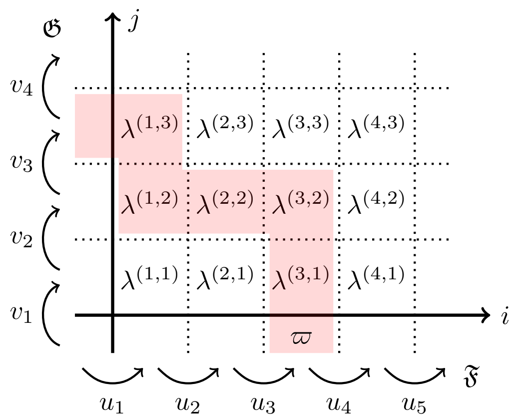

Figure 3.1: A down-right path (highlighted) in a random field, and edge decorations.

In this thesis, particularly interesting instances of $\mathfrak{F}/\mathfrak{G}$ processes will be those arising when considering paths ϖ of the form $(0,T) \to (N,T) \to (N,0)$. Taking the marginal distribution of $\lambda^{(N,1)}, \ldots, \lambda^{(N,T)}$, we arrive at the following definition:

Definition 3.1.3. The *ascending* $\mathfrak{F}/\mathfrak{G}$ *process* is the probability measure on the set of Young diagrams (or signatures)

$$\lambda^1 \subseteq \lambda^2 \subseteq \cdots \subseteq \lambda^N,$$

assigning to each such sequence the probability weight

$$\frac{1}{\prod_{i=1}^N \prod_{j=1}^T \Pi(u_i; v_j)} \mathfrak{F}_{\lambda^1}(u_1)\, \mathfrak{F}_{\lambda^2/\lambda^1}(u_2) \cdots \mathfrak{F}_{\lambda^N/\lambda^{N-1}}(u_N)\, \mathfrak{G}_{\lambda^N}(v_1, \cdots, v_T).$$

3.1.2 Fields based on spin Hall-Littlewood and spin q-Whittaker polynomials

Here we specialize skew Cauchy structures to three cases involving spin q-Whittaker and spin Hall–Littlewood functions.

Definition 3.1.4 (sHL/sHL field)**.** Let $s \in (-1, 0)$ and take parameters $u_i, v_j \in [0, 1)$. The *sHL/sHL field* is obtained by specializing $\mathfrak{F}_{\lambda/\mu}(x_i) = \mathsf{F}_{\lambda'/\mu'}(x_i)$ and $\mathfrak{G}_{\lambda/\mu}(v_j) = \mathsf{F}^*_{\lambda'/\mu'}(v_j)$.

The corresponding skew Cauchy identity is given in Theorem 2.2.5. One readily verifies that the sHL functions specialized like this are nonnegative, which leads to probability distributions. Joint distributions along down-right paths in this field are given by *sHL/sHL processes* which are specializations of (3.2).

Definition 3.1.5 (sqW/sHL field)**.** Let $s \in (-1, 0)$ and take parameters $x_i \in [-s, -s^{-1}]$, $v_j \in [0, 1)$. The *sqW/sHL field* is obtained by specializing $\mathfrak{F}_{\lambda/\mu}(x_i) = \mathbb{F}_{\lambda/\mu}(x_i)$ and $\mathfrak{G}_{\lambda/\mu}(v_j) = \mathsf{F}^{\bullet}_{\lambda'/\mu'}(v_j)$.

The corresponding skew Cauchy identity is given in Theorem 2.3.10. One readily verifies that the sHL and sqW functions specialized like this are nonnegative, which leads to probability distributions. Joint distributions along down-right paths in this field are given by *sqW/sHL processes* which are specializations of (3.2).

Definition 3.1.6 (sqW/sqW field)**.** Let $s \in (-1, 0)$ and take parameters $x_i, y_j \in [-s, -s^{-1}]$. The *sqW/sqW field* is obtained by specializing $\mathfrak{F}_{\lambda/\mu}(x_i) = \mathbb{F}_{\lambda/\mu}(x_i)$ and $\mathfrak{G}_{\lambda/\mu}(y_j) = \mathbb{F}^*_{\lambda/\mu}(y_j)$.

The corresponding skew Cauchy identity is Theorem 2.3.15. The range of parameters here also leads to nonnegative functions $\mathbb{F}, \mathbb{F}^*$, thus producing probability measures. Joint distributions along down-right paths in the sqW/sqW field are given by *sqW/sqW processes* which are specializations of (3.2).

3.1.3 Sampling a field via bijectivization

As mentioned in Remark 3.1.2, a random field is not determined uniquely. Moreover, its properties (like marginal stochastic dynamics) heavily rely on a particular choice of the field's construction. This choice can be encoded by certain Markov transition operators. Let us return to the general formalism of skew Cauchy structures.

Suppose that we have Markov transition operators

$$\mathsf{U}^{\mathrm{fwd}}_{u,v}(\varkappa \to \nu \mid \lambda, \mu) \qquad \text{and} \qquad \mathsf{U}^{\mathrm{bwd}}_{u,v}(\nu \to \varkappa \mid \lambda, \mu),$$

that satisfy the *reversibility condition*

$$\mathsf{U}^{\mathrm{fwd}}_{u,v}(\varkappa \to \nu \mid \lambda, \mu)\Pi(u; v)\mathfrak{F}_{\mu/\varkappa}(u)\mathfrak{G}_{\lambda/\varkappa}(v) = \mathsf{U}^{\mathrm{bwd}}_{u,v}(\nu \to \varkappa \mid \lambda, \mu)\mathfrak{F}_{\nu/\lambda}(u)\,\mathfrak{G}_{\nu/\mu}(v). \quad (3.4)$$

Here $\mathsf{U}^{\mathrm{fwd}}_{u,v}(\varkappa \to \nu \mid \lambda, \mu)$ encodes the probability of a transition $\varkappa \to \nu$ conditioned on λ, μ, whereas $\mathsf{U}^{\mathrm{bwd}}_{u,v}(\nu \to \varkappa \mid \lambda, \mu)$ describes the probability of the opposite move (specializations u, v are assumed positive). See Figure 1.3, left, for an illustration. Summing (3.4) over both ν and $\varkappa$ and using the Markov property of $\mathsf{U}^{\mathrm{fwd}}, \mathsf{U}^{\mathrm{bwd}}$, one recovers the skew Cauchy Identity (3.1). Condition (3.4) determines $\mathsf{U}^{\mathrm{bwd}}$ once $\mathsf{U}^{\mathrm{fwd}}$ if given, and vice versa.

If $\mathsf{U}^{\mathrm{fwd}}$ is given, we can construct a random field $\{\lambda^{(i,j)} : i, j \in \mathbb{Z}_{\geq 0}\}$ as in fig. 1.3, right panel. Namely, fix empty boundary conditions. Inductively for $n \geq 2$, assuming we already sampled Young diagrams $\lambda^{(i,j)}$ with $i+j \le n$, pick $\lambda^{(i',j')}$ for each $i'+j'=n+1$ at random with probabilities

$$\mathsf{U}^{\mathrm{fwd}}_{u_{i'},v_{j'}}(\lambda^{(i'-1,j'-1)} \to \lambda^{(i',j')} \mid \lambda^{(i'-1,j')}, \lambda^{(i',j'-1)}),$$

independently for various pairs (i',j'). We say that the field is *generated* by $\mathsf{U}^{\mathrm{fwd}}$.

Proposition 3.1.7. *Assume that $\mathsf{U}^{\mathrm{fwd}}$ is known. Then the procedure described right above samples an $\mathfrak{F}/\mathfrak{G}$ field.*

Proof. One has to show that the distribution of the Young diagrams along any down-right path is described by the corresponding $\mathfrak{F}/\mathfrak{G}$ process. This is readily verified by induction on adding one box to the area below the down-right path, and using (3.4). We omit the details. □

3.1.4 Borodin–Ferrari fields

Let us now describe a particular choice of the forward transition probabilities which guarantees the existence of a field for a skew Cauchy structure. This construction is based on [BF14] and follows an earlier coupling idea of [DF90]. Choose

$$\begin{aligned}
\mathsf{U}^{\mathrm{fwd}}_{u,v}(\varkappa \to \nu \mid \lambda, \mu) &= \frac{\mathfrak{F}_{\nu/\lambda}(u)\mathfrak{G}_{\nu/\mu}(v)}{\Pi(u;v)\sum_{\varkappa}\mathfrak{F}_{\mu/\varkappa}(u)\mathfrak{G}_{\lambda/\varkappa}(v)},\\
\mathsf{U}^{\mathrm{bwd}}_{u,v}(\nu \to \varkappa \mid \lambda, \mu) &= \frac{\Pi(u;v)\mathfrak{F}_{\mu/\varkappa}(u)\mathfrak{G}_{\lambda/\varkappa}(v)}{\sum_{\nu}\mathfrak{F}_{\nu/\lambda}(u)\mathfrak{G}_{\nu/\mu}(v)}.
\end{aligned} \tag{3.5}$$

In general, although transition probabilities (3.5) are explicit, in particular examples their concrete meaning may be far from transparent.

A helpful simplification can be made if we assume that $\mathfrak{G}$ admits expansion

$$\mathfrak{G}_{\nu/\mu}(v) = (v-v^*)^{d(\nu/\mu)}(g_{\nu/\mu} + \mathsf{O}(v-v^*)), \tag{3.6}$$

for some fixed value v^* independent of ν, μ, coefficients $g_{\nu/\mu}$, and a "nice" degree function d such that $d(\nu/\nu)=0$. Then one can consider a Poisson-type scaling limit of the field (3.5) as $v_j \to v^*$ for all j. Under this scaling, the discrete vertical axis becomes continuous, and the field turns into a Markov dynamics $\{\lambda^{(i,t)} \colon i \in \mathbb{Z}_{\ge 0}, t \in \mathbb{R}_{\ge 0}\}$, where t is the continuous time variable. The dynamics lives on sequences of signatures.

When $\mathfrak{F}, \mathfrak{G}$ are Schur functions, such continuous processes is the *push–block dynamics* introduced in [BF14].

3.1.5 Bijectivization of the Yang–Baxter equation

In many cases, skew Cauchy Identities descend directly from the Yang–Baxter equation and we have seen examples of this phenomenon in chapter 2. This observation was used in [BP19], [BMP19] to provide an explicit construction of random fields for sHL and sqW functions, which we briefly recall here. In general, this approach produces fields which *differ* from the Borodin–Ferrari ones. On the other hand, *Yang–Baxter fields* by design possess Markovian marginals.

For any given identity with positive terms

$$\sum_{a\in A} \mathsf{w}(a) = \sum_{b\in B} \mathsf{w}(b), \tag{3.7}$$

we say that two stochastic matrices $\mathbf{p}^{\mathrm{fwd}}(a,b)$ and $\mathbf{p}^{\mathrm{bwd}}(b,a)$ (with indices $a \in A$, $b \in B$) form a (stochastic) *bijectivization of identity* (3.7) if they satisfy the reversibility condition

$$\mathbf{p}^{\mathrm{fwd}}(a \to b)\, \mathsf{w}(a) = \mathbf{p}^{\mathrm{bwd}}(b \to a)\, \mathsf{w}(b) \qquad \text{for all } a \in A,\ b \in B.$$

A bijectivization always exists since we can take $\mathbf{p}^{\mathrm{fwd}}(a \to b) \propto \mathsf{w}(b)$. A bijectivization is unique only when A or B has a single element. Another simple case is given when both A and B have only two elements.

Example 3.1.8. When $A = \{a_1, a_2\}$ and $B = \{b_1, b_2\}$, identity (3.7) becomes

$$\mathsf{w}(a_1) + \mathsf{w}(a_2) = \mathsf{w}(b_1) + \mathsf{w}(b_2).$$

In this case all stochastic bijectivizations $\mathbf{p}^{\mathrm{fwd}}$, $\mathbf{p}^{\mathrm{bwd}}$ are expressed as

$$\begin{aligned}
\mathbf{p}^{\mathrm{fwd}}(a_1 \to b_1) &= \gamma, & \mathbf{p}^{\mathrm{fwd}}(a_2 \to b_1) &= \frac{\mathsf{w}(a_2) - \mathsf{w}(b_2) + (1-\gamma)\mathsf{w}(a_1)}{\mathsf{w}(a_2)},\\
\mathbf{p}^{\mathrm{fwd}}(a_1 \to b_2) &= 1 - \gamma, & \mathbf{p}^{\mathrm{fwd}}(a_2 \to b_2) &= 1 - \mathbf{p}^{\mathrm{fwd}}(a_2 \to b_1),
\end{aligned}$$

for a parameter $\gamma \in [0, 1]$.

Let now (3.7) be one of the Yang–Baxter equations from Chapter B, corresponding to fig. B.5 (b) or fig. B.7 (b). Let us rewrite them in a unified notation as

$$\sum_{K} \mathsf{wl}(K \mid I, J) = \sum_{K'} \mathsf{wr}(K' \mid I, J), \tag{3.8}$$

where $I = \{i_1, i_2, i_3\}$, $J = \{j_1, j_2, j_3\}$, $K = \{k_1, k_2, k_3\}$ and $K' = \{k'_1, k'_2, k'_3\}$, and weight functions wl, wr denote the terms in the left and right-hand sides of each of the Yang-Baxter equations of chapter B involving pairs of non-dual and dual weights. Equations (B.26) and (B.27) involving corner weights, by agreement, correspond to the choice $j_1 = \varnothing$.

Denote by $\mathbf{p}^{\mathrm{fwd}}_{I,J}(K \to K')$ and $\mathbf{p}^{\mathrm{bwd}}_{I,J}(K' \to K)$ a stochastic bijectivization of (3.8). Then $\mathbf{p}^{\mathrm{fwd}}_{I,J}$ is the probability of moving the cross from left to right (in the local configuration in Figure B.5 (b)), while transforming the occupation numbers K into K'. The probabilities $\mathbf{p}^{\mathrm{bwd}}_{I,J}(K' \to K)$ similarly correspond to moving the cross from right to left. By the conservation of paths at each vertex, once I, J are fixed, the configuration K is completely determined specifying only one of the numbers k_1, k_2, or k_3 (and similarly for K').

Bijectivizations of the Yang–Baxter equation are building blocks of operators $\mathsf{U}^{\mathrm{fwd}}, \mathsf{U}^{\mathrm{bwd}}$. Given Young diagrams $\varkappa, \mu, \lambda, \nu$ we identify path configurations through two rows of vertices as in Figure 3.2, that is using their dual path representation[1] as discussed in Section 2.1.2. Vertices crossed by blue paths are assigned non dual weights (w or W) (2.12)–(2.14) whereas those in red have dual weights (w^* or W^*). We assume that at the leftmost column an infinite number of paths flows in the vertical direction. The transition probability $\mathsf{U}^{\mathrm{fwd}}(\varkappa \to \nu \mid \lambda, \mu)$ is the product of probabilities of sequential local moves $\mathbf{p}^{\mathrm{fwd}}$ obtained dragging the cross vertex from the leftmost column to the right. In case we are considering transition probabilities between signatures such dragging will terminate at a specific location N, where the corner weights $W^{\lrcorner}$ will necessarily have to be employed.

The operator $\mathsf{U}^{\mathrm{bwd}}$ is constructed using the opposite local moves with probabilities $\mathbf{p}^{\mathrm{bwd}}$, starting from a column very far to the right. See Figure 3.2 for an illustration.

Definition 3.1.9. The random field constructed from operators $\mathsf{U}^{\mathrm{fwd}}$ takes the name of *Yang-Baxter field*. In this case we say that $\mathsf{U}^{\mathrm{fwd}}$ is generated by local moves $\mathbf{p}^{\mathrm{fwd}}$.

3.1.6 Three Yang-Baxter fields

In this subsection we specialize the construction described in section 3.1.5 to demonstrate that Yang-Baxter fields sample random fields weighted by sHL and sqW functions.

We consider first a stochastic bijectivization $\mathbf{p}^{\mathrm{fwd}}$ and $\mathbf{p}^{\mathrm{bwd}}$ of the Yang-Baxter equation (B.2). We fix parameters $q \in (0,1)$, $s \in (-1,0)$, and $u_i, v_j \in [0,1)$, $i,j \in \mathbb{Z}_{\geq 1}$. To distinguish this case from the one that we will follow we will denote the Markov operators generated by $\mathbf{p}^{\mathrm{fwd}}$ and $\mathbf{p}^{\mathrm{bwd}}$ respectively as $\mathsf{U}^{\mathrm{fwd}}_{\mathrm{sHL}(u),\mathrm{sHL}(v)}$ and $\mathsf{U}^{\mathrm{bwd}}_{\mathrm{sHL}(u),\mathrm{sHL}(v)}$.

Proposition 3.1.10. *The random field $\{\lambda^{(i,j)} : i,j \in \mathbb{Z}_{\geq 0}\}$ generated by $\mathsf{U}^{\mathrm{fwd}}_{\mathrm{sHL}(u_i),\mathrm{sHL}(v_j)}$ is a sHL/sHL field as in definition 3.1.4. In particular the single-point distributions have the form*

$$\mathrm{Prob}\big(\lambda^{(i,j)} = \nu\big) = \prod_{\substack{1 \leq i' \leq i \\ 1 \leq j' \leq j}} \frac{1 - u_{j'} v_{i'}}{1 - q u_{j'} v_{i'}} \, \mathsf{F}_{\nu'}(u_1, \ldots, u_i) \, \mathsf{F}^*_{\nu'}(v_1, \ldots, v_j),$$

where ν is an arbitrary fixed Young diagram.

The proof of proposition 3.1.10 is a straightforward consequence of the following bijective proof of the skew Cauchy identity (2.11).

Proposition 3.1.11. *For any four Young diagrams $\mu, \varkappa, \lambda, \nu$ we have*

$$\frac{1 - quv}{1 - uv} \mathsf{U}^{\mathrm{fwd}}_{\mathrm{sHL}(u),\mathrm{sHL}(v)}(\varkappa \to \nu \mid \lambda, \mu) \, \mathsf{F}_{\lambda'/\varkappa'}(u) \, \mathsf{F}^*_{\mu'/\varkappa'}(v) \\ = \mathsf{U}^{\mathrm{bwd}}_{\mathrm{sHL}(u),\mathrm{sHL}(v)}(\nu \to \varkappa \mid \lambda, \mu) \, \mathsf{F}^*_{\nu'/\lambda'}(v) \, \mathsf{F}_{\nu'/\mu'}(u). \quad (3.9)$$

Summing (3.9) over both $\varkappa$ and ν, we obtain the skew Cauchy identity for the stable sHL functions (Theorem 2.2.5).

[1] to a Young diagram λ we associate the arrow representation $|\lambda'\rangle$. We switch to this convention in order to treat random fields corresponding to sHL and sqW functions on an equal footing

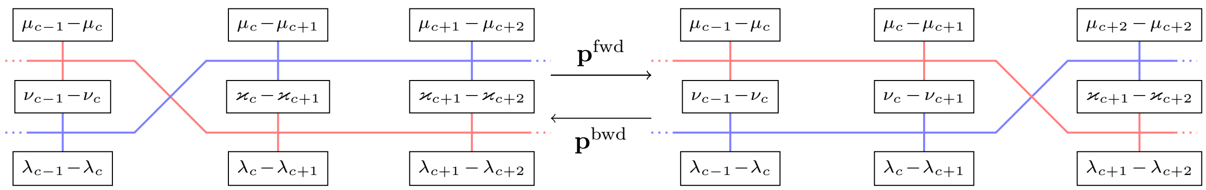

Figure 3.2: A local random move in a Yang–Baxter field. Moving the cross through the column c updates the value of $\varkappa_c - \varkappa_{c+1}$ to $\nu_c - \nu_{c+1}$.

Proof. The product $\mathsf{F}_{\lambda'/\varkappa'}(u)\mathsf{F}^*_{\mu'/\varkappa'}(v)$ is the weight of a configuration $\mu \succ \varkappa \prec \lambda$ in a vertex model obtained attaching a $w_{u,s}$-weighted row of vertices on top of a $w^*_{v,s}$-weighted row of vertices. The leftmost column is occupied by infinitely many paths. The factor $(1-quv)/(1-uv)$ is the R_{uv} weight of a cross 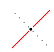 attached at the left of the lattice. Now we employ the definition of $\mathsf{U}^{\mathrm{fwd}}_{\mathrm{sHL}(u),\mathrm{sHL}(v)}$ and drag the cross all the way to the right, replacing $\varkappa$ by the random ν. This procedure, along with the local reversibility condition of the bijectivization leaves us with the right-hand side of the desired identity (3.9). □

Results of proposition 3.1.10 and proposition 3.1.11 extend naturally to the case when we consider Yang-Baxter equations related to sqW polynomials. In the following we report these results omitting the details of proofs.

Proposition 3.1.12. *Let $\mathbf{p}^{\mathrm{fwd}}$ and $\mathbf{p}^{\mathrm{bwd}}$ be a stochastic bijectivization of Yang–Baxter equations* (B.11), (B.26) *for the weights W, w^*, and $\mathsf{U}^{\mathrm{fwd}}$ be constructed from sequential local moves $\mathbf{p}^{\mathrm{fwd}}$. Then the random field generated by $\mathsf{U}^{\mathrm{fwd}}$ is a sqW/sHL field.*

Proposition 3.1.13. *Let $\mathbf{p}^{\mathrm{fwd}}$ and $\mathbf{p}^{\mathrm{bwd}}$ be a stochastic bijectivization of Yang–Baxter equations* (B.12), (B.26) *for the weights W, W^*, and $\mathsf{U}^{\mathrm{fwd}}$ be constructed from sequential local moves $\mathbf{p}^{\mathrm{fwd}}$. Then the random field generated by $\mathsf{U}^{\mathrm{fwd}}$ is a sqW/sqW field.*

3.1.7 Markov marginals of a Yang-Baxter field

By the very construction, we see that for any fixed $c \geq 1$, the update $(\varkappa_1, \dots, \varkappa_c) \to (\nu_1, \dots, \nu_c)$ in a Yang-Baxter field is independent of $\varkappa_i, \mu_i, \lambda_i$ for all $i \geq c+1$. Therefore, we have:

Proposition 3.1.14. *Let $\{\lambda^{(i,j)} \colon i,j \in \mathbb{Z}_{j\in\geq 0}\}$ be a Yang–Baxter random field as above. For any $c \in \mathbb{Z}_{\geq 1}$, the marginal process $\{(\lambda_1^{(i,j)} \geq \cdots \geq \lambda_c^{(i,j)}) : i,j \in \mathbb{Z}_{\geq 0}\}$ is a Markov process.*

Proof. This is [BP19, Proposition 6.2]. □

In the simplest case $c = 1$, transition probabilities of the one-dimensional marginal field can be written down explicitly:

Proposition 3.1.15. *Let $\{\lambda^{(i,j)} : i,j \in \mathbb{Z}_{\geq}0\}$ be a random field generated by $\mathsf{U}^{\mathrm{fwd}}$ constructed from bijectivization of the Yang–Baxter equation. Let $\{\lambda_1^{(i,j)} : i,j \in \mathbb{Z}_{\geq 0}\}$ be the first row marginal process. Then for all $i,j \geq 1$ we have*

$$\mathrm{Prob}\{\lambda_1^{(i,j)} = n \mid \lambda_1^{(i,j-1)} = m, \lambda_1^{(i-1,j)} = \ell, \lambda_1^{(i-1,j-1)} = k\} = \mathbf{L}_{u_i,v_i}(m-k, \ell-k; n-\ell, n-m), \tag{3.10}$$

for all $n,m,k,n \geq 0$, where $\mathbf{L}$ is the stochastic vertex weight

$$\mathbf{L}_{u,v}(j_2, j_1; k_1', k_2') = \frac{\mathsf{wr}_{\{0,0,\infty\},\{j_1,j_2,\infty\}}(\{k_1', k_2', \infty\})}{\sum_{k_1,k_2} \mathsf{wl}_{\{0,0,\infty\},\{j_1,j_2,\infty\}}(\{k_1,k_2,\infty\})}. \tag{3.11}$$

Note that interlacing implies that $k \leq m \leq n$, $k \leq \ell \leq n$, so the arguments of $\mathbf{L}_{u_i,v_i}$ in (3.10) are all nonnegative.

Proof of Proposition 3.1.15. This is proven in [BMP19, Section 6.4] and we briefly reproduce the argument here. The update $\lambda_1^{(i-1,j-1)} \to \lambda_1^{(i,j)}$, once $\lambda_1^{(i-1,j)}, \lambda_1^{(i,j-1)}$ are fixed, is determined only by a single random move at the leftmost column of vertices. By construction, the vertical direction at the leftmost column has infinitely many paths. The corresponding Yang–Baxter equation is

$$\sum_{k_1,k_2} \mathsf{wl}(\{k_1,k_2,\infty\} \mid \{0,0,\infty\},\{j_1,j_2,\infty\}) = \sum_{k_1',k_2'} \mathsf{wr}(\{k_1',k_2',\infty\} \mid \{0,0,\infty\},\{j_1,j_2,\infty\}). \tag{3.12}$$

This implies that taking

$$\mathbf{p}^{\mathrm{fwd}}_{\{0,0,\infty\},\{j_1,j_2,\infty\}}(\{k_1,k_2,\infty\} \to \{k_1',k_2',\infty\}) = \mathbf{L}_{u,v}(j_2,j_1;k_2',k_1')$$

indeed produces a bijectivization.[2] Here u,v denote generic spectral parameters of weights appearing in the Yang–Baxter equation. Recall that occupation numbers are related to signatures as

$$\begin{aligned} j_1 &= \lambda_1^{(i-1,j)} - \lambda_1^{(i-1,j-1)}, \qquad & j_2 &= \lambda_1^{(i,j-1)} - \lambda_1^{(i-1,j-1)}, \\ k_1' &= \lambda_1^{(i,j)} - \lambda_1^{(i,j-1)}, \qquad & k_2' &= \lambda_1^{(i,j)} - \lambda_1^{(i-1,j)}. \end{aligned} \tag{3.13}$$

This completes the proof. □

The fact that the sqW functions are parametrized by signatures with specified number of rows also allows to access the random dynamics of *last rows* of a field by writing down explicit bijectivizations. In particular, the evolution of $\{\lambda_i^{(i,j)} : i,j \geq 0\}$ is related to the Yang–Baxter equations (B.26), (B.27) corresponding to configurations depicted in Figure B.5 (b).

Remark 3.1.16. The construction of a random field using stochastic bijectivizations *does not guarantee* that the evolution of last rows is autonomous. This contrasts with the fact that the first rows form autonomous Markov marginal processes by the very construction of Yang–Baxter fields (Proposition 3.1.14). In Theorems 3.3.10 and 3.3.16 below we show that the marginals $\{\lambda_i^{(i,j)} : i,j \geq 0\}$ of sqW/sHL and sqW/sqW fields, respectively, are in fact autonomous for a particular bijectivization we construct.

[2] This bijectivization is in fact unique for our choices of weights (this follows similarly to [BMP19]). However, we do not need this fact.

3.2 Schur case: Robinson–Schensted–Knuth from Yang–Baxter

In this section, as a simpler illustration, we consider the degeneration of the vertex weights and the Yang–Baxter equation obtained by setting $q = s = 0$, and show how this produces (via bijectivization) the classical Robinson–Schensted–Knuth (RSK) row insertion algorithm [Knu70], [Ful97], [Sta01]. We would obtain a "local" description of the RSK insertion in terms of "toggle" operations. We refer to, e.g., [Pak01], [KB95], [Fom95] and also to the recent notes [Hop14] for this description.

We consider the $q = s = 0$ degeneration of the Yang–Baxter equations ((B.12)(B.26)) proving the sqW/sqW skew Cauchy identity (Theorem 2.3.15). Note that for $q = s = 0$, the spin q-Whittaker polynomials become the Schur polynomials. The Yang–Baxter equations we need are illustrated in Figure B.5. In fact, in the Schur degeneration the corner Yang–Baxter equation Equation (B.27) illustrated in Figure B.7 (b) is the same as the usual one, and so we only need the equation from Equation (B.12).

The weights entering the Yang–Baxter equation degenerate as follows:

$$\begin{aligned} W_{x,0}(i_1, j_1; i_2, j_2) &= \mathbf{1}_{i_1+j_1=i_2+j_2}\, \mathbf{1}_{i_1 \geq j_2}\, x^{j_2}, \\ W^*_{y,0}(i_1, j_1; i_2, j_2) &= \mathbf{1}_{i_1+j_2=i_2+j_1}\, \mathbf{1}_{i_2 \geq j_2}\, y^{j_2}, \\ \mathbb{R}_{x,y,s}(i_1, j_1; i_2, j_2) &= \mathbf{1}_{i_2+j_1=i_1+j_2}\, (xy)^{\min(j_1,j_2)}. \end{aligned} \tag{3.14}$$

Equation (B.12) thus reads for all fixed $i_1, i_2, i_3, j_1, j_2, j_3 \in \mathbb{Z}_{\geq 0}$:

$$\begin{aligned} &\sum_{k_1,k_2,k_3 \geq 0} \mathbf{1}_{\text{arrow preservation}}\, \mathbf{1}_{k_3 \geq \max(j_1,j_2)}\, x^{j_2} y^{j_1} (xy)^{\min(k_1,k_2)} \\ &\qquad = \sum_{k_1',k_2',k_3' \geq 0} \mathbf{1}_{\text{arrow preservation}}\, \mathbf{1}_{i_3 \geq k_2'} \mathbf{1}_{j_3 \geq k_1'} (xy)^{\min(j_1,j_2)} x^{k_2'} y^{k_1'}, \end{aligned} \tag{3.15}$$

where by "arrow preservation" we mean the intersection of all the conditions of the form $a_1 + b_1 = a_2 + b_2$ in (3.14) which the indices k_1, k_2, k_3 and k_1', k_2', k_3' must satisfy. In particular, by arrow preservation we have

$$k_2 = i_2 + k_1 - i_1, \qquad k_3 = i_3 + j_1 - k_1, \qquad k_2' = j_2 + k_1' - j_1, \qquad k_3' = i_1 + j_3 - k_1',$$

and thus the summands in the left- and right-hand sides of (3.15) are indexed only by k_1 or k_1', respectively. Equation (3.15) admits a bijective proof (or, in terms of Section 3.1, a bijectivization which is deterministic):

Lemma 3.2.1. *Setting*

$$k_1' = j_1 - \min(j_1, j_2) + \min(k_1, i_2 + k_1 - i_1) \tag{3.16}$$

produces a bijection between the terms in both sides of (3.15).

Proof. By (3.16) we see that the powers of y in the corresponding terms match. The powers of x match, too:

$$j_2 + \min(k_1, i_2 + k_1 - i_1) = \min(j_1, j_2) + j_2 + k_1' - j_1,$$

where k_1' is given by (3.16). It remains to check that if k_1 is such that the product of indicators in the left-hand side of (3.15) is nonzero, then the same holds for k_1' in the right-hand side. This check is straightforward. □

Let us now interpret a sequence of bijective Yang–Baxter transformations as a row RSK insertion. Fix signatures λ, μ and use Lemma 3.2.1 to construct a bijection between the sets

$$\{\varkappa\colon \varkappa \prec \lambda,\ \varkappa \prec \mu\} \times \mathbb{Z}_{\geq 0} \longleftrightarrow \{\nu\colon \nu \succ \lambda,\ \nu \succ \mu\}. \tag{3.17}$$

This bijection would correspond to a local move in the "Fomin growth diagram" [Fom95] interpretation of the RSK.

Interpret $\mu, \varkappa, \lambda$ as a path configuration as in Figure 3.2. The numbers of paths through vertical edges are then equal to $\mu_c - \mu_{c+1}$, $\varkappa_c - \varkappa_{c+1}$, and $\lambda_c - \lambda_{c+1}$. One can also check that the horizontal edges carry $\mu_c - \varkappa_c$ and $\lambda_c - \varkappa_c$ paths.

Attach a cross at the leftmost boundary of the path configuration. This cross is not uniquely determined since at the leftmost boundary (with $i_3 = j_3 = \infty$, $i_1 = i_2 = 0$) the Yang–Baxter equation (3.15) takes the form

$$x^{j_2} y^{j_1} \sum_{k=0}^{\infty} (xy)^k = (xy)^{\min(j_1,j_2)} x^{j_2 - j_1} \sum_{k_1' \geq 0} \mathbf{1}_{\text{arrow preservation}}\, x^{k_1'} y^{k_1'}.$$

Arrow preservation in the right-hand side here means that there exists an arrow configuration with the given k_1'.

Selecting an arbitrary k in the left-hand side is equivalent to selecting an element of $\mathbb{Z}_{\geq 0}$ in the left-hand side of (3.17). Then we set based on the Yang–Baxter equation (see Lemma 3.2.1):

$$k_1' = j_1 - \min(j_1, j_2) + k.$$

In terms of signatures, k_1' corresponds to the new number of paths on the horizontal edge, and so the above equation means that

$$\nu_1 - \mu_1 = \lambda_1 - \varkappa_1 - \min(\lambda_1 - \varkappa_1, \mu_1 - \varkappa_1) + k,$$

that is,

$$\nu_1 = k + \max(\lambda_1, \mu_1). \tag{3.18}$$

After dealing with the leftmost boundary, we move the cross one by one to the right, updating each $\varkappa_c - \varkappa_{c+1}$ to $\nu_c - \nu_{c+1}$, where $c \geq 2$. At each step the signatures correspond to the path numbers as

$$j_1 = \lambda_{c+1} - \varkappa_{c+1}, \qquad j_2 = \mu_{c+1} - \varkappa_{c+1}, \qquad k_1 = \lambda_c - \varkappa_c, \qquad k_2 = i_2 + k_1 - i_1 = \mu_c - \varkappa_c,$$
$$k_1' = \nu_{c+1} - \mu_{c+1}, \qquad k_2' = j_2 + k_1' - j_1 = \nu_{c+1} - \lambda_{c+1}.$$

The local bijection of Lemma 3.2.1 then leads to

$$\begin{aligned} k_1' &= j_1 - \min(j_1, j_2) + \min(k_1, k_2) \\ &= \lambda_{c+1} - \varkappa_{c+1} - \min(\lambda_{c+1} - \varkappa_{c+1}, \mu_{c+1} - \varkappa_{c+1}) + \min(\lambda_c - \varkappa_c, \mu_c - \varkappa_c) \\ &= \lambda_{c+1} - \min(\lambda_{c+1}, \mu_{c+1}) - \varkappa_c + \min(\lambda_c, \mu_c), \end{aligned}$$

which leads to

$$\nu_{c+1} = \max(\lambda_{c+1}, \mu_{c+1}) + \min(\lambda_c, \mu_c) - \varkappa_c. \tag{3.19}$$

Formulas (3.18)–(3.19) for ν in terms of $\varkappa$ provide the local RSK bijection between the two sets (3.17). Moreover, these formulas have the "toggle" form, e.g., see [Hop14].

Therefore, we see that in the Schur degeneration the Yang–Baxter equation of Equation (B.12) produces a bijection, and this bijection coincides with the "toggle" bijection in the local description of the classical Robinson–Schensted–Knuth row insertion.

3.3 Marginals of spin Hall-Littlewood and spin q-Whittaker fields

In this section we characterize marginals of random fields defined in Section 3.1.2 corresponding to the first and last coordinates $\lambda_1^{(i,j)}$ and $\lambda_i^{(i,j)}$. These are matched with stochastic vertex models or particle dynamics introduced in [GS92] [Pov13], [CP16], [CMP19]. In case of fields weighter by sqW functions, these results extend the characterization of marginals of the q-Whittaker processes given in [MP17] by adding the spin parameter s into the picture. The matchings are summarized in the table in Figure 3.3.

	first row $\lambda_1^{(i,j)}$	last row $\lambda_i^{(i,j)}$
sHL/sHL field	[3.3.2] Stochastic six vertex model [GS92],[BCG16]	
sqW/sHL field	[3.3.4] Stochastic higher spin six vertex model [CP16], [BP18a]	[3.3.3] Stochastic higher spin six vertex model [CP16], [BP18a]
sqW/sqW field	[3.3.6] ${}_4\phi_3$ vertex model and q-Hahn PushTASEP [CMP19], [BMP19]	[3.3.5, 3.3.7] q-Hahn TASEP / Boson particle systems [Pov13], [Cor14]

Figure 3.3: A summary of matchings of Section 3.3, with numbers of relevant subsections.

3.3.1 Stochastic vertex models

We work with two typologies of stochastic vertex models: *up-right* or *up-left*. These are probability measures on directed path ensembles (of the corresponding direction) in the integer quadrant, constructed from families of *stochastic vertex weights* $L_{(i,j)}$. By "stochastic" we mean that the weights must satisfy the sum to one condition

$$\sum_{\alpha_2,\beta_2\geq 0} L_{(i,j)}(\alpha_1,\beta_1;\alpha_2,\beta_2)=1 \tag{3.20}$$

for all α_1,β_1, where $\alpha_1,\alpha_2,\beta_1,\beta_2\in\mathbb{Z}_{\geq 0}$ are the occupation numbers of edges at a vertex (i,j).

For the first type of stochastic vertex models, equip the lattice with *up-right* vertex weights $L^{\mathrm{ur}}_{(i,j)}$ subject to the arrow preservation condition

$$L^{\mathrm{ur}}_{(i,j)}(\alpha_1,\beta_1;\alpha_2,\beta_2)=0 \qquad \text{if} \qquad \alpha_1+\beta_1\neq\alpha_2+\beta_2.$$

Definition 3.3.1 (Up-right stochastic vertex model)**.** The *up-right stochastic vertex model* with weights $L^{\mathrm{ur}}_{(i,j)}$ and boundary conditions $B^{\mathrm{h}}=\{b^{\mathrm{h}}_1,b^{\mathrm{h}}_2,\dots\}$, $B^{\mathrm{v}}=\{b^{\mathrm{v}}_1,b^{\mathrm{v}}_2,\dots\}$, with $b^{\mathrm{h}}_i,b^{\mathrm{v}}_j\geq 0$, is the unique probability measure on the set of up-right directed paths on $\mathbb{Z}_{\geq 1}\times\mathbb{Z}_{\geq 0}$, such that:

- each vertex $(1,j)$ emanates b^{v}_j paths initially directed to the right;
- each vertex $(i,0)$ emanates b^{h}_i paths initially directed upwards;
- the probability of observing a configuration $(\alpha_1,\beta_1;\alpha_2,\beta_2)$ at vertex (i,j), conditioned on the configuration at all vertices (i',j') with $i'+j'<i+j$, is given by $L^{\mathrm{ur}}_{(i,j)}(\alpha_1,\beta_1;\alpha_2,\beta_2)$. Moreover, this event is independent of choosing arrow configurations at other vertices $\dots,(i-1,j+1),(i+1,j-1),\dots$ on the same diagonal.

Up-right directed lattice path configurations can be encoded by the *height function*:

$$\mathcal{H}^{\mathrm{ur}}(i,j)=\#\{\text{occupations at horizontal edges}\}-\#\{\text{occupations at vertical edges}\}, \tag{3.21}$$

where occupations are counted along the path $(\frac{1}{2},\frac{1}{2})\to(i+\frac{1}{2},\frac{1}{2})\to(i+\frac{1}{2},j+\frac{1}{2})$ (equivalently, along any up-right directed path from $(\frac{1}{2},\frac{1}{2})$ to $(i+\frac{1}{2},j+\frac{1}{2})$). See Figure 3.4, right, for an illustration of the vertex model and the corresponding height function.

Remark 3.3.2 (Up-right model and TASEPs)**.** Path configurations can be interpreted as trajectories of particles performing totally asymmetric random walks, with time running in the upward direction. In particular, one can define a process

$$\{\mathsf{X}(t)=(\mathsf{x}_1(t)>\mathsf{x}_2(t)>\cdots)\}_{t\in\mathbb{Z}_{\geq 0}}$$

by setting $\mathsf{x}_n(t):=\mathcal{H}^{\mathrm{ur}}(n,t)-n$. Then X is a discrete time totally asymmetric simple exclusion process, in which the random jump $\mathsf{x}_n(t-1)\to\mathsf{x}_n(t)$ of the n-th particle at time t is governed by

$$L^{\mathrm{ur}}_{(n,t)}\big(\mathsf{x}_{n-1}(t-1)-\mathsf{x}_n(t-1)-1,\mathsf{x}_{n-1}(t)-\mathsf{x}_{n-1}(t-1);\mathsf{x}_{n-1}(t)-\mathsf{x}_n(t)-1,\mathsf{x}_n(t)-\mathsf{x}_n(t-1)\big).$$

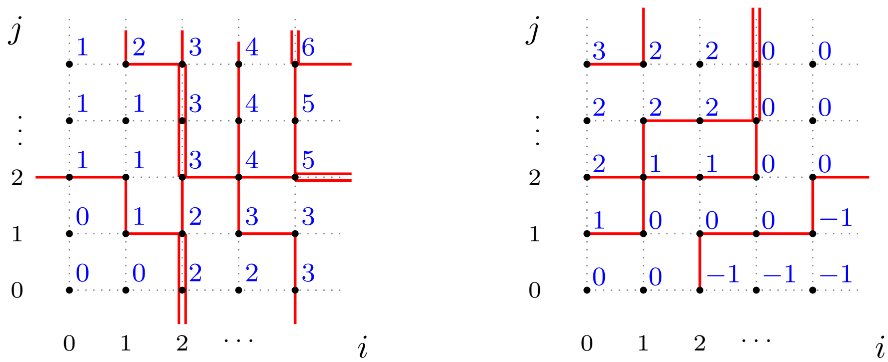

Figure 3.4: Realizations of the up-left and the up-right stochastic vertex models (left and right panels, respectively).

Let us now turn to up-left path ensembles. The *up-left* weights $L^{\mathrm{ul}}_{(i,j)}$ satisfy the following arrow preservation property:

$$L^{\mathrm{ul}}_{(i,j)}(\alpha_1, \beta_1; \alpha_2, \beta_2) = 0 \qquad \text{if} \qquad \alpha_1 + \beta_2 \neq \beta_1 + \alpha_2.$$

Definition 3.3.3 (Up-left stochastic vertex model)**.** The *up-left stochastic vertex model* with weights $L^{\mathrm{ul}}_{(i,j)}$ and boundary conditions $B^{\mathrm{h}} = \{b^{\mathrm{h}}_1, b^{\mathrm{h}}_2, \dots\}$, $B^{\mathrm{v}} = \{b^{\mathrm{v}}_1, b^{\mathrm{v}}_2, \dots\}$, with $b^{\mathrm{h}}_i, b^{\mathrm{v}}_j \geq 0$, is the unique probability measure on the set of up-left directed path on $\mathbb{Z}_{\geq 1} \times \mathbb{Z}_{\geq 0}$, such that:

- each vertex $(1, j)$ has b^{v}_j paths entering from its left;
- each vertex $(i, 0)$ emanates b^{h}_i paths initially directed upwards;
- the probability of observing a configuration $(\alpha_1, \beta_1; \alpha_2, \beta_2)$ at a vertex (i, j), conditioned on the path configuration at vertices (i', j') with $i' + j' < i + j$, is given by $L^{\mathrm{ul}}_{(i,j)}(\alpha_1, \beta_1; \alpha_2, \beta_2)$. Moreover, this event is independent of choosing arrow configurations at other vertices $\dots, (i-1, j+1), (i+1, j-1), \dots$ on the same diagonal.

Up-left directed lattice path configurations can be encoded by the *height function*:

$$\mathcal{H}^{\mathrm{ul}}(i, j) = \#\{\text{occupations at horizontal edges}\} + \#\{\text{occupations at vertical edges}\}, \tag{3.22}$$

where occupations are counted along the path $(\frac{1}{2}, \frac{1}{2}) \to (i + \frac{1}{2}, \frac{1}{2}) \to (i + \frac{1}{2}, j + \frac{1}{2})$ (equivalently, along any up-right directed path from $(\frac{1}{2}, \frac{1}{2})$ to $(i + \frac{1}{2}, j + \frac{1}{2})$). Notice the difference in sign with the definition of $\mathcal{H}^{\mathrm{ur}}$ (3.21). See Figure 3.4, left, for an illustration of the up-left vertex model and the corresponding height function.

Remark 3.3.4 (Up-left model and PushTASEPs)**.** Define a process

$$\{\mathsf{Y}(t) = (\mathsf{y}_1(t) > \mathsf{y}_2(t) > \cdots)\}_{t \in \mathbb{Z}_{\geq 0}}$$

by setting $\mathsf{y}_n(t) = -\mathcal{H}^{\text{ul}}(n,t) - n$. Then Y is a discrete time totally asymmetric simple exclusion process under which particles jump to the left, and a *pushing mechanism* is present. The random jump $\mathsf{y}_n(t-1) \to \mathsf{y}_n(t)$ of the n-th particle at time t is governed by $L^{\text{ul}}_{(n,t)}\big(\mathsf{y}_{n-1}(t-1) - \mathsf{y}_n(t-1) - 1, \mathsf{y}_{n-1}(t-1) - \mathsf{y}_{n-1}(t); \mathsf{y}_{n-1}(t) - \mathsf{y}_n(t) - 1, \mathsf{y}_n(t-1) - \mathsf{y}_n(t)\big)$.

In the rest of this section we establish the matching results outlined in Figure 3.3.

3.3.2 First row in the sHL/sHL field

Here we study the scalar Markov marginal $\lambda_1^{(i,j)}$ of the sHL/sHL Yang-Baxter field, and match it to the stochastic six vertex model.

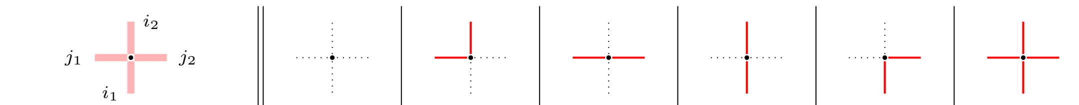

$\mathsf{L}_{uv}(i_1, j_1; i_2, j_2)$	1	$\frac{uv(1-t)}{1-tuv}$	$\frac{1-uv}{1-tuv}$	$\frac{t(1-uv)}{1-tuv}$	$\frac{1-t}{1-tuv}$	1

Figure 3.5: The vertex weights $\mathsf{L}_{uv}(i_1, j_1; i_2, j_2)$ in the stochastic six vertex model. This parametrization of the vertex weights follows, e.g., [BM18].

Definition 3.3.5 ([GS92], [BCG16])**.** Specialize the up-right stochastic vertex model of Definition 3.3.1 by taking $L^{\text{ur}}_{(i,j)} = \mathsf{L}_{u_i v_j}$ given in Figure 3.5. We refer to this model as the *stochastic six vertex model.* We consider the *step* boundary conditions:

$$b^{\text{v}}_j = 1 \qquad \text{and} \qquad b^{\text{h}}_i = 0, \tag{3.23}$$

The next theorem is analogous to [BP19, Proposition 7.3].

Theorem 3.3.6. *Let $\mathcal{H}^{\text{ur}}_{6\text{V}}(i,j)$ be the height function of the six vertex model with step boundary conditions and let $\{\lambda^{(i,j)}\}$ be the sHL/sHL field. Then the two random fields $\{j - \lambda_1^{(i,j)} : i, j \in \mathbb{Z}_{\geq 0}\}$ and $\{\mathcal{H}^{\text{ur}}_{6\text{V}}(i,j) : i, j \in \mathbb{Z}_{\geq 0}\}$ are equal in distribution.*

Proof. Recall that, by proposition 3.1.15, the Markov evolution of the scalar marginal $\lambda_1^{(x,y)}$ is determined by the quantity $\mathbf{L}$ of eq. (3.11) corresponding to Yang-Baxter equation (B.2). Its expression can be readily written down using (2.2), (2.9), and Figure B.3. Comparing these quantities to the stochastic six vertex weights L_{uv} in Figure 3.5, while taking into account the relation between $j_2, j_1; k_1', k_2'$ and $\lambda_1^{(i,j)}$ (3.13), we see that $\mathbf{L}_{\text{sHL}(u),\text{sHL}(v)}(j_2, 1-j_1; k_1', 1-k_2') = \mathsf{L}_{uv}(j_2, j_1; k_1', k_2')$ for all $j_2, j_1; k_1', k_2' \in \{0,1\}$. This implies the claim. □

Remark 3.3.7. While Theorem 3.3.6 essentially follows from [BP19], let us emphasize what is different here. Theorem 3.3.6 connects the ordinary stochastic six vertex model with stable spin Hall-Littlewood polynomials. On the other hand, previously the same stochastic six vertex model was matched to Hall-Littlewood processes and measures [BBW18], [BM18], and the non-stable spin Hall-Littlewood polynomials gave rise to a dynamic version of the stochastic six vertex model [BP19]. Therefore, formally Theorem 3.3.6 is a new statement.

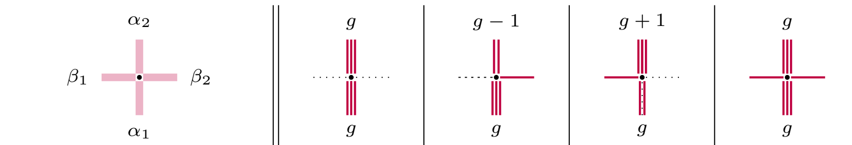

$\mathsf{L}^{\mathrm{ur}}_{x,v}(\alpha_1,\beta_1;\alpha_2,\beta_2)$	$\frac{1+q^g xv}{1+xv}$	$\frac{xv(1-q^g)}{1+xv}$	$\frac{1+q^g sx}{1+xv}$	$\frac{xv-q^g sx}{1+xv}$

Figure 3.6: The stochastic vertex weights $\mathsf{L}^{\mathrm{ur}}_{x,v}$ for the up-right stochastic higher spin six vertex model.

3.3.3 Last row in sqW/sHL field

We start by defining the stochastic higher spin six vertex model:

Definition 3.3.8 ([CP16], [BP18a])**.** Specialize the up-right stochastic vertex model of Definition 3.3.1 by taking $L^{\mathrm{ur}}_{(i,j)} = \mathsf{L}^{\mathrm{ur}}_{x_i,v_j}$, where the latter are given in Figure 3.6. We refer to this model as the *up-right stochastic higher spin six vertex model.* We consider the *step-stationary* boundary conditions:

$$b^{\mathrm{v}}_j \sim \mathrm{Ber}\left(\frac{x_1 v_j}{1+x_1 v_j}\right) \qquad \text{and} \qquad b^{\mathrm{h}}_i = 0, \tag{3.24}$$

where $\mathrm{Ber}(\cdot)$ are independent Bernoulli random variables with the probability of success given in the parentheses.[3]

Remark 3.3.9. The model in Definition 3.3.8 is equivalent to that of [BP18a] (the latter with step boundary conditions $b^{\mathrm{v}}_j = 1$, $b^{\mathrm{h}}_i = 0$), under specializations $\xi_1 \mathsf{s}_1 \to x_1$, $\mathsf{s}_1^2 \to 0$, $\mathsf{s}_\alpha \xi_\alpha \to x_\alpha$, $\mathsf{s}_\alpha^2 \to -s x_\alpha$ and $u_\beta \to -v_\beta$.

Theorem 3.3.10 (sqW/sHL last row)**.** *The last row marginal* $\{\lambda_i^{(i,j)}\}_{i\geq 1, j\geq 0}$ *of the sqW/sHL field has the same distribution as the height function* $\{\mathcal{H}^{\mathrm{ur}}_{\mathrm{HS}}(i,j)\}_{i\geq 1, j\geq 0}$ *of the up-right higher spin six vertex model with step-stationary boundary conditions.*

Proof. We use Proposition 3.1.12. During the update

$$\lambda^{(n-1,t-1)} \to \lambda^{(n,t)}, \qquad \text{for fixed} \qquad \lambda^{(n-1,t)}, \lambda^{(n,t-1)}, \tag{3.25}$$

weighted by the stochastic matrix $\mathsf{U}^{\mathrm{fwd}}$, the law of the rightmost local move is given by a stochastic bijectivization of the Yang–Baxter equation (B.26). A computation shows that one such bijectivization is given by the choice

$$\mathbf{p}^{\mathrm{fwd}}_{\{i_1,i_2,i_3\},\{\varnothing,j_2,j_3\}}(\{k_1,k_2,k_3\} \to \{k_1',k_2',k_3'\}) = \mathsf{L}^{\mathrm{ur}}_{x,v}(j_3 - i_2 - k_1, k_1; j_3 - i_2 - k_1', k_1'). \tag{3.26}$$

[3] A slightly broader class of boundary conditions than the step-stationary ones, where also b^{h}_i are allowed to be positive numbers, can be considered using the fusion argument introduced in [Agg18]; see also [IMS20], [BMP19].

This can be readily verified using the parametrization from Example 3.1.8. In terms of elements of signatures in (3.25), the integers i_2, j_3, k_1, k_1' are interpreted as

$$
\begin{aligned}
i_2 &= \lambda_{n-1}^{(n,t-1)} - \lambda_{n-1}^{(n-1,t)}, \qquad & j_3 &= \lambda_{n-1}^{(n,t-1)} - \lambda_{n}^{(n,t-1)} \\
k_1 &= \lambda_{n-1}^{(n-1,t)} - \lambda_{n-1}^{(n-1,t-1)}, \qquad & k_1' &= \lambda_{n}^{(n,t)} - \lambda_{n}^{(n,t-1)}.
\end{aligned}
$$

Remarkably, transition weight (3.26) only depends on the difference $j_3 - i_2$ and on k_1, k_1', but not on other edge occupation numbers. Therefore, the law of $\lambda_n^{(n,t)}$ is solely determined by $\lambda_{n-1}^{(n-1,t)}$,$\lambda_n^{(n,t-1)}$,$\lambda_{n-1}^{(n-1,t-1)}$. This implies that the last row marginal $\{\lambda_i^{(i,j)}\}_{i\geq 1, j\geq 0}$ is an autonomous Markov process. Moreover, this autonomous process has the same multitime joint distribution as the height function of the up-right higher spin six vertex model because L^{ur} appears in (3.26). This completes the proof. □

In [CP16], [BP18a], joint q-moments of the up-right stochastic higher spin six vertex model were expressed in terms of nested contour integrals. These moments completely determine the joint distribution of the model's height function $\mathcal{H}^{\mathrm{ur}}_{\mathrm{HS}}(\cdot, j)$ along any given horizontal line (because $q \in (0,1)$ and the random variables in question are nonnegative). Let us reproduce the q-moment formula:

Proposition 3.3.11 ([BP18a])**.** *Consider the up-right stochastic higher spin six vertex model with step-stationary boundary conditions and assume $v_\alpha \neq q v_\beta$. For any $i_1 \geq \ldots \geq i_\ell \geq 1$ we have*

$$
\begin{aligned}
\mathbb{E}\prod_{k=1}^{\ell} q^{\mathcal{H}^{\mathrm{ur}}_{\mathrm{HS}}(i_k,j)} = q^{\binom{\ell}{2}} \oint_{\gamma[-\bar{\mathbf{v}}|1]} \frac{dz_1}{2\pi\mathrm{i}} \cdots \oint_{\gamma[-\bar{\mathbf{v}}|\ell]} \frac{dz_\ell}{2\pi\mathrm{i}} \prod_{1\leq A<B\leq \ell} \frac{z_A - z_B}{z_A - q z_B} \\
\times \prod_{k=1}^{\ell} \left(\frac{1}{z_k(1+s z_k)} \prod_{\alpha=1}^{i_k} \frac{x_\alpha(1+s z_k)}{x_\alpha - z_k} \prod_{\alpha=1}^{j} \frac{1+q v_\alpha z_k}{1+v_\alpha z_k} \right).
\end{aligned}
\tag{3.27}
$$

Here, integration contours are $\gamma[-\bar{\mathbf{v}}|k] = \gamma[-\bar{\mathbf{v}}] \cup r^{k-1} c_0$, where $\gamma[-\bar{\mathbf{v}}]$ encircles $-1/v_1, \ldots, -1/v_j$ and no other singularity, c_0 is a small circle around 0, and $r > q^{-1}$. All curves are positively oriented, and $r^{k-1}c_0$ never intersects $\gamma[-\bar{\mathbf{v}}]$ for $k = 1, \ldots, \ell$.

Proof. This follows from Theorem 9.8 in [BP18a] by identifying the parameters as in Remark 3.3.9 and noting that $\mathcal{H}^{\mathrm{ur}}_{\mathrm{HS}}(i,j)$ is the same as the height function $\mathfrak{h}(i)$ at the j-th horizontal slice. Note also that [BP18a, Corollary 10.3] is essentially the same as our q-moments (3.27), but with contours dragged through infinity, and identification of s_1^2 with x_1. The latter follows by comparing (3.24) with [BP18a, Remark 6.14]. □

Eigenrelations for sqW polynomials given in Theorem 2.6.11 can be employed to provide an alternative proof of the moment formula (3.27).

Alternative proof of Proposition 3.3.11. We express q-moments of last rows of the sqW/sHL process using the q-difference operators $\mathfrak{D}_1$ (2.85) at several levels, following the argument in [Bor+16, Proposition 4.4].

Denote by $\mathfrak{D}_1^{(i)}$ the operator $\mathfrak{D}_1$ acting on i variables $x_1, \dots, x_i$. Then for any ℓ and any sequence $1 \le i_1 \le \dots \le i_\ell$, we have

$$\mathbb{E} \prod_{k=1}^{\ell} q^{\lambda_{i_k}^{(i_k,j)}} = \frac{\mathfrak{D}_1^{(i_1)} \cdots \mathfrak{D}_1^{(i_\ell)} \Pi(x_1, \dots, x_N; v_1, \dots, v_j)}{\Pi(x_1, \dots, x_N; v_1, \dots, v_j)}, \tag{3.28}$$

where $N \ge i_\ell$ is arbitrary, and

$$\Pi(x_1, \dots, x_N; v_1, \dots, v_j) = \prod_{r=1}^{j} \left(\frac{1}{1 - s v_r} \right)^{N-1} \prod_{i=1}^{N} \prod_{r=1}^{j} (1 + v_r x_i)$$

is the partition function in the right-hand side of the sqW/sHL Cauchy identity (2.27). Equality (3.28) is a straightforward consequence of the Cauchy identities (2.25), (2.27), eigenrelation (2.87), and the branching rules for the sqW functions.

Let us now express the right-hand side of (3.28) in terms of nested contour integrals. For

$$h(z) = \prod_{r=1}^{j} (1 + v_r z),$$

we have

$$\text{r.h.s. } (3.28) = \frac{\mathfrak{D}_1^{(i_1)} \cdots \mathfrak{D}_1^{(i_\ell)} h(x_1) \cdots h(x_N)}{h(x_1) \cdots h(x_N)}.$$

Moreover, for any meromorphic function $\widetilde{h}$ we have

$$\mathfrak{D}_1^{(n)} \left(\widetilde{h}(x_1) \cdots \widetilde{h}(x_n) \right) = \frac{1}{2\pi \mathrm{i}} \oint_{\gamma_{\widetilde{h}}} \prod_{\alpha=1}^{n} \left(\widetilde{h}(x_\alpha) \frac{x_\alpha (1 + s z)}{x_\alpha - z} \right) \frac{\widetilde{h}(qz)}{\widetilde{h}(z)} \frac{dz}{z(1 + s z)},$$

where the curve $\gamma_{\widetilde{h}}$ encircles 0 and all poles of $\widetilde{h}(qz)/\widetilde{h}(z)$. The latter poles may include infinity, too. In other words, the integral over $\gamma_{\widetilde{h}}$ is equal to the sum of minus residues of the integrand at $x_1, \dots, x_n$.

By iterating this integral representation, we can evaluate (3.28) and match the resulting expression with the q-moment formula (3.27). The equivalence of processes $\lambda_i^{(i,j)}$ and $\mathcal{H}_{\mathrm{HS}}^{\mathrm{ur}}(i,j)$ stated in Theorem 3.3.10 allows us to complete the proof. □

3.3.4 First row in sqW/sHL field

Let us define an *up-left version of the stochastic higher spin six vertex model*. Take an up-left model in the sense of Definition 3.3.3, with the weights $L_{(i,j)}^{\mathrm{ul}} = \mathsf{L}_{x_i,v_j}^{\mathrm{ul}}$, given in Figure 3.7. We take this model with the same step-stationary boundary conditions (3.24). In fact, this model is essentially the same as the one from Definition 3.3.8:

Remark 3.3.12. When at most one path occupies each horizontal edge (as in our case), swapping the horizontal occupation numbers $0 \leftrightarrow 1$ is a bijection between up-left and up-right models. Their height functions are related as $\mathcal{H}_{\mathrm{HS}}^{\mathrm{ur}}(i,j) = j - \mathcal{H}_{\mathrm{HS}}^{\mathrm{ul}}(i,j)$. Moreover, the weights $\mathsf{L}_{x,v}^{\mathrm{ul}}$ become the weights $\mathsf{L}_{x,v}^{\mathrm{ur}}$ from Figure 3.6 after this swapping of horizontal occupations, and the inversion of the parameters $(x, v) \mapsto (x^{-1}, v^{-1})$.

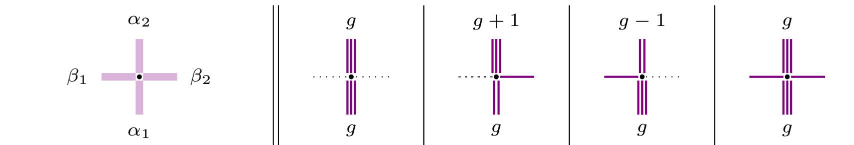

$\mathsf{L}^{\mathrm{ul}}_{x,v}(\alpha_1,\beta_1;\alpha_2,\beta_2)$	$\frac{1-q^g sv}{1+xv}$	$\frac{xv+q^g sv}{1+xv}$	$\frac{1-q^g}{1+xv}$	$\frac{xv+q^g}{1+xv}$

Figure 3.7: The stochastic vertex weights $\mathsf{L}^{\mathrm{ul}}_{x,v}$ for the up-left stochastic higher spin six vertex model.

However, it is convenient to work with the up-right and the up-left models separately, as in the sqW/sqW case they are genuinely different.

Theorem 3.3.13 (sqW/sHL first row)**.** *The first row marginal $\{\lambda_1^{(i,j)}\}_{i\ge 1, j\ge 0}$ of the sqW/sHL field has the same distribution as the height function $\{\mathcal{H}^{\mathrm{ul}}_{\mathrm{HS}}(i,j)\}_{i\ge 1,j\ge 0}$ of the up-left stochastic higher spin six vertex model with step-stationary boundary conditions.*

Proof. We use Yang–Baxter fields similarly to the approach taken in [BMP19, Section 7.3]. Let us specialize the general notation of Proposition 3.1.15. We need to match the stochastic vertex weight $\mathbf{L}$ of (3.11) with L^{ul}, and verify boundary conditions.

The random move $\lambda_1^{(i-1,j-1)} \to \lambda_1^{(i,j)}$, conditioned on $\lambda_1^{(i,j-1)}, \lambda_1^{(i-1,j)}$ is determined by the bijectivization of the Yang–Baxter equation (B.11) for $i > 1, j \ge 1$ and by the bijectivization of (B.26), if $i = 1$. We start with the first case, where in (3.11) we get (after canceling common factors)

$$\mathsf{wl}_{\{0,0,\infty\},\{j_1,j_2,\infty\}}(\{k_1,k_2,\infty\}) = \mathcal{R}_{x,v,s}(0,0;k_1,k_2)\,\frac{v^{j_1}}{1-sv}\,x^{j_2}\,\frac{(-s/x;q)_{j_2}}{(q;q)_{j_2}},$$
$$\mathsf{wr}_{\{0,0,\infty\},\{j_1,j_2,\infty\}}(\{k_1',k_2',\infty\}) = \mathcal{R}_{x,v,s}(k_2',k_1';j_2,j_1)\frac{v^{k_1'}}{1-sv}\,x^{k_2'}\,\frac{(-s/x;q)_{k_2'}}{(q;q)_{k_2'}}.$$

One readily sees that then (3.11) gives the stochastic weight $\mathsf{L}^{\mathrm{ul}}_{x,v}$.

For the boundary signature $\lambda_1^{(1,j)}$ case, configuration weights wl, wr become (after canceling common factors)

$$\mathsf{wl}_{\{0,0,\infty\},\{\varnothing,j_2,\infty\}}(\{k_1,k_2,\infty\}) = \mathcal{R}_{x,v,s}(0,0;k_1,k_2)\,x^{j_2},$$
$$\mathsf{wr}_{\{0,0,\infty\},\{\varnothing,j_2,\infty\}}(\{k_1',k_2',\infty\}) = \frac{v^{k_1'}}{1-sv}\,x^{k_2'},$$

which leads to the step-stationary boundary conditions (3.24) since $\lambda^{(i,0)} = \varnothing$ for all i. □

3.3.5 Last row in sqW/sqW field

Define the up-right stochastic weight by

$$\mathbb{L}^{\mathrm{ur}}_{x,y}(\alpha_1,\beta_1;\alpha_2,\beta_2) := \mathbf{1}_{\alpha_1+\beta_1=\alpha_2+\beta_2}\,\varphi_{q,xy,-sx}(\beta_2 \mid \alpha_1), \tag{3.29}$$

where φ is the q-beta-binomial distribution (A.16)–(A.17).

Definition 3.3.14 ([Pov13])**.** The *q-Hahn vertex model* is the up-right stochastic vertex model, in the sense of Definition 3.3.1, with weights $L^{\mathrm{ur}}_{i,j} = \mathbb{L}^{\mathrm{ur}}_{x_i,y_j}$. We consider *step-stationary* boundary conditions:

$$b^{\mathrm{v}}_j \sim \varphi_{q,x_1y_j,-sx_1}(\bullet \mid \infty) \qquad \text{and} \qquad b^{\mathrm{h}}_i = 0, \tag{3.30}$$

where the random variables for b^{v}_j are independent. Denote the corresponding height function by $\mathcal{H}^{\mathrm{ur}}_{q\text{-Hahn}}$.

Remark 3.3.15. The model of Definition 3.3.14 is equivalent to that of [BP18a, Section 6.6.2], where parameters have been specialized as $\mathsf{s}_\alpha^2 \to -sx_\alpha$ and $q^{J_\alpha} \to -y_\alpha/s$.

Theorem 3.3.16 (sqW/sqW last row)**.** *The last row marginal* $\{\lambda_i^{(i,j)}\}_{i\ge 1, j\ge 0}$ *of the sqW/sqW field has the same distribution as the height function* $\{\mathcal{H}^{\mathrm{ur}}_{q\text{-Hahn}}(i,j)\}_{i\ge1,j\ge0}$ *of the up-right q-Hahn vertex model.*

Proof. This follows from Theorem 3.3.10 which established an analogous result matching the last row of the sqW/sHL field and the height function of the up-right higher spin six vertex model. By fusion, the dual sHL functions turn into the dual sqW functions (cf. [BW17]). Therefore, the sqW/sHL field under fusion turns into the sqW/sqW field.

On the other hand, the same fusion procedure turns the up-right higher spin six vertex model into the up-right q-Hahn vertex model[4]. This completes the proof. □

In [BP18a, Corollary 10.4] the multi-point q-moments of the up-right q-Hahn vertex model were expressed in terms of nested contour integrals:

Proposition 3.3.17 ([BP18a], Corollary 10.4)**.** *Assume* $\min_\alpha |sx_\alpha| > q \max_\alpha |sx_\alpha|$. *For any* $i_1 \ge \ldots \ge i_\ell \ge 1$ *we have*

$$\mathbb{E} \prod_{k=1}^{\ell} q^{\mathcal{H}^{\mathrm{ur}}_{q\text{-Hahn}}(i_k,j)} = (-1)^\ell q^{\binom{\ell}{2}} \oint_{\gamma_1^+[-s\mathbf{x}]} \frac{dw_1}{2\pi \mathrm{i}} \cdots \oint_{\gamma_\ell^+[-s\mathbf{x}]} \frac{dw_\ell}{2\pi\mathrm{i}} \prod_{1\le A<B\le \ell} \frac{w_A - w_B}{w_A - qw_B}$$
$$\times \prod_{k=1}^{\ell} \left(\frac{1}{w_k(1-w_k)} \prod_{\alpha=1}^{i_k} \frac{1-w_k}{1+w_k/(sx_\alpha)} \prod_{\alpha=1}^{j} \frac{1+w_k y_\alpha/s}{1-w_k} \right). \tag{3.31}$$

Integration contours encircle $-sx_1, -sx_2, \ldots,$ *and leave out 0,1 and are q-nested in the sense that* $q\gamma_{k+1}^+[-s\mathbf{x}]$ *is inside* $\gamma_k^+[-s\mathbf{x}]$ *for all* $k = 1, \ldots, \ell-1$.

Proposition 3.3.17 was obtained in [BP18a] as a corollary (under fusion) of the multi-point q-moment formula (3.27) for the up-right higher spin six vertex model. Both of these q-moment formulas have several different proofs: via duality [CP16], manipulations with symmetric functions using Bethe Ansatz [BP18a], or distributional matchings and difference operators [OP17]. Eigenrelations for the sqW polynomials provide yet another independent proof:

[4]For a practical explanation of fusion in the context of $\mathfrak{sl}_2$ stochastic vertex models see [BW17] and [CP16], [BP18a] and references therein.

Alternative proof of Proposition 3.3.17. Similarly to the alternative proof of Proposition 3.3.11 given in Section 3.3.3, we will use eigenrelations of the sqW polynomials to compute q-moments. To express q-moments of the sqW/sqW field, we use formula (3.28), after replacing the function Π with the right-hand side of (2.34). The action of the difference operator $\mathfrak{D}_1$ (2.85) (in n variables) on a meromorphic function $\widetilde{h}$ can be written as

$$\mathfrak{D}_1\left(\widetilde{h}(x_1)\cdots\widetilde{h}(x_n)\right) = -\frac{1}{2\pi \mathrm{i}}\oint_{x_1,\dots,x_n}\prod_{\alpha=1}^{n}\left(\widetilde{h}(x_\alpha)\,\frac{x_\alpha(1+sz)}{x_\alpha - z}\right)\frac{\widetilde{h}(qz)}{\widetilde{h}(z)}\frac{dz}{z(1+sz)},$$

where the integration contour contains $x_1,\dots,x_n$, but doesn't contain 0 or any pole of $\widetilde{h}(qz)/\widetilde{h}(z)$. Using this formula repeatedly, we can match the q-moments of the marginal $\lambda_i^{(i,j)}$ to expression (3.31). The equivalence of processes between last row of the sqW/sqW field and height function of the q-Hahn vertex model stated in Theorem 3.3.16 yields the proof. □

3.3.6 First row in sqW/sqW field

For our fourth and final vertex model, define the up-left stochastic weight by

$$\begin{aligned}\mathbb{L}^{\mathrm{ul}}_{x,y}(\alpha_1,\beta_1;\alpha_2,\beta_2) \coloneqq \mathbf{1}_{\alpha_1+\beta_2=\alpha_2+\beta_1}\,&\frac{y^{\alpha_2}s^{\alpha_1}x^{\alpha_2-\alpha_1}\,q^{\beta_1\beta_2+\frac{1}{2}\alpha_1(\alpha_1-1)}\,(-s/x;q)_{\alpha_2}(-s/y;q)_{\beta_2}}{(-s/x;q)_{\alpha_1}(-s/y;q)_{\beta_1}(q;q)_{\beta_2}(-q/(sy);q)_{\beta_2-\alpha_2}}\\ &\times\frac{(s^2q^{\alpha_1+\beta_2};q)_\infty(xy;q)_\infty}{(-sy;q)_\infty(-sx;q)_\infty}\,{}_4\overline{\phi}_3\left(\begin{matrix}q^{-\beta_1};q^{-\beta_2},-sx,-q/(sy)\\ -s/y,q^{1+\alpha_1-\beta_1},-xq^{1-\beta_2-\alpha_1}/s\end{matrix}\,\middle|\,q,q\right),\end{aligned}\tag{3.32}$$

where ${}_4\overline{\phi}_3$ is the regularized q-hypergeometric function (A.10).

Remark 3.3.18. An expression equivalent to (3.32) for the stochastic weight $\mathbb{L}^{\mathrm{ul}}_{x,y}$ is given by

$$\mathbb{L}^{\mathrm{ul}}_{x,y}(g,\ell;g+L-\ell,L) = \sum_{k=0}^{\min(\ell,L)}\varphi_{q^{-1},q^g,-syq^{g-1}}(k\mid\ell)\,\psi_{q,-q^ks/y,-q^gs/x,s^2q^{g+k}}(L-k),\tag{3.33}$$

where we used the q-beta-binomial and the q-hypergeometric distributions (A.16), (A.20). This can be proved through simple manipulations of the q-Pochhammer terms. From (3.33) it is immediate to see that $\mathbb{L}^{\mathrm{ul}}_{x,y}$ possesses the sum to one property (3.20). The positivity of the weights (under certain restrictions on the parameters) is proven in section B.3.

Definition 3.3.19. The ${}_4\phi_3$ *vertex model* is the up-left stochastic vertex model, in the sense of Definition 3.3.3, with weights $L^{\mathrm{ur}}_{i,j}=\mathbb{L}^{\mathrm{ul}}_{x_i,y_j}$. We consider the same *step-stationary* boundary conditions as in (3.30). The height function of this model is denoted by $\mathcal{H}^{\mathrm{ul}}_{\phi}$.

Theorem 3.3.20 (sqW/sqW first row)**.** *Let $s\in(-\sqrt{q},0)$. The first row marginal $\{\lambda_1^{(i,j)}\}_{i,j\in\mathbb{Z}_{\geq 0}}$ of the sqW/sqW field has the same distribution as the height function $\{\mathcal{H}^{\mathrm{ul}}_{\phi}(i,j)\}_{i,j\in\mathbb{Z}_{\geq 0}}$ of the ${}_4\phi_3$ stochastic vertex model.*

Proof. The proof of this matching is similar to that of Theorem 3.3.13, and follows from Proposition 3.1.15. Namely, we specialize formula (3.11) using the Yang–Baxter equations (B.12), (B.27). For updates of "bulk" transition $\lambda_1^{(i-1,j-1)} \to \lambda_1^{(i,j)}$, for $i > 1, j \geq 1$, conditioned on $\lambda_1^{(i,j-1)}, \lambda_1^{(i-1,j)}$, the stochastic weight (3.11) uses

$$\mathsf{wl}_{\{0,0,\infty\},\{j_1,j_2,\infty\}}(\{k_1,k_2,\infty\}) = \mathbb{R}_{x,y,s}(0,0;k_1,k_2)\, y^{j_1}\frac{(-s/y;q)_{j_1}}{(q;q)_{j_1}}\, x^{j_2}\frac{(-s/x;q)_{j_2}}{(q;q)_{j_2}},$$
$$\mathsf{wr}_{\{0,0,\infty\},\{j_1,j_2,\infty\}}(\{k_1',k_2',\infty\}) = \mathbb{R}_{x,y,s}(k_2',k_1';j_2,j_1)\, y^{k_1'}\frac{(-s/y;q)_{k_1'}}{(q;q)_{k_1'}}\, x^{k_2'}\frac{(-s/x;q)_{k_2'}}{(q;q)_{k_2'}}.$$

Using the expression of the R-matrix $\mathbb{R}_{x,y,s}$ and summation identity (B.10) one can match $\mathbf{L}_{x,y}$ with $\mathbb{L}_{x,y}$. At the boundary $\lambda_1^{(1,j)}$, we use a stochastic bijectivization of (B.27) and therefore in this case we have

$$\mathsf{wl}_{\{0,0,\infty\},\{\varnothing,j_2,\infty\}}(\{k_1,k_2,\infty\}) = \mathbb{R}_{x,y,s}(0,0;k_1,k_2)\, x^{j_2},$$
$$\mathsf{wr}_{\{0,0,\infty\},\{\varnothing,j_2,\infty\}}(\{k_1',k_2',\infty\}) = y^{k_1'}\frac{(-s/y;q)_{k_1'}}{(q;q)_{k_1'}}\frac{(-sy;q)_\infty}{(s^2;q)_\infty}\, x^{k_2'},$$

that yields boundary conditions (3.30) after using again summation identity (B.10). □

3.3.7 Push–block dynamics for sqW/sqW process

Let us now present another, more explicit matching of last rows of the sqW/sqW field in a "Plancherel" (or "Poisson-type") continuous time limit. Here the dynamics of the last rows is matched to the corresponding continuous time limit of the q-Hahn TASEP. This construction is very similar to how the continuous time q-TASEP emerges from q-Whittaker processes in [BC14].

Consider the Borodin–Ferrari forward transition map (cf. Section 3.1.4)

$$\mathsf{U}^{\mathrm{fwd}}_{x,y}(\varkappa \to \nu \mid \lambda,\mu) = \frac{\mathbb{F}_{\nu/\lambda}(x)\mathbb{F}^*_{\nu/\mu}(y)}{\Pi(x;y)\sum_{\varkappa}\mathbb{F}_{\mu/\varkappa}(x)\mathbb{F}^*_{\lambda/\varkappa}(y)}, \tag{3.34}$$

where $\Pi(x;y) = \frac{(-sx;q)_\infty(-sy;q)_\infty}{(xy;q)_\infty(s^2;q)_\infty}$. In the limit as $y = -s + \varepsilon(1-q)$, $\varepsilon \to 0$, the dual sqW function at a single variable becomes (we use the notation $[r]_q = (1-q^r)/(1-q)$)

$$\mathbb{F}^*_{\lambda/\mu}(-s+\varepsilon(1-q)) = \begin{cases} 1+\mathsf{O}(\varepsilon), & \lambda=\mu; \\ \varepsilon\,\dfrac{(-s)^{r-1}}{[r]_q}\dfrac{(q^{\mu_{i-1}-\lambda_i+1};q)_r}{(q^{\mu_{i-1}-\lambda_i}s^2;q)_r} + \mathsf{O}(\varepsilon^2), & \lambda = \mu + r\mathbf{e}_i \text{ for some } i, r>0. \end{cases}$$

see (2.31). Take $y_j = -s + \varepsilon(1-q)$ for all j and rescale $M = \lfloor t/\varepsilon \rfloor$, $t \in \mathbb{R}_{\geq 0}$, in the sqW/sqW field. Thus, we get a continuous time dynamics on interlacing arrays $\lambda^1(t) \prec \lambda^2(t) \prec \cdots$, where at time t, each λ_i^k jumps to $\lambda_i^k + r$, $r \geq 1$, according to an exponential clock with rate (see (3.34))

$$\mathrm{rate}(\lambda^k \to \lambda^k + r\mathbf{e}_i \mid \lambda^{k-1}) = x_k^r\,\frac{(-s)^{r-1}}{[r]_q}\,\frac{(-q^{\lambda_i^k-\lambda_i^{k-1}}s/x_k\,,\, q^{\lambda_i^k-\lambda_{i+1}^k+1}\,,\, q^{\lambda_{i-1}^{k-1}-\lambda_i^k+1-r}\,;\,q)_r}{(q^{\lambda_i^k-\lambda_i^{k-1}+1}\,,\, q^{\lambda_i^k-\lambda_{i+1}^k}s^2\,,\, -q^{\lambda_{i-1}^{k-1}-\lambda_i^k-r}sx_k\,;\,q)_r}. \tag{3.35}$$

When an update occurs at level j bringing $\lambda^j \to \widetilde{\lambda}^j = \lambda^j + r\mathbf{e}_i$, the signature λ^{j+1} is instantaneously updated to $\widetilde{\lambda}^{j+1}$ in the following way:

- if $\widetilde{\lambda}^j_i \le \lambda^{j+1}_i$, then $\widetilde{\lambda}^{j+1} = \lambda^{j+1}$
- if $\widetilde{\lambda}^j_i > \lambda^{j+1}_i$, then assume $\widetilde{\lambda}^j_i - \lambda^{j+1}_i = m$ and set $\widetilde{\lambda}^{j+1} = \lambda^{j+1} + (m+\ell)\mathbf{e}_i$ with probability

$$\mathrm{prob}(\lambda^{j+1} \to \widetilde{\lambda}^{j+1} \mid \lambda^j \to \widetilde{\lambda}^j) = \lim_{\varepsilon \to 0} \frac{\mathbb{F}_{\widetilde{\lambda}^{j+1}/\widetilde{\lambda}^j}(x)\mathbb{F}^*_{\widetilde{\lambda}^{j+1}/\lambda^{j+1}}(y)}{\sum_{\eta=\lambda^{j+1}+(m+\ell')\mathbf{e}_i} \mathbb{F}_{\eta/\widetilde{\lambda}^j}(x)\mathbb{F}^*_{\eta/\lambda^{j+1}}(y)}\Bigg|_{y=-s+\varepsilon(1-q)}.$$

for any $\ell \ge 0$ (for ℓ large enough this probability vanishes). See Figure 3.8 for an illustration.

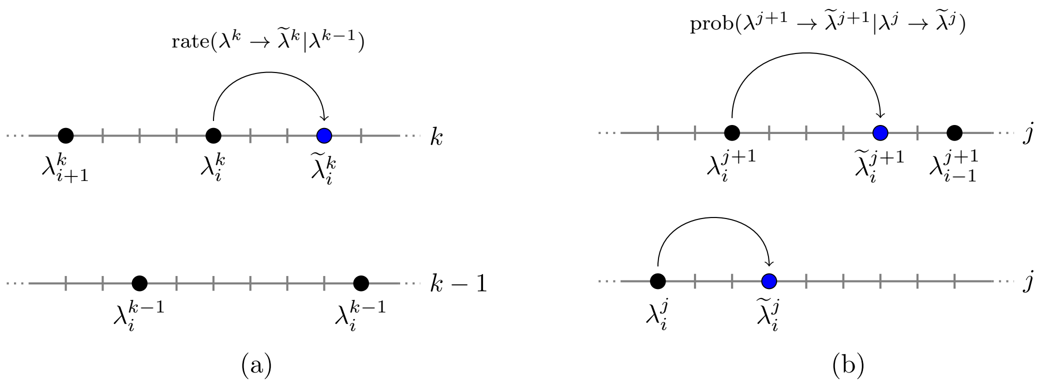

Figure 3.8: Push–block mechanism in the half-continuous sqW/sqW field. Each λ^k_i jumps to $\widetilde{\lambda}^k_i = \lambda^k_i + r$ at rate (3.35), which only depends on λ^{k-1}; see left panel. When a jump happens at level k and breaks interlacing, it triggers an instantaneous push at levels above to re-establish interlacing; see right panel.

When $s = 0$ and $q \in (0,1)$ in our dynamics, we recover the continuous time q-Whittaker 2d-growth model introduced in [BC14, Definition 3.3.3]. Further setting $q = 0$ brings the original Borodin–Ferrari's push–block process corresponding to Schur measures [BF14]. Note that in our case, in contrast with the Schur and q-Whittaker situations, jumps are long range.

Restricting attention to the last rows (leftmost diagonal) of the array and setting $i = k$ in (3.35), we see that the rate only depends on λ^k_k and λ^{k-1}_{k-1}. Moreover, the pushing mechanism does not affect the leftmost diagonal of the array. Thus, the marginal evolution of the particles in the leftmost diagonal is an autonomous Markov process. Its jump rates are

$$\mathrm{rate}(\lambda^k_k \to \lambda^k_k + r \mid \lambda^{k-1}_{k-1}) = x^r_k \frac{(-s)^{r-1}}{[r]_q} \frac{(q^{\lambda^{k-1}_{k-1}-\lambda^k_k+1-r}; q)_r}{(-q^{\lambda^{k-1}_{k-1}-\lambda^k_k-r} s x_k; q)_r}.$$

These rates correspond to an inhomogeneous version of the continuous time q-Hahn TASEP studied in [BC16b], which is also a continuous time degeneration of the q-Hahn

TASEP of [Cor14]. Thus, we see that the continuous time push–block dynamics in the sqW case agrees with the last row marginal evolution.

3.4 Random boundary conditions

In this section we show how to generalize the construction of the Yang-Baxter fields given in sections 3.1 and 3.3 in order to produce fields with random boundary conditions.

3.4.1 Fields with scaled geometric specializations

Stochastic bijectivizations of Yang-Baxter equations with scaled geometric specializations (B.22), (B.24) can be employed to produce fields with random boundary conditions. Fix additional parameters $\alpha, \beta \in [0, -s^{-1}]$, and consider specializations ρ_i^{v}, ρ_i^{h}, $i = -1, 0, 1, \ldots$:

$$\rho_{-1}^{\mathrm{h}} = \mathrm{sg}(\alpha), \qquad \rho_{-1}^{\mathrm{v}} = \mathrm{sg}(\beta), \qquad \rho_i^{\mathrm{h}} = \mathrm{sHL}(u_i), \qquad \rho_j^{\mathrm{v}} = \mathrm{sHL}(v_j), \tag{3.36}$$

as in section 2.5. Let $\boldsymbol{\eta}$ be the Yang-Baxter field on the lattice $\mathbb{Z}_{\geq -1} \times \mathbb{Z}_{\geq -1}$ generated by the Markov transition operators $\mathsf{U}^{\mathrm{fwd}}_{\rho_j^{\mathrm{v}}, \rho_i^{\mathrm{h}}}$. Restricting the field $\boldsymbol{\eta}$ to the nonnegative quadrant, denote $\boldsymbol{\lambda} = \boldsymbol{\eta}|_{\mathbb{Z}_{\geq 0} \times \mathbb{Z}_{\geq 0}}$. We call $\boldsymbol{\lambda}$ the *sHL/sHL Yang-Baxter field with two-sided stationary boundary conditions*.

Proposition 3.4.1. *The single-point distributions in the sHL/sHL Yang-Baxter field with the two-sided stationary boundary conditions are given by*

$$\mathrm{Prob}\{\lambda^{(i,j)} = \nu\} = \frac{(\alpha\beta; q)_\infty}{\prod_{j'=1}^{j} (1 + v_{j'}\alpha) \prod_{i'=1}^{i} (1 + u_{i'}\beta)} \prod_{\substack{1 \leq i' \leq i \\ 1 \leq j' \leq j}} \frac{1 - u_{i'}v_{j'}}{1 - q u_{i'}v_{j'}} \mathsf{F}_{\nu'}(u_1, \ldots, u_i; \breve{\alpha}) \mathsf{F}^*_{\nu'}(v_1, \ldots, v_j; \breve{\beta}).$$

Joint distributions in this field along down-right paths are expressed through products of skew functions similarly to eq. (3.2).

Proposition 3.4.2. *Consider positive specializations*

$$\rho_i^{\mathrm{h}} = \mathrm{sqW}(x_i), \qquad \rho_{-1}^{\mathrm{v}} = \mathrm{sg}(\beta), \qquad \rho_j^{\mathrm{v}} = \mathrm{sHL}(v_j), \qquad i, j \geq 0 \tag{3.37}$$

and let $\boldsymbol{\eta}$ be the Yang-Baxter field on the lattice $\mathbb{Z}_{\geq 0} \times \mathbb{Z}_{\geq -1}$ generated by the Markov transition operators $\mathsf{U}^{\mathrm{fwd}}_{\rho_j^{\mathrm{v}}, \rho_i^{\mathrm{h}}}$. Denote $\boldsymbol{\lambda} = \boldsymbol{\eta}|_{\mathbb{Z}_{\geq 0} \times \mathbb{Z}_{\geq 0}}$. We call $\boldsymbol{\lambda}$ the sqW/sHL Yang-Baxter field with two-sided stationary boundary conditions. *Then $\boldsymbol{\lambda}$ is an sqW/sHL field with mixed specializations. In particular its single-point distribution is given by*

$$\mathrm{Prob}\{\lambda^{(i,j)} = \nu\} = \frac{\prod_{1 \leq i' \leq i} (\beta x_{i'}; q)_\infty}{(-s\beta; q)_\infty^{i-1}} \prod_{1 \leq j' \leq j} \frac{(1 - s v_{j'})^{i-1}}{\prod_{1 \leq i' \leq i} (1 + v_{j'} x_{i'})} \mathbb{F}_\nu(x_1, \ldots, x_i) \mathsf{F}^{\bullet}_{\nu'}(v_1, \ldots, v_j, \breve{\beta}).$$

Remark 3.4.3. The use of Yang-Baxter equations with corner weights automatically produces random entries along the vertical boundary. This is the reason why to produce a random sqW/sHL field we only employ scaled geometric specializations in the dual term.

Proposition 3.4.4. *Consider positive specializations*

$$\rho_i^{\mathrm{h}} = \mathrm{sqW}(x_i), \qquad \rho_{-1}^{\mathrm{v}} = \mathrm{sg}(\beta), \qquad \rho_j^{\mathrm{v}} = \mathrm{sqW}(y_j), \qquad i,j \geq 0 \tag{3.38}$$

and let $\boldsymbol{\eta}$ *be the Yang-Baxter field on the lattice* $\mathbb{Z}_{\geq 0} \times \mathbb{Z}_{\geq -1}$ *generated by the Markov transition operators* $\mathsf{U}^{\mathrm{fwd}}_{\rho_j^{\mathrm{v}},\rho_i^{\mathrm{h}}}$. *Denote* $\boldsymbol{\lambda} = \boldsymbol{\eta}|_{\mathbb{Z}_{\geq 0}\times\mathbb{Z}_{\geq 0}}$. *We call* $\boldsymbol{\lambda}$ *the* sqW/sqW Yang-Baxter field with two-sided stationary boundary conditions. *Then* $\boldsymbol{\lambda}$ *is an sqW/sqW field with mixed specializations. In particular its single-point distribution is given by*

$$\mathrm{Prob}\{\lambda^{(i,j)} = \nu\} = \frac{\prod_{1\leq i'\leq i}(\beta x_{i'};q)_\infty}{(-s\beta;q)_\infty^{i-1}} \prod_{1\leq j'\leq j}\left(\frac{(s^2;q)_\infty}{(-sy_j;q)_\infty}\right)^{i-1} \prod_{\substack{1\leq i'\leq i\\ 1\leq j'\leq j}} \frac{(x_{i'}y_{j'};q)_\infty}{(-sx_{i'};q)_\infty} \mathbb{F}_\nu(x_1,\dots,x_i)\mathbb{F}^*_{\nu'}(y_1,\dots,y_j$$

3.4.2 Vertex models with double sided stationary boundary conditions

Let us now turn to the marginal of fields with the two-sided stationary boundary conditions described in Section 3.4.1. We will consider the behavior of $\lambda_1^{(i,j)}$ at the boundary:

Proposition 3.4.5. *Consider the transition probabilities* $\mathbf{L}$ *given in* (3.11). *Then we have*

$$\mathbf{L}_{\mathrm{sg}(\alpha),\mathrm{sHL}(v)}(0,j_1;k_1',k_2') = \mathbf{1}_{j_1+k_1'=k_2'}\frac{(v\alpha)^{k_1'}}{1+v\alpha}, \tag{3.39}$$

$$\mathbf{L}_{\mathrm{sHL}(u),\mathrm{sg}(\beta)}(j_2,0;k_1',k_2') = \mathbf{1}_{j_2+k_2'=k_1'}\frac{(u\beta)^{k_2'}}{1+u\beta}, \tag{3.40}$$

$$\mathbf{L}_{\mathrm{sg}(\alpha),\mathrm{sg}(\beta)}(0,0;k_1',k_2') = \mathbf{1}_{k_1'=k_2'}\frac{(\alpha\beta)^{k_2'}}{(q;q)_{k_2'}}(\alpha\beta;q)_\infty, \tag{3.41}$$

$$\mathbf{L}_{\mathrm{sg}(\beta),\mathrm{sqW}(x)}(0,j_1;k_1',k_2') = \mathbf{1}_{j_1+k_1'=k_2'}(\beta x)^{k_1'}\frac{(-s/x;q)_{k_1'}}{(q;q)_{k_1'}}\frac{(\beta x;q)_\infty}{(-s\beta;q)_\infty}, \tag{3.42}$$

$$\mathbf{L}_{\mathrm{sg}(\beta),\mathrm{sqW}_\lrcorner(x)}(0,0;k_1',k_2') = \mathbf{1}_{k_1'=k_2'}\frac{(\beta x)^{k_2'}}{(q;q)_{k_2'}}(\beta x;q)_\infty. \tag{3.43}$$

The cases (3.39), (3.42) correspond to the bottom of the lattice and the left boundaries and (3.41), (3.43) arise from the bottom left corner. Finally (3.40) is found at the vertical boundary of the two sided stationary sHL/sHL Yang-Baxter field. Observe that (3.41) defines the q-Poisson distribution (cf. eq. (A.19)).

Proof of Proposition 3.4.5. All expressions follows by direct evaluation of (3.11) with the indicated choice of vertex weights. Normalization constant always come from the correct specialization of (B.10) when evaluating the sum of the cross vertex weight. □

Now take the stochastic six vertex model with independent Bernoulli boundary conditions (we call these the *two-sided stationary boundary conditions*:

$$b_i^{\mathrm{h}} \sim \mathrm{Ber}\left(\frac{u_i\beta}{1+u_i\beta}\right) \qquad \text{and} \qquad b_j^{\mathrm{v}} \sim \mathrm{Ber}\left(\frac{1}{1+v_j\alpha}\right). \tag{3.44}$$

That is, given a realization of these random variables, we then consider the stochastic six vertex model with these boundary conditions according to Definition 3.3.5. We have the following

Theorem 3.4.6. *Let $\mathcal{M}$ be a q-Poisson random variable with parameter $\alpha\beta$ independent of the stochastic six vertex model with two-sided stationary boundary conditions (3.44). Let $\{\lambda^{(i,j)} : i, j \geq 0\}$ be a sHL/sHL field two sided stationary boundary conditions. Then two random fields $\{j - \lambda_1^{(i,j)} : i, j \in \mathbb{Z}_{\geq 0}\}$ and $\{\mathcal{H}_{6V}^{\mathrm{ur}}(i,j) - \mathcal{M} : i, j \in \mathbb{Z}_{\geq 0}\}$ are equal in distribution.*

Proof. Theorem 3.4.6 follows in essentially the same way as Theorem 3.3.6 by matching the value of vertex weights L_{u_y,v_x} and probability laws of entries $b_x^{\mathrm{h}}, b_x^{\mathrm{v}}$ with those given by $\mathbf{L}$ (on the boundary this follows from Proposition 3.4.5). We will not repeat the argument. □

Result of theorem 3.4.6 extends with little modifications to all other marginal fields we considered in section 3.3 and summarized in fig. 3.3. We report the cases concerning the λ_1 marginal in the following list of theorems.

Theorem 3.4.7. *Let $\boldsymbol{\lambda} = \{\lambda^{(i,j)} : i, j \geq 0\}$ be a sqW/sHL field with mixed specializations and let $\mathcal{M} \sim q\text{-}Poi(\beta x_1)$ be independent of $\boldsymbol{\lambda}$. Then the marginal field $\{\lambda_1^{(i,j)} : i, j \geq 0\}$ is equivalent in distribution to $\{\mathcal{H}_{\mathrm{HS}}^{\mathrm{ul}}(i,j) + \mathcal{M}; i, j \geq 0\}$, where $\mathcal{H}_{\mathrm{HS}}^{\mathrm{ul}}$ is the height function of the up-left higher spin vertex model with boundary conditions*

$$b_i^{\mathrm{h}} \sim \varphi_{q,x_i\beta,-s/x_i}(\bullet|\infty), \qquad \text{and} \qquad b_j^{\mathrm{v}} \sim \mathrm{Ber}\left(\frac{v_j x_1}{1+v_j x_1}\right). \tag{3.45}$$

Proof. The proof is equivalent to that of theorem 3.4.6 and consist in matching weights $\mathbf{L}$ with vertex weights and boundary conditions of the up-left higher spin vertex model. □

Theorem 3.4.8. *Let $\boldsymbol{\lambda} = \{\lambda^{(i,j)} : i, j \geq 0\}$ be a sqW/sqW field with mixed specializations and let $\mathcal{M} \sim q\text{-}Poi(\beta x_1)$ be independent of $\boldsymbol{\lambda}$. Then the marginal field $\{\lambda_1^{(i,j)} : i, j \geq 0\}$ is equivalent in distribution to $\{\mathcal{H}_{\phi}^{\mathrm{ul}}(i,j) + \mathcal{M}; i, j \geq 0\}$, where $\mathcal{H}_{\mathrm{HS}}^{\mathrm{ul}}$ is the height function of the ${}_4\phi_3$ vertex model with boundary conditions*

$$b_i^{\mathrm{h}} \sim \varphi_{q,x_i\beta,-s/x_i}(\bullet|\infty), \qquad \text{and} \qquad b_j^{\mathrm{v}} \sim \varphi_{q,x_1y_j,-sx_1}(\bullet|\infty). \tag{3.46}$$

We conclude our discussion about marginals of fields with random boundary conditions with the following remark.

Remark 3.4.9. It is possible to extend the characterization of marginals of fields with two-sided stationary boundary conditions to include the last row case $\lambda_i^{(i,j)}$. Here the resulting processes would be the up-right higher spin vertex model with boundary conditions (3.45) and the q-Hahn vertex model with boundary conditions (3.46) respectively for the sqW/sHL field and the sqW/sqW field. To justify our claim we should construct sqW functions labeled by signatures λ with integer parts (possibly negative) and define yet another class of specializations for dual functions analogous to the scaled geometric ones. The scheme is the one employed in [IS19]. We will not repeat the construction here.

3.5 Fredholm determinants from q-moment formulas

Here we derive Fredholm determinant expressions for the q-Laplace transform of the random variable $\lambda_1^{(i,j)}$, where $\boldsymbol{\lambda} = \{\lambda^{(i,j)}\}$ is one of the Yang-Baxter fields described in Section 3.1.2 In the sHL/sHL case, these Fredholm formulas are known [BCG16], [Agg18]. In the sHL/sqW case, they are present in the literature for the step and step-stationary boundary conditions [CP16], [BP18a], [BP18b]. A Fredholm determinantal formula for the stochastic higher spin six vertex model appears also in [IMS20] and we recall it below in chapter 4, though the expression we establish here is different for this case. In the sqW/sqW case, a similar Fredholm formula for the q-Hahn PushTASEP was conjectured in [CMP19], and here we prove this conjecture.

For the sake of this section in many cases we use the Borodin-Wheeler's version of the sqW functions, as for the sake of marginal $\lambda_1^{(i,j)}$ there is no difference between the two variants. The derivation of Fredholm determinantal formulas for marginals $\lambda_i^{(i,j)}$ can be carried on the same footing, but for brevity we will not treat this case here.

3.5.1 Six vertex model observables through difference operators

In this subsection we rederive known results about the q-moments of the six vertex model [BCG16], [BP18a] making use of the difference operators acting on spin Hall-Littlewood functions. Consider the inhomogeneous stochastic six vertex model with the step boundary conditions and height function $\mathcal{H}^{\mathrm{ur}}_{6\mathrm{V}}$. Recall that the model depends on the parameters v_j and u_i, $i,j \in \mathbb{Z}_{\geq 1}$, which we assume positive (cf. definition 3.1.4). Let $v_1, v_2, \dots$ be spaced in such a way that

$$q \sup_j \{v_j\} < \inf_j \{v_j\}. \tag{3.47}$$

Proposition 3.5.1. *Under (3.47) we have*

$$\mathbb{E}^{\mathrm{step}}\left(q^{l\,\mathcal{H}^{\mathrm{ur}}_{6\mathrm{V}}(i,j)}\right) = q^{l(l-1)/2} \oint_{\gamma[\mathbf{v}|1]} \cdots \oint_{\gamma[\mathbf{v}|l]} \prod_{1\leq A<B\leq l} \frac{z_A - z_B}{z_A - q z_B} \times \prod_{k=1}^{l} \left\{ \prod_{\alpha=1}^{j} \frac{q z_k - v_\alpha}{z_k - v_\alpha} \prod_{\alpha=1}^{i} \frac{1 - z_k u_\alpha}{1 - q z_k u_\alpha} \frac{dz_k}{2\pi \mathrm{i} z_k} \right\}, \tag{3.48}$$

where the positively orientated contour $\gamma[\mathbf{v}|j] = \gamma_{\mathbf{v}} \cup r^{j-1} C_0$ for z_j is the union of a curve $\gamma_{\mathbf{v}}$ that encircles $v_1, \dots, v_j$ and no other pole of the integrand, and the dilation $r^{j-1}C_0$ of an arbitrary small circle C_0 around 0. Moreover, $r > q^{-1}$, and the shifted contour $q\gamma_{\mathbf{v}}$ must lie completely to the left of $\gamma_{\mathbf{v}}$ and completely to the right of $r^{l-1}C_0$.

Proof. This is an application of the eigenrelations from Theorem 2.6.2. Define the operator $\widetilde{\mathfrak{D}}$ as

$$\widetilde{\mathfrak{D}} := q^{-j}\left(Id + (q-1)\overline{\mathfrak{D}}_1^{*} \right), \tag{3.49}$$

acting on v variables and diagonally on the sHL functions as

$$\widetilde{\mathfrak{D}} \mathsf{F}^*_\lambda(v_1, \dots, v_j) = q^{-\ell(\lambda)} \mathsf{F}^*_\lambda(v_1, \dots, v_j).$$

This operator, acting on product functions $H(v_1,\ldots,v_j)=h(v_1)\cdots h(v_j)$ admits an integral representation

$$\widetilde{\mathfrak{D}}H(v_1,\ldots,v_j)=H(v_1,\ldots,v_j)\frac{1}{2\pi\mathrm{i}}\oint_{\gamma_{0,\boldsymbol{v}}}\prod_{\alpha=1}^{j}\frac{w-q^{-1}v_\alpha}{w-v_\alpha}\frac{1}{h(w)}\frac{dw}{w}. \tag{3.50}$$

From theorem 3.3.6 we have the identification $\mathcal{H}^{\mathrm{ur}}_{6\mathrm{V}}(i,j)=j-\lambda_1^{(i,j)}$, where $\lambda^{(i,j)}$ is the sHL/sHL field. Therefore, we have

$$\mathbb{E}^{\mathrm{step}}\big(q^{l\,\mathcal{H}^{\mathrm{ur}}_{6\mathrm{V}}(i,j)}\big)=q^{lj}\,\frac{\widetilde{\mathfrak{D}}^{l}\Pi(u_1,\ldots,u_i;v_1,\ldots,v_j)}{\Pi(u_1,\ldots,u_i;v_1,\ldots,v_j)},$$

where

$$\Pi(u_1,\ldots,u_i;v_1,\ldots,v_j)=\prod_{\alpha=1}^{j}\prod_{\beta=1}^{i}\frac{1-qu_\beta v_\alpha}{1-u_\beta v_\alpha}.$$

The nested contour formula (3.48) follows by recursively applying integral expression (3.50) for the action of $\widetilde{\mathfrak{D}}$ on factorized functions. □

Proposition 3.5.1 combined with well-known manipulations of summations of nested contour integrals like (3.48) (e.g., see [BCS14, Section 3]) give rise to a Fredholm determinant[5] expression for the one-point distribution of $\mathcal{H}^{\mathrm{ur}}_{6\mathrm{V}}$.

Theorem 3.5.2. *Consider the stochastic six vertex model with step boundary conditions. We have*

$$\mathbb{E}^{\mathrm{step}}\left(\frac{1}{(\zeta q^{\mathcal{H}^{\mathrm{ur}}_{6\mathrm{V}}(i,j)};q)_\infty}\right)=\det\left(Id+\mathsf{K}\right)_{L^2(\mathsf{C})},\qquad \zeta\in\mathbb{C}\setminus\mathbb{R}_{>0}. \tag{3.51}$$

The expression in the right-hand side of (3.51) is the Fredholm determinant of the kernel

$$\mathsf{K}(w,w')=\frac{1}{2\mathrm{i}}\int_{d+\mathrm{i}\mathbb{R}}\frac{(-\zeta)^r}{\sin(\pi r)}\frac{\mathsf{f}(w)/\mathsf{f}(q^r w)}{q^r w-w'}\,dr, \tag{3.52}$$

where $d\in(0,1)$, and

$$\mathsf{f}(w)=\prod_{\alpha=1}^{j}(w-v_\alpha)^{-1}\prod_{\alpha=1}^{i}(1-u_\alpha w).$$

The kernel K is defined on the Hilbert space $L^2(\mathsf{C})$, where C is a closed positively oriented curve encircling $0,v_1,v_2,\ldots$ such that, for all $r\in d+\mathrm{i}\mathbb{R}$, C contains $q^r\mathsf{C}$ but not $q^{-r}u_i^{-1}$ for $i=1,2,\ldots$.

We present the main steps of the proof of the Fredholm determinantal formula, and refer to [BC14] or [BCS14] for detailed explanations.

[5] On Fredholm determinants in general see, e.g., [Bor10].

Idea of proof of Theorem 3.5.2. Assume first (3.47) and $|\zeta| < 1/q$, and consider the nested contour expression (3.48). We can deform all contours, one by one, to be the same C around $0, v_1, v_2, \ldots$, and such that C contains its image under multiplication by q. This contour shift will cross poles $z_A = qz_B$, $A < B$, and one can rewrite (3.48) as

$$(q;q)_l \sum_{\lambda \vdash l} \frac{1}{m_1! m_2! \cdots} \int_{\mathsf{C}} \cdots \int_{\mathsf{C}} \det_{i,j=1}^{\ell(\lambda)} \left(\frac{1}{w_i - q^{\lambda_j} w_j} \right) \prod_{k=1}^{\ell(\lambda)} f(w_k)/f(q^{\lambda_k} w_k) \frac{dz_k}{2\pi \mathrm{i}},$$

where the sum is taken over all partitions λ of l, and $m_i = m_i(\lambda)$ are the multiplicities of the parts i in λ. Summing over l, we have

$$\sum_{l \geq 0} \frac{\zeta^l}{(q;q)_l} \mathbb{E}^{\mathrm{step}} \left(q^{l\, \mathcal{H}^{\mathrm{ur}}_{6\mathrm{V}}(i,j)} \right) = \mathbb{E}^{\mathrm{step}} \left(\frac{1}{(\zeta q^{\mathcal{H}^{\mathrm{ur}}_{6\mathrm{V}}(i,j)}; q)_\infty} \right),$$

where we used the absolute summability of the left-hand side (since $0 < q^{l\, \mathcal{H}^{\mathrm{ur}}_{6\mathrm{V}}} < 1$ and we assumed $|\zeta| < 1/q$) to exchange the summation with the expectation sign and the q-binomial theorem. The result we obtain is the Fredholm determinant of the kernel

$$\sum_{n \geq 0} \frac{\zeta^n}{w' - q^n w} \mathsf{f}(w)/\mathsf{f}(q^n w) = \frac{1}{2\mathrm{i}} \int_{d+\mathrm{i}\mathbb{R}} \frac{(-\zeta)^r}{\sin(\pi r)} \frac{\mathsf{f}(w)/\mathsf{f}(q^r w)}{q^r w - w'}.$$

Once we reach (3.51), we can relax conditions on u_i's and ζ since both side are analytic functions of their parameters. Formula (3.51) holds for any choice of $u_i, v_j \in (0,1)$ and $\zeta \in \mathbb{C} \setminus q^{\mathbb{Z}_{\geq 0}}$ (in particular, we can always find d in (3.52) such that C satisfies the required properties). □

In the next theorem we perform fusion of the sHL parameters. Recall the principal specializations $\mathfrak{F}^{(J_0,\ldots,J_i)}(u_0,\ldots,u_i)$, $\mathfrak{G}^{(I_0,\ldots,I_j)}(v_0,\ldots,v_j)$ defined in (2.38), (2.39). Parameters u_l, J_l, v_k, I_k are complex numbers satysfying (2.40) which we reproduce here:

$$|s|, |u_k|, |v_l|, |q^{J_k} u_k|, |q^{I_l} v_l|, \left| \frac{q^i u_k - s}{1 - q^i s u_k} \right|, \left| \frac{q^i v_l - s}{1 - q^i s v_l} \right| < \delta \qquad \text{for all } 0 \leq k \leq y,\ 0 \leq l \leq x,\ i \geq 0. \tag{3.53}$$

for sufficiently small $\delta > 0$ which might depend on x, y, but not on the other parameters.

Theorem 3.5.3. *With the above notation, we have for all $\zeta \in \mathbb{C} \setminus \mathbb{R}_{>0}$:*

$$\prod_{\substack{0 \leq \alpha \leq i \\ 0 \leq \beta \leq j}} \frac{(u_\alpha v_\beta; q)_\infty (u_\alpha v_\beta q^{I_\beta + J_\alpha}; q)_\infty}{(u_\alpha v_\beta q^{I_\beta}; q)_\infty (u_\alpha v_\beta q^{J_\alpha}; q)_\infty} \times \sum_\lambda \frac{\mathfrak{F}^{(J_0,\ldots,J_i)}_\lambda(u_0,\ldots,u_i) \mathfrak{G}^{(I_0,\ldots,I_j)}_\lambda(v_0,\ldots,v_j)}{(\zeta q^{-\ell(\lambda)}; q)_\infty} = \det\left(Id + K\right)_{L^2(C)}. \tag{3.54}$$

The kernel K is defined as

$$K(w,w') = \frac{1}{2\mathrm{i}} \int_{d+\mathrm{i}\mathbb{R}} \frac{(-\zeta)^r}{\sin(\pi r)} \frac{f(w)/f(q^r w)}{q^r w - w'} dr,$$

where $d \in (0,1)$ and

$$f(w) = \prod_{\alpha=0}^{j} \frac{(q^{I_\alpha} v_\alpha / w; q)_\infty}{(v_\alpha/w;q)_\infty} \prod_{\alpha=0}^{i} \frac{(u_\alpha w;q)_\infty}{(q^{J_\alpha} u_\alpha w; q)_\infty}.$$

The contour C is a closed positively oriented curve encircling $0, q^k v_i$ for $k, i \geq 0$ and such that, for all $r \in d + \mathrm{i}\mathbb{R}$, C contains $q^r C$ and $q^{r+k} q^{I_l} v_l$ for all $k, l \geq 0$, but leaves outside $1/(q^{r+k} u_l)$ and $1/(q^k q^{J_l} u_l)$ for all $k, l \geq 0$.

Proof. Considering principal specializations in Theorem 3.5.2, we see that (3.54) holds for any $J_0, \dots J_i, I_0, \dots, I_j$ positive integers. Indeed, this follows from the computation for $I, J \in \mathbb{Z}_{\geq 1}$:

$$\begin{aligned} &\frac{q^r w - v}{w - v} \frac{q^r w - qv}{w - qv} \cdots \frac{q^r w - vq^{I-1}}{w - vq^{I-1}} \frac{1 - uw}{1 - q^r uw} \frac{1 - quw}{1 - q^r uvw} \cdots \frac{1 - q^{J-1} uw}{1 - q^r q^{J-1} uw} \\ &\qquad = q^{rI} \frac{(vq^I/w;q)_\infty}{(v/w;q)_\infty} \frac{(q^{-r} v/w;q)_\infty}{(q^{-r} v q^I / w; q)_\infty} \frac{(uw;q)_\infty}{(uq^J w;q)_\infty} \frac{(uq^J w q^r; q)_\infty}{(uwq^r;q)_\infty}. \end{aligned} \tag{3.55}$$

The factor q^{rI} (leading to $q^{r(I_0+\dots+I_j)}$ in the kernel) disappears after replacing ζ by $\zeta q^{-I_0-\dots-I_j}$. This change of variable accounts for the fact that in the left-hand side of (3.54) we take the q-Laplace transform of $q^{-\ell(\lambda)}$ as opposed to the height function in Theorem 3.5.2.

By the absolute convergence result of Proposition 2.4.4 and the boundedness of $1/(\zeta q^{-\ell(\lambda)};q)_\infty$, the left-hand side of (3.54) is an analytic function of q^{J_k}, q^{I_l} under the bounds (3.53). In order to establish the analyticity of the Fredholm determinant we first observe that, due to the compactness of C and of the image of $r \to q^r$ for $r \in d + \mathrm{i}\mathbb{R}$, there exists a constant M_1 independent of J_k or I_l such that

$$\sup_{\substack{w,w' \in C, \\ r \in d+\mathrm{i}\mathbb{R}}} \left| \frac{f(w)/f(q^r w)}{q^r w - w'} \right| < M_1.$$

This implies that $|K(w,w')| < M_2$ integrating over r due to the exponential decay of $1/\sin \pi r$ for large $|r|$. We can thus estimate the Fredholm determinant of K with

$$\sum_{l \geq 0} \frac{1}{l!} \int_C \cdots \int_C \left| \det_{i,j=1}^{l} (K(w_i,w_j)) \right| dw_1 \cdots dw_l \leq \sum_{l \geq 0} \frac{l^{l/2} M_3^l}{l!},$$

where we used the Hadamard inequality to bound the determinant of $K(w_i, w_j)$, and $M_3 = M_2 \ell(C)$. This shows that the right-hand side of (3.54) is an absolutely convergent sum of analytic functions and hence it is analytic. This completes the proof. □

Remark 3.5.4. Fredholm determinantal expression (3.54) degenerates to a number of known results. In particular, considering the specialization $v_0 = -\alpha\epsilon$, $u_0 = -\beta\epsilon$ $q^{I_0} = q^{J_0} = 1/\epsilon$, $\epsilon \to 0$, and $J_1 = \ldots = J_i = I_1 = \ldots = I_j = 1$, we recover the expression for the q-Laplace transform of the height function of the six vertex model with two-sided stationary bound conditions from [Agg18, Proposition 4.1] (in the latter one has to set $\mu = 0$). The latter formula is obtained by a more involved analytic continuation in q^{I_0} than in the proof of Theorem 3.5.3.

3.5.2 Higher spin six vertex model observables

The eigenrelations for the sqW or sHL functions give rise to moment formulas for the stochastic higher spin six vertex model. Consider the model with step-Bernoulli boundary conditions (see eq. (3.24)). Assume that the parameters $x_1, x_2, \ldots$ are spaced in such a way that

$$q \sup(1/x_i)_{i\geq 1} < \inf(1/x_i)_{i\geq 1}. \tag{3.56}$$

Following the same approach as in the proof of Proposition 3.5.1 (applying either $\widetilde{\mathfrak{D}}$ or $\overline{\mathfrak{D}}_1$ from Section 2.6 to the sum of the corresponding Cauchy identity), we obtain a q-moment formula which was essentially first written down in [CP16]:

Proposition 3.5.5. *We have*

$$\begin{aligned}\mathbb{E}\left(q^{-l\,\mathcal{H}^{\mathrm{ul}}_{\mathrm{HS}}(i,j)}\right) = (-1)^l q^{l(l-1)/2} \oint_{\Gamma[\boldsymbol{x}|1]} \cdots \oint_{\Gamma[\boldsymbol{x}|l]} \prod_{1\leq A<B\leq l} \frac{z_A - z_B}{z_A - q z_B} \\ \times \prod_{k=1}^{l} \left\{ \prod_{\alpha=1}^{i} \frac{1+s z_k}{1-x_\alpha z_k} \prod_{\alpha=1}^{j} \frac{z_k + v_\alpha/q}{z_k + v_\alpha} \frac{dz_k}{2\pi \mathrm{i} z_k(1+s z_k)} \right\},\end{aligned} \tag{3.57}$$

where the positively oriented contour $\Gamma[\boldsymbol{x}|k]$ is around $1/x_1, \ldots 1/x_i$, $q\Gamma[\boldsymbol{x}, \beta|k+1]$, and no other pole of the integrand.

The following determinantal expression for the q-Laplace transform of the height $\mathcal{H}^{\mathrm{ul}}_{\mathrm{HS}}$ is obtained specializing the general formula (3.54).

Theorem 3.5.6. *Consider the higher spin six vertex model with two-sided stationary boundary conditions (3.45) and let $\mathcal{M} \sim q$-Poi$(x_1\beta)$ be independent of the vertex model. Then we have*

$$\mathbb{E}\left(\frac{1}{(\zeta q^{-\mathcal{H}^{\mathrm{ul}}_{\mathrm{HS}}(i,j)-\mathcal{M}}; q)_\infty}\right) = \det(Id + \mathcal{K})_{L^2(\mathcal{C})}. \tag{3.58}$$

The kernel $\mathcal{K}$ is defined by

$$\mathcal{K}(w, w') = \frac{1}{2\mathrm{i}} \int_{d+\mathrm{i}\mathbb{R}} \frac{(-\zeta)^r}{\sin(\pi r)} \frac{f(w)/f(q^r w)}{q^r w - w'} dr, \tag{3.59}$$

where $d \in (0,1)$ and

$$f(w) = \frac{(-\beta/w; q)_\infty}{(-x_1 w; q)_\infty} \prod_{l=1}^{j} \frac{1}{w - v_l} \prod_{l=2}^{i} \frac{(sw; q)_\infty}{(-x_l w; q)_\infty}. \tag{3.60}$$

Here $\mathcal{C}$ is a closed complex contour encircling $0, v_1, v_2, \ldots$ and such that for all $r \in d+\mathrm{i}\mathbb{R}$, $\mathcal{C}$ contains $-q^{r+k}\beta$ for all $k \geq 0$, but leaves outside $1/(q^{r+k}s)$ and $1/(q^k x_l)$ for all $k, l \geq 1$.

Proof. We use an analytic continuation argument staring from identity (3.54). Considering specializations $\mathrm{sg}(\beta)$ for v_0, q^{J_0} and $\mathrm{sg}(x_1), \mathrm{sqW}(x_1), \mathrm{sqW}(x_2), \ldots,$ respectively for $u_0, q^{I_0}, u_1, q^{I_1}, u_2, q^{I_2}, \ldots,$ we can prove expression (3.58) for values β, v_l, x_l is a small neighborhood of the origin. Once (3.58) is established for parameters in an open set, we can perform an analytic continuation, always keeping them in a region where they define a probability measure. This is possible since both sides of (3.58) can be written as absolutely convergent series of holomorphic functions in β, v_l, x_l. □

Using the integral expression for the q-moments (3.57) we can obtain an alternative expression for the Fredholm determinant:

Theorem 3.5.7. *Assume conditions (3.56). Let $\widetilde{\mathcal{C}}$ be a closed positively oriented contour encircling $-1/x_1, -1/x_2, \ldots$ and which does not contain any point of the interior of $q\,\widetilde{\mathcal{C}}$. Then the Fredholm determinantal formula (3.58) holds when replacing $\mathcal{C}$ with $\widetilde{\mathcal{C}}$.*

Proof. The proof of this alternative representation can be given as in theorem 3.5.2. We can start from step-Bernoulli boundary conditions and then obtain stationary boundary conditions via fusion. For detail we refer to [BMP19] □

Remark 3.5.8. Another Fredholm determinantal formula for the stochastic higher spin six vertex model with two-sided stationary boundary conditions was obtained in [IMS20] and we use this below in chapter 4. While the two formulas differ from each other, one should in principle be able to transform one to the other. We do not focus on this in the present work.

3.5.3 $_4\phi_3$ stochastic vertex model observables.

By using the fact that the $_4\phi_3$ vertex model is equivalent in distribution to a marginal of the sqW/sqW field we can obtain contour integral expressions for the q-moments of the height function $\mathcal{H}_\phi^{\mathrm{ul}}$. Indeed, this is possible by employing the eigenoperator $\overline{\mathfrak{D}}_1$. However, only finitely many of the q-moments exist, and this also involves certain bounds on the parameters. Consider the model with step-stationary boundary conditions (3.30). Assume that $x_1, x_2, \ldots$ satisfy (3.56).

Proposition 3.5.9. *If l is such that $q^l > \max_{1 \leq t \leq j}\{x_1 y_t\}$, we have*

$$\mathbb{E}^{\mathrm{step}}\left(q^{-l\,\mathcal{H}_\phi^{\mathrm{ul}}(i,j)}\right) = (-1)^l q^{l(l-1)/2} \oint_{\Gamma[\boldsymbol{x}|1]} \cdots \oint_{\Gamma[\boldsymbol{x}|l]} \prod_{1 \leq A < B \leq l} \frac{z_A - z_B}{z_A - q z_B} \times \prod_{k=1}^{l} \left\{ \prod_{\alpha=1}^{i} \frac{1 + s z_k}{1 - x_\alpha z_k} \prod_{\alpha=1}^{j} \frac{z_k + s/q}{z_k - y_\alpha/q} \frac{dz_k}{2\pi\mathrm{i} z_k (1 + s z_k)} \right\}, \tag{3.61}$$

where $\Gamma[\boldsymbol{x}|j]$ is a positively oriented contour around $1/x_1, 1/x_2, \ldots,\ q\Gamma[\boldsymbol{x}|j+1]$, and no other pole of the integrand. In case $q^l \leq \max_{1 \leq t \leq y}\{x_1 y_t\}$ we have $\mathbb{E}^{\mathrm{step}}\left(q^{-l\,\mathcal{H}_\phi^{\mathrm{ul}}(i,j)}\right) = \infty$.

Despite the fact that the distribution of $\mathcal{H}_\phi^{\mathrm{ul}}$ is not characterized by its q-moments since only finitely many of them exist, we can still write down Fredholm determinant expressions for the q-Laplace transform of $\mathcal{H}_\phi^{\mathrm{ul}}$.

Theorem 3.5.10. *Consider the* ${}_4\phi_3$ *stochastic vertex model with two-sided stationary boundary conditions with parameters* (3.46). *Let* $\mathcal{M} \sim q\text{-Poi}(x_1\beta)$ *be independent of the vertex model. We have*

$$\mathbb{E}\Big(\frac{1}{(\zeta q^{-\mathcal{H}_\phi^{\mathrm{ul}}(i,j)-\mathcal{M}};q)_\infty}\Big) = \det(Id+\mathbb{K})_{L^2(\mathfrak{C})}. \tag{3.62}$$

The kernel $\mathbb{K}$ *is defined by*

$$\mathbb{K}(w,w') = \frac{1}{2\mathrm{i}}\int_{d+\mathrm{i}\mathbb{R}} \frac{(-\zeta)^r}{\sin(\pi r)} \frac{\mho(w)/\mho(q^r w)}{q^r w - w'} dr, \tag{3.63}$$

where $d \in (0,1)$ *and*

$$\mho(w) = \frac{(-\beta/w;q)_\infty}{(-x_1 w;q)_\infty} \prod_{l=1}^{j} \frac{(-y_l/w;q)_\infty}{(s/w;q)_\infty} \prod_{l=2}^{i} \frac{(sw;q)_\infty}{(-x_l w;q)_\infty} \tag{3.64}$$

Here $\mathfrak{C}$ *is a closed complex contour encircling* $0, q^k s$ *for* $k \geq 0$ *and such that, for any* $r \in d+\mathrm{i}\mathbb{R}$, $\mathfrak{C}$ *contains* $q^r\mathfrak{C}$ *and* $-q^{r+k}y_l, -q^{r+k}\beta$ *for all* $k, l \geq 0$, *but leaves outside* $1/(q^{r+k}s)$ *and* $-1/(q^k x_l)$ *for all* $k, l \geq 0$.

Proof. Expression (3.62) is derived from the general summation identity (3.54) in the same way as Theorem 3.5.6. First we establish (3.62) for parameters β, s, y_l, x_l is a small neighborhood of the origin by considering specializations of $u_0, q^{J_0}, u_1, q^{J_1}, \dots, v_0, q^{I_0}, v_1, q^{I_1}$ in (3.54). Subsequently we relax conditions on these parameters moving them away from the origin but keeping them in real intervals in such a way that they always define a probability measure. This is possible due to the analyticity of both sides of (3.62) in the parameters. □

Theorem 3.5.11. *Assume* (3.56) *and let* $\widetilde{\mathfrak{C}}$ *be a closed complex contour encircling* $-1/x_1, -1/x_2, \dots$ *and that does not contain any point of the interior of* $q\widetilde{\mathfrak{C}}$. *Then expression* (3.62) *holds with contour* $\mathfrak{C}$ *replaced by* $\widetilde{\mathfrak{C}}$.

Proof. This alternative determinantal expression for the q-Laplace transform follows from Theorem 3.5.7 using the sqW specializations and subsequent analytic continuation. □

Remark 3.5.12. Both Theorems 3.5.10 and 3.5.11 degenerate to Fredholm determinantal formulas for the q-Hahn pushTASEP. In particular, expression given by Theorem 3.5.11 was conjectured in [CMP19] (Conjecture 3.11) for step initial conditions. Therefore, we have established this conjecture. Moreover, by sending all parameters to 1, one can also get the proof of [CMP19, Conjecture 4.6] on the Laplace transform of the one-point observable in the beta polymer like model introduced in [CMP19].

Chapter 4

KPZ fluctuation of the Higher Spin Vertex Model

This chapter presents results contained in sections 5 and 6 of

[IMS20] T. Imamura, M. Mucciconi, and T. Sasamoto. "Stationary Higher Spin Six Vertex Model and q-Whittaker measure". In: *Probability Theory and Related Fields* (Mar. 2020)

4.1 Fredholm determinants from elliptic determinants

In section 3.5 we derived a number of determinantal formulas for the higher spin vertex model and its degenerations. There the scheme we employed was to use nice nested contours representations for q-moment formulas, that after a certain shift of contours give rise to terms of the series expansion of a Fredholm determinant. Nevertheless this is not the only way such nice expressions can be derived. A possibly more straightforward procedure was discovered in [IS19] and makes use of Frobenius elliptic generalization of Cauchy determinant (see [KN03]). In this section we will report an alternative representation for the q-Laplace transform of the height function of the higher spin six vertex model found in [IMS20] and we will omit the details of the derivation of our formulas, which can be found in [IS19; IMS20].

4.1.1 Double sided stationary higher spin vertex model

Techniques employing elliptic determinants allow to consider a more general vertex model than the one discussed in chapter 3. In fact throughout the section we will allow spin parameter to be completely inhomogeneous in space. This requires a change of notation the and stochastic weights we use are those reported in table 4.1. Moreover, since in this chapter we only consider the up-right higher spin vertex model and no other model we will drop the use of superscripts $^{\mathrm{ur}}$ and we will refer to the stochastic weight as $\mathsf{L}^{\mathrm{ur}} = \mathsf{L}$ and to the height function $\mathcal{H}^{\mathrm{ur}}_{\mathrm{HS}} = \mathcal{H}$.

	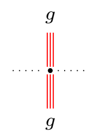	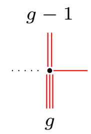	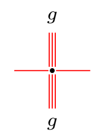	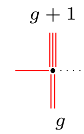
$\mathsf{L}_{\xi_x u_t, s_x}$	$\frac{1-q^g \xi_x s_x u_t}{1-s_x \xi_x u_t}$	$\frac{-s_x \xi_x u_t + q^g \xi_x s_x u_t}{1-s_x \xi_x u_t}$	$\frac{-s_x \xi_x u_t + s_x^2 q^g}{1-s_x \xi_x u_t}$	$\frac{1-s_x^2 q^g}{1-s_x \xi_x u_t}$

Table 4.1: Fully inhomogeneous stochastic weights

Definition 4.1.1 ([BP18a])**.** Specialize the up-right stochastic vertex model of Definition 3.3.1 by taking $L^{\mathrm{ur}}_{(x,t)} = \mathsf{L}_{\xi_x u_t, s_x}$, where the latter are given in table 4.1. We refer to this model as the *fully inhomogeneous stochastic higher spin six vertex model.* To ensure well posedness of the model we assume that parameters are

$$0 \le q < 1, \qquad 0 \le s_x < 1, \qquad \xi_x > 0, \qquad u_t < 0, \qquad \text{for all } x, t. \tag{4.1}$$

We consider the *two sided-stationary* boundary conditions:

$$b^{\mathrm{h}}_x \sim q\mathrm{NB}(s_x^2, v/(\xi_x s_x)), \qquad b^{\mathrm{h}}_t \sim \mathrm{Ber}(\mathpzc{d} u_t/(\mathpzc{d} u_t - 1)), \tag{4.2}$$

where Ber$(\cdot)$ are independent Bernoulli random variables and qNB$(\cdot)$ are independent q-negative binomial random variables (A.18). Parameters $v, \mathpzc{d}$ play the role of densities and we assume

$$q \sup_i \{\xi_i s_i\} < \mathpzc{d} < \inf_i \{\xi_i s_i\} \le \sup_i \{\xi_i s_i\} < \inf_i \{\xi_i / s_i\} \tag{4.3}$$

and

$$0 \le v < \inf_x \{\xi_x s_x\}. \tag{4.4}$$

It was proven in [IMS20] that even for a fully inhomogeneous model such as that of definition 4.1.1 a notion of translation invariance and hence stationarity can be defined. For this consider random boundary conditions $B^{\mathrm{h}}, B^{\mathrm{v}}$ and their shifts $B^{\mathrm{h}}_{+i} = (b^{\mathrm{h}}_{i+1}, b^{\mathrm{h}}_{i+2}, \dots)$, $B^{\mathrm{v}}_{+j} = (b^{\mathrm{v}}_{j+1}, b^{\mathrm{v}}_{j+2}, \dots)$. We say that a measure $\mathcal{P}(B^{\mathrm{h}}, B^{\mathrm{v}})$ is *translation invariant* if the restriction of the ensemble to the quadrant $\mathbb{Z}_{\ge i} \times \mathbb{Z}_{\ge j}$ originating from a generic point (i, j) is equivalent in distribution to $\mathcal{P}(B^{\mathrm{h}}_{+i}, B^{\mathrm{v}}_{+j})$.

We have the following

Theorem 4.1.2 ([IMS20])**.** *Consider the higher spin six vertex model of definition 4.1.1 with double sided-stationary boundary conditions of densities $v, \mathpzc{d}$. Then, if $v = \mathpzc{d}$ the model is transfation invariant and we call it stationary higher spin vertex model with density $\mathpzc{d}$.*

4.1.2 Fredholm determinants for two sided stationary boundary conditions: elliptic determinants form

In this section we give a Fredholm determinant expression for the q-Laplace transform of the probability mass function of the shifted height function $\mathcal{H}(x,t) - \mathcal{M}$. The proof of theorem 4.1.3 is based on calculations involving an elliptic version of the Cauchy determinant that were developed in [IS19] and it is therefore omitted.

Theorem 4.1.3. *Consider the higher spin vertex model of definition 4.1.1 and let $v < \mathpzc{d}$. Also set $\mathcal{M}$ to be an independent q-Poisson random variable of parameter $v/\mathpzc{d}$ (see (A.19) for the definition). Then we have*

$$\mathbb{E}_{\mathrm{HS}(v,\mathpzc{d})\otimes\mathcal{M}}\left(\frac{1}{(\zeta q^{\mathcal{H}(x,t)-\mathcal{M}};q)_\infty}\right) = \det(\mathbf{1} - fK)_{l^2(\mathbb{Z})}. \tag{4.5}$$

where

$$f(n) = \frac{1}{1-q^n/\zeta}, \tag{4.6}$$

$$K(n,m) = \sum_{l=1}^{x-1} \phi_l(m)\psi_l(n) + (\mathpzc{d} - v)\Phi_x(m)\Psi_x(n), \tag{4.7}$$

$$\phi_l(n) = \tau(n)\int_D \frac{dw}{2\pi \mathrm{i}}\frac{1}{w^{x+n-l+1}}\prod_{k=1}^{l}\frac{1}{(w-\xi_{k+1}s_{k+1})}\frac{(qv/w;q)_\infty}{F(w)}, \tag{4.8}$$

$$\psi_l(n) = \frac{\xi_{l+1}s_{l+1}}{\tau(n)}\int_C \frac{dz}{2\pi\mathrm{i}} z^{n+x-l-1}\prod_{k=2}^{l}(z-\xi_k s_k)\frac{F(z)}{(qv/z;q)_\infty}, \tag{4.9}$$

$$\Phi_x(n) = \tau(n)\int_D \frac{dw}{2\pi\mathrm{i}}\frac{1}{w^{n+1}}\frac{1}{w-\mathpzc{d}}\prod_{k=2}^{x}\frac{1}{w-\xi_k s_k}\frac{(qv/w;q)_\infty}{F(w)}, \tag{4.10}$$

$$\Psi_x(n) = \frac{1}{\tau(n)}\int_C \frac{dz}{2\pi\mathrm{i}}\frac{z^{n-1}}{(v/z;q)_\infty}\prod_{k=2}^{x}(z-\xi_k s_k)F(z). \tag{4.11}$$

The contour D encircles $\{\mathpzc{d}, \xi_2 s_2, \dots, \xi_x s_x\}$ and no other singularity, whereas C contains 0 and vq^k, for any k in $\mathbb{Z}_{\geq 0}$. Finally, $\tau(n)$ is taken to be

$$\tau(n) = \begin{cases} b^n & \text{if } n \geq 0, \\ c^n & \text{if } n < 0, \end{cases} \tag{4.12}$$

with

$$v < b < \mathpzc{d} \leq \inf_{i\geq 2}\{\xi_i s_i\} \leq \sup_{i\geq 2}\{\xi_i s_i\} < c < \inf_{i \geq 2}\{\xi_i/s_i\},$$

and

$$F(z) = (qz/\mathpzc{d};q)_\infty \prod_{j=1}^{t}(1-zu_j)\prod_{k=2}^{x}\frac{(qz/(\xi_k s_k);q)_\infty}{(zs_k/\xi_k;q)_\infty}. \tag{4.13}$$

The next proposition ensures that the Fredholm determinant expression (4.5) makes sense.

Proposition 4.1.4. *The kernel fK defined by eqs. (4.6) to (4.11) is trace class.*

Proof. From fK being a finite sum of products of operators of rank one, it is enough to show that each one of these operators is of Hilbert-Schmidt class. This is essentially proven in Appendix C.1. In fact the generic terms $f(n)\phi_l(n)\psi_l(m)$ and $f(n)\Phi_x(n)\Psi_x(m)$ are bounded in absolute value by quantities exponentially small in $|n|+|m|$, thanks to Proposition C.1.1, and therefore the double summation

$$\sum_{n,m\in\mathbb{Z}} |f(n)K(n,m)|^2$$

is indeed convergent. □

An alternative expression for the kernel K is given defining an auxiliary kernel A as

$$A(n,m) = \sum_{l=1}^{x-1} \phi_l(n)\psi_l(m) \tag{4.14}$$

of which we report the explicit form.

Proposition 4.1.5 (Double integral kernel)**.** *The discrete kernel A admits the following expression*

$$\begin{aligned} A(n,m) =& \frac{\tau(n)}{\tau(m)} \frac{1}{(2\pi \mathrm{i})^2} \int_D dw \int_C dz \frac{z^m}{w^{n+1}} \prod_{j=1}^{t} \left(\frac{1-u_j z}{1-u_j w} \right) \\ & \times \prod_{k=2}^{x} \left(\frac{(z/(\xi_k s_k), w s_k/\xi_k; q)_\infty}{(w/(\xi_k s_k), z s_k/\xi_k; q)_\infty} \right) \frac{(qv/w, qz/d\!\!\!/; q)_\infty}{(qv/z, qw/d\!\!\!/; q)_\infty} \frac{1}{z-w}. \end{aligned} \tag{4.15}$$

Proof. All it takes to show (4.15) is to perform the summation

$$\sum_{l=1}^{x-1} \phi_l(n)\psi_l(m),$$

using the rather tricky identity

$$\frac{1}{z-w}\left[\frac{w^{x-1}}{z^{x-1}} \prod_{k=2}^{x} \frac{z-a_k}{w-a_k} - 1 \right] = \sum_{l=1}^{x-1} \frac{a_{l+1}}{w-a_{l+1}} \frac{w^{l-1}}{z^l} \prod_{k=2}^{l} \frac{z-a_k}{w-a_k},$$

which can be proven by induction. We see that the addend $(z-w)^{-1}$ in the left hand side doesn't give any contribution to the integral as integrating over the variable z it only leaves an integral in w over a path containing no singularities. □

We like now to state some regularity properties of the integral kernel fA defined by (4.6),(4.14) that hold for parameters $v, d\!\!\!/$ such that

$$qv < d\!\!\!/ < v/q. \tag{4.16}$$

Proposition 4.1.6. *Let $\zeta < 0$ and take f, A as in (4.6), (4.14). Then $\mathbf{1} - fA$ is an invertible operator. Moreover both fA and $(\mathbf{1} - fA)^{-1}$ are well defined, bounded operators in the region (4.16).*

In the proof of Proposition 4.1.6 we use the following biorthogonality property.

Lemma 4.1.7. *Let $v, đ$ be such that $v < đ$ or (4.16) holds. Then we have*

$$\sum_{n \in \mathbb{Z}} \phi_l(n) \psi_m(n) = \delta_{l,m}. \tag{4.17}$$

Proof. This is a simple consequence of the contour integral expressions (4.8), (4.9). The generic term in the summation in the left hand side of (4.17) is

$$\phi_l(n)\psi_m(n) = \xi_{m+1} s_{m+1} \int_D \int_C \frac{dwdz}{(2\pi \mathrm{i})^2} \left(\frac{z}{w}\right)^n \frac{w^{l-1}}{z^{m+1}} \frac{\prod_{k=2}^m (z - \xi_k s_k)}{\prod_{k=2}^{l+1} (w - \xi_k s_k)} \frac{G(w)}{G(z)},$$

where, in the function G, we gathered together the factors independent on n or l, m as

$$G(u) = \frac{(qv/u; q)_\infty}{u^x F(u)}.$$

We see that in order to take the summation over all integers inside the integrals we need $|z/w|$ to be suitably defined depending on the positivity of n itself.

Consider the contour $\widetilde{C}$ being a circle of radius r such that $\max_i |\xi_i s_i| < r < \min_i |\xi_i / s_i|$. We can write

$$\begin{aligned}
\sum_{n \in \mathbb{Z}} \phi_l(n)\psi_m(n) &= \xi_{m+1} s_{m+1} \Bigg[\sum_{n \geq 0} \int_D \int_C \frac{dwdz}{(2\pi \mathrm{i})^2} \left(\frac{z}{w}\right)^n \frac{w^{l-1}}{z^{m+1}} \frac{\prod_{k=2}^m (z - \xi_k s_k)}{\prod_{k=2}^{l+1} (w - \xi_k s_k)} \frac{G(w)}{G(z)} \\
&\qquad + \sum_{n < 0} \int_D \int_{\widetilde{C}} \frac{dwdz}{(2\pi \mathrm{i})^2} \left(\frac{z}{w}\right)^n \frac{w^{l-1}}{z^{m+1}} \frac{\prod_{k=2}^m (z - \xi_k s_k)}{\prod_{k=2}^{l+1} (w - \xi_k s_k)} \frac{G(w)}{G(z)} \Bigg] \\
&= \xi_{m+1} s_{m+1} \left[\int_D \left(\int_{\widetilde{C}} - \int_C \right) \frac{dwdz}{(2\pi \mathrm{i})^2} \frac{1}{z - w} \frac{w^l}{z^{m+1}} \frac{\prod_{k=2}^m (z - \xi_k s_k)}{\prod_{k=2}^{l+1} (w - \xi_k s_k)} \frac{G(w)}{G(z)} \right] \\
&= \xi_{m+1} s_{m+1} \left[\int_D \int_{\widetilde{D}} \frac{dwdz}{(2\pi \mathrm{i})^2} \frac{1}{z - w} \frac{w^l}{z^{m+1}} \frac{\prod_{k=2}^m (z - \xi_k s_k)}{\prod_{k=2}^{l+1} (w - \xi_k s_k)} \frac{G(w)}{G(z)} \right],
\end{aligned}$$

where, for the last equality, we deformed $\widetilde{C}$ into an union or the two contours C and $\widetilde{D}$, with the latter being a curve encircling D and no other singularity for the z variable. Performing the z integral we get

$$\xi_{m+1} s_{m+1} \int_D \frac{dw}{2\pi \mathrm{i}} w^{l-m-1} \left(\mathbb{1}_{m=l+1} + \mathbb{1}_{m \leq l} \prod_{k=m+1}^{l+1} \frac{1}{w - \xi_k s_k} + \mathbb{1}_{m \geq l+2} \prod_{k=l+2}^{m} (w - \xi_k s_k) \right).$$

Naturally, when $m > l$ there is no pole inside D and the integral vanishes. On the other hand, if $m \leq l$ we can evaluate the residue at infinity and obtain the result. □

Proof of Proposition 4.1.6. We want to show that $\|fA\|_{l^2(\mathbb{Z})} < 1$, so to define $(\mathbf{1} - fA)^{-1}$ through the geometric series

$$\sum_{k \geq 0} (fA)^k.$$

A first observation is that $\|A\| = 1$ and this follows from the biorthogonality relation (4.17). For this set $V = \text{span}\{\psi_i | \, i = 1, \dots, x-1\}$ and notice that, by biorthogonality, we also have $V = \text{span}\{\phi_i | \, i = 1, \dots, x-1\}$ (if $\widetilde{v} = \sum c_i \phi_i$ such that $\widetilde{v} \perp V$, then $\widetilde{v} = 0$). For any $h \in \ell^2(\mathbb{Z})$ write the orthogonal decomposition $h = h_V + h_{V^\perp}$ where $h_V \in V$ and $h_{V^\perp} \in V^\perp$. Then we have $Ah = Ah_V = h_V$ for all h since $A\phi_i = \phi_i$ for all $i = 1, \dots, x-1$ and we conclude that

$$\|A\| = \sup_{h_V \in V} \frac{\|Ah_V\|}{\|h_V\|} = 1.$$

To show that the operator norm of fA is strictly smaller than 1, consider the following bound for the function f, defined in (4.6),

$$f(n) \leq (1 - \varepsilon) f(n + n_0) + \varepsilon P_{n_1}(n),$$

with $P_{n_1}(n) = \mathbb{1}_{n \geq n_1}$ and ε, n_0, n_1, suitably chosen. In particular, taking n_0 large enough and ε small we can let n_1 be an arbitrary big number. Moreover, the fact that f is a diagonal operator implies the simple estimate

$$\|fA\| \leq (1 - \varepsilon)\|f\|\|A\| + \varepsilon \|P_{n_1} A\| \leq 1 - \varepsilon + \varepsilon \|P_{n_1} A\|.$$

Let's consider now an element η in the unitary sphere of $l^2(\mathbb{Z})$. By simply using the definition of the kernel A and the Schwartz inequality we have

$$\|P_{n_1} A \eta\| \leq \sum_{l=1}^{x-1} \left(\sum_{n \in \mathbb{Z}} \left| \mathbb{1}_{n \geq n_1} \phi_l(n) \sum_{m \in \mathbb{Z}} \psi_l(m) \eta(m) \right|^2 \right)^{1/2} \leq \sum_{l=1}^{x-1} \|\psi_l\| \left(\sum_{n \geq n_1} |\phi_l(n)|^2 \right)^{1/2},$$

which, thanks to the bound (C.1), can be shown to be geometrically small in n_1. Therefore $\|fA\| < 1$.

Finally, we remark that for sequences ϕ_l or ψ_l the bounds (C.1) hold true also in the region (4.16), so A is analytic in this domain, so are its powers and so is $(\mathbf{1} - fA)^{-1}$ as one can show the geometrical decay of derivatives of $(fA)^N$ as well. □

4.1.3 Decoupling and stationary limit

In this Section we give a proof of Theorem 4.1.8, that characterizes the probability distribution of the height function $\mathcal{H}$ in the higher spin vertex model with double sided stationary boundary conditions. Our starting point is the Fredholm determinant formula stated in Theorem 4.1.3. Removing the effect of the independent q-Poisson random variable $\mathcal{M}$ from expression (4.5) we find that determinantal expressions we obtain are well defined in the region (4.16). In Corollary 4.1.10 we specialize the result of Theorem 4.1.8 to the relevant case of the stationary higher spin vertex model with density $\mathscr{d}$.

Theorem 4.1.8. *Consider the higher spin vertex model of definition 4.1.1 and assume $v, \text{đ}$ satisfy (4.16). Then we have*

$$\mathbb{E}\left(\frac{1}{(\zeta q^{\mathcal{H}(x,t)};q)_\infty}\right) = \frac{1}{(qv/\text{đ};q)_\infty}\sum_{k\geq 0}\frac{(-1)^k q^{\binom{k}{2}}}{(q;q)_k}\left(\frac{v}{\text{đ}}\right)^k V_{x;v,\text{đ}}(\zeta q^{-k}), \tag{4.18}$$

where the function $V_{x;v,\text{đ}}$ is defined as

$$V_{x;v,\text{đ}}(\zeta) = \frac{1}{1-v/\text{đ}}\det(\mathbf{1}-fK)_{l^2(\mathbb{Z})}.$$

The following lemma offers a tool to decouple a generic process from the contribution of an independent q-Poisson random variable.

Lemma 4.1.9. *Let $\mathcal{M}\sim qPoi(p)$. Then, for any bounded function B, we have*

$$B(z) = \frac{1}{(p;q)_\infty}\sum_{k\geq 0}\frac{(-1)^k q^{\binom{k}{2}}}{(q;q)_k}p^k\mathbb{E}_{\mathcal{M}}(B(z-\mathcal{M}-k)). \tag{4.19}$$

Proof. To verify identity (4.19) we simply open up the average in the right hand side with respect to $\mathcal{M}$, as

$$\mathbb{E}_{\mathcal{M}}(B(z-\mathcal{M}-k)) = \sum_{l\geq 0}p^l\frac{(p;q)_\infty}{(q;q)_l}B(z-l-k).$$

We can now rearrange the double summation in the indices k, l, naming $L = l+k$, as

$$\text{rhs of (4.19)} = \sum_{L\geq 0}B(z-L)\sum_{k=0}^{L}\frac{(-1)^k q^{\binom{k}{2}}}{(q;q)_k(q;q)_{L-k}},$$

which completes the proof, after recognizing, in the right hand side, the q-Pochhammer expansion (A.3) (with $z=1$) that is one for $L=0$ and zero otherwise. □

In the remaining part of the paper we will use the following decomposition of terms Φ_x, Ψ_x:

$$\Phi_x(n) = \Phi_x^{(1)}(n) + \Phi_x^{(2)}(n), \tag{4.20}$$
$$\Psi_x(n) = \Psi_x^{(1)}(n) + \Psi_x^{(2)}(n), \tag{4.21}$$

obtained separating from the integration (4.10) (resp. (4.11)) the contribution of pole $w = \text{đ}$ (resp. $z = v$) from that of other poles. The exact expressions are

$$\Phi_x^{(1)}(n) = \frac{\tau(n)}{\text{đ}^{n+1}}\prod_{k=2}^{x}\frac{1}{\text{đ}-\xi_k s_k}\frac{(qv/\text{đ};q)_\infty}{F(\text{đ})}, \tag{4.22}$$

$$\Phi_x^{(2)}(n) = \tau(n) \int_{D_1} \frac{dw}{2\pi\mathrm{i}} \frac{1}{w^{n+1}} \frac{1}{w-d\!\!\!/} \prod_{k=2}^{x} \frac{1}{w-\xi_k s_k} \frac{(qv/w;q)_\infty}{F(w)}, \tag{4.23}$$

$$\Psi_x^{(1)}(n) = \frac{v^n}{\tau(n)} \prod_{k=2}^{x} (v-\xi_k s_k) \frac{F(v)}{(q;q)_\infty}, \tag{4.24}$$

$$\Psi_x^{(2)}(n) = \frac{1}{\tau(n)} \int_{C_1} \frac{dz}{2\pi\mathrm{i}} \frac{z^{n-1}}{(v/z;q)_\infty} \prod_{k=2}^{x} (z-\xi_k s_k) F(z), \tag{4.25}$$

where F was given in (4.13), contour D_1 contains $\{\xi_i s_i\}_{i\geq 2}$ and no other singularity and C_1 contains $\{q^k v\}_{k\geq 1}$ and no other singularity.

Proof of Theorem 4.1.8. Using Lemma 4.1.9 setting $B: z \to \mathbb{E}(1/(\zeta q^{\mathcal{H}+z};q)_\infty)$ and expressing the q-Laplace transform $\mathbb{E}_{\mathrm{HS}(v,d\!\!\!/)}(1/(\zeta q^{\mathcal{H}-\mathcal{M}};q)_\infty)$ as in (4.5) we obtain formula (4.18). Therefore we only need to show that expression (4.18) is well posed in the region (4.16).

Using basic properties of Fredholm determinants, along with the regularity of the kernel fA proved in Proposition 4.1.6, we can write

$$\det(\mathbf{1}-fK) = \det\left(\mathbf{1}-fA-(d\!\!\!/-v)f\Phi_x\Psi_x\right) = \det(\mathbf{1}-fA)\det\left(\mathbf{1}-(d\!\!\!/-v)(\varrho f\Phi_x)\Psi_x\right),$$

where we called $\varrho = (\mathbf{1}-fA)^{-1}$. This allows us to express $V_{x;v,d\!\!\!/}(\zeta)$ as

$$V_{x;v,d\!\!\!/}(\zeta) = \det(\mathbf{1}-fA)\frac{1}{1-v/d\!\!\!/}\left(1-(d\!\!\!/-v)\sum_{n\in\mathbb{Z}}(\varrho f\Phi_x)(n)\Psi_x(n)\right), \tag{4.26}$$

We turn our attention to the term

$$\sum_{n\in\mathbb{Z}}(\varrho f\Phi_x)(n)\Psi_x(n) = \sum_{n\in\mathbb{Z}} f(n)\Phi_x(n)\Psi_x(n) + \sum_{n\in\mathbb{Z}}(fA\varrho\Phi_x)(n)\Psi_x(n), \tag{4.27}$$

that we rewrite, using eqs. (4.22) to (4.25) as

$$(4.27) = \sum_{n\in\mathbb{Z}} f(n)\Phi_x^{(1)}(n)\Psi_x^{(1)}(n) + \sum_{\substack{i,j=1,2\\(i,j)\neq(1,1)}}\sum_{n\in\mathbb{Z}} f(n)\Phi_x^{(i)}(n)\Psi_x^{(j)}(n) + \sum_{n\in\mathbb{Z}}(fA\varrho f\Phi_x)(n)\Psi_x(n). \tag{4.28}$$

We easily see that, thanks to bounds stated in Appendix C.1, the second and the third terms in the right hand side of (4.28) are geometrically convergent summations in the region (4.16). On the other hand, the generic term of the summation in the first addend of the right hand side of (4.28) takes the form

$$\frac{1}{1-q^n/\zeta}\frac{1}{d\!\!\!/}\left(\frac{v}{d\!\!\!/}\right)^n \prod_{k=2}^{x} \frac{v-\xi_k s_k}{d\!\!\!/-\xi_k s_k} \frac{(qv/d\!\!\!/;q)_\infty}{(q;q)_\infty}\frac{F(v)}{F(d\!\!\!/)}.$$

We can perform the summation over n through the Ramanujan ${}_1\psi_1$ formula ([Ism05], Theorem 12.3.1) as

$$\sum_{n\in\mathbb{Z}} \frac{1}{1-q^n/\zeta}\left(\frac{v}{\mathscr{d}}\right)^n = \frac{(v/(\mathscr{d}\zeta), q\zeta\mathscr{d}/v, q, q; q)_\infty}{(v/\mathscr{d}, q\mathscr{d}/v, 1/\zeta, q\zeta; q)_\infty}.$$

which itself leads to the expression

$$\sum_{n\in\mathbb{Z}} f(n)\Phi_x^{(1)}(n)\Psi_x^{(1)}(n) = \frac{1}{\mathscr{d}} \frac{(v/(\mathscr{d}\zeta), q\zeta\mathscr{d}/v, q; q)_\infty}{(v/\mathscr{d}, 1/\zeta, q\zeta; q)_\infty} \frac{F(v)}{F(\mathscr{d})} \prod_{k=2}^{x} \frac{v-\xi_k s_k}{\mathscr{d}-\xi_k s_k}. \tag{4.29}$$

Combining the explicit formula (4.29) with (4.28) and (4.26) we see that $V_{x;v,\mathscr{d}}$ does not in fact present any singularity in $v=\mathscr{d}$ by virtue of the Taylor expansion

$$\text{rhs of (4.29)} = \frac{1}{\mathscr{d}-v} + \frac{1}{\mathscr{d}}\left(\upsilon_0(1/\zeta) - \upsilon_0(q\zeta) + 2\upsilon_0(q) + xh_0(\mathscr{d}) - \sum_{j=1}^{t} a_0(\mathscr{d};j)\right) + \mathcal{O}(\mathscr{d}-v), \tag{4.30}$$

where we used the q-polygamma type functions υ_k defined in Appendix A, their combinations a_0, h_0 presented in (4.34) and the notation $a_0(\mathscr{d};j)$ stresses the dependence on the spectral parameters u_j as

$$a_k(\mathscr{d};j) = \upsilon_k(qu_j\mathscr{d}) - \upsilon_k(u_j\mathscr{d}).$$

Therefore $V_{x;v,\mathscr{d}}$ is an analytic function of both parameters $v, \mathscr{d}$ in the region (4.16) and this concludes the proof. □

Calculations performed during the proof of Theorem 4.1.8 can be exploited to obtain determinantal formulas for for the stationary higher spin vertex model.

Corollary 4.1.10. *Consider stationary higher spin vertex model as in definition 4.1.1. Then we have*

$$\mathbb{E}_{\mathrm{HS}(\mathscr{d},\mathscr{d})}\left(\frac{1}{(\zeta q^{\mathcal{H}(x,t)};q)_\infty}\right) = \frac{1}{(q;q)_\infty}\sum_{k\geq 0}\frac{(-1)^k q^{\binom{k}{2}}}{(q;q)_k} q^k \left(V_x(\zeta q^{-k}) - V_x(\zeta q^{-k-1})\right), \tag{4.31}$$

with the function $V_x = V_{x;\mathscr{d},\mathscr{d}}$ being

$$V_x(\zeta) = \det(\mathbf{1} - fA)\Bigg(-\upsilon_0(1/\zeta) + \upsilon_0(q\zeta) - 2\upsilon_0(q) - xh_0(\mathscr{d}) + \sum_{j=1}^{t} a_0(\mathscr{d};j) - \mathscr{d}\sum_{\substack{i,j=1,2\\(i,j)\neq(1,1)}}\sum_{n\in\mathbb{Z}} f(n)\Phi_x^{(i)}(n)\Psi_x^{(j)}(n) - \mathscr{d}\sum_{n\in\mathbb{Z}}(fA\varrho f\Phi_x)(n)\Psi_x(n)\Bigg). \tag{4.32}$$

Proof. All it takes to show (4.31) is to take the limit $v \to đ$ of both sides of equality (4.5). We exchange the limit sign in $v \to đ$ and the summation sign in the right hand side of (4.5) and this can be done as, in the proof of Theorem 4.1.8, the function $V_{x;v,đ}$ was shown to be uniformly bounded in a neighborhood of $v = đ$ and its limit $V_{x;v,đ} \to V_{x;đ,đ}$ is readily computed using (4.30). This is enough to prove that

$$\lim_{v \to đ} \mathbb{E}_{\mathrm{HS}(v,đ)} \left(\frac{1}{(\zeta q^{\mathcal{H}(x,t)}; q)_\infty} \right) = \frac{1}{(q;q)_\infty} \sum_{k \geq 0} \frac{(-1)^k q^{\binom{k}{2}}}{(q;q)_k} V_x(\zeta q^{-k}). \tag{4.33}$$

Finally, substituting $V_x(\zeta q^{-k})$ with $q^k V_x(\zeta q^{-k}) + (1-q^k) V_x(\zeta q^{-k})$ and rearranging the summation in the right hand side of (4.33) we obtain (4.31). □

4.2 Asymptotic analysis in the stationary regime

In this section we prove that the asymptotic fluctuations of the stationary higher spin vertex model obey the Baik-Rains distribution, when taken along a special direction. For simplicity we will suppress time inhomogeneities and we will take the model in definition 4.1.1 with $u_t = u$ and $v = đ$.

We first fix a number of scaling parameters and for this make use of q-polygamma type functions $\boldsymbol{\upsilon}_k$ defined in Appendix A. For non-negative integers k consider the functions

$$a_k(đ) = \boldsymbol{\upsilon}_k(quđ) - \boldsymbol{\upsilon}_k(uđ), \qquad h_k(đ) = \frac{1}{x} \sum_{y=2}^{x} \left(\boldsymbol{\upsilon}_k(đ/(\xi_y s_y)) - \boldsymbol{\upsilon}_k(đ s_y/\xi_y) \right) \tag{4.34}$$

and, depending on the parameter $đ$, define the quantities

$$\kappa_0 = \frac{h_1(đ)}{a_1(đ)}, \qquad \eta_0 = \kappa_0 a_0(đ) - h_0(đ), \qquad \gamma = -\left(\frac{1}{2} (\kappa_0 a_2(đ) - h_2(đ)) \right)^{1/3}. \tag{4.35}$$

We assume that the functions h_k always converge in the large x limit and we refer to the curve $(x, \kappa_0 x)$ as the *characteristic line* of the stationary higher spin vertex model. For random growth models usually the characteristic line is expressed as a function of the time t, rather than of the coordinate x, but in our case, since the system exhibits spatial inhomogeneities we find more natural to adopt the notation $(x, \kappa_0 x)$. The parameter η_0 multiplied by x is readily understood as the expectation $\mathbb{E}(\mathcal{H}(x, \kappa_0 x))$, whereas γ will be used to describe the size of the characteristic fluctuations of $\mathcal{H}$ around η_0. By slightly perturbing quantities κ_0, η_0 we can analyze the asymptotic behavior of $\mathcal{H}$ in a region of size $x^{2/3}$ around the characteristic line. For this we extend the definitions given in (4.35) setting

$$\kappa_\varpi = \kappa_0 + \frac{h_2 a_1 - h_1 a_2}{a_1^2} \frac{\varpi}{\gamma x^{1/3}} \tag{4.36}$$

$$\eta_\varpi = \eta_0 + \frac{a_0(h_2 a_1 - h_1 a_2)}{a_1^2} \frac{\varpi}{\gamma x^{1/3}} + \frac{h_2 a_1 - h_1 a_2}{a_1} \frac{\varpi^2}{\gamma^2 x^{2/3}}, \tag{4.37}$$

where ϖ is a real number parameterizing the displacement from the characteristic line and functions a_k, h_k are evaluated at $đ$. We come now to state our main result.

Theorem 4.2.1. *Consider the stationary higher spin vertex model with density ð as in theorem 4.1.2. Assume that parameter satisfy additional conditions given below in definition 4.2.5. Then, for any real numbers ϖ, r we have*

$$\lim_{x\to\infty} \mathbb{P}_{\mathrm{HS}(\text{ð},\text{ð})}\left(\frac{\mathcal{H}(x,\kappa_\varpi x)-\eta_\varpi x}{\gamma x^{1/3}} > -r\right) = F_\varpi(r), \tag{4.38}$$

where $F_\varpi(r)$ is the Baik-Rains distribution presented below in Definition 4.2.3.

4.2.1 The KPZ scaling for the Higher Spin Six Vertex Model

Before we enter the discussion it is appropriate to recall the definition of the Baik-Rains distribution [BR00], which will ultimately describe long time fluctuations of the stationary height function $\mathcal{H}$ under a suitable scaling. Rather than showing the original definition given by authors in [BR00], formula (2.16), we present an equivalent expression first found in [IS13] (see also [FS06]).

The building blocks for the construction of the Baik-Rains distributions are given in the following

Definition 4.2.2 (Airy function and Airy kernel)**.** The Airy function Ai is given by

$$Ai(\nu) = \frac{1}{2\pi\mathrm{i}}\int_{e^{-\frac{\mathrm{i}}{3}\pi}\infty}^{e^{\frac{\mathrm{i}}{3}\pi}\infty} \exp\left\{\frac{z^3}{3} - z\nu\right\} dz,$$

where the integration contour is any open complex curve having the half lines $\{Re^{\frac{\mathrm{i}}{3}\pi}|R \geq 0\}$ and $\{Re^{-\frac{\mathrm{i}}{3}\pi}|R \geq 0\}$ as asymptotes.

The Airy kernel[1] K_{Airy} is defined as

$$K_{Airy}(\nu,\theta) = \int_{e^{-\frac{2}{3}\pi\mathrm{i}}\infty}^{e^{\frac{2}{3}\pi\mathrm{i}}\infty} \frac{dz}{2\pi\mathrm{i}} \int_{e^{\frac{\pi}{3}\mathrm{i}}\infty}^{e^{-\frac{\pi}{3}\mathrm{i}}\infty} \frac{dw}{2\pi\mathrm{i}} \frac{1}{z-w} \exp\left\{\frac{w^3}{3} - \frac{z^3}{3} - w\nu + z\theta\right\}, \tag{4.39}$$

where again integration contours are non intersecting complex curves whose asymptotes are half lines $\{Re^{\pm\frac{\mathrm{i}}{3}\pi}|R \geq 0\}$ for w and $\{Re^{\mp\mathrm{i}\frac{2}{3}\pi}|R \geq 0\}$ for z.

We come to the next

Definition 4.2.3 (Baik-Rains distribution)**.** Let $\varpi \in \mathbb{R}$ and define the one parameter family of functions

$$\begin{aligned}\chi_\varpi(r) = F_2(r)\Bigg(r - \varpi^2 - &\sum_{\substack{i,j=1,2\\(i,j)\neq(1,1)}} \int_r^\infty \Upsilon_{-\varpi}^{(i)}(\nu)\Upsilon_{\varpi}^{(j)}(\nu)d\nu \\ &- \int_r^\infty d\nu \Upsilon_\varpi(\nu)\int_r^\infty d\lambda_1 \int_r^\infty d\lambda_2 \varrho_{Airy;r}(\nu,\lambda_1)K_{Airy}(\lambda_1,\lambda_2)\Upsilon_{-\varpi}(\lambda_2)\Bigg)\end{aligned} \tag{4.40}$$

where terms $F_2, \varrho_{Airy;r}, \Upsilon_\varpi^{(i)}, \Upsilon_\varpi$ are given by:

[1] Sometimes the equivalent expression $K_{\mathrm{Airy}}(\nu,\theta) = \int_0^\infty \mathrm{Ai}(\lambda+\nu)\mathrm{Ai}(\lambda+\theta)d\lambda$ is found in literature.

- $F_2(r)$ is the GUE Tracy-Widom distribution ([TW94])

$$F_2(r) = \det\left(\mathbf{1} - \mathbb{1}_{[r,\infty)} K_{Airy}\right)_{\mathcal{L}^2(\mathbb{R})}; \tag{4.41}$$

- $\varrho_{Airy;r}(\nu, \lambda)$ is the kernel

$$\varrho_{Airy;r}(\nu,\lambda) = \left(\mathbf{1} - \mathbb{1}_{[r,\infty)} K_{Airy}\right)^{-1}(\nu,\lambda); \tag{4.42}$$

- auxiliary functions $\Upsilon^{(1)}_{\varpi}, \Upsilon^{(2)}_{\varpi}$ are

$$\Upsilon^{(1)}_{\varpi}(\nu) = e^{\frac{\varpi^3}{3} - \nu\varpi}, \qquad \Upsilon^{(2)}_{\varpi}(\nu) = \int_{e^{-\frac{2}{3}\mathrm{i}\pi}\infty}^{e^{\frac{2}{3}\mathrm{i}\pi}\infty} \frac{d\omega}{2\pi\mathrm{i}} \frac{\exp\{-\frac{\omega^3}{3} + \omega\nu\}}{\omega + \varpi}, \tag{4.43}$$

  where the integration contour passes to the left of $-\varpi$;

- lastly

$$\Upsilon_{\varpi}(\nu) = \Upsilon^{(1)}_{\varpi}(\nu) + \Upsilon^{(2)}_{\varpi}(\nu). \tag{4.44}$$

The Baik-Rains distribution F_{ϖ} is

$$F_{\varpi}(r) = \frac{\partial}{\partial r}\chi_{\varpi}(r). \tag{4.45}$$

Remark 4.2.4. The equivalence between F_{ϖ} of (4.45) and an analogous expression found in [FS06] is discussed in the Remark at the end of Section 5 of [IS19]. Further, in Appendix A of [FS06] the authors prove that their definition of the Baik-Rains distribution is equivalent to the original one introduced in [BR00].

We now possess all the ingredients to give a brief explanation of the KPZ scaling theory, which gives a precise conjecture to describe stationary (asymptotic) fluctuations of the height function of models in the KPZ universality class ([PS00]).

We start considering a properly rescaled version of our model, where, for convenience we interpret the vertical spatial coordinate as a time direction and where we regard space and time as continuous parameters. In this case the height function $\mathcal{H}$, defined for the higher spin vertex model in (3.21), still contains every information on the random dynamics thanks to relations

$$\mathcal{H}(x,t) - \mathcal{H}(x+dx,t) = \#\text{ of paths in } [x, x+dx] \text{ at time } t, \tag{4.46}$$

$$\mathcal{H}(x,t+dt) - \mathcal{H}(x,t) = \#\text{ of paths crossing } x \text{ during the time interval } [t, t+dt]. \tag{4.47}$$

For the sake of argument assume that the average of space and time infinitesimal increments of $\mathcal{H}$ are regular enough to define the deterministic density ρ and current j as

$$\mathbb{E}\left(\mathcal{H}(x+dx,t) - \mathcal{H}(x,t)\right) \approx -\rho(x,t)dx, \qquad \mathbb{E}\left(\mathcal{H}(x,t+dt) - \mathcal{H}(x,t)\right) \approx j(x,t)dt.$$

The system is autonomous, or, in other words, its evolution depends on space and time only implicitly, therefore the current j must only be a function of ρ and the continuity equation linking these quantities reads

$$\partial_t \rho(x,t) + \partial_x j(\rho(x,t)) = 0. \tag{4.48}$$

At this stage the height $\mathcal{H}$ remains defined, through (4.46), (4.47), only up to a global constant and to remove this ambiguity we fix its value at the reference point $x = 0, t = 0$ to be $\mathcal{H}(0,0) = 0$. With this choice the average profile of $\mathcal{H}$ at the generic space time point (x,t) can be expressed as

$$\eta(x,t) = -\int_0^x \rho(y,0)dy + \int_0^t j(\rho(x,s))ds \tag{4.49}$$

and the study of fluctuations of the height is, by definition, the study of the random quantity

$$\mathcal{H}(x,t) - \eta(x,t). \tag{4.50}$$

Assume now that the system has reached its steady state, or equivalently assume that at time zero the measure is stationary. Qualitatively, the randomness of (4.50) is affected by two different contributions. One is coming from the stochastic evolution of the system and the other is given by initial conditions. For growth processes in the KPZ universality class, when initial conditions are deterministic and sufficiently regular, fluctuations in the long time scale are expected to present with size of order $t^{1/3}$. This conjecture goes back to the seminal paper [KPZ86], where authors argued such property to hold for the solution of the one dimensional KPZ equation itself. On the other hand, from our knowledge of the stationary measure of the higher spin vertex model displayed in theorem 4.1.2, we certainly expect fluctuations in the space direction to have size of order $x^{1/2}$, as a result of the Central Limit Theorem applied to independent occupation numbers at each site. This means that the information we have about $\mathcal{H}$, which is the choice $\mathcal{H}(0,0) = 0$, will be transported by the random dynamics along the direction of growth of the surface and along this line we can observe the emergence of the $1/3$ exponent. Along all other lines, the distribution of (4.50) will be affected very little by the process, and asymptotic fluctuations remain of gaussian nature. An earlier evidence of this last fact was found in [FF94] (see also [BFP10], Appendix D).

The direction along which nontrivial fluctuations are observed is given by the characteristic line of partial differential equation (4.48). This is the curve (x_t, t), where x_t is set to be the solution of the differential equation

$$\begin{cases} \dot{x}_t = j'(\rho(x_t,t)), \\ x_0 = 0. \end{cases} \tag{4.51}$$

When the system is in its stationary state, equation (4.51) loses its dependence on time and the $\dot{x}_t$ is only function of the stationary density profile ρ_{st}. In case the model does not present space inhomogeneities the characteristic curve is simply the line $(j'(\rho_{\mathrm{st}})t, t)$, but when the stationary density is not constant, this is no more true. We use the explicit parametrization (x, t_x), rather than (x_t, t) and by integration of (4.51), we obtain

$$t_x = \int_0^x \frac{dy}{j'(\rho_{\rm st}(y))}. \tag{4.52}$$

To reiterate what we just explained, consider diverging x and t. Assume first that

$$|t - t_x| = \mathcal{O}(x^{2/3+\delta}),$$

for some $\delta > 0$. Then, asymptotically (4.50) obeys the gaussian distributions and its size becomes of order $x^{1/2}$. When on the other hand, (x, t) is taken in the vicinity of the characteristic curve, say

$$|t - t_x| = \mathcal{O}(x^{2/3}),$$

then fluctuations become of size $x^{1/3}$ and their law is described by the Baik-Rains distribution.

We can be more precise. Take at first $t = t_x$. The convergence result, in this case, is

$$\frac{\mathcal{H}(x, t_x) - \eta(x, t_x)}{\gamma x^{1/3}} \xrightarrow[x\to\infty]{\mathcal{D}} F_0,$$

where, calling $\sigma_y^2 dy$ the variance of the number of paths lying at time 0 in the infinitesimal segment $[y, y + dy]$ and its mean

$$\overline{\sigma^2} = \lim_{x\to\infty} \frac{1}{x} \int_0^x \sigma_y^2 dy,$$

then the constant γ is given by

$$\gamma^3 = - \lim_{x\to\infty} \frac{1}{2} j''(\rho_{\rm st}) (\overline{\sigma^2})^2 \frac{t_x}{x}. \tag{4.53}$$

The explicit parametrization of a fan of size $x^{2/3}$ around the characteristic line can be still expressed in terms of macroscopic quantities. Consider a perturbation of t_x of the form

$$t_{x,\varpi} = t_x - \varpi \frac{\overline{\sigma}^2 j''(\rho_{\rm st})}{\gamma j'(\rho_{\rm st})^2} x^{2/3}. \tag{4.54}$$

with ϖ being a real number. The resulting effect on the expression of η reads, up to order $x^{1/3}$, as

$$\eta_{x,\varpi} = \eta(x, t_x) - \varpi \frac{\overline{\sigma}^2 j''(\rho_{\rm st}) j(\rho_{\rm st})}{\gamma j'(\rho_{\rm st})^2} x^{2/3} - \frac{1}{2} \varpi^2 \frac{(\overline{\sigma^2})^2 j''(\rho_{\rm st})}{\gamma^2 j'(\rho_{\rm st})} x^{1/3}. \tag{4.55}$$

In this case, the convergence result for fluctuations along the line $(x, t_{x,\varpi})$ becomes

$$\frac{\mathcal{H}(x, t_{x,\varpi}) - \eta_{x,\varpi}}{\gamma x^{1/3}} \xrightarrow[x\to\infty]{\mathcal{D}} F_\varpi. \tag{4.56}$$

The same kind of results are conjectured for discrete time systems, where the characteristic curves can be again explicitly expressed through relation (4.52). In the next section we will establish result (4.56) for the stationary higher spin vertex model. For this model, the scaling parameters $\kappa_\varpi, \eta_\varpi, \gamma$ were defined in eqs. (4.35) to (4.37) and it is a simple exercise to verify that they match with expressions given in eqs. (4.53) to (4.55).

4.2.2 The Baik-Rains limit

This subsection is devoted to the proof of Theorem 4.2.1, that characterizes the asymptotic fluctuations of the height function in the stationary higher spin vertex model. Throughout the proof we will assume that the model presents only spatial inhomogeneities and hence the spectral parameters $\mathbf{U}$ are taken as

$$\mathbf{U} = (u, u, u, \dots). \tag{4.57}$$

Our strategy relies on taking the large x limit of the q-Laplace transform of the height functions $\mathcal{H}$ given in (4.31). The computation of such a limit for the right hand side of (4.31) might look complicated, but the expression will simplify after the right change of variables (discussed in detail below in Section 4.2.3). Motivated by the KPZ scaling theory discussed in Section 4.2.1, we fix parameters t and ζ as

$$t = \kappa x \qquad \text{and} \qquad \zeta = -q^{-\eta x + \gamma x^{1/3} r}. \tag{4.58}$$

Here and in the rest of the Section, for the sake of a cleaner notation, we set

$$\eta = \eta_{\varpi}, \qquad \text{and} \qquad \kappa = \kappa_{\varpi},$$

dropping the explicit dependence on the real number ϖ from $\eta_{\varpi}, \kappa_{\varpi}$ introduced in eqs. (4.36) and (4.37). The first choice in (4.58) means that we are considering the behaviour of the height along the critical line, while the choice for ζ reflects the fact that we study fluctuations of size $\gamma x^{1/3}$ around the expected value η of the height function. We assume the parameter r of (4.58) to be fixed throughout the entire section and it will ultimately represent the argument of the Baik-Rains distribution, as in (4.38).

The asymptotic analysis of expressions given in Corollary 4.1.10 will be performed via a rigorous steep descent method. Although we postpone the details of the analysis to Subsections 4.2.4 and 4.2.5, we now fix hypothesis on parameters $q, \Xi, \mathbf{S}$, that will hold true throughout the rest of the Section.

Definition 4.2.5 (Conditions on parameters)**.** Take a, σ such that $a > \text{đ}$ and $\sigma \in [0, 1)$. Parameters $q, \text{đ}, \Xi, \mathbf{S}$ are assumed to satisfy (4.1),(4.3) and they are spaced so that there exist R_a, R_σ, R_q, with the properties that

$$a \le \xi_k s_k \le a + R_a, \qquad \sigma \le s_k^2 \le \sigma + R_\sigma, \qquad \text{for all } k, \qquad 0 \le q \le R_q \tag{4.59}$$

and

$$a + R_a < \frac{2a}{1+\sigma} < \text{đ}/q. \tag{4.60}$$

Numbers R_a, R_σ, R_q are strictly positive, yet small in the sense given by Proposition C.2.3.

The first and the second conditions in (4.59) are not too much prohibitive and they essentially say that we can consider perturbations of a general homogeneous model, since parameters a and σ can be chosen freely. The strongest assumption in Definition 4.2.5

is indeed the third one in (4.59) and it says that the parameter q has to remain reasonably close to 0. The reason for such restrictions in the choice of parameters lies in the perturbative approach we used to prove Proposition C.2.3. There, we showed the steep ascent property (for the function g defined below in (4.80)) of integration contour D, in the case where $q = 0, \xi_k s_k = a, s_k^2 = \sigma$ for each $k \geq 2$. Subsequently, through a continuity argument we concluded that the same property must hold also when parameters are taken in suitably small neighborhoods of our original choices, hence (4.59).

Although numerical checks show that a steep ascent contour D indeed exists also for q reasonably greater than zero (yet not too much close to 1), obtaining sharp bounds for parameters becomes difficult due to the complicated expressions we encounter setting $q > 0$. More precisely, to prove Theorem 4.2.1 when q is taken far from 0 would mean constructing an explicit closed contour D on which one would be able to show that the function g assumes a global minimum in a neighborhood of $\not{d}$. This is indeed possible in principle, but obtaining explicit bounds for parameters q, ξ_k, s_k becomes prohibitive.

The first inequality in (4.60) is also technical and not very restrictive. It is used in the construction of the explicit steep ascent contour D in Proposition C.2.3. On the other hand the assumption $2a/(1+\sigma) < \not{d}/q$, reported in (4.60), is used to ensure the exponential decay of rear tails of $f\Phi_x\Psi_x$ in Propositions 4.2.9, 4.2.10.

Remark 4.2.6. Conditions stated in Definition 4.2.5 are far from being optimal and they are essentially consequences of our choice for the representation of the integral kernels K, Φ_x, Ψ_x in (4.7),(4.10),(4.11). In particular these technical assumptions are consequence of the fact that D is a closed contour.

We will now present limiting expressions of terms entering the definition (4.32) of function $V_x(\zeta)$, for $x \to \infty$. The proof of the next Proposition is reported in Section 4.2.4.

Proposition 4.2.7. *We have*

$$\det(\mathbf{1} - fA)_{l^2(\mathbb{Z})} = F_2(r) + \frac{1}{\gamma x^{1/3}} R_x^{(1)}(r), \tag{4.61}$$

where F_2 is defined in (4.41) and the error term $R_x^{(1)}$ satisfies the following properties

1. *For each $r^* \in \mathbb{R}$, there exists $M_{r^*} > 0$ such that, for all x,*

$$\left| R_x^{(1)}(r^*) \right| < M_{r^*}; \tag{4.62}$$

2. *There exist $\epsilon > 0$, such that, for all $r^* \in [r - \epsilon, r]$, we have*

$$\lim_{x \to \infty} \left(R_x^{(1)}(r^*) - R_x^{(1)}(r^* - \frac{1}{\gamma x^{1/3}}) \right) = 0, \tag{4.63}$$

   uniformly.

Let's now see what is the asymptotic behavior of remaining terms of (4.32). The proofs of the following three Propositions are given in Section 4.2.5 below.

Proposition 4.2.8. *Recall choice (4.58). Then we have*

$$\frac{1}{\gamma x^{1/3}}\left(ta_0(\text{đ}) - \upsilon_0(1/\zeta) - 2\upsilon_0(q) + \upsilon_0(q\zeta) - xh_0(\text{đ})\right) = r - \varpi^2 + \frac{1}{\gamma x^{1/3}} R_x^{(2)}(r). \quad (4.64)$$

The error term $R_x^{(2)}$ satisfies the following properties

1. *for each $r^* \in \mathbb{R}$, there exists $M_{r^*} > 0$ such that, for all x,*

$$\left|R_x^{(2)}(r^*)\right| < M_{r^*}; \quad (4.65)$$

2. *there exist $\epsilon > 0$, such that, foe all $r^* \in [r-\epsilon, r]$ we have*

$$\lim_{x\to\infty}\left(R_x^{(2)}(r^*) - R_x^{(2)}(r^* - \frac{1}{\gamma x^{1/3}})\right) = 0. \quad (4.66)$$

   uniformly.

Lastly we state the convergence result for terms $\Phi_x^{(i)}, \Phi_x, \Psi_x^{(j)}, \Psi_x$.

Proposition 4.2.9. *We have*

$$\frac{\text{đ}}{\gamma x^{1/3}}\sum_{n\in\mathbb{Z}}\sum_{\substack{i,j=1,2\\(i,j)\neq(1,1)}} f(n)\Phi_x^{(i)}(n)\Psi_x^{(j)}(n) = \sum_{\substack{i,j=1,2\\(i,j)\neq(1,1)}}\int_r^\infty \Upsilon_{-\varpi}^{(i)}(\nu)\Upsilon_{\varpi}^{(j)}(\nu)d\nu + \frac{1}{\gamma x^{1/3}}R_x^{(3)}(r), \quad (4.67)$$

where functions $\Upsilon^{(1)}, \Upsilon^{(2)}$ are defined in (4.43) and the error term $R_x^{(3)}$ satisfies the following properties

1. *for each $r^* \in \mathbb{R}$ there exists $M_{r^*} > 0$ such that, for all x,*

$$\left|R_x^{(3)}(r^*)\right| < M_{r^*}; \quad (4.68)$$

2. *there exists $\epsilon > 0$, such that, for all $r^* \in [r-\epsilon, r]$ we have*

$$\lim_{x\to\infty}\left(R_x^{(3)}(r^* + \frac{1}{\gamma x^{1/3}}) - R_x^{(3)}(r^*)\right) = 0. \quad (4.69)$$

   uniformly.

Proposition 4.2.10. *We have*

$$\frac{\text{đ}}{\gamma x^{1/3}}\sum_{n\in\mathbb{Z}}(fA\varrho f\,\Phi_x)(n)\Psi_x(n) =$$
$$\int_r^\infty d\nu\Upsilon_\varpi(\nu)\int_r^\infty d\lambda_1\int_r^\infty d\lambda_2\varrho_{\text{Airy};r}(\nu,\lambda_1)K_{\text{Airy}}(\lambda_1,\lambda_2)\Upsilon_{-\varpi}(\lambda_2) + \frac{1}{\gamma x^{1/3}}R_x^{(4)}(r), \quad (4.70)$$

where the integral kernel $\varrho_{\text{Airy};r}$ and the function Υ_ϖ were defined in (4.42), (4.44) and the error term $R_x^{(4)}$ satisfies the following properties

1. *for each* $r^* \in \mathbb{R}$ *there exists* $M_{r^*} > 0$ *such that, for all* x

$$\left|R_x^{(4)}(r^*)\right| < M_{r^*}; \tag{4.71}$$

2. *there exists* $\epsilon > 0$ *such that, for all* $r^* \in [r-\epsilon, r]$, *we have*

$$\lim_{x\to\infty}\left(R_x^{(4)}(r^*) - R_x^{(4)}(r^* - \frac{1}{\gamma x^{1/3}})\right) = 0. \tag{4.72}$$

uniformly.

Using convergence results reported in the Propositions 4.2.7, 4.2.8, 4.2.9, 4.2.10 we are now ready to prove our main Theorem.

Proof of Theorem 4.2.1. Using a rather elementary argument, detailed in Secion 5 of [FV15], it is possible to show that proving (4.38) is equivalent to showing that

$$\lim_{x\to\infty}\mathbb{E}_{\mathrm{HS}(\mathscr{d},\mathscr{d})}\left(\frac{1}{(-q^{\mathcal{H}(x,\kappa x)-\eta x+r\gamma x^{1/3}};q)_\infty}\right) = F_\varpi(r).$$

To do so we use formula (4.31) to express the q-Laplace transform on the left hand side. We want to evaluate

$$\lim_{x\to\infty}\frac{1}{(q;q)_\infty}\sum_{k\geq 0}\frac{(-1)^k q^{\binom{k+1}{2}}}{(q;q)_k}\left(V_x(\zeta q^{-k}) - V_x(\zeta q^{-k-1})\right), \tag{4.73}$$

and to do so we aim to bring the limit inside the summation symbol. We start by fixing a small number ϵ and we split the summation in (4.73) into two different contributions. One comes from the sum over k ranging in the region $[0, \epsilon\gamma x^{1/3}]$ and the other is given by k in $(\epsilon\gamma x^{1/3}, \infty)$. For each of these terms we can use different estimates.

We start with the latter, that is we take $k > \epsilon\gamma x^{1/3}$. A general inequality that can be deduced from the definition of $V_x = \lim_{v\to\mathscr{d}} V_{x;v,\mathscr{d}}$ and from Theorem 4.1.3, in case ζ is a negative number, is

$$\begin{aligned}V_x(\zeta q^{-k}) &= \lim_{v\uparrow\mathscr{d}}\frac{1}{1-v/\mathscr{d}}\mathbb{E}_{\mathrm{HS}(v,\mathscr{d})\otimes\mathcal{M}}\left(\frac{1}{(\zeta q^{-k}q^{\mathcal{H}-\mathcal{M}};q)_\infty}\right)\\ &\leq \lim_{v\uparrow\mathscr{d}}\frac{1}{1-v/\mathscr{d}}\mathbb{E}_{\mathrm{HS}(v,\mathscr{d})\otimes\mathcal{M}}\left(\frac{1}{(\zeta q^{-k^*}q^{\mathcal{H}-\mathcal{M}};q)_\infty}\right) = V_x(\zeta q^{-k^*}),\end{aligned}$$

which holds for every $k^* < k$. By taking $k^* = \epsilon\gamma x^{1/3}$ and $r^* = r - \epsilon$ we obtain the estimate

$$\begin{aligned}q^{\binom{k+1}{2}}\left(V_x(\zeta q^{-k}) - V_x(\zeta q^{-k-1})\right) &\leq 2q^{\binom{k+1}{2}}V_x(\zeta q^{(r^*-r)\gamma x^{1/3}})\\ &= 2q^{\binom{k+1}{2}}\left(\gamma x^{1/3}\chi_\varpi(r^*) + \sum_{i=1}^{4}S^{(i)}(r^*)R_x^{(i)}(r^*) + \mathcal{O}(x^{-1/3})\right).\end{aligned} \tag{4.74}$$

In the right hand side of (4.74) we used results of Propositions 4.2.7, 4.2.8, 4.2.9, 4.2.10 to provide the approximate expression of V_x. Function χ_ϖ was defined in (4.40) and terms $S^{(i)}$'s are explicit, bounded functions which for convenience we do not report explicitly. We can therefore write

$$\frac{1}{(q;q)_\infty} \sum_{k>\epsilon\gamma x^{1/3}} \frac{(-1)^k q^{\binom{k+1}{2}}}{(q;q)_k} \big(V_x(\zeta q^{-k}) - V_x(\zeta q^{-k-1})\big) = \mathsf{o}(e^{-cx^{2/3}}), \tag{4.75}$$

for some positive constant c, since, from (4.74) we see that the right hand side is a quantity exponentially small in $x^{2/3}$, due to the presence of the term $q^{\binom{k+1}{2}}$.

We now consider the contribution of the summation in (4.73), when the index k is smaller than $\epsilon\gamma x^{1/3}$. Once again, using results of Propositions 4.2.7, 4.2.8, 4.2.9, 4.2.10 we have

$$\begin{aligned} V_x(\zeta q^{-k}) - V_x(\zeta q^{-k-1}) = \gamma x^{1/3} &\left(\chi_\varpi(r - \frac{k}{\gamma x^{1/3}}) - \chi_\varpi(r - \frac{k+1}{\gamma x^{1/3}}) \right) \\ &+ \sum_{i=1}^{4} S^{(i)}(r - \frac{k}{\gamma x^{1/3}}) \left(R_x^{(i)}(r - \frac{k}{\gamma x^{1/3}}) - R_x^{(i)}(r - \frac{k+1}{\gamma x^{1/3}}) \right) \\ &+ \mathcal{O}(x^{-1/3}), \end{aligned} \tag{4.76}$$

which immediately implies

$$\left| V_x(\zeta q^{-k}) - V_x(\zeta q^{-k-1}) \right| \leq \text{const}, \tag{4.77}$$

after expanding χ_ϖ around $r - \frac{k}{\gamma x^{1/3}}$.

We can finally evaluate the limit (4.73). Using the bound (4.75), we write

$$\begin{aligned} (4.73) &= \lim_{x\to\infty} \left(\sum_{k=0}^{\epsilon\gamma x^{1/3}} + \sum_{k>\epsilon\gamma x^{1/3}} \right) \frac{(-1)^k q^{\binom{k+1}{2}}}{(q;q)_\infty (q;q)_k} (V_x(\zeta q^{-k}) - V_x(\zeta q^{-k-1})) \\ &= \lim_{x\to\infty} \sum_{k\geq 0} \frac{(-1)^k q^{\binom{k+1}{2}}}{(q;q)_\infty (q;q)_k} (V_x(\zeta q^{-k}) - V_x(\zeta q^{-k-1})) \mathbb{1}_{[0,\epsilon\gamma x^{1/3}]}(k) \end{aligned} \tag{4.78}$$

and following estimate (4.77), we can employ the bounded convergence theorem to exchange the limit and summation symbols in the right hand side of (4.78). Here the pointwise convergence

$$\lim_{x\to\infty} V_x(\zeta q^{-k}) - V_x(\zeta q^{-k-1}) = \frac{\partial}{\partial r} \chi_\varpi(r)$$

can be established through the expansion (4.76), using the fact that the difference between remainder terms $R_x^{(i)}$'s converges to zero, as reported in Propositions 4.2.7, 4.2.8, 4.2.9, 4.2.10. We can therefore write

$$(4.73) = \sum_{k\geq 0} \frac{(-1)^k q^{\binom{k+1}{2}}}{(q;q)_\infty (q;q)_k} \frac{\partial}{\partial r} \chi_\varpi(r) = \frac{\partial}{\partial r} \chi_\varpi(r),$$

which concludes the proof. □

4.2.3 Scaling form of determinantal formulas

In this Section we present expressions of kernels $f(n), A(n,m), \Phi^{(i)}(n), \Psi^{(j)}(n), \varrho(n,m)$ one finds in the definition of function V_x given in (4.32), that are amaenable to rigorous asymptotic analysis.

We fix a parametrization of integer indeces n, m as

$$n = n_\nu = -\eta x + \nu \gamma x^{1/3}, \qquad m = m_\theta = -\eta x + \theta \gamma x^{1/3}. \tag{4.79}$$

Here ν, θ belong to the set of rescaled integers

$$\widetilde{\mathbb{Z}} = \{\nu \in \mathbb{R} | -\eta x + \nu \gamma x^{1/3} \in \mathbb{Z}\}$$

and we will use the symbol $\widetilde{\sum}$ to denote a summation where the index ranges over $\widetilde{\mathbb{Z}}$ rather than $\mathbb{Z}$. We also introduce the scaling function

$$g(z) = -\eta \log(z) + \kappa a_{-1}(z) - h_{-1}(z), \tag{4.80}$$

where

$$a_{-1}(z) = \log(1 - zu) \qquad \text{and} \qquad h_{-1}(z) = \frac{1}{x} \sum_{y=2}^{x} \log\left(\frac{(z s_y/\xi_y; q)_\infty}{(z/(\xi_y s_y); q)_\infty} \right).$$

Functions a_k, h_k, for $k \geq 0$, were defined in (4.34) and they satisfy the properties

$$z \frac{d}{dz} a_k(z) = a_{k+1}(z) \qquad \text{and} \qquad z \frac{d}{dz} h_k(z) = h_{k+1}(z),$$

for all $k \geq -1$.

The combination of the KPZ scaling (4.58) and of the change of variable (4.79) is summarized in the following:

Proposition 4.2.11. *Assume* (4.58), (4.79) *and fix a real number L such that*

$$-L < r. \tag{4.81}$$

Define the sequence

$$\widetilde{\tau}(\nu) = \begin{cases} \varsigma^{\nu \gamma x^{1/3}}, & \text{if } \nu > -L, \\ \tau(n_\nu), & \text{if } \nu \leq -L, \end{cases} \tag{4.82}$$

where ς is a number in a neighborhood of order $x^{-1/3}$ of $\mathscr{d}$ and its exact expression in given below in (4.86). *Define also*

$$\widetilde{f}(\nu) = f(n_\nu) = \frac{1}{1 + q^{(\nu - r)\gamma x^{1/3}}}, \tag{4.83}$$

$$\widetilde{A}(\nu, \theta) = \frac{\widetilde{\tau}(\nu)}{\widetilde{\tau}(\theta)} \int_D \frac{dw}{2\pi \mathrm{i} w} \int_C \frac{dz}{2\pi \mathrm{i}} \frac{z^{\theta \gamma x^{1/3}}}{w^{\nu \gamma x^{1/3}}} \frac{e^{x g(z)}}{e^{x g(w)}} \frac{(q\mathscr{d}/w, qz/\mathscr{d}; q)_\infty}{(q\mathscr{d}/z, qw/\mathscr{d}; q)_\infty} \frac{1}{z - w}, \tag{4.84}$$

$$\widetilde{\Phi}_x^{(1)}(\nu) = \eth^{-\nu\gamma x^{1/3}-1} e^{-xg(\eth)}, \qquad \widetilde{\Phi}_x^{(2)}(\nu) = \int_{D_1} \frac{dw}{2\pi \mathrm{i} w} w^{-\nu\gamma x^{1/3}} e^{-xg(w)} \frac{(q\eth/w;q)_\infty}{(qw/\eth;q)_\infty} \frac{1}{w-\eth},$$

$$\widetilde{\Psi}_x^{(1)}(\nu) = \eth^{\nu\gamma x^{1/3}} e^{xg(\eth)}, \qquad \widetilde{\Psi}_x^{(2)}(\nu) = \int_{C_1} \frac{dz}{2\pi \mathrm{i}} z^{\nu\gamma x^{1/3}} e^{xg(z)} \frac{(qz/\eth;q)_\infty}{(q\eth/z;q)_\infty} \frac{1}{z-\eth}.$$

$$\widetilde{\Phi}_x(\nu) = \widetilde{\Phi}_x^{(1)}(\nu) + \widetilde{\Phi}_x^{(2)}(\nu), \qquad \widetilde{\Psi}_x(\nu) = \widetilde{\Psi}_x^{(1)}(\nu) + \widetilde{\Psi}_x^{(2)}(\nu)$$

Then formula (4.31) for the q-Laplace transform still holds if we substitute, in the expression of V_x (4.32), $f, A, \Phi_x^{(i)}, \Psi_x^{(j)}, \Phi_x, \Psi_x$ with $\widetilde{f}, \widetilde{A}, \widetilde{\Phi}_x^{(i)}, \widetilde{\Psi}_x^{(j)}, \widetilde{\Phi}_x, \widetilde{\Psi}_x$ and we change the summation signs $\sum$ with $\widetilde{\sum}$.

Proof. We can easily see that the tilde notation corresponds to applying to functions in (4.32) the change of variables (4.79). The Fredholm determinant $\det(\mathbf{1} - fA)_{l^2(\mathbb{Z})}$ is clearly not affected by the multiplication of A with the gauge factor $\frac{\widetilde{\tau}(\nu)}{\widetilde{\tau}(\theta)} \frac{\tau(m_\theta)}{\tau(n_\nu)}$, nor by the change of variables and it is therefore equal to $\det(\mathbf{1} - \widetilde{f}\widetilde{A})_{l^2(\widetilde{\mathbb{Z}})}$. Similar considerations are true also for the remaining functions in (4.32). □

The function g was used to simplify the expression of integrands of quantities $A, \Phi^{(i)}, \Psi^{(j)}$. Its crucial feature is that, in a neighborhood of size $x^{-1/3}$ of $\eth$, it admits the expansion

$$g(z) = g(\varsigma) + g'''(\varsigma)\frac{(z-\varsigma)^3}{6!} + \mathsf{o}(x^{-1/3}),$$

where ς is another point in a neighborhood of size $x^{-1/3}$ of $\eth$. In other words g has a double critical point ς in the vicinity of $\eth$ and this will enable us to analyze the asymptotic form of $A, \Phi^{(i)}, \Psi^{(j)}$ through saddle point method. This is precisely stated in the following:

Proposition 4.2.12. *With the choice $\varpi = 0$, the function g has a double critical point at $\eth$, that is $g'(\eth) = g''(\eth) = 0$. When $\varpi \neq 0$, there exists a point $\varsigma = \varsigma(\varpi)$ such that*

$$g'(\varsigma) = g''(\varsigma) = \mathcal{O}(1/x), \qquad g'''(\varsigma) = -2\frac{\gamma^3}{\varsigma^3} + \mathcal{O}(x^{1/3}) \tag{4.85}$$

and $g'''(\varsigma) < 0$ for x large enough. Moreover, such ς admits the expansion

$$\varsigma = \eth\left(1 + \frac{\varpi}{\gamma x^{1/3}} + \frac{1}{2}\frac{\varpi^2}{\gamma^2 x^{2/3}}\left(1 + \frac{a_1^2 h_3 - a_1 a_2 h_2 + 2a_2^2 h_1 - a_1 a_3 h_1}{a_1(a_2 h_1 - a_1 h_2)}\right)\right) + \mathsf{o}(1/x^{2/3}), \tag{4.86}$$

where $a_k = a_k(\eth), h_k = h_k(\eth)$ are as in (4.34).

Proof. Equalities reported in (4.85) can be verified by direct inspection making use of the approximate form of ς (4.86). Therefore the only thing we are left to prove is that γ is a positive quantity. From expression (4.35) we write

$$\gamma^3 = \frac{1}{2}\left(h_2(\eth) - \frac{h_1(\eth)}{a_1(\eth)}a_2(\eth)\right). \tag{4.87}$$

Functions a_1, a_2 have the explicit expressions

$$a_1(\eth) = \sum_{j=0}^{J-1} \frac{-\eth u q^j}{(1-\eth u q^j)^2}, \qquad a_2(\eth) = \sum_{j=0}^{J-1} \frac{-\eth u q^j(1+\eth u q^j)}{(1-\eth u q^j)^3},$$

that can be recovered using the form (A.12) to compute υ_1, υ_2. On the other hand, expressing the υ_k's in h_1, h_2 using (A.11) we can write, after some algebraic manipulations, the right hand side of (4.87) as

$$\frac{1}{2}\frac{1}{x}\sum_{y=2}^{x}\sum_{k\geq 1}\left(\frac{\eth}{\xi_y s_y}\right)^k \frac{k(1-s_y^{2k})}{1-q^k}\sum_{j=0}^{J-1}\frac{-u\eth q^j}{(1-u\eth q^j)^2}\left(k - \frac{1+u\eth q^j}{1-u\eth q^j}\right),$$

that is a sum of positive terms since $u < 0$. □

4.2.4 Proof of Proposition 4.2.7

In this Section we present the proof of Proposition 4.2.7 that establishes the convergence of the Fredholm determinant $\det(\mathbf{1} - fA)$ to the GUE Tracy-Widom distribution. Rather than using the original expressions (4.6) and (4.14) for f and A we will use their riscaled forms $\widetilde{f}, \widetilde{A}$ discussed in Proposition 4.2.11. Before we move to the more rigorous part of the presentation we like to outline the strategy we will follow:

Step 1 We first establish the pointwise convergence of the kernel $\widetilde{A}(\nu,\theta)$ to the Airy kernel $K_{\text{Airy}}(\nu,\theta)$ and this is done in Lemma 4.2.13. Our analysis relies on a saddle point method and because of this we can control the error term up to order $x^{-1/3}$ for (ν,θ) lying in an enlarging rectangle $[-L, x^{\delta/3}]^2$ with $\delta \in (0,1/3)$. This corresponds to the red region in Figure 4.1. The reason why we consider the convergence on rectangles that grow with x is that this will allow us to control the difference between $\det(\mathbf{1}-\widetilde{f}\widetilde{A})$ and F_2 as a function of x (see also Remark 4.2.18).

Step 2 We estimate the decay of the kernel $\widetilde{A}(\nu,\theta)$ for (ν,θ) in the set $[-L,\infty]^2 \setminus [-L, x^{\delta/3}]^2$, corresponding to the yellow region in Figure 4.1. This is also done through a saddle point analysis; see Lemma 4.2.14. (4.88)

Step 3 Combining the exponential decay in x of $\widetilde{f}(\nu)$ for $\nu < r$ and the fact that terms $\widetilde{A}(\nu,\theta)$ are bounded in modulus by 1 (see Lemma 4.2.15), we can estimate $\det(\mathbf{1}-\widetilde{f}\widetilde{A})_{l^2(\widetilde{\mathbb{Z}})}$ with $\det(\mathbf{1}-\widetilde{f}\widetilde{A})_{l^2(\widetilde{\mathbb{Z}}_{\geq -L})}$ up to an error of order $e^{-\text{const}.x^{1/3}}$. This is the result of Lemma 4.2.16.

Step 4 As a result of the exponential decay of front tails of the kernel $\widetilde{A}(\nu,\theta)$ we can further approximate $\det(\mathbf{1}-\widetilde{f}\widetilde{A})_{l^2(\widetilde{\mathbb{Z}}_{\geq -L})}$ with $\det(\mathbf{1}-\widetilde{f}\widetilde{A})_{l^2(\widetilde{\mathbb{Z}}\cap[-L,x^{\delta/3}))}$ up to an error of order $e^{-\text{const}.x^{1/3}}$. This is the result of Lemma 4.2.17.

Step 5 We can finally evaluate the convergence of $\det(\mathbf{1}-\widetilde{f}\widetilde{A})_{l^2(\widetilde{\mathbb{Z}}\cap[-L,x^{\delta/3}))}$ to the Tracy-Widom distribution and we can verify the "continuity" properties of the remainder $R_x^{(1)}(r^*)$ in a neighborhood of r.

Let us now start.

Step 1: we have the following Lemma.

Lemma 4.2.13 (Convergence on moderately large sets)**.** *Let δ be a number in the interval $(0,1/3)$. Then for $(\nu,\theta) \in [-L, x^{\delta/3}]^2$ we have* [2]*,*

$$\widetilde{A}(\nu,\theta) = \frac{1}{\gamma x^{1/3}} K_{\text{Airy}}(\nu,\theta) + \frac{1}{\gamma^2 x^{2/3}} Q(\nu,\theta) + \mathcal{O}\left(x^{2\delta/3-1}\right) \tag{4.89}$$

and the error term satisfies

$$x^{2/3}\mathcal{O}(x^{2\delta/3-1}) \xrightarrow[x\to\infty]{} 0, \tag{4.90}$$

uniformly in the sequence of sets $(\nu,\theta) \in [-L, x^{\delta/3}]^2$. Moreover the exponential estimates,

$$|K_{\text{Airy}}(\nu,\theta)|, |Q(\nu,\theta)| < c_1 e^{-c_2(\nu+\theta)}, \tag{4.91}$$

[2] for motivation on the choice of sets $[-L, x^{\delta/3}]$ see Remark 4.2.18.

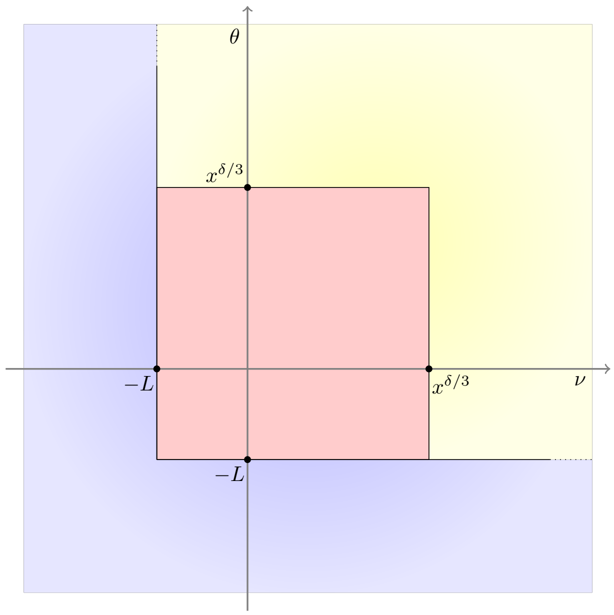

Figure 4.1: We estimate the kernel $\widetilde{A}(\nu, \theta)$ in the red the region (see Lemma 4.2.13) and in the yellow region (see Lemma 4.2.14). Because $\widetilde{f}(\nu)$ converges to the indicator function $\mathbb{1}_{(r,\infty)}$ and $-L < r$, the contribution to the Fredholm determinant of $\widetilde{f}\widetilde{A}$ of integrations in the blue region is negligible (see Lemma 4.2.16).

hold for all $(\nu, \theta) \in [-L, x^{\delta/3}]^2$, for an opportune choice of positive constants c_1, c_2 which do not depend on x.

Proof. The definition itself of scaling parameters is functional to perform a saddle point analysis. In particular we want to show that, when ν and θ are relatively small quantities, compared to $x^{1/3}$, the integrals in (4.84) are dominated by the value of the integrands at the double critical point ς. To do so we suitably deform contours C, D in such a way that, for x large enough, the following properties hold:[3]

1. $\max_{z\in C} \mathfrak{Re}\{g(z)\} = g(\varsigma(1 - \frac{1}{2\gamma x^{1/3}}))$;

2. $\max_{z\in C} |z| = \varsigma(1 - \frac{1}{2\gamma x^{1/3}})$;

3. $\min_{w\in D} \mathfrak{Re}\{g(z)\} = g(\varsigma(1 + \frac{1}{2\gamma x^{1/3}}))$;

4. $\min_{w\in D} |w| = \varsigma(1 + \frac{1}{2\gamma x^{1/3}})$.

The idea is to take paths like those depicted in Figure 4.2. Based on results of Appendix C.2, we now construct the steep descent contour C. The same procedure can be applied to provide an exact expression for D as well and therefore we will omit this in the discussion.

[3]for the sake of the uniform convergence over compact sets conditions 2,4 are not necessary, but we still state them as they will become useful later in Lemma 4.102.

Fix an arbitrarily small positive number ϵ and consider C to be the union of two curves $\widetilde{C}_1$, $\widetilde{C}_2$ such that

$$\widetilde{C}_1 = \partial \mathsf{D}\left(0, \varsigma(1-\epsilon)\right) \cap \left\{ z \in \mathbb{C} | \; \mathfrak{Re}(z) \leq \frac{\varsigma}{4}(3+\sqrt{1-8\epsilon+4\epsilon^2}) \right\}, \tag{4.92}$$

$$\widetilde{C}_2 = \left\{ \mathbb{1}_{[0,\frac{2}{\gamma x^{1/3}}]}(|\rho|)\varsigma \left(1 - \frac{4+\gamma^2 x^{2/3}\rho^2}{8\gamma x^{1/3}} + \mathrm{i}\frac{\sqrt{3}}{2}\rho \right) \right.$$
$$\left. + \mathbb{1}_{[\frac{2}{\gamma x^{1/3}},\infty)}(|\rho|)\varsigma \left(1 - \frac{|\rho|}{2} + \mathrm{i}\frac{\sqrt{3}}{2}\rho \right) : \; |\rho| \leq \frac{1}{2}(1-\sqrt{1-8\epsilon+4\epsilon^2}) \right\}, \tag{4.93}$$

where $\partial \mathsf{D}(c, R)$ indicates a circumference of center c and radius R. To put it in simple terms C is a circle of radius $\varsigma(1-\epsilon)$ up until it intersects for the first time (from the left) the two complex lines exiting from ς with slope $\pm\frac{2\pi}{3}$ (as in Figure 4.2, b)). After C meets these intersection points, denoted with $p_\pm$, it becomes $\widetilde{C}_2$, a regular curve which coincides with such lines for a while and passes strictly to the left of ς.

We claim that the contribution of the integral in the z variable in (4.84) are given, up to an error which is exponentially small in x, by the integral along the contour $\widetilde{C}_2$. To show this, we first notice that from Proposition C.2.1, if ϵ is small enough we can assume that, along $\widetilde{C}_1$ the real part of $g(z)$ is a decreasing function. Therefore, the contribution of the term $e^{xg(z)}$ can be estimated by its values at the extremal points of $\widetilde{C}_1$,

$$p_\pm = \frac{\varsigma}{4}\left(3+\sqrt{1-8\epsilon+4\epsilon^2}\right) \pm \mathrm{i}\frac{\sqrt{3}}{4}\varsigma(1-\sqrt{1-8\epsilon+4\epsilon^2}) \approx \varsigma\left(1-\epsilon\pm\mathrm{i}\sqrt{3}\epsilon\right).$$

Let us evaluate the quantity $\mathfrak{Re}\{g(p_\pm)\} - g(\varsigma)$ through a Taylor expansion. By using (4.85), we have

$$\mathfrak{Re}\{g(p_\pm)\} - g(\varsigma) = \frac{8g'''(\varsigma)\varsigma^3}{3!}\epsilon^3 + R(\epsilon)\epsilon^4,$$

where $R(\epsilon)$ is the Taylor remainder and it is a regular, bounded function in a neighborhood of zero. The factor $\varsigma^3 g'''(\varsigma)$ is strictly negative, as stated in Proposition 4.2.12 and therefore we obtain the bound

$$e^{x(g(z)-g(\varsigma))} \leq e^{-cx}, \qquad \text{for each } z \in \widetilde{C}_1,$$

which holds for some positive constant c.

Through an analogous argument we can deform the D contour too and separate it in an union of two curves $\widetilde{D}_1$ and $\widetilde{D}_2$ (see Figure 4.2). As for the C contour case, we can take $\widetilde{D}_2$ to be a curve that follows the two complex half lines $\{\varsigma + e^{\pm\mathrm{i}\frac{\pi}{3}}\rho : \rho \geq 0\}$ in a neighborhood of size ϵ of ς and that passes strictly to the right of ς. For ϵ small enough, but still of order 1, the remaining contour $\widetilde{D}_1$ can be chosen so that the contribution of the w integral over $\widetilde{D}_1$ to the kernel $\widetilde{A}$ are exponentially small in x.

We also remark that curves $\widetilde{C}_2, \widetilde{D}_2$ are kept at a distance of size $x^{-1/3}$ from ς (and hence from each other) due to the presence in the integral expression of $\widetilde{A}$ of a singularity at $z = w$.

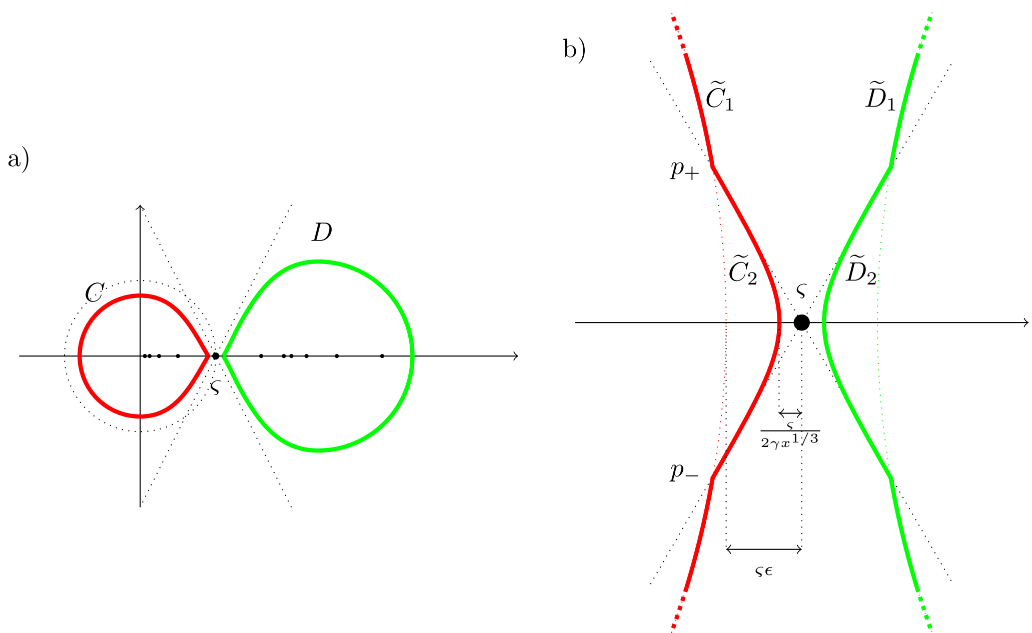

Figure 4.2: a) Choices of integration contours in Lemma 4.2.13. The red contour C encircles the sigularities $\{q^k \not{d}\}_{k\geq 1}$, is contained inside a circle of radius $\varsigma(1-\epsilon)$ and joins the point $\varsigma(1-\frac{1}{2\gamma x^{1/3}})$ with slope $\frac{\pi}{3}$ from above (resp. $-\frac{\pi}{3}$ from below). The green contour D contains the singularities $\{\xi_k s_k\}_{k=2,\dots,x}$ and forms at the point $\varsigma(1+\frac{1}{2\gamma x^{1/3}})$ a cusp of width $\frac{2}{3}\pi$, symmetric to that of C. b) A representation of contours C and D in the immediate vicinity of the critical point ς.

We can summarize discussion made so far expressing the kernel $\widetilde{A}$ as

$$\widetilde{A}(\nu,\theta) = \frac{\varsigma^{\nu\gamma x^{1/3}}}{\varsigma^{\theta\gamma x^{1/3}}} \frac{1}{(2\pi \mathrm{i})^2} \int_{\widetilde{D}_2} \frac{dw}{w} \int_{\widetilde{C}_2} dz \frac{z^{\theta\gamma x^{1/3}}}{w^{\nu\gamma x^{1/3}}} \frac{\exp\{xg(z)\}}{\exp\{xg(w)\}} \frac{(q\not{d}/w, qz/\not{d};q)_\infty}{(q\not{d}/z, qw/\not{d};q)_\infty} \frac{1}{z-w} + \mathcal{O}(e^{-cx}), \tag{4.94}$$

where we notice that, with respect to (4.84), the integration contours have become $\widetilde{C}_2$ and $\widetilde{D}_2$ and the remainder is a quantity which decays as an exponential in x. We can now safely employ the saddle point method to give an estimate of the integral expression in (4.94). The only significant contribution to the double integral (4.84) is given when variables z, w are separated from ς by a distance of order $x^{-1/3}$. For this reason we like to apply the change of variables

$$z = \varsigma\left(1 - \frac{Z}{\gamma x^{1/3}}\right), \qquad w = \varsigma\left(1 - \frac{W}{\gamma x^{1/3}}\right),$$

and we write, through simple Taylor expansions, different terms of the integrand function in (4.94) as

$$\frac{z^{\theta\gamma x^{1/3}}}{w^{\nu\gamma x^{1/3}}} = \frac{\varsigma^{\theta\gamma x^{1/3}}}{\varsigma^{\nu\gamma x^{1/3}}}\frac{e^{-\theta Z}}{e^{-\nu W}}\left[1+\frac{1}{\gamma x^{1/3}}\left(\frac{\nu W^2}{2}-\frac{\theta Z^2}{2}\right)+\mathcal{O}\left(\frac{Z^3\theta}{x^{2/3}},\frac{W^3\nu}{x^{2/3}},\frac{Z^4\theta^2}{x^{2/3}},\frac{W^4\nu^2}{x^{2/3}}\right)\right], \tag{4.95}$$

$$\frac{e^{xg(z)}}{e^{xg(w)}} = \frac{e^{Z^3/3}}{e^{W^3/3}}\left[1+\frac{1}{\gamma x^{1/3}}\left(E_1Z^4-E_1W^4\right)+\mathcal{O}\left(\frac{Z^8}{x^{2/3}},\frac{W^8}{x^{2/3}}\right)\right], \tag{4.96}$$

$$\frac{(q\mathscr{d}/w, qz/\mathscr{d};q)_\infty}{(q\mathscr{d}/z, qw/\mathscr{d};q)_\infty} = 1+\frac{1}{\gamma x^{1/3}}(E_2Z-E_2W)+\mathcal{O}\left(\frac{Z^2}{x^{2/3}},\frac{W^2}{x^{2/3}}\right). \tag{4.97}$$

In these expressions, coefficients E_1, E_2, naturally possess exact expressions, which we do not report as they are irrelevant for the computations.

Thanks to (4.94),(4.95),(4.96),(4.97) we obtain an expansion of $\widetilde{A}$ in the infinitesimal quantity $1/(\gamma x^{1/3})$. Collecting together terms of order $1/(\gamma x^{1/3})$ and $1/(\gamma x^{1/3})^2$ we obtain

$$\widetilde{A}(\nu,\theta) = \frac{1}{\gamma x^{1/3}}\int_{e^{-\frac{2}{3}\pi\mathrm{i}}\infty}^{e^{\frac{2}{3}\pi\mathrm{i}}\infty}\frac{dW}{2\pi\mathrm{i}}\int_{e^{\frac{\pi}{3}\mathrm{i}}\infty}^{e^{-\frac{\pi}{3}\mathrm{i}}\infty}\frac{dZ}{2\pi\mathrm{i}}\frac{e^{Z^3/3-\theta Z}}{e^{W^3/3-\nu W}}\frac{1}{W-Z}+\frac{1}{(\gamma x^{1/3})^2}Q(\nu,\theta)+\mathcal{O}(x^{2\delta/3-1}). \tag{4.98}$$

with the kernel Q being given by

$$Q(\nu,\theta) = \int_{e^{-\frac{2}{3}\pi\mathrm{i}}\infty}^{e^{\frac{2}{3}\pi\mathrm{i}}\infty}\frac{dW}{2\pi\mathrm{i}}\int_{e^{\frac{\pi}{3}\mathrm{i}}\infty}^{e^{-\frac{\pi}{3}\mathrm{i}}\infty}\frac{dZ}{2\pi\mathrm{i}}\frac{e^{Z^3/3-\theta Z}}{e^{W^3/3-\nu W}}\left(\frac{\nu W^2}{2}-\frac{\theta Z^2}{2}+E_1(Z^4-W^4)+E_2(Z-W)\right)\frac{1}{W-Z}. \tag{4.99}$$

By recognizing the expression of the Airy kernel (4.39) in (4.98) we write $\widetilde{A}$ as in (4.89).

All we are left to do is to prove the exponential bound (4.91) for Q, since the same type of estimate for K_{Airy} follows from well known decay properties of the Airy functions. To do this consider the following parametrization of the integration variables

$$Z=\frac{\widetilde{b}}{2}+|\varrho_1|e^{-\operatorname{sign}(\varrho_1)\mathrm{i}\pi/3}, \qquad W=-\frac{\widetilde{b}}{2}+|\varrho_2|e^{-\operatorname{sign}(\varrho_2)\mathrm{i}2\pi/3}, \tag{4.100}$$

for $\rho_1,\rho_2\in\mathbb{R}$ and $\widetilde{b}$ being a positive real number. Applying the substitution (4.100) in (4.99), we straightforwardly obtain an inequality like

$$|Q(\nu,\theta)| < e^{-\frac{\widetilde{b}}{2}(\theta+\nu)}\frac{e^{\widetilde{b}^3/12}}{\widetilde{b}}\int_0^\infty d\varrho_1\int_0^\infty d\varrho_2\Big(|\theta|P_{\widetilde{b}}(\rho_1)+|\nu|P_{\widetilde{b}}(\rho_2)+S_{\widetilde{b}}(\varrho_1)+S_{\widetilde{b}}(\varrho_2)\Big) \times e^{-\frac{\widetilde{b}}{4}(\rho_1^2+\rho_2^2)-\left(\frac{\theta}{2}-\frac{\widetilde{b}^2}{8}\right)\rho_1-\left(\frac{\nu}{2}-\frac{\widetilde{b}^2}{8}\right)\rho_2}, \tag{4.101}$$

where $P_{\widetilde{b}}$ and $S_{\widetilde{b}}$ are polynomials and by making use of elementary estimates on the integrals on the right hand side of (4.101), we can finally show (4.91).

The error term $\mathcal{O}(x^{2\delta/3-1})$ in (4.89) is obtained taking into account quantities

$$\mathcal{O}\left(\frac{Z^3\theta}{x^{2/3}},\frac{W^3\nu}{x^{2/3}},\frac{Z^4\theta^2}{x^{2/3}},\frac{W^4\nu^2}{x^{2/3}}\right),\mathcal{O}\left(\frac{Z^8}{x^{2/3}},\frac{W^8}{x^{2/3}}\right),\mathcal{O}\left(\frac{Z^2}{x^{2/3}},\frac{W^2}{x^{2/3}}\right),\mathcal{O}(e^{-cx})$$

from (4.94) and (4.95), (4.96), (4.97) in the saddle point integration. Due to the presence of the exponentially decaying term $e^{Z^3/3-W^3/3-Z\theta+W\nu}$ we can formulate bounds like (4.101) for these remainders as well, to finally show (4.90). This concludes our proof. $\square$

Step 2: the following lemma establishes the exponential decay of $\widetilde{A}(\nu,\theta)$ in the yellow region in Figure 4.1.

Lemma 4.2.14 (Exponential decay of front tails)**.** *Let L' be an arbitrary large positive real numbers (possibly of order x raised to some power). Then there exists x_*, such that for all $x > x_*$ the bound*

$$\left|\gamma x^{1/3}\widetilde{A}(\nu,\theta)\right| < e^{-\nu-\theta} \tag{4.102}$$

holds for each $(\nu,\theta)\in[-L,\infty)^2\setminus[-L,L']^2$.

Proof. We use again suitable deformations of contours described in Lemma 4.2.13 to estimate, for large x, the contribution of the factor

$$\frac{z^{\theta\gamma x^{1/3}}}{w^{\nu\gamma x^{1/3}}}$$

to the double integral (4.84). Let's first prove (4.102) in the case $\theta \geq \nu$. When this is the case, we take the contour D exactly as in Lemma 4.2.13 and we modify $C = \widetilde{C}_1 \cup \widetilde{C}_2$, where

$$\widetilde{C}_1 = \partial\mathsf{D}\left(0, \varsigma - \frac{2\varsigma}{\gamma x^{1/3}}\right) \cap \{z\in\mathbb{C}|\ \mathfrak{Re}(z) \leq \varsigma(1-\frac{3}{\gamma x^{1/3}})\},$$
$$\widetilde{C}_2 = \varsigma(1-\frac{3}{\gamma x^{1/3}}) + \mathrm{i}[-\varsigma\widetilde{a}, \varsigma\widetilde{a}]$$

and $\widetilde{a}$ is given by the intersections of the vertical complex line $\{\varsigma(1-\frac{3}{\gamma x^{1/3}})+\mathrm{i}y|\ y\in\mathbb{R}\}$ with the circle $\partial\mathsf{D}\left(0,\varsigma-\frac{2\varsigma}{\gamma x^{1/3}}\right)$. We can also write down its exact expression as

$$\widetilde{a} = \sqrt{\frac{2}{\gamma x^{1/3}} - \frac{5}{\gamma^2 x^{2/3}}} \approx \sqrt{\frac{2}{\gamma}}\frac{1}{x^{1/6}} + \mathcal{O}(x^{-1/3}).$$

From Proposition C.2.1, $\partial\mathsf{D}\left(0,\varsigma(1-\frac{2}{\gamma x^{1/3}})\right)$ is a steep descent contour for $\mathfrak{Re}(g)$ and we can assume that

$$\max_{z\in C_1}\mathfrak{Re}\{g(z)\} = \mathfrak{Re}\{g(\varsigma(1-\frac{3}{\gamma x^{1/3}}+\mathrm{i}\widetilde{a}))\}.$$

To evaluate the real part of the function g on the complex segment $\widetilde{C}_2$ we use the parametrization

$$z = \varsigma\left(1-\frac{3}{\gamma x^{1/3}} + \mathrm{i}\frac{Z}{\gamma x^{1/3}}\right). \tag{4.103}$$

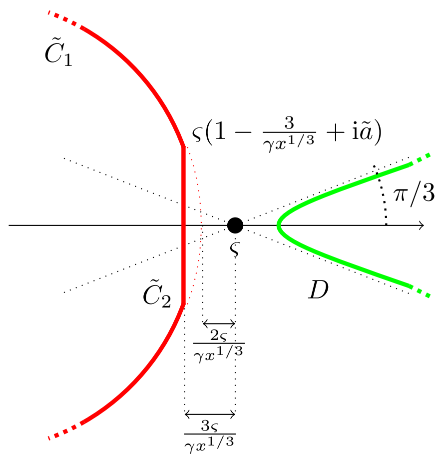

Figure 4.3: Choice of integration contours of Lemma 4.2.14. The red contour C is the union of $\widetilde{C}_1$, an arc of the circle of center 0 and radius $\varsigma(1-\frac{2}{\gamma x^{1/3}})$, and $\widetilde{C}_2$, a vertical segment passing for the point $\varsigma(1-\frac{3}{\gamma x^{1/3}})$ on the real axis. On the other hand D, in the vicinity of the critical point ς, stays close to the lines exiting from ς with slope $\pm\frac{\pi}{3}$ (dotted lines).

In this case Z is a real number ranging in an interval which, up to corrections of order $x^{-1/3}$ is $[-\sqrt{2\gamma}x^{1/6}, \sqrt{2\gamma}x^{1/6}]$. Expanding g in Taylor series around ς and recalling (4.85), we have

$$\mathfrak{Re}\{g(z)\}-g(\varsigma) = \frac{1}{x}\frac{\varsigma^3 g'''(\varsigma)}{3!\gamma^3}(-27+9Z^2)+\frac{1}{x^{4/3}}\frac{\varsigma^4 g^{(4)}(\varsigma)}{4!\gamma^4}Z^4+\mathcal{O}\left(\frac{Z^2}{x^{4/3}},\frac{Z^4}{x^{5/3}},\frac{Z^6}{x^2}\right), \quad (4.104)$$

where the presence of terms of order higher than three takes into account the fact that Z can be of order $x^{1/6}$. When $Z/(\gamma x^{1/3}) = \widetilde{a}$, (4.104) becomes

$$\mathfrak{Re}\{g(\varsigma(1-\frac{3}{\gamma x^{1/3}}+\mathrm{i}\widetilde{a}))\} - g(\varsigma) = \frac{1}{\gamma^2 x^{2/3}}\left(3\varsigma^3 g'''(\varsigma)+\frac{1}{6}\varsigma^4 g^{(4)}(\varsigma)\right)+\mathcal{O}(x^{-1})$$

and the term on the right hand side of order $x^{-2/3}$ is negative. This can be shown either directly computing the derivatives of g or simply recalling that the point $\varsigma(1-\frac{3}{\gamma x^{1/3}}+\mathrm{i}\widetilde{a})$ lies on a steep descent contour. These calculations imply the estimate

$$|e^{x(g(z)-g(\varsigma))}| \le e^{-cx^{1/3}}, \qquad \text{for each } z\in\widetilde{C}_1, \quad (4.105)$$

for some positive constant c. On the other hand, when z belongs to $\widetilde{C}_2$, (4.104) gives us that

$$|e^{x(g(z)-g(\varsigma))}| \le e^{9-\widetilde{c}Z^2}, \qquad \text{for each } |Z|\le\gamma\widetilde{a}x^{1/3}, \quad (4.106)$$

for some other positive constant $\widetilde{c}$.

To complete the list of preliminary estimates for terms depending on z in the integral formula (4.84) of the kernel $\widetilde{A}$, we need to address the factor $z^{\theta\gamma x^{1/3}}$. First we notice that, since the contour C lies inside the circle centered at 0 with radius $\varsigma(1-2/(\gamma x^{1/3}))$, we have

$$\left|\frac{z}{\varsigma}\right|^{\theta\gamma x^{1/3}} \leq \exp\left\{\theta\gamma x^{1/3}\log\left(1-\frac{2}{\gamma x^{1/3}}\right)\right\} \leq e^{-2\theta}, \qquad \text{for each } z \in C, \tag{4.107}$$

as a result of the simple inequlity $\log(1+y) \leq y$, valid for all $y > -1$. Moreover, when z is on $\widetilde{C}_2$, using the parametrization (4.103), we have

$$\left|\frac{z}{\varsigma}\right|^{\theta\gamma x^{1/3}} = \exp\left\{\theta\gamma x^{1/3}\log\left|1-\frac{3}{\gamma x^{1/3}}+\frac{\mathrm{i}Z}{\gamma x^{1/3}}\right|\right\} \leq \exp\left\{-\theta\left(3-\frac{9+Z^2}{2\gamma x^{1/3}}\right)\right\}. \tag{4.108}$$

To evaluate the kernel $\widetilde{A}$ we also need to provide some estimates for quantities involving the variable w. The choice of contours C, D implies that

$$\frac{1}{z-w} \leq \frac{\varsigma}{\gamma x^{1/3}} \qquad \text{and} \qquad \left|\frac{(q\text{ď}/w, qz/\text{ď};q)_\infty}{(q\text{ď}/z, qw/\text{ď};q)_\infty}\right| \leq \Gamma_1, \tag{4.109}$$

for some constant Γ_1. In addition, since $\nu > -L$ and $|w| > \varsigma$, combined with the fact that D is steep ascent for the function $\mathfrak{Re}\{g\}$, as proved in Proposition C.2.3, we have that

$$\left|\frac{\varsigma}{w}\right|^{\nu\gamma x^{1/3}} \exp\{x(g(\varsigma)-g(w))\} \leq \left|\frac{\varsigma}{w}\right|^{-L\gamma x^{1/3}} \exp\{x(g(\varsigma)-g(w))\} \leq \Gamma_2, \tag{4.110}$$

for some other constant Γ_2. Combining together inequalities (4.108), (4.109), (4.110), we can write

$$\begin{aligned}|\widetilde{A}(\nu,\theta)| &= \frac{\varsigma^{\nu\gamma x^{1/3}}}{\varsigma^{\theta\gamma x^{1/3}}}\left|\int_C \frac{dz}{2\pi}\int_D \frac{dw}{2\pi w}\frac{z^{\theta\gamma x^{1/3}}}{w^{\nu\gamma x^{1/3}}}\frac{\exp\{xg(z)\}}{\exp\{xg(w)\}}\frac{(q\text{ď}/w, qz/\text{ď};q)_\infty}{(q\text{ď}/z, qw/\text{ď};q)_\infty}\frac{1}{z-w}\right| \\ &\leq \frac{\Gamma_1\Gamma_2 l(D)}{(2\pi)^2\gamma x^{1/3}}\int_C\left|dz\left(\frac{z}{\varsigma}\right)^{\theta\gamma x^{1/3}}\exp\{x(g(z)-g(\varsigma))\}\right|,\end{aligned} \tag{4.111}$$

where $l(D)$ is the length of the curve D. The integral over C is naturally split into different contributions coming from contours $\widetilde{C}_1$ and $\widetilde{C}_2$. On $\widetilde{C}_1$, utilizing (4.105) and (4.107) we have

$$\int_{\widetilde{C}_1}\left|dz\left(\frac{z}{\varsigma}\right)^{\theta\gamma x^{1/3}}\exp\{x(g(z)-g(\varsigma))\}\right| \leq e^{-2\theta}e^{-cx^{-1/3}}l(\widetilde{C}_1), \tag{4.112}$$

whereas on $\widetilde{C}_2$, from (4.106), (4.108) we obtain

$$\int_{\widetilde{C}_2}\left|dz\left(\frac{z}{\varsigma}\right)^{\theta\gamma x^{1/3}}\exp\{x(g(z)-g(\varsigma))\}\right| \leq \int_{-a\gamma x^{1/3}}^{a\gamma x^{1/3}} dZ\exp\left\{-\theta\left(3-\frac{9+Z^2}{2\gamma x^{1/3}}\right)+9-\widetilde{c}Z^2\right\}. \tag{4.113}$$

To estimate the integral on the right hand side of (4.113), set a large integer N and split the integration segmant into $|Z| < N$ and $N < |Z| < \widetilde{a}\gamma x^{1/3}$. When $|Z| < N$ the term $\frac{9+Z^2}{2\gamma x^{1/3}}$ is small and we can denote it with $\mathcal{O}(N^2/x^{1/3})$. On the other hand, when

$N < |Z| < \widetilde{a}\gamma x^{1/3}$, since $(3 - \frac{9+Z^2}{2\gamma x^{1/3}}) > 2$, the integrand becomes very small due to the presence of the exponential of $-\widetilde{c}Z^2$. We can therefore write

$$\begin{aligned}\text{rhs } (4.113) &\leq e^{-2\theta}\left(e^{-\theta(1-\mathcal{O}(N^2/x^{1/3}))}\int_{-N}^{N} e^{9-\widetilde{c}Z^2}dZ + \int_{N<|Z|\widetilde{a}\gamma x^{1/3}} dZ e^{9-\widetilde{c}Z^2}\right)\\ &= e^{-2\theta}\left(e^{-\theta(1-\mathcal{O}(N^2/x^{1/3}))}\Gamma_3 + \mathcal{O}(e^{-\widetilde{c}N^2})\right),\end{aligned} \tag{4.114}$$

with Γ_3 being a constant coming from the integration of the exponential.

We can now plug (4.112), (4.113), (4.114) into the right hand side of (4.111) to finally obtain

$$|\widetilde{A}(\nu,\theta)| < e^{-2\theta}\left(e^{-cx^{1/3}}l(C_1) + e^{-\theta(1-\mathcal{O}(N^2/x^{1/3}))}\Gamma_3 + \mathcal{O}(e^{-\widetilde{c}N^2})\right)\frac{\Gamma_1\Gamma_2 l(D)}{(2\pi)^2\gamma x^{1/3}}. \tag{4.115}$$

The term inside the parentheses can be made smaller than $\frac{(2\pi)^2}{\Gamma_1\Gamma_2 l(D)}$ taking $x \gg 0$ and $L' \gg 0$ (remember $L' < \theta$), so that (4.115) reduces to

$$|\widetilde{A}(\nu,\theta)| < e^{-2\theta}\frac{1}{\gamma x^{1/3}},$$

which implies (4.102) since $-2\theta < -\theta - \nu$.

The complementary case $\nu > \theta$ can be studied analogously, deforming the contour D, instead of C, symmetrically with respect to the critical point ς. $\square$

Up to this point we estimated the kernel $\widetilde{A}$ in a region where both θ and ν are bounded from below. When this is not the case the saddle point method cannot be applied any longer as the contribution to the integral (4.84) of the term

$$\frac{z^{\gamma x^{1/3}\theta}}{w^{\gamma x^{1/3}\nu}}$$

is no more negligible. In the following Lemma we show how to control the rear tails of $\widetilde{A}$.

Lemma 4.2.15. *The kernel $\widetilde{A}$ defines a trace class operator on $l^2(\widetilde{\mathbb{Z}})$ with $\|\widetilde{A}\| = 1$. In particular we have the bound*

$$|\widetilde{A}(\nu,\theta)| \leq 1. \tag{4.116}$$

Proof. Since $\widetilde{A}$ is obtained from the kernel A through a simple change of variable and a multiplication by a gauge factor $\frac{\widetilde{\tau}(\nu)}{\widetilde{\tau}(\theta)}\frac{\tau(m_\theta)}{\tau(n_\nu)}$, we can still write the expansion

$$\widetilde{A}(\nu,\theta) = \sum_{l=1}^{x-1}\frac{\widetilde{\tau}(\nu)}{\tau(n_\nu)}\phi_l(n_\nu)\frac{\tau(m_\theta)}{\widetilde{\tau}(\theta)}\psi_l(m_\theta) = \sum_{l=1}^{x-1}\widetilde{\phi}_l(\nu)\widetilde{\psi}_l(\theta),$$

where $\widetilde{\phi}_l(\nu) = \frac{\widetilde{\tau}(\nu)}{\tau(n_\nu)}\phi_l(n_\nu)$ and $\widetilde{\psi}_l(\theta) = \frac{\tau(m_\theta)}{\widetilde{\tau}(\theta)}\psi_l(m_\theta)$. Functions $\widetilde{\phi}_l, \widetilde{\psi}_l$, like ϕ_l, ψ_l, are still a biorthogonal family and to prove this we only have to check that the summation

$\widetilde{\sum_\nu} \widetilde{\phi}_l(\nu)\widetilde{\psi}_k(\nu)$ is absolutely convergent. This can be done establishing exponential decay of tails of $\widetilde{\phi}_l, \widetilde{\psi}_k$. For the rear tails this is done as in Appendix C.1 for functions ϕ_l, ψ_l (for the real tails), while front tails are estimated using a saddle point analysis as that performed for the kernel $\widetilde{A}$ in Lemma 4.2.13, 4.2.14. Such exponential bounds imply that $\widetilde{A}$ is trace class for each x, following the argument in the proof of Proposition 4.1.4. Also, the biorthogonality of $\widetilde{\phi}_l, \widetilde{\psi}_k$ implies that $\|\widetilde{A}\| = 1$ as shown in the proof of Proposition 4.1.6. □

Step 3: we can now start the evaluation of the Fredholm determinant of the kernel $\widetilde{f}\widetilde{A}$.

Lemma 4.2.16. *There exist constants c, x^* such that, for each $x > x^*$, we have*

$$\left|\det\left(\mathbf{1} - \widetilde{f}\widetilde{A}\right)_{l^2(\widetilde{\mathbb{Z}})} - \det\left(\mathbf{1} - \widetilde{f}\widetilde{A}\right)_{l^2(\widetilde{\mathbb{Z}}\cap[-L,\infty))}\right| < e^{-cL\gamma x^{1/3}}. \tag{4.117}$$

Proof. First we set constants c_1, c_2 such that the estimate

$$\left|\sqrt{\widetilde{f}(\nu)\widetilde{f}(\theta)}\widetilde{A}(\nu,\theta)\right| < \begin{cases} \frac{1}{\gamma x^{1/3}} c_1 e^{-\theta-\nu}, & \text{if } \theta,\nu \in [-L,\infty), \\ \frac{1}{\gamma x^{1/3}} e^{c_2(\min(\theta,-L)+\min(\nu,-L))\gamma x^{1/3}}, & \text{else,} \end{cases}$$

holds, for each x sufficiently large. This is always possible as a result of Lemmas 4.2.13, 4.2.14, 4.2.15 and from the fact that $\widetilde{f}(\nu)$, given in (4.83), decays exponentially in $x^{1/3}$ when $\nu \ll 0$. In particular we can easily deduce the additional bound

$$\left|\sqrt{\widetilde{f}(\nu)\widetilde{f}(\theta)}\widetilde{A}(\nu,\theta)\right| < c_3 \frac{1}{\gamma x^{1/3}} e^{-|\theta|-|\nu|},$$

true for any θ, ν, for some constant c_3. We have

$$\begin{aligned} \text{lhs of (4.117)} &= \left| \sum_{k\geq 1} \frac{(-1)^k}{k!} \widetilde{\sum_{(\nu_1,\dots,\nu_k)\notin[-L,\infty)^k}} \det_{i,j=1}^{k}\left(\sqrt{\widetilde{f}(\nu_i)\widetilde{f}(\nu_j)}\widetilde{A}(\nu_i,\nu_j)\right)\right| \\ &\leq \sum_{k\geq 1} \frac{(-1)^k}{(k-1)!} \widetilde{\sum_{\nu_1\leq -L}} \sum_{\nu_2,\dots,\nu_k} \left|\det_{i,j=1}^{k}\left(\sqrt{\widetilde{f}(\nu_i)\widetilde{f}(\nu_j)}\widetilde{A}(\nu_i,\nu_j)\right)\right|. \end{aligned} \tag{4.118}$$

Thanks to the Hadamard's inequality we can estimate the determinantal term in the sum as

$$\begin{aligned} \left|\det_{i,j=1}^{k}\left(\sqrt{\widetilde{f}(\nu_i)\widetilde{f}(\nu_j)}\widetilde{A}(\nu_i,\nu_j)\right)\right| &\leq \prod_{i=1}^{k}\left(\sum_{j=1}^{k}\widetilde{f}(\nu_i)\widetilde{f}(\nu_j)\left|\widetilde{A}(\nu_i,\nu_j)\right|^2\right)^{1/2} \\ &\leq \frac{k^{k/2}}{(\gamma x^{1/3})^k} e^{c_2\nu_1\gamma x^{1/3}} c_3^{k-1}\prod_{j=2}^{k} e^{-|\nu_j|}, \end{aligned}$$

so that, using this bound in (4.118), we obtain our result. □

Step 4:

Lemma 4.2.17. *Take constants L, δ such that $-L < r$ and $\delta \in (0, 1/3)$. Then there exist constants C, x^* such that, for each $x > x^*$, we have*

$$\left| \det \left(\mathbf{1} - \widetilde{f}\widetilde{A} \right)_{l^2(\widetilde{\mathbb{Z}}_{\geq -L})} - \det \left(\mathbf{1} - \widetilde{f}\widetilde{A} \right)_{l^2(\widetilde{\mathbb{Z}} \cap [-L, x^{\delta/3}))} \right| < Ce^{-x^{\delta/3}}. \tag{4.119}$$

Proof. The proof of (4.119) makes use of the exponential bound (4.102) choosing $L' = x^{\delta/3}$ and it is similar to that of Lemma 4.2.16, therefore we omit it. □

Step 5: we can finally combine all previous preliminary Lemmas and give the proof of Proposition 4.2.7.

Proof of Proposition 4.2.7. To prove this result we first use Lemma 4.2.16 and Lemma 4.2.17 to restrict our attention to the Fredholm determinant of $\widetilde{f}\widetilde{A}$ in $l^2(\widetilde{\mathbb{Z}} \cap [-L, x^{\delta/3}])$. The error we make while considering this restriction is exponentially small in x and hence it is irrelevant when it comes to a decomposition like (4.61). Using results of Lemma 4.2.13 we have

$$\widetilde{A}(\nu, \theta) = \frac{1}{\gamma x^{1/3}} K_{\mathrm{Airy}}(\nu, \theta) + \frac{1}{(\gamma x^{1/3})^2} Q(\nu, \theta) + \mathcal{O}(x^{2\delta/3 - 1}),$$
$$\widetilde{f}(\nu) = \mathbb{1}_{[r, \infty)}(\nu) + \Delta_r(\nu),$$

where the term Δ_r is simply expressed as

$$\Delta_r(\nu) = \begin{cases} \frac{1}{1 + q^{(\nu - r)\gamma x^{1/3}}}, & \text{if } \nu < r, \\ \frac{-q^{(\nu - r)\gamma x^{1/3}}}{1 + q^{(\nu - r)\gamma x^{1/3}}}, & \text{if } \nu \geq r. \end{cases}$$

We can saparate the terms of the product $\widetilde{f}(\nu)\widetilde{A}(\nu, \theta)$ based on their order in $x^{-1/3}$ as

$$B^{(1)}(\nu, \theta) = \mathbb{1}_{[r, \infty)}(\nu) K_{\mathrm{Airy}}(\nu, \theta), \qquad B^{(2)}(\nu, \theta) = \frac{1}{\gamma x^{1/3}} \mathbb{1}_{[r, \infty)}(\nu) Q(\nu, \theta),$$
$$B^{(3)}(\nu, \theta) = \Delta_r(\nu) K_{\mathrm{Airy}}(\nu, \theta), \qquad B^{(4)}(\nu, \theta) = \frac{1}{\gamma x^{1/3}} \Delta_r(\nu) Q(\nu, \theta),$$
$$B^{(5)}_{i,j}(\nu, \theta) = \mathcal{O}(x^{2(\delta - 1)/3}).$$

In this notation we write the Fredholm determinant of $\widetilde{f}\widetilde{A}$ as

$$\det \left(\mathbf{1} - \widetilde{f}\widetilde{A} \right)_{l^2(\widetilde{\mathbb{Z}} \cap [-L, x^{\delta/3}])} = 1 + \sum_{k \geq 1} \frac{(-1)^k}{k!} \widetilde{\sum_{\substack{\nu_l \in [-L, x^{\delta/3}] \\ l = 1, \dots, k}}} \left(\frac{1}{\gamma x^{1/3}} \right)^k \det_{i,j=1}^{k} \left(B^{(1)}(\nu_i, \nu_j) + \cdots + B^{(5)}(\nu_i, \nu_j) \right) \tag{4.120}$$

and our goal is to separate the contribution of higher order terms $B^{(2)}, \dots, B^{(5)}$ from that of $B^{(1)}$. To do so we use a formula that expresses the determinant of a sum of matrices

$B^{(1)} + \cdots + B^{(N)}$ in terms of sums of determinants of matrices having for column i, the i-th column of exactly one of the $B^{(1)}, \ldots, B^{(N)}$. More precisely we have

$$\det\left(B^{(1)} + \cdots + B^{(N)}\right) = \sum_{\substack{\cup_{i=1}^N I_i = \{1,\ldots,k\} \\ I_i \cap I_j = \emptyset \text{ if } i \neq j}} \det\left(B^{(I_1,\ldots,I_N)}\right), \tag{4.121}$$

where

$$B^{(I_1,\ldots,I_N)}_{i,j} = B^{(l)}_{i,j} \qquad \text{if } i \in I_l.$$

This expansion holds for generic $k \times k$ matrices $B^{(1)}, \ldots, B^{(N)}$ and it follows directly from the multi linearity of the determinant. Using (4.121) can rewrite the determinant in the right hand side of (4.120) as

$$\det\left(B^{(1)} + \cdots + B^{(5)}\right) = \det\left(B^{(1)}\right) + \sum_{\substack{\cup_{i=1}^5 I_i = \{1,\ldots,k\} \\ I_i \cap I_j = \emptyset \text{ if } i \neq j \\ I_1 \neq \varnothing}} \det\left(B^{(I_1,I_2,I_3,I_4,I_5)}\right). \tag{4.122}$$

The Hadamard inequality provides the bound

$$\left|\det(B^{(I_1,I_2,I_3,I_4,I_5)})\right| \leq \prod_{l=1}^{5} \prod_{i \in I_l} \left(\sum_{j=1}^{k} |B^{(l)}(\nu_i, \nu_j)|^2 \right)^{1/2},$$

while exponential inequality (4.91) allows us to write

$$B^{(1)}(\nu_i,\nu_j) < c_1 e^{-c_2 \nu_i}, \qquad B^{(2)}(\nu_i,\nu_j) < \frac{1}{\gamma x^{1/3}} c_1 e^{-c_2 \nu_i}, \qquad B^{(3)}(\nu_i,\nu_j) < c_1 q^{|\nu_i - r|\gamma x^{1/3}},$$

$$B^{(4)}(\nu_i,\nu_j) < \frac{c_1 q^{|\nu_i - r|\gamma x^{1/3}}}{\gamma x^{1/3}}, \qquad B^{(5)}(\nu_i,\nu_j) = \mathcal{O}(x^{2(\delta-1)/3}).$$

Integrating the generic term of the summation in (4.122) we obtain

$$\widetilde{\sum_{\substack{\nu_l \in [-L, x^{\delta/3}] \\ l=1,\ldots,k}}} \left(\frac{1}{\gamma x^{1/3}}\right)^k \left|\det(B^{(I_1,I_2,I_3,I_4,I_5)})\right| = k^{k/2} \mathcal{O}\left(x^{-|I_2|/3 - |I_3|/3 - 2|I_4|/3 - |I_5|(2/3-\delta)}\right), \tag{4.123}$$

where the exponents $-|I_3|/3$ and $-2|I_4|/3$ appear due to the fact that the function $q^{|\nu - r|\gamma x^{1/3}}$ is exponentially small in x outside of a neighborhood of size $x^{-1/3}$ of r. Because at least one among $I_2, \ldots, I_5$ is not empty, we have proven that

$$\begin{aligned} \det\left(\mathbf{1} - \widetilde{f}\widetilde{A}\right)_{l^2(\widetilde{\mathbb{Z}} \cap [-L, x^{\delta/3}])} &= \det\left(\mathbf{1} - \mathbb{1}_{[r,\infty)} K_{\text{Airy}}\right)_{l^2(\widetilde{\mathbb{Z}} \cap [-L, x^{\delta/3}])} + \frac{1}{\gamma x^{1/3}} S_x^{(1)}(r) \\ &= \det\left(\mathbf{1} - \mathbb{1}_{[r,\infty)} K_{\text{Airy}}\right)_{\mathcal{L}^2(\mathbb{R})} + \frac{1}{\gamma x^{1/3}} \left(S_x^{(1)}(r) + S_x^{(2)}(r)\right). \end{aligned} \tag{4.124}$$

In the right hand side the error $S^{(1)}$ comes from contribution to the Fredholm determinant of matrices $B^{(2)}, \dots, B^{(5)}$, while $S^{(2)}$ comes from substituting discrete integrations $\widetilde{\sum}$ with integral symbols. Both these quantities are explicit and clearly bounded due to the exponential estimates (4.91) and this proves (4.61), (4.62).

The continuity of the remainder term (4.63) can be proven following the same strategy used to prove its boundedness. In fact for any r^*, $S_x^{(1)}(r^*), S_x^{(2)}(r^*)$ are sums of determinants of kernels depending on r^* and to evaluate the differences

$$S_x^{(i)}(r^*) - S_x^{(i)}(r^* - 1/\gamma x^{1/3})$$

we can first expand these kernels around r^* and subsequently analyse the contributions of terms of order zero and one in $x^{-1/3}$ using an expansion of the form (4.122). We don't discuss these details any further.

□

Remark 4.2.18. The statement of Proposition 4.2.7 not only tells us that

$$\det(\mathbf{1} - \widetilde{f}\widetilde{A}) \xrightarrow[x\to\infty]{} F_2(r),$$

but also it gives us an estimate of the error depending on x and this will be essential in the proof of Theorem 4.2.1. To measure such error term, namely $\frac{1}{\gamma x^{1/3}} R_x^{(1)}$ in (4.61), we approximated the kernel $\widetilde{f}\widetilde{A}$ on $l^2(\widetilde{\mathbb{Z}}^2)$ with its truncated version defined only on $(\widetilde{\mathbb{Z}} \cap [-L, x^{\delta/3}])^2$. The choice of the supremum of the segment $[-L, x^{\delta/3}]$ is actually very relevant and possibly differentiate our analysis of the Fredholm determinant from that of earlier works, such as [BFS08]. Had we considered the convergence of $\widetilde{f}\widetilde{A}$ only on compact sets like $[-L, L']$, with L' being some finite constant, we would have ended up, in Lemma 4.2.17 (replacing every $x^{\delta/3}$ with L'), with a bound like

$$\textit{lhs of } (4.119) < Ce^{-L'}. \tag{4.125}$$

This clearly would have not been enough for our purposes, as the right hand side of (4.125) has no dependence on x and in particular does not decay when x becomes infinite.

4.2.5 Proof of Propositions 4.2.8, 4.2.9, 4.2.10

In this Section we carry out proofs of Propositions 4.2.8, 4.2.9 and 4.2.10, that were stated in Section 4.2.2 and used in the proof of our main result Theorem 4.2.1. As in Section 4.2.4, rather than the original expressions of $f, A, \Phi^{(i)}, \Psi^{(j)}$ we will make use of their rescaled forms $\widetilde{f}, \widetilde{A}, \widetilde{\Phi}^{(i)}, \widetilde{\Psi}^{(j)}$ discussed in Proposition 4.2.11. First we present the proof of Proposition 4.2.8 and the argument we follow traces that given in Lemma 5.12 of [IS19].

Proof of Proposition 4.2.8. First we see that the term

$$\upsilon_0(1/\zeta) + 2\,\upsilon_0(q) = \sum_{n\geq 0} \left(\frac{q^n/\zeta}{1-q^n/\zeta} + 2\frac{q^{n+1}}{1-q^{n+1}} \right)$$

plays no role in the limit as it is a bounded quantity in x for each fixed r.

Less trivial is to calculate the limiting form of $\upsilon_0(q\zeta)$, which is a summation like

$$\sum_{n\geq 0} \frac{q^{n+1-X}}{1+q^{n+1-X}},$$

for X being large. The kicker here is understanding that the main contribution to the sum is given by terms where m runs between 0 and $2\lceil X \rceil$ [4]. Coupling the $(k-1)$th and the $(2\lceil X \rceil - k - 1)$th addends and using the simple inequality

$$1 - \frac{1-q^2}{1+q^2+q^{k-X}+q^{X-k+2}} \leq \frac{1}{1+q^{X-k}} + \frac{1}{1+q^{X-2\lceil X \rceil + k}} \leq 1,$$

we see that

$$\sum_{n\geq 0} \frac{1}{1+q^{X-n-1}} = X + \mathcal{O}(1).$$

We are interested in the case when $X = \eta x - \gamma x^{1/3} r$, so that, plugging this result into (4.64) we are left to calculate

$$\begin{aligned}
&\lim_{x\to\infty} \frac{1}{\gamma x^{1/3}} \left(\kappa x a_0(\text{đ}) - x h_0(\text{đ}) - \eta x + r\gamma x^{1/3}\right) \\
&= r + \lim_{x\to\infty} \frac{x^{2/3}}{\gamma} \text{đ}\, g'(\text{đ}),
\end{aligned}$$

which gives (4.64) and (4.65) after expanding g' around its critical point ς as

$$g'(\text{đ}) \approx \frac{1}{2} g'''(\varsigma)(\text{đ} - \varsigma)^2 = \frac{\varsigma^2}{2\gamma^2} g'''(\varsigma) \frac{\varpi^2}{x^{2/3}} + \mathsf{o}(x^{-2/3}).$$

This procedure also proves the boundedness of the remainder $R_x^{(3)}$ due to the generality of r.

Result (4.66) follows from expression (4.64). We have

$$R_x^{(2)}(r^*) = -\gamma x^{1/3} r^* - \sum_{n\geq 0} \left(\frac{q^n/\zeta}{1-q^n/\zeta} - \frac{q^{n+1}\zeta}{1-q^{n+1}\zeta} \right) + (\text{terms independent of } r^*),$$

where $\zeta = -q^{-\eta x + \gamma x^{1/3} r^*}$. In this way the difference $R_x^{(2)}(r^*) - R_x^{(2)}(r^* - 1/(\gamma x^{1/3}))$ becomes

$$-1 + \frac{q^{\eta x - \gamma x^{1/3} r^*}}{1+q^{\eta x - \gamma x^{1/3} r^*}} + \frac{q^{-\eta x + \gamma x^{1/3} r^*}}{1+q^{-\eta x + \gamma x^{1/3} r^*}},$$

which converges to zero exponentially as x goes to infinity. □

[4] here $\lceil\rceil$ is the ceiling function

Next we present the proofs of Propositions 4.2.9, 4.2.10. Our approach follows a saddle point analysis analogous to that showed in Section 4.2.4. The only difference between the argument we present next and that used for the evaluation of the Fredholm determinant of $\widetilde{f}\widetilde{A}$ consists in the proof of the exponential decay of rear tails of $\widetilde{f}(\nu)\widetilde{\Phi}_x^{(i)}(\nu)\widetilde{\Psi}_x^{(j)}(\nu)$. In fact in Section 4.2.4 the decay of rear tails of $\widetilde{f}\widetilde{A}$ was implied by the bound (4.116) and by the convergence $\widetilde{f} \to \mathbb{1}_{(r,\infty)}$. Below to obtain similar estimates we use more direct computations and hypothesis (4.60).

Proof of Proposition 4.2.9. By making use of the saddle point method it is easy, at this stage, to obtain a convergence result as

$$\mathfrak{d} \sum_{\substack{i,j=1,2 \\ (i,j)\neq(1,1)}} \widetilde{f}(\nu)\widetilde{\Phi}_x^{(i)}(\nu)\widetilde{\Psi}_x^{(j)}(\nu) \xrightarrow[x\to\infty]{} \sum_{\substack{i,j=1,2 \\ (i,j)\neq(1,1)}} \mathbb{1}_{[r,\infty)}(\nu)\Upsilon_{-\varpi}^{(i)}(\nu)\Upsilon_{\varpi}^{(j)}(\nu) \tag{4.126}$$

and to estimate the error term depending on x and r. This holds for ν in relatively large sets of the form $[-L, x^{\delta/3}]$ for some fixed $L > 0$ and $\delta \in (0, 1/3)$. Also, assuming a suitably strong decay of tails of summands in the left hand side of (4.126), this easily leads to an expansion of type (4.67).

Using suitable deformations of contours in the integral expressions of $\widetilde{\Phi}_x^{(2)}, \widetilde{\Psi}_x^{(2)}$, such as those seen in Lemma 4.2.14, one can also establish an exponential type decay for the front tail ($\nu \gg 0$) of (4.126).

The exponential decay we have in the left hand side of (4.126), when ν goes to $-\infty$ is slightly different from what seen previously and in particular, here we make use of the hypothesis $\frac{2a}{1+\sigma} < q^{-1}\mathfrak{d}$ stated in (4.60). We evaluate separately each one of the three summands in the left hand side of (4.67), when (i,j) is either equal to $(1,2),(2,1)$ or $(2,2)$.

We start with the $(i,j) = (1,2)$ term. From expressions reported in Proposition 4.2.11, we write

$$\mathfrak{d}\widetilde{f}(\nu)\widetilde{\Phi}_x^{(1)}(\nu)\widetilde{\Psi}_x^{(2)}(\nu) = \frac{1}{1+q^{\gamma x^{1/3}(\nu-r)}} \int_{C_1} \frac{dz}{2\pi \mathrm{i} z} \left(\frac{z}{\mathfrak{d}}\right)^{\gamma x^{1/3}\nu} e^{x(g(z)-g(\mathfrak{d}))} \frac{(qz/\mathfrak{d};q)_\infty}{(q;q)_\infty}. \tag{4.127}$$

We take C_1 to be a circle of center in 0 and radius $\varsigma(1 - h/(\gamma x^{1/3}))$, where h is chosen so that $|z| < \mathfrak{d}$ for all z in C_1 (e.g. take $h > \varpi$). When x is large enough, such C_1 is a steep descent contour for $\mathfrak{Re}\{g\}$, as proven in Proposition C.2.1. This, along with the fact that ς is a double critical point for g allows us to state the bound

$$|\exp\{x(g(z) - g(\mathfrak{d}))\}| < \text{const} \qquad \text{for all } z \in C_1. \tag{4.128}$$

Moreover, the choice of C_1 also allows us to write

$$\begin{aligned} \left|\frac{z}{\mathfrak{d}}\right|^{\gamma x^{1/3}\nu} &= \exp\left\{\gamma x^{1/3}\nu\left(\log\left(1-\frac{h}{\gamma x^{1/3}}\right) - \log\left(1-\frac{w}{\gamma x^{1/3}}\right)\right) + \mathsf{o}(1)\right\} \\ &\leq \exp\left\{\nu(\varpi - h) + \mathsf{o}(1)\right\}, \end{aligned} \tag{4.129}$$

having used the simple logarithmic inequality $\frac{y}{1+y} \le \log(1+y) \le y$, valid for all $y > -1$. Despite the right hand side of (4.129) is a quantity which diverges exponentially when $\nu \to -\infty$, its contribution is easily balanced by the term $1/(1 + q^{\gamma x^{1/3}(\nu - r)})$ in (4.127), which, for $\nu < -L$, decays as $q^{-(1-r/L)\gamma x^{1/3}\nu}$. Following (4.128), (4.129) we come to the estimate

$$|(4.127)| < \text{const}\frac{l(C_1)}{2\pi} e^{(h-\varpi)\nu} q^{-(1-r/L)\gamma x^{1/3}\nu}$$

where in the right hand side the constant term also includes a trivial bound for the factor $\frac{(qz/d;q)_\infty}{(q;q)_\infty}$. This is enough to show that for L large enough, we have

$$|(4.127)| < c_1 e^{c_2 \gamma x^{1/3} \nu}, \qquad \text{for all } \nu < -L, \tag{4.130}$$

where c_1 and c_2 are two suitably chosen positive constants.

We now want to establish a type of bound similar to (4.130) for the term $(i, j) = (2, 1)$ of the left hand side of (4.67). Again, from (4.23), (4.24) we write

$$d\widetilde{f}(\nu)\widetilde{\Phi}_x^{(2)}(\nu)\widetilde{\Psi}_x^{(1)}(\nu) = \frac{1}{1 + q^{\gamma x^{1/3}(\nu - r)}} \int_{D_1} \frac{dw}{2\pi \mathrm{i} w} \left(\frac{d}{w}\right)^{\gamma x^{1/3}\nu} e^{x(g(d)-g(w))} \frac{(qd/w;q)_\infty}{(qw/d;q)_\infty} \frac{d}{w-d}. \tag{4.131}$$

As a contour D_1 we can simply take the contour D described in Proposition C.2.3. Since we can always deform the integration contour in a neighborhood of size $x^{-1/3}$ of ς, without loss of generality, we assume that d lies strictly at the left of D_1. With this choice, we know that D_1 is a steep ascent contour for $\mathfrak{Re}\{g\}$ and this, along with the fact that ς is double critical point for g implies the bound

$$|\exp\{x(g(d) - g(w))\}| < \text{const} \qquad \text{for all } w \in D_1.$$

Another consequence of the choice of contour D_1 is that

$$\max_{w \in D_1} |w| \le \frac{2a}{1+\sigma},$$

as reported in (C.8). This immediately gives us the estimate

$$\left|\frac{d}{w}\right|^{\gamma x^{1/3}\nu} \le \left|\frac{(1+\sigma)d}{2a}\right|^{\gamma x^{1/3}\nu} \qquad \text{for all } w \in D_1,$$

since in this case ν is taken to be negative. In expression (4.131), the contribution of the factor $d/(w - d)$ is bounded, in absolute value, by a quantity of order $x^{1/3}$ and therefore we come to write

$$|(4.131)| < \text{const}\frac{l(D_1)}{2\pi} x^{1/3} \left|\frac{(1+\sigma)}{2a} q^{-(1-r/L)} d\right|^{\gamma x^{1/3}\nu}. \tag{4.132}$$

When L is large enough, the assumption $2a/(1 + \sigma) < q^{-1}d$ of (4.60) guarantees that the right hand side of (4.132) is bounded by an exponential function in $\gamma x^{1/3}\nu$ whenever $\nu < -L$ and this concludes our analysis of the rear tail of the term $(i, j) = (2, 1)$.

To obtain the same type of result also for the case when $(i, j) = (2, 2)$ one can reproduce, with minor adjustments, the same argument we used for $(i, j) = (2, 1)$ and therefore we omit details on this part.

We have, at this point proved a bound for the summands in expression (4.67) of the form

$$\left| \sum_{\substack{i,j=1,2 \\ (i,j)\neq(1,1)}} \widetilde{f}(\nu)\widetilde{\Phi}_x^{(i)}(\nu)\widetilde{\Psi}_x^{(j)}(\nu) \right| < c_1 e^{c_2 \gamma x^{1/3} \nu} \qquad \text{for all } \nu < -L,$$

for suitably chosen positive constants c_1, c_2. This concludes our argument. □

We conclude this Section presenting the proof of Proposition 4.2.10.

Proof of Proposition 4.2.10. First we expand the expression in the left hand side of (4.70) as

$$\frac{d\!\!\!^-}{\gamma x^{1/3}} \widetilde{\sum_{\nu,\lambda_1,\lambda_2 \in \widetilde{\mathbb{Z}}}} \widetilde{f}(\nu)\widetilde{A}(\nu,\lambda_1)\widetilde{\varrho}(\lambda_1,\lambda_2)\widetilde{f}(\lambda_2)\widetilde{\Phi}_x(\lambda_2)\widetilde{\Psi}_x(\nu). \tag{4.133}$$

We can split the summation (4.133) as

$$\frac{d\!\!\!^-}{\gamma x^{1/3}} \left(\widetilde{\sum_{(\nu,\lambda_1,\lambda_2)\in[-L,x^{\delta/3}]^3}} + \widetilde{\sum_{\nu,\lambda_1,\lambda_2 \notin [-L,x^{\delta/3}]^3}} \right) \left(\widetilde{f}(\nu)\widetilde{A}(\nu,\lambda_1)\widetilde{\varrho}(\lambda_1,\lambda_2)\widetilde{f}(\lambda_2)\widetilde{\Phi}_x(\lambda_2)\widetilde{\Psi}_x(\nu) \right).$$

Using estimates already encountered in the proofs of Proposition 4.2.7, 4.2.9, we know that the contribution of summation where indices do not belong to $[-L, x^{\delta/3}]^3$ is exponentially small in some power of x. On the other hand, when all $\nu, \lambda_1, \lambda_2$ belong to $[-L, x^{\delta/3}]$, we can safely employ the saddle point method to estimate the summand terms in and obtain their expansion in power of $x^{-1/3}$, as done in (4.89) for $\widetilde{A}$. This would ultimately lead to the convergence result (4.70) and to a verification of properties (4.71), (4.72) for the remainder term. The procedure is analogous to what explained throughout the rest of the section and therefore we do not describe its details any further. □

Chapter 5

Spin Whittaker functions from $q \to 1$ limit

This chapter presents results contained in sections 7,8 and 9 of

[MP20] M. Mucciconi and L. Petrov. "Spin q-Whitaker polynomials and deformed quantum Toda". In: *arXiv preprint* (2020). arXiv:2003.14260 [math.PR]

5.1 Spin Whittaker functions

In this section we introduce new one-parameter deformations of the $\mathfrak{gl}_n$ Whittaker functions [Jac67], [Kos78]. These deformations arise from our version of spin q-Whittaker polynomials in a scaling limit as $q \to 1$. The deformation parameter is denoted by $S > 0$.

5.1.1 Whittaker functions

Before proceeding with deformations of Whittaker functions, let us recall the usual $\mathfrak{gl}_N$ Whittaker functions. These functions play a central role in representation theory and integrable systems [Kos80], [Eti99], [Giv97] as well as are related to several models of random polymers [OCo12], [Cor+14], [OSZ14], [BC14].

The $\mathfrak{gl}_N$ Whittaker functions $\psi_{\lambda_1,\dots,\lambda_N}(\underline{u}_N)$ are indexed[1] by N-tuples $\underline{u}_N = (u_{N,1}, \dots, u_{N,N}) \in \mathbb{R}^N$, depend on $\underline{\lambda} = (\lambda_1, \dots, \lambda_N) \in \mathbb{C}^N$, and may be defined through the recursion (following from the Givental integral representation [Giv97], cf. [Ger+06]):

$$\psi_{\lambda_1,\dots,\lambda_N}(\underline{u}_N) = \int_{\mathbb{R}^{N-1}} \psi_{\lambda_1,\dots,\lambda_{N-1}}(\underline{u}_{N-1})\, Q_{\lambda_N}^{N\to N-1}(\underline{u}_N, \underline{u}_{N-1}) \prod_{k=1}^{N-1} du_{N-1,k}, \tag{5.1}$$

[1] To match the historical notation for Whittaker functions, here and in the discussion of the spin Whittaker functions we place the "variables" into the subscript of a Whittaker function, and the "index" in the parentheses.

where

$$Q_{\lambda}^{N\to N-1}(\underline{u}_N,\underline{u}_{N-1}) = e^{\mathrm{i}\lambda\left(\sum_{i=1}^{N}u_{N,i}-\sum_{i=1}^{N-1}u_{N-1,i}\right)}\prod_{i=1}^{N-1}\exp\left\{-e^{u_{N-1,i}-u_{N,i}}-e^{u_{N,i+1}-u_{N-1,i}}\right\} \tag{5.2}$$

is known as the Baxter Q-operator. The function $\underline{\lambda}\mapsto\psi_{\underline{\lambda}}(\underline{u}_N)$ is an entire function of $\underline{\lambda}\in\mathbb{C}^N$ for all $\underline{u}_N\in\mathbb{R}^N$. For $N=1$, we have $\psi_\lambda(u)=e^{\mathrm{i}\lambda u}$. For $N=2$, the Whittaker functions can be expressed through the (single-variable) Bessel K function $K_v(z)=\frac{1}{2}\int_{-\infty}^{\infty}e^{xv}\exp\left(-\frac{z}{2}(e^x+e^{-x})\right)dx$.

For the Whittaker functions, $Q_{\lambda_N}^{N\to N-1}(\underline{u}_N,\underline{u}_{N-1})$ plays the role of a branching function like the single-variable sqW function $\mathbb{F}_{\nu/\mu}(x)$ (2.15) (here x plays the same role as λ_N, and ν,μ correspond to $\underline{u}_N,\underline{u}_{N-1}$). Note that the Whittaker functions are not indexed by ordered sequences of numbers $\underline{u}_N$. Rather, in the Baxter Q-operator, the interlacing condition among arrays $\underline{u}_{N-1},\underline{u}_N$ is replaced by the "mild interlacing". Namely, $Q^{N\to N-1}$ (5.2) decays doubly exponentially whenever $u_{N,i+1}>u_{N-1,i}$ or $u_{N-1,i}>u_{N,i}$.

The Whittaker functions satisfy the following analogue of the Cauchy identity due to Bump and Stade [Bum89], [Sta02], [GLO08]:

$$\int_{\mathbb{R}^N}e^{-e^{-u_{N,N}}}\overline{\psi_{\underline{\lambda}_N}(\underline{u}_N)}\psi_{\underline{\nu}_N}(\underline{u}_N)\prod_{j=1}^{N}du_{N,j}=\prod_{j,k=1}^{N}\Gamma(\mathrm{i}\nu_j-\mathrm{i}\lambda_k). \tag{5.3}$$

See also [Cor+14, (1.2)], [BC14, Section 4.2.1] for a generalization when one of the Whittaker functions is replaced by a certain integral coming from the limit of the torus product representation of Macdonald polynomials:

$$\theta_{\underline{Y}}(\underline{u}_N):=\int_{\mathbb{R}^N}\overline{\psi_{\underline{\nu}}(\underline{u}_N)}\prod_{i=1}^{T}\prod_{k=1}^{N}\Gamma(Y_i-\mathrm{i}\nu_k)\cdot\frac{1}{(2\pi)^N N!}\prod_{1\le A\ne B\le N}\frac{1}{\Gamma(\mathrm{i}\nu_A-\mathrm{i}\nu_B)}\,d\underline{\nu}, \tag{5.4}$$

where $\underline{Y}=(Y_1,\ldots,Y_T)\in\mathbb{R}^T$. We refer to $\theta_{\underline{Y}}(\underline{u}_N)$ as the *dual Whittaker function.*

Similar integral representations for dual spin Hall–Littlewood functions are found in [Bor17, Proposition 7.3], [BP18a, Section 7.3].

The Whittaker functions are eigenfunctions of the $\mathfrak{gl}_N$ quantum Toda Hamiltonian $\mathcal{H}_2^{\mathrm{Toda}}$, see formula (1.36) in the Introduction.

Convention on multiplicative notation. The papers [Cor+14], [OSZ14] use *multiplicative parameters* $U_{N,i}=e^{u_{N,i}}\in\mathbb{R}_{>0}$ instead of the additive ones. In multiplicative notation, the integration in (5.1) and (5.3) is over the product measures of the form $\prod\frac{dU_{m,i}}{U_{m,i}}$. It is convenient for us to adopt multiplicative notation throughout most of the discussion of the spin Whittaker functions. We will often denote multiplicative variables and parameters by capital letters.

5.1.2 Signatures in continuous space

In contrast with the usual Whittaker functions indexed by unordered N-tuples of reals, the spin Whittaker functions will be indexed by *nondecreasing* sequences of real numbers.

Introduce the *Weyl chamber* of $\mathbb{R}^N_{\geq 1}$ by

$$\mathcal{W}_N \coloneqq \{\underline{L}_N = (L_{N,i})_{1\leq i\leq N} \in \mathbb{R}^N_{\geq 1} \colon L_{N,N} \leq L_{N,N-1} \leq \ldots \leq L_{N,1}\}. \tag{5.5}$$

By $\mathring{\mathcal{W}}_N$ denote the interior of the Weyl chamber with strict inequalities in (5.5).

Given two sequences $\underline{L}_{N-1} \in \mathcal{W}_{N-1}$ and $\underline{L}_N \in \mathcal{W}_N$, we say that they *interlace* if

$$L_{N,i+1} \leq L_{N-1,i} \leq L_{N,i}, \qquad \text{for } 1 \leq i \leq N-1. \tag{5.6}$$

As in discrete setting, we denote interlacing by $\underline{L}_{N-1} \prec \underline{L}_N$. The interlacing relation is naturally extended to sequences of the same length by dropping the last inequality in (2.1).

We endow the Weyl chamber $\mathcal{W}_N$ with the measure $\frac{d\underline{L}_N}{\underline{L}_N} = \prod_{k=1}^N \frac{dL_{N,k}}{L_{N,k}}$. In most cases we do not explicitly indicate the integration domain $\mathcal{W}_N$ when the measure $\frac{d\underline{L}_N}{\underline{L}_N}$ is used.

Define the *continuous Gelfand-Tsetlin cone* as

$$\mathcal{GT}_N \coloneqq \{\underline{\underline{L}}_N = (L_{k,i})_{1\leq i\leq k\leq N} \in \mathbb{R}^{N(N+1)/2}_{\geq 1} \colon L_{k+1,i+1} \leq L_{k,i} \leq L_{k+1,i}\}, \tag{5.7}$$

which is the set of interlacing sequences $\underline{L}_1 \prec \cdots \prec \underline{L}_N$. The set $\mathcal{GT}_N$ is endowed with the measure $\frac{d\underline{\underline{L}}_N}{\underline{\underline{L}}_N} = \prod_{1\leq i\leq j\leq N} \frac{dL_{j,i}}{L_{j,i}}$.

5.1.3 Spin Whittaker functions

We begin with a branching function from which we can recursively build spin Whittaker functions. The branching function is an analogue of the skew polynomial evaluated at a single variable.

Fix a deformation parameter $S > 0$ throughout the section. Let us denote

$$\mathcal{A}_{S,X}(u,v,z) \coloneqq \frac{1}{\mathrm{B}(S+X,S-X)} \left(1-\frac{v}{z}\right)^{S-X-1} \left(1-\frac{u}{v}\right)^{S+X-1} \left(1-\frac{u}{z}\right)^{1-2S}, \tag{5.8}$$

where $1 \leq u < v < z$ are real, and $|X| < S$. Here $\mathrm{B}(\cdot,\cdot)$ is the beta function (A.21).

Definition 5.1.1. Let $|X| < S$ and $k \geq 1$. The *spin Whittaker branching functions* are given by

$$\mathfrak{f}_X(\underline{L}_k; \underline{L}_{k+1}) \coloneqq \mathbf{1}_{\underline{L}_k \prec \underline{L}_{k+1}} \left(\frac{L_{k+1,k+1}\cdots L_{k+1,1}}{L_{k,k}\cdots L_{k,1}}\right)^{-X} \prod_{i=1}^k \mathcal{A}_{S,X}(L_{k+1,i+1}, L_{k,i}, L_{k+1,i}).$$

We now introduce the main object of the present section.

Definition 5.1.2 (Spin Whittaker functions)**.** For $N \geq 1$, consider parameters $X_1, \ldots, X_N$ and S such that $|X_i| < S$ for all i. The *spin Whittaker functions* $\mathfrak{f}_{X_1,\ldots,X_N}(\underline{L}_N)$, $\underline{L}_N \in \mathcal{W}_N$, are defined recursively by

$$\mathfrak{f}_{X_1}(L_{1,1}) \coloneqq L_{1,1}^{-X_1} \tag{5.9}$$

for $N = 1$, and via the branching rule

$$\mathfrak{f}_{X_1,\dots,X_N}(\underline{L}_N) := \int_{\underline{L}_{N-1} \prec \underline{L}_N} \mathfrak{f}_{X_1,\dots,X_{N-1}}(\underline{L}_{N-1})\, \mathfrak{f}_{X_N}(\underline{L}_{N-1}; \underline{L}_N) \frac{d\underline{L}_{N-1}}{\underline{L}_{N-1}} \tag{5.10}$$

for $N \geq 2$.

Example 5.1.3 (Two-variable spin Whittaker function)**.** Let us compute the integral (5.10) for $N = 2$. Denote $\underline{X}_2 = (X, Y)$, $\underline{L}_2 = (u, u + \alpha)$, where $u \geq 1$, $\alpha > 0$. Then

$$\begin{aligned}
&\mathfrak{f}_{X,Y}(u, u+\alpha) \\
&\quad = \frac{(u(u+\alpha))^{-Y}}{\mathrm{B}(S+Y, S-Y)} \left(1 - \frac{u}{u+\alpha}\right)^{1-2S} \int_u^{u+\alpha} v^{Y-X-1} \left(1 - \frac{v}{u+\alpha}\right)^{S-Y-1} \left(1 - \frac{u}{v}\right)^{S+Y-1} dv \\
&\quad = \frac{u^{-Y}(u+\alpha)^S}{\mathrm{B}(S+Y, S-Y)} \int_0^1 (u + t\alpha)^{-X-S} (1-t)^{S-Y-1} t^{S+Y-1} dt,
\end{aligned}$$

where we changed the variable as $v = u + \alpha t$, $t \in [0, 1]$. The integral can now be evaluated using Euler's representation of the Gauss hypergeometric function ${}_2F_1$ (A.24). Let us also rename back $z = u + \alpha$. We have

$$\mathfrak{f}_{X,Y}(u, z) = (z/u)^S u^{-X-Y} {}_2F_1 \left(\begin{matrix} S+X, & S+Y \\ 2S & - \end{matrix} \middle| \, 1 - \frac{z}{u} \right). \tag{5.11}$$

When $|1 - z/u| \geq 1$, the hypergeometric function in (5.11) should be understood in the sense of analytic continuation.

We remark that most of the properties of the spin Whittaker functions given below in this section can be directly derived for $N = 2$ from known properties of the Gauss hypergeometric function ${}_2F_1$.

Proposition 5.1.4. *For $\underline{X}_N = (X_1, \dots, X_N)$ with $|X_i| < S$, the spin Whittaker function $\mathfrak{f}_{\underline{X}_N}(\underline{L}_N)$ is well-defined and continuous in $\underline{L}_N \in \mathcal{W}_N$.*

In particular, we can first define $\mathfrak{f}_{\underline{X}_N}(\underline{L}_N)$ for $\underline{L}_N \in \mathring{\mathcal{W}}_N$, and then extend to the whole Weyl chamber by continuity. (Note that $\mathcal{A}_{S,X}(u, v, z)$ (5.8) might have a singularity at $u = z$.) The proof of Proposition 5.1.4 is based on the next two lemmas.

Lemma 5.1.5. *Let $\ell_1 > 0$ and let $f(\cdot)$ be a left continuous function on $\mathbb{R}_{\geq 1}$. Then, we have*

$$\lim_{\ell_3 \to \ell_1^-} \int_{\ell_3}^{\ell_1} \frac{d\ell_2}{\ell_2} \mathcal{A}_{S,X}(\ell_3, \ell_2, \ell_1) f(\ell_2) = f(\ell_1). \tag{5.12}$$

Proof. To compute the limit set $\ell_3 = \ell_1 - \delta$ for a small positive δ. After a change of variable $\ell_2 = \ell_1 - \delta(1 - \ell_2')$, the integral in (5.12) becomes

$$\frac{1}{\mathrm{B}(S+X, S-X)} \int_0^1 d\ell_2' \left(\frac{\ell_1}{\ell_1 - \delta(1 - \ell_2')} \right)^{S+X} (1 - \ell_2')^{S-X-1} \ell_2'^{S+X-1} f(\ell_1 - \delta(1 - \ell_2')).$$

Using the left continuity of f, we see that the integrand converges to $(1-\ell_2')^{S-X-1} \ell_2'^{S+X-1} f(\ell_1)$ as $\delta \to 0$. The limiting integrand integrates to $\mathrm{B}(S+X, S-X)$, and so by the Dominated Convergence Theorem the lemma follows. □

Lemma 5.1.6. *Let $f : \mathcal{W}_{N-1} \to \mathbb{C}$ be left continuous in each of $L_{N-1,i}$. Define $F : \mathring{\mathcal{W}}_N \to \mathbb{C}$ as*

$$F(\underline{L}_N) = \int f(\underline{L}_{N-1})\, \mathfrak{f}_X(\underline{L}_{N-1}; \underline{L}_N) \frac{d\underline{L}_{N-1}}{\underline{L}_{N-1}}. \tag{5.13}$$

Then F is continuous and can be extended by continuity to $\mathcal{W}_N$.

Proof. For $\underline{L}_N \in \mathring{\mathcal{W}}_N$, the singularities of the integrand in (5.13) come only from the branching function $\mathfrak{f}_X(\underline{L}_{N-1}, \underline{L}_N)$ and they are of the form

$$\left(1 - \frac{L_{N-1,i}}{L_{N,i}}\right)^{S-X-1}, \qquad \text{or} \qquad \left(1 - \frac{L_{N,i+1}}{L_{N-1,i}}\right)^{S+X-1}$$

for some i. Because $|X| < S$ these singularities are summable. Therefore F, is continuous inside the interior $\mathring{\mathcal{W}}_N$ of the Weyl chamber.

To prove that F can be extended by continuity to $\mathcal{W}_N$ we first define, from small positive increments $\delta_1, \ldots, \delta_{N-1}$, the quantities $d_i = \delta_i + \cdots + \delta_{N-1}$ for each $i = 1, \ldots, N-1$. We aim to compute the limit

$$\lim_{\delta_1, \ldots, \delta_{N-1} \to 0} F(L_{N,N}, L_{N,N-1} + d_{N-1}, \ldots, L_{N,1} + d_1),$$

when some of the $L_{N,i}$'s are equal to each other. Before the limit, this function is equal to

$$\int_{L_{N,N}}^{L_{N,N-1}+\delta_{N-1}} \mathcal{A}_{S,X}(L_{N,N}, L_{N-1,N-1}, L_{N,N-1} + \delta_{N-1}) \frac{dL_{N-1,N-1}}{L_{N-1,N-1}}$$
$$\cdots \int_{L_{N,2}+d_2}^{L_{N,1}+d_2+\delta_1} \mathcal{A}_{S,X}(L_{N,2} + d_2, L_{N-1,1}, L_{N,1} + d_2 + \delta_1) \frac{dL_{N-1,1}}{L_{N-1,1}} f(\underline{L}_{N-1}) \left(\frac{\prod_{i=1}^{N-1} L_{N-1,i}}{\prod_{i=1}^{N} (L_{N,i} + d_i)}\right)^X.$$

For any i such that $L_{N,i} = L_{N,i+1}$, make the change of variables $L_{N-1,i} = L_{N,i} + d_{i+1} - \delta_i(1 - \ell_{N-1,i})$. As in the proof of Lemma 5.1.5, this removes all the corresponding singularities. Therefore, the limit as $\delta_1, \ldots, \delta_{N-1} \to 0$ exists, is finite, and can be computed using (5.12). □

Proof of Proposition 5.1.4. For $N = 1$ the spin Whittaker function (5.9) is clearly continuous. Therefore, by Lemma 5.1.6, $\mathfrak{f}_{X_1,X_2}(\underline{L}_2)$ is well defined and continuous on $\mathcal{W}_2$. Proceeding by induction on N, we get the result of Proposition 5.1.4. □

The next corollary gives a Givental type representation of the spin Whittaker functions, obtained by writing down explicitly the recursive definition (5.10).

Corollary 5.1.7. *We have*

$$\mathfrak{f}_{X_1,\ldots,X_N}(\underline{L}_N) = \int \prod_{1\le k\le N} \frac{\prod_{i=1}^{k-1} L_{k-1,i}^{X_k}}{\prod_{i=1}^{k} L_{k,i}^{X_k}} \prod_{1\le i\le k\le N-1} \mathcal{A}_{S,X_{k+1}}(L_{k+1,i+1}, L_{k,i}, L_{k+1,i}) \frac{d\underline{\underline{L}}_{N-1}}{\underline{\underline{L}}_{N-1}}. \tag{5.14}$$

Proof. Because the sequence of integrations as in (5.10) leading to $\mathfrak{f}_{\underline{X}_N}(\underline{L}_N)$ is (absolutely) convergent, so is the integration over the Gelfand-Tsetlin array $\mathcal{GT}_{N-1}$. The two integration procedures give the same result by the Fubini–Tonelli theorem. □

5.1.4 Dual Spin Whittaker functions

In this section we define a dual family of functions. Given interlacing sequences $\underline{\widetilde{L}}_k \prec \underline{L}_k$ of the same length k, introduce the *dual spin Whittaker branching functions*

$$\mathfrak{g}_Y(\underline{\widetilde{L}}_k; \underline{L}_k) := \mathbf{1}_{\underline{\widetilde{L}}_k \prec \underline{L}_k} \frac{1}{\Gamma(S-Y)} \left(\frac{\widetilde{L}_{k,k} \cdots \widetilde{L}_{k,1}}{L_{k,k} \cdots L_{k,1}} \right)^Y \left(1 - \frac{\widetilde{L}_{k,1}}{L_{k,1}}\right)^{S-Y-1} \times \prod_{i=2}^{k} \mathcal{A}_{S,-Y}(\widetilde{L}_{k,i}, L_{k,i}, \widetilde{L}_{k,i-1}). \tag{5.15}$$

For pairs of interlacing sequences $\underline{L}_{k-1} \prec \underline{L}_k$, $k \geq 1$, of different lengths, set

$$\mathfrak{g}_Y(\underline{L}_{k-1}; \underline{L}_k) := \mathfrak{g}_Y((1, \underline{L}_{k-1}); \underline{L}_k).$$

Remark 5.1.8. One can also write $\mathfrak{g}_Y$ as

$$\mathfrak{g}_Y(\underline{\widetilde{L}}_k; \underline{L}_k) = \frac{L_{k,1}^{-Y}}{\Gamma(S-Y)} \left(1 - \frac{\widetilde{L}_{k,1}}{L_{k,1}}\right)^{S-Y-1} \mathfrak{f}_{-Y}(\underline{\ell}_{k-1}; \underline{\widetilde{L}}_k), \tag{5.16}$$

where $\underline{L}_k = (\underline{\ell}_{k-1}, L_{k,1})$.

Definition 5.1.9. Let $N \leq M$ and consider parameters $Y_1, \ldots, Y_M$ such that $|Y_i| < S$ for all i. The *dual spin Whittaker functions* are defined recursively by

$$\mathfrak{g}_{Y_1,\ldots,Y_M}(\underline{L}_N) = \begin{cases} \displaystyle\int \mathfrak{g}_{Y_1,\ldots,Y_{M-1}}(\underline{\widetilde{L}}_N) \mathfrak{g}_{Y_M}(\underline{\widetilde{L}}_N; \underline{L}_N) \frac{d\underline{\widetilde{L}}_N}{\underline{\widetilde{L}}_N} & \text{if } N < M, \\ \displaystyle\int \mathfrak{g}_{Y_1,\ldots,Y_{N-1}}(\underline{\widetilde{L}}_{N-1}) \mathfrak{g}_{Y_N}(\underline{\widetilde{L}}_{N-1}; \underline{L}_N) \frac{d\underline{\widetilde{L}}_{N-1}}{\underline{\widetilde{L}}_{N-1}} & \text{if } N = M. \end{cases} \tag{5.17}$$

In particular, for $M = N = 1$ we have

$$\mathfrak{g}_Y(L) = \mathfrak{g}_Y(1; L) = \frac{L^{-Y}(1 - L^{-1})^{S-Y-1}}{\Gamma(S-Y)}.$$

The next two propositions explain that $\mathfrak{g}_{Y_1,\ldots,Y_M}$ are well-defined as elements of the "dual" space of compactly supported continuous functions on the Weyl chamber $\mathcal{W}_N$.

Proposition 5.1.10. *Let $f(\underline{L}_N)$ be a compactly supported continuous function on $\mathcal{W}_N$. Then the function*

$$\underline{\widetilde{L}}_N \mapsto \int \mathfrak{g}_Y(\underline{\widetilde{L}}_N; \underline{L}_N) f(\underline{L}_N) \frac{d\underline{L}_N}{\underline{L}_N}, \tag{5.18}$$

is also compactly supported and continuous.

Proof. We evaluate the integral (5.18) using expression (5.16) for $\mathfrak{g}_Y$ as

$$\int \frac{dL_{N,1}}{L_{N,1}^{1+Y}} \frac{1}{\Gamma(S-Y)} \left(1 - \frac{\widetilde{L}_{N,1}}{L_{N,1}}\right)^{S-Y-1} \int f(\underline{\ell}_{N-1}, L_{N,1}) \frac{d\underline{\ell}_{N-1}}{\underline{\ell}_{N-1}} \mathfrak{f}_{-Y}(\underline{\ell}_{N-1}; \widetilde{\underline{L}}_k).$$

By Lemma 5.1.6, the integral in the variables $\underline{\ell}_{N-1}$ defines a family of continuous bounded functions in $\widetilde{\underline{L}}_N$, depending on $L_{N,1}$. The (improper) integral in $L_{N,1}$ is convergent both at $\widetilde{L}_{N,1}$ and ∞ (the latter because f vanishes for $L_{N,1}$ large enough). This proves the claim. □

Proposition 5.1.11. *Let $f(\underline{L}_N)$ be a compactly supported continuous function. Then the integral*

$$\int \mathfrak{g}_{Y_1,\dots,Y_M}(\underline{L}_N) f(\underline{L}_N) \frac{d\underline{L}_N}{\underline{L}_N}$$

is absolutely convergent.

Proof. This follows from Proposition 5.1.10 applied recursively after expanding $\mathfrak{g}_{Y_1,\dots,Y_M}$ using the branching rules (5.17). □

5.1.5 Convergence of the sqW functions as $q \to 1$

Here and in the following subsection we establish that the spin Whittaker functions $\mathfrak{f}_{\underline{X}}(\underline{L}_N)$ and $\mathfrak{g}_{\underline{Y}}(\underline{L}_N)$ are scaling limits, as $q \to 1$, of the spin q-Whittaker functions $\mathbb{F}_\lambda(x_1, \dots, x_N)$ and $\mathbb{F}^*_\mu(y_1, \dots, y_k)$, respectively. Recall that they also depend on two parameters, $q \in (0,1)$ and $s \in (-1, 0)$.

First, this subsection we deal with the non-dual functions. Let us fix a scaling of all parameters.

Definition 5.1.12 (Scaling)**.** We consider the following renormalization of parameters:

$$x_i = q^{X_i}, \qquad s = -q^S, \qquad \lambda^i_j = \left\lfloor \log_q(1/L_{i,j}) \right\rfloor. \tag{5.19}$$

We will assume throughout that

$$S > 0, \qquad |X_i| < S, \qquad \text{and} \qquad 1 \le L_{i+1,j+1} \le L_{i,j} \le L_{i+1,j}$$

for all i, j. Therefore, the pre-limit quantities in (5.19) satisfy $s \in (0,1)$, $x_i \in (-s, -s^{-1})$, and $0 \le \lambda^{i+1}_{j+1} \le \lambda^i_j \le \lambda^{i+1}_j$.

For any triple of real numbers $1 \le \ell_3 \le \ell_2 \le \ell_1$, set $n_i := \left\lfloor \log_q(1/\ell_i) \right\rfloor$ (so $0 \le n_3 \le n_2 \le n_1$).

Lemma 5.1.13. *With the above notation, for any function $f : \mathbb{Z} \to \mathbb{R}$ we have*

$$\sum_{n_2=n_3}^{n_1} f(n_2) = \int_{\ell_3}^{\ell_1} \frac{1}{\Delta_q(\ell_3, \ell_2, \ell_1)} f(\left\lfloor \log_q(1/\ell_2) \right\rfloor) \frac{d\ell_2}{\ell_2}, \tag{5.20}$$

where

$$\Delta_q(\ell_3, \ell_2, \ell_1) := \int_{\max(\ell_3, q^{-n_2})}^{\min(\ell_1, q^{-n_2-1})} \frac{d\ell_2'}{\ell_2'} = \begin{cases} -\log q & \textit{if } n_3 < n_2 < n_1; \\ \log(q^{n_1}\ell_1) & \textit{if } n_3 < n_2 = n_1; \\ -\log(q^{n_3+1}\ell_3) & \textit{if } n_3 = n_2 < n_1; \\ \log(\ell_1/\ell_3) & \textit{if } n_3 = n_2 = n_1. \end{cases} \tag{5.21}$$

When $\ell_3 = \ell_1$, the integral in (5.20) is understood in the limiting sense.

Proof. This follows by observing that Δ_q is the measure of intervals where the function $\ell_2 \mapsto \lfloor \log_q(1/\ell_2) \rfloor$ is constant, and simultaneously ℓ_2 lies in the interval $[\ell_3, \ell_1]$. □

The rescaled spin q-Whittaker functions are defined recursively as

$$\begin{aligned} \mathfrak{f}^{(q)}_{X_N}(\underline{L}_{N-1}; \underline{L}_N) &= \prod_{k=1}^{N-1} \frac{1}{\Delta_q(L_{N,k+1}, L_{N-1,k}, L_{N,k})} \mathbb{F}_{\lambda^N/\lambda^{N-1}}(x_N) \Big|_{\text{scaling (5.19)}}; \\ \mathfrak{f}^{(q)}_{X_1}(L_{1,1}) &= x_1^{\lambda_1^1} \Big|_{\text{scaling (5.19)}} = q^{X_1 \lfloor \log_q(1/L_{1,1}) \rfloor}; \\ \mathfrak{f}^{(q)}_{X_1,\dots,X_N}(\underline{L}_N) &= \int \mathfrak{f}^{(q)}_{X_1,\dots,X_{N-1}}(\underline{L}_{N-1})\, \mathfrak{f}^{(q)}_{X_N}(\underline{L}_{N-1}; \underline{L}_N) \frac{d\underline{L}_{N-1}}{\underline{L}_{N-1}}, \end{aligned}$$

The next theorem is the main result of this subsection:

Theorem 5.1.14. *We have*

$$\lim_{q \to 1} \mathfrak{f}^{(q)}_{X_1,\dots,X_N} = \mathfrak{f}_{X_1,\dots,X_N}, \tag{5.22}$$

uniformly on any compact subset of $\mathcal{W}_N$.

Pointwise convergence in (5.22) is a consequence of a simpler result stated in Lemma 2.2 of [BC16a] (reproduced as Lemma 5.1.25 in Section 5.1.9):

$$\lim_{q \to 1} \frac{(\ell q^A; q)_\infty}{(\ell q^B; q)_\infty} = (1 - \ell)^{B-A}, \tag{5.23}$$

for any $\ell \in (0, 1)$ and $A, B > 0$.

By (5.23) and through a repeated use of the identity

$$\frac{(q^a; q)_n}{(q^b; q)_n} = \mathbf{1}_{n=0} + \mathbf{1}_{n \geq 1} \frac{\Gamma_q(b)}{\Gamma_q(a)} (1 - q)^{b-a} \frac{(q^{b+n}; q)_\infty}{(q^{a+n}; q)_\infty}, \tag{5.24}$$

where Γ_q is the q-Gamma function (A.15), one readily gets the pointwise convergence of the branching function $\mathfrak{f}^{(q)}_X(\underline{L}_{N-1}; \underline{L}_N)$ to $\mathfrak{f}_X(\underline{L}_{N-1}; \underline{L}_N)$. Nevertheless, for the finer uniform convergence result of Theorem 5.1.14, a slightly more accurate analysis of ratios of q-Pochhammer symbols appearing in the sqW functions is required. We postpone this technical discussion to Section 5.1.9. Let us summarize the main technical result proven in Section 5.1.9:

Proposition 5.1.15. *Let $f(\underline{L}_{N-1})$ be a continuous function on $\mathcal{W}_{N-1}$. Then for any $\underline{L}_N \in \mathcal{W}_N$ we have*

$$\lim_{q\to 1}\int f(\underline{L}_{N-1})\,\mathfrak{f}_X^{(q)}(\underline{L}_{N-1};\underline{L}_N)\frac{d\underline{L}_{N-1}}{\underline{L}_{N-1}} = \int f(\underline{L}_{N-1})\,\mathfrak{f}_X(\underline{L}_{N-1};\underline{L}_N)\frac{d\underline{L}_{N-1}}{\underline{L}_{N-1}}, \tag{5.25}$$

and the convergence is uniform on compact subsets of $\mathcal{W}_N$.

The continuous function f in Proposition 5.1.15 can also be replaced by a uniformly converging sequence:

Corollary 5.1.16. *Let $f^{(q)}(\underline{L}_{N-1})$ be a sequence uniformly convergent as $q \to 1$ on compact subsets of $\mathcal{W}_{N-1}$ to a continuous function $f(\underline{L}_{N-1})$. Then*

$$\lim_{q\to 1}\int f^{(q)}(\underline{L}_{N-1})\,\mathfrak{f}_X^{(q)}(\underline{L}_{N-1};\underline{L}_N)\,\frac{d\underline{L}_{N-1}}{\underline{L}_{N-1}} = \int f(\underline{L}_{N-1})\,\mathfrak{f}_X(\underline{L}_{N-1};\underline{L}_N)\,\frac{d\underline{L}_{N-1}}{\underline{L}_{N-1}}$$

and the convergence is uniform on compact subsets of $\mathcal{W}_N$.

Proof. This follows from Proposition 5.1.15 and the fact that for fixed $\underline{L}_N \in \mathcal{W}_N$, the functions $\underline{L}_{N-1} \mapsto \mathfrak{f}_X^{(q)}(\underline{L}_{N-1};\underline{L}_N)$ and $\underline{L}_{N-1} \mapsto \mathfrak{f}_X(\underline{L}_{N-1};\underline{L}_N)$ are compactly supported on $\mathcal{W}_{N-1}$. □

Proof of Theorem 5.1.14. For $N = 1$ we have

$$\mathfrak{f}_{X_1}^{(q)}(L) = q^{X_1\lfloor \log_q(1/L)\rfloor} \xrightarrow[q\to 1]{} L^{-X_1} = \mathfrak{f}_{X_1}(L),$$

uniformly with respect to $L \geq 1$ varying in any compact domain. Corollary 5.1.16 then implies Theorem 5.1.14 by induction on N. □

5.1.6 Convergence of the dual sqW functions as $q \to 1$

We now establish the convergence of functions $\mathbb{F}^*$ to the dual spin Whittaker functions $\mathfrak{g}$. The scaling of parameters we adopt is that of Definition 5.1.12. For consistency with the previous sections, dual functions will depend on y variables for which the scaling is

$$y_i = q^{Y_i}, \qquad |Y_i| < S. \tag{5.26}$$

For two interlacing arrays $\underline{\widetilde{L}}_k \prec \underline{L}_k$ define the rescaled dual spin Whittaker branching functions

$$\mathfrak{g}_{Y_k}^{(q)}(\underline{\widetilde{L}}_k;\underline{L}_k) = (1-q)^{S-Y_k}\left(\prod_{j=1}^{k}\frac{1}{\Delta_q(\widetilde{L}_{k,j},L_{k,j},\widetilde{L}_{k,j-1})}\right)\mathbb{F}^*_{\lambda^k/\widetilde{\lambda}^k}(y_k)\Big|_{\text{scaling (5.19),(5.26)}}, \tag{5.27}$$

where, by agreement, $\widetilde{L}_{k,0} = \infty$, and Δ_q is given by (5.21). In particular, the rescaled one-variable function is (assuming $L > 1$ and q close enough to 1)

$$\mathfrak{g}_Y^{(q)}(L) = \mathfrak{g}_Y^{(q)}(1;L) = (1-q)^{S-Y}\frac{1}{(-\log q)}\frac{(q^{S-Y};q)_{\lfloor \log_q(1/L)\rfloor}}{(q;q)_{\lfloor \log_q(1/L)\rfloor}}\,q^{Y\lfloor \log_q(1/L)\rfloor}.$$

For interlacing arrays of different lengths $\underline{L}_{k-1} \prec \underline{L}_k$, we set $\mathfrak{g}^{(q)}_Y(\underline{L}_{k-1};\underline{L}_k) = \mathfrak{g}^{(q)}_Y((1,\underline{L}_{k-1});\underline{L}_k)$, as before. Define the rescaled dual spin q-Whittaker functions recursively as

$$\mathfrak{g}^{(q)}_{Y_1,\dots,Y_M}(\underline{L}_N) = \begin{cases} \displaystyle\int \mathfrak{g}^{(q)}_{Y_1,\dots,Y_{M-1}}(\widetilde{\underline{L}}_N)\mathfrak{g}^{(q)}_{Y_M}(\widetilde{\underline{L}}_N;\underline{L}_N)\frac{d\widetilde{\underline{L}}_N}{\widetilde{\underline{L}}_N} & \text{if } N < M, \\ \displaystyle\int \mathfrak{g}^{(q)}_{Y_1,\dots,Y_{N-1}}(\widetilde{\underline{L}}_{N-1})\mathfrak{g}^{(q)}_{Y_N}(\widetilde{\underline{L}}_{N-1};\underline{L}_N)\frac{d\widetilde{\underline{L}}_{N-1}}{\widetilde{\underline{L}}_{N-1}} & \text{if } N = M. \end{cases}$$

The next result establishes a weak convergence of rescaled branching functions $\mathfrak{g}^{(q)}$.

Theorem 5.1.17. *Let $f(\underline{L}_N)$ be a compactly supported continuous function on $\mathcal{W}_N$. Then*

$$\lim_{q\to 1}\int \mathfrak{g}^{(q)}_Y(\widetilde{\underline{L}}_N;\underline{L}_N)f(\underline{L}_N)\,\frac{d\underline{L}_N}{\underline{L}_N} = \int \mathfrak{g}_Y(\widetilde{\underline{L}}_N;\underline{L}_N)f(\underline{L}_N)\,\frac{d\underline{L}_N}{\underline{L}_N}, \tag{5.28}$$

and the convergence is uniform with respect to $\widetilde{\underline{L}}_N$.

Proof. We start by rewriting the branching function $\mathfrak{g}^{(q)}_Y(\widetilde{\underline{L}}_N;\underline{L}_N)$ as (this follows from straightforward algebraic manipulations with (5.27))

$$q^{Y\lambda_1^k}\frac{(q^{S-Y};q)_{\lambda_1^k-\tilde{\lambda}_1^k}}{(q;q)_{\lambda_1^k-\tilde{\lambda}_1^k}}\frac{(1-q)^{S-Y}}{\Delta_q(\widetilde{L}_{k,1},L_{k,1},\infty)}\,\mathfrak{f}^{(q)}_{-Y}(\underline{\ell}_{k-1};\widetilde{\underline{L}}_k).$$

The integral in the left-hand side of (5.28) becomes

$$\int\frac{dL_{k,1}}{L^1_{k,1}}\left(q^{Y\lambda_1^k}\frac{(q^{S-Y};q)_{\lambda_1^k-\tilde{\lambda}_1^k}}{(q;q)_{\lambda_1^k-\tilde{\lambda}_1^k}}\frac{(1-q)^{S-Y}}{\Delta_q(\widetilde{L}_{k,1},L_{k,1},\infty)}\right)\int\frac{d\underline{\ell}_{k-1}}{\underline{\ell}_{k-1}}\,\mathfrak{f}^{(q)}_{-Y}(\underline{\ell}_{k-1};\widetilde{\underline{L}}_k)f(\underline{\ell}_{k-1},L_{k,1}). \tag{5.29}$$

The inner integral involving the function $\mathfrak{f}^{(q)}_{-Y}$ is uniformly (with respect to $\widetilde{\underline{L}}_k$) convergent to

$$\int\frac{d\underline{\ell}_{k-1}}{\underline{\ell}_{k-1}}\,\mathfrak{f}_{-Y}(\underline{\ell}_{k-1};\widetilde{\underline{L}}_k)f(\underline{\ell}_{k-1},L_{k,1})$$

by virtue of Proposition 5.1.15. On the other hand, the term inside the parentheses in (5.29) is uniformly convergent to

$$\frac{L_{k,1}^{-Y}}{\Gamma(S-Y)}\left(1-\widetilde{L}_{k,1}/L_{k,1}\right)^{S-Y-1},$$

when $L_{k,1}$ is kept away from $\widetilde{L}_{k,1}$. Moreover, the term inside the parentheses is absolutely bounded by const $\times\ (1-\widetilde{L}_{k,1}/L_{k,1})^{S-Y-1}$ when $L_{k,1}$ approaches $\widetilde{L}_{k,1}$, thanks to Lemma 5.1.26. Since the resulting term after the $q\to 1$ limit coincides with the expression (5.16) for the dual branching function $\mathfrak{g}_Y(\widetilde{\underline{L}}_N;\underline{L}_N)$, we are done. ◻

Similarly to Corollary 5.1.16, we can let the test function f depend on q:

Corollary 5.1.18. *Let $f^{(q)}(\underline{L}_N)$ converge, as $q \to 1$, to a compactly supported continuous function $f(\underline{L}_N)$, uniformly on $\mathcal{W}_N$. Then*

$$\lim_{q\to 1} \int \mathfrak{g}_Y^{(q)}(\underline{\widetilde{L}}_N; \underline{L}_N) f^{(q)}(\underline{L}_N) \frac{d\underline{L}_N}{\underline{L}_N} = \int \mathfrak{g}_Y(\underline{\widetilde{L}}_N; \underline{L}_N) f(\underline{L}_N) \frac{d\underline{L}_N}{\underline{L}_N}$$

and the convergence is uniform with respect to $\underline{\widetilde{L}}_N$.

5.1.7 Properties of the spin Whittaker functions

In this subsection we describe the properties of the spin Whittaker functions which follow in the $q \to 1$ limit from the corresponding properties of the spin q-Whittaker functions.

Proposition 5.1.19 (Symmetry and shifting)**.** *The spin Whittaker function $\mathfrak{f}_{X_1,\dots,X_N}(\underline{L}_N)$ is symmetric in the X_i's for all $\underline{L}_N \in \mathcal{W}_N$. They also satisfy the shifting property:*

$$\mathfrak{f}_{X_1,\dots,X_N}(a\underline{L}_N) = a^{-X_1-\dots-X_N} \mathfrak{f}_{X_1,\dots,X_N}(\underline{L}_N), \qquad a > 1.$$

Proof. The symmetry follows from the corresponding symmetry of the sqW polynomial $\mathbb{F}_\lambda(x_1, \dots, x_N)$, which ultimately is a consequence of the Yang–Baxter equation. The shifting property can either be deduced from Proposition 2.3.7, or obtained in a similar way by noting that the branching spin Whittaker functions themselves satisfy $\mathfrak{f}_X(a\underline{L}_k; a\underline{L}_k) = a^{-X} \mathfrak{f}_X(\underline{L}_k; \underline{L}_k)$. □

We now turn to Cauchy type identities for the spin Whittaker functions.

Theorem 5.1.20 (Skew Cauchy type identity)**.** *Assume $|X|, |Y| < S$ and $X + Y > 0$. Then, for any $\underline{L}_{N-1}, \underline{\widetilde{L}}_N$ we have*

$$\int \mathfrak{f}_X(\underline{L}_{N-1}; \underline{L}_N) \mathfrak{g}_Y(\underline{\widetilde{L}}_N; \underline{L}_N) \frac{d\underline{L}_N}{\underline{L}_N} = \frac{\Gamma(X+Y)\Gamma(2S)}{\Gamma(S+X)\Gamma(S+Y)} \int \mathfrak{f}_X(\underline{\widetilde{L}}_{N-1}; \underline{\widetilde{L}}_N) \mathfrak{g}_Y(\underline{\widetilde{L}}_{N-1}; \underline{L}_{N-1}) \frac{d\underline{\widetilde{L}}_{N-1}}{\underline{\widetilde{L}}_{N-1}} \quad (5.30)$$

and, when $N = 1$ we have

$$\int \mathfrak{f}_X(L_{1,1}) \mathfrak{g}_Y(\widetilde{L}_{1,1}; L_{1,1}) \frac{dL_{1,1}}{L_{1,1}} = \frac{\Gamma(X+Y)}{\Gamma(S+X)} \mathfrak{f}_X(\widetilde{L}_{1,1}). \quad (5.31)$$

Proof. We first observe that (5.31) is equivalent to the integral representation of $\mathrm{B}(S - Y, X + Y)$.

In order to prove the general case (5.30) we use Corollaries 5.1.16 and 5.1.18. Take a compactly supported continuous test function $\phi(\underline{L}_{N-1})$, and set

$$\Phi_{\mathfrak{f}}(\underline{L}_N) := \int \phi(\underline{L}_{N-1}) \mathfrak{f}_X(\underline{L}_{N-1}; \underline{L}_N) \frac{d\underline{L}_{N-1}}{\underline{L}_{N-1}}, \quad \Phi_{\mathfrak{g}}(\underline{\widetilde{L}}_{N-1}) := \int \mathfrak{g}_Y(\underline{\widetilde{L}}_{N-1}; \underline{L}_{N-1}) \phi(\underline{L}_{N-1}) \frac{d\underline{L}_{N-1}}{\underline{L}_{N-1}}.$$

Analogously define $\Phi_{\mathfrak{f}}^{(q)}$ and $\Phi_{\mathfrak{g}}^{(q)}$ by substituting respectively $\mathfrak{f}_X$ and $\mathfrak{g}_Y$ with $\mathfrak{f}_X^{(q)}$ and $\mathfrak{g}_Y^{(q)}$ in the above formulas. It follows from the skew Cauchy Identity for sqW functions (theorem 2.3.15) that

$$\int \Phi_{\mathfrak{f}}^{(q)}(\underline{L}_N)\mathfrak{g}_Y^{(q)}(\underline{\widetilde{L}}_N;\underline{L}_N)\frac{d\underline{L}_N}{\underline{L}_N} = \frac{\Gamma_q(X+Y)\Gamma_q(2S)}{\Gamma_q(S+X)\Gamma_q(S+Y)}\int \mathfrak{f}_X^{(q)}(\underline{\widetilde{L}}_{N-1};\underline{\widetilde{L}}_N)\Phi_{\mathfrak{g}}^{(q)}(\underline{\widetilde{L}}_{N-1})\frac{d\underline{\widetilde{L}}_{N-1}}{\underline{\widetilde{L}}_{N-1}}. \tag{5.32}$$

By Corollary 5.1.18 we have $\Phi_{\mathfrak{g}}^{(q)} \to \Phi_{\mathfrak{g}}$ uniformly, and further $\Phi_{\mathfrak{g}}$ is compactly supported and continuous by Proposition 5.1.10. This implies, by Corollary 5.1.16, that the right-hand side of (5.32) converges to

$$\frac{\Gamma(X+Y)\Gamma(2S)}{\Gamma(S+X)\Gamma(S+Y)}\int \mathfrak{f}_X(\underline{\widetilde{L}}_{N-1};\underline{\widetilde{L}}_N)\Phi_{\mathfrak{g}}(\underline{\widetilde{L}}_{N-1})\frac{d\underline{\widetilde{L}}_{N-1}}{\underline{\widetilde{L}}_{N-1}}.$$

The integral in the left-hand side of (5.32) is absolutely convergent when $X+Y>0$. Since $\Phi_{\mathfrak{f}}^{(q)} \to \Phi_{\mathfrak{f}}$ uniformly by Proposition 5.1.15, Corollary 5.1.18 implies that the left-hand side of (5.32) converges to

$$\int \Phi_{\mathfrak{f}}(\underline{L}_N)\mathfrak{g}_Y(\underline{\widetilde{L}}_N;\underline{L}_N)\frac{d\underline{L}_N}{\underline{L}_N}.$$

Since the function ϕ was arbitrary, equality (5.30) follows. □

Corollary 5.1.21 (Full Cauchy type identity)**.** *Let $N \le M$ and $|X_i|, |Y_j| < S$, $X_i+Y_j>0$ for all i,j. We have*

$$\int \mathfrak{f}_{X_1,\dots,X_N}(\underline{L}_N)\,\mathfrak{g}_{Y_1,\dots,Y_M}(\underline{L}_N)\,\frac{d\underline{L}_N}{\underline{L}_N} = \prod_{j=1}^{M}\frac{\Gamma(X_1+Y_j)}{\Gamma(S+X_1)}\left(\prod_{i=2}^{N}\frac{\Gamma(X_i+Y_j)\Gamma(2S)}{\Gamma(S+X_i)\Gamma(S+Y_j)}\right). \tag{5.33}$$

Proof. Immediately follows from Theorem 5.1.20 and the branching rules for the functions $\mathfrak{f},\mathfrak{g}$. □

We also have an identity involving a single spin Whittaker function:

Proposition 5.1.22. *Let $|X_i| < S$. Then we have*

$$\int_{L_{N,N}=1}\mathfrak{f}_{X_1,\dots,X_N}(\underline{L}_N)\prod_{j=1}^{N-1}\left(1-\frac{L_{N,j+1}}{L_{N,j}}\right)^{2S-1}\frac{dL_{N,j}}{L_{N,j}^{1+S}} = \frac{\Gamma(S+X_1)\cdots\Gamma(S+X_N)}{\Gamma(SN+X_1+\cdots+X_N)}.$$

Proof. This is a scaling limit of Proposition 2.3.9. □

We now consider the scaling limits of eigenrelations for the sqW functions stated in Theorems 2.6.11 and 2.6.12. This produces two operators acting in the X_i variables which are diagonal in the spin Whittaker functions. For the next definition we use the shift operator

$$\mathcal{T}_X f(X) := f(X+1). \tag{5.34}$$

Definition 5.1.23. For any $N \geq 1$ set

$$\mathcal{D}_1 := \sum_{i=1}^{N} \prod_{\substack{j=1 \\ j \neq i}}^{N} \frac{X_i + S}{X_i - X_j} \mathcal{T}_{X_i}, \qquad \overline{\mathcal{D}}_1 := \sum_{i=1}^{N} \prod_{\substack{j=1 \\ j \neq i}}^{N} \frac{X_i - S}{X_i - X_j} \mathcal{T}_{X_i}^{-1}.$$

The next proposition represents a partial generalization of eigenrelations satisfied by Whittaker functions (e.g., see [KL01]).

Proposition 5.1.24 (Eigenrelations for spin Whittaker functions)**.** *We have*

$$\mathcal{D}_1 \mathfrak{f}_{X_1,\dots,X_N}(\underline{L}_N) = L_{N,N}^{-1} \mathfrak{f}_{X_1,\dots,X_N}(\underline{L}_N),$$
$$\overline{\mathcal{D}}_1 \mathfrak{f}_{X_1,\dots,X_N}(\underline{L}_N) = L_{N,1} \mathfrak{f}_{X_1,\dots,X_N}(\underline{L}_N).$$

Proof. We easily see that operators $\mathcal{D}_1, \overline{\mathcal{D}}_1$ are limiting forms of $\mathfrak{D}_1, \overline{\mathfrak{D}}_1$ (Definition 2.6.9) under the scaling (5.19). At the same time we have $q^{\lambda_N} \to L_{N,N}^{-1}$ and $q^{-\lambda_1} \to L_{N,1}$ under the same scaling. Therefore, (2.87), (2.91) and convergence (5.22) imply the claimed eigenrelation. □

5.1.8 Formal reduction to the usual Whittaker functions

Just like the sqW polynomials reduce to the q-Whittaker polynomials setting $s = 0$, it should be possible to prove that, under the correct scaling, our spin Whittaker functions converge to the Whittaker functions. An evidence for this is suggested by the following computation.

Set

$$L_{k,i} = S^{k+1-2i} e^{u_{k,i}}, \qquad X_k = -\mathrm{i}\lambda_k, \tag{5.35}$$

then, in the limit $S \to \infty$ we have

$$\begin{aligned}
\left(\frac{L_{k,k} \cdots L_{k,1}}{L_{k+1,k+1} \cdots L_{k+1,1}}\right)^{X_{k+1}} &\longrightarrow \exp\left\{\mathrm{i}\lambda_k \left(\sum_{i=1}^{k+1} u_{k+1,i} - \sum_{i=1}^{k} u_{k,i}\right)\right\}; \\
\left(1 - \frac{L_{k,i}}{L_{k+1,i}}\right)^{S - X_{k+1} - 1} &\longrightarrow \exp\left\{-e^{u_{k,i} - u_{k+1,i}}\right\}; \\
\left(1 - \frac{L_{k+1,i+1}}{L_{k,i}}\right)^{S + X_{k+1} - 1} &\longrightarrow \exp\left\{-e^{u_{k+1,i+1} - u_{k,i}}\right\}; \\
\left(1 - \frac{L_{k+1,i+1}}{L_{k+1,i}}\right)^{1-2S} &\longrightarrow 1; \\
4^S S^{\frac{1}{2}} \,\mathrm{B}(S + X, S - X) &\longrightarrow 2\sqrt{\pi}.
\end{aligned} \tag{5.36}$$

All the limits in (5.36) are straightforward (note that the last one requires the Stirling approximation). Thus, the branching function $\mathfrak{f}$, rescaled by a factor depending solely on S, converges locally uniformly to the Baxter Q-operator $Q^{N\to N-1}$ (5.2) for the usual Whittaker functions:

$$\left(\frac{4\pi}{S16^S}\right)^{\frac{N-1}{2}} \mathfrak{f}_{X_N}(\underline{L}_{N-1};\underline{L}_N) \xrightarrow[S\to\infty]{\text{scaling (5.35)}} Q^{N\to N-1}_{\lambda_N}(\underline{u}_N,\underline{u}_{N-1}).$$

These computations suggest that the same type of convergence should hold for the full functions. Namely, under (5.35) and as $S\to+\infty$, the spin Whittaker functions $\mathfrak{f}_{\underline{X}_N}(\underline{L}_N)$ rescaled by $(4S^{-1}\pi/16^S)^{\frac{N(N-1)}{4}}$ should converge to the usual Whittaker functions $\psi_{\underline{\lambda}_N}(\underline{u}_N)$. A proof of this convergence would require a finer analysis to justify the exchange of the $S\to+\infty$ limit and integration, and goes beyond the scope of this thesis.

5.1.9 Proof of Proposition 5.1.15

Lemma 5.1.25 ([BC16a], Lemma 2.2)**.** *Let $A,B>0$. Then*

$$\lim_{q\to 1}\frac{(\ell q^A;q)_\infty}{(\ell q^B;q)_\infty}=(1-\ell)^{B-A}, \tag{5.37}$$

uniformly in ℓ belonging to any compact subset of $(0,1)$.

Note that the uniformity in ℓ in (5.37) is not claimed in [BC16a] but easily follows from the uniformity of all Taylor expansions involved in the proof in the cited paper (which we do not reproduce).

Lemma 5.1.26. *Let $A,B>0$. Then, for all $n\in\mathbb{Z}_{\geq 1}$ and all $q\in(\frac{1}{2},1)$, we have*

$$\frac{(q^{A+n};q)_\infty}{(q^{B+n};q)_\infty}\leq c\,(1-q^n)^{B-A}, \tag{5.38}$$

where c is a constant independent of q,n.

Proof. Set $q=e^{-\varepsilon}$. The result of the Lemma is restated, taking the logarithm of both sides of (5.38), as

$$\sum_{k\geq 0}\log\frac{(1-e^{-\varepsilon(A+n+k)})}{(1-e^{-\varepsilon(B+n+k)})}-(B-A)\log(1-e^{-\varepsilon n})\leq c', \tag{5.39}$$

for all $\varepsilon\in(0,-\log 2)$ and a constant c' independent of ε,n. Using Lagrange mean value theorem, we can rewrite the generic term of the infinite sum as

$$\log\frac{(1-e^{-\varepsilon(A+n+k)})}{(1-e^{-\varepsilon(B+n+k)})}=(A-B)\,\frac{\varepsilon}{e^{\varepsilon(\widetilde{t}_k+n+k)}-1},$$

where numbers $\widetilde{t}_k$ belong to the interval $(\min(A,B),\max(A,B))$. We show that for any positive bounded sequence $\{t_k\}_k\subset(0,M)$, with M fixed, the quantity

$$\sum_{k\geq 0}\frac{\varepsilon}{e^{\varepsilon(t_k+n+k)}-1}+\log(1-e^{-\varepsilon n}) \tag{5.40}$$

is absolutely bounded uniformly in ε and n and this would prove (5.39) and hence (5.38). To evaluate the infinite sum over k we fix a positive constant δ and distinguish two cases.

Case 1, $k \geq \delta/\varepsilon$. We use the estimate

$$\frac{\varepsilon}{e^{\varepsilon(t_k+n+k)}-1} \leq e^{-\varepsilon k}\frac{\varepsilon}{1-e^{-\delta}},$$

that implies, summing over k,

$$\sum_{k\geq\delta/\varepsilon} \frac{\varepsilon}{e^{\varepsilon(t_k+n+k)}-1} \leq \frac{1}{e^{\delta}-1}\frac{\varepsilon}{1-e^{-\varepsilon}} \leq \frac{2\log 2}{e^{\delta}-1}. \tag{5.41}$$

Case 2, $k < \delta/\varepsilon$. In this case we use again Lagrange mean value theorem to express the denominator of the generic term of the summation of (5.40) as

$$\frac{\varepsilon}{e^{\varepsilon(t_k+n+k)}-1} = \frac{e^{-\varepsilon\xi_{k,n}}}{t_k+n+k}, \qquad \text{for some } \xi_{k,n} \in (0, t_k+n+k).$$

This implies the bounds

$$\frac{e^{-\varepsilon(M+n+k)}}{M+n+k} \leq \frac{\varepsilon}{e^{\varepsilon(t_k+n+k)}-1} \leq \frac{1}{n+k}. \tag{5.42}$$

We focus first on the lower bound given by the first inequality in (5.42). Summing over k we find

$$\sum_{k=0}^{\delta/\varepsilon} \frac{e^{-\varepsilon(M+n+k)}}{M+n+k} \geq \int_0^{\delta/\varepsilon} \frac{e^{-\varepsilon(M+n+k)}}{M+n+k}dk = \int_{\varepsilon(M+n)}^{\delta+\varepsilon(M+n)} \frac{e^{-k'}}{k'}dk' \geq \int_{\varepsilon(M+n)}^{\delta+\varepsilon(M+n)} \left(\frac{1}{k'}-1\right)dk',$$

which gives

$$\sum_{k=0}^{\delta/\varepsilon} \frac{\varepsilon}{e^{\varepsilon(t_k+n+k)}-1} \geq \log\left(1+\frac{\delta}{\varepsilon(M+n)}\right) - \delta. \tag{5.43}$$

We turn now our attention to the second inequality in (5.42) and, since

$$\sum_{k=0}^{\delta/\varepsilon} \frac{1}{n+k} \leq \int_n^{\delta/\varepsilon+n} \frac{dk}{k-1/2},$$

we obtain

$$\sum_{k=0}^{\delta/\varepsilon} \frac{\varepsilon}{e^{\varepsilon(t_k+n+k)}-1} \leq \log\left(1+\frac{\delta}{\varepsilon(n-1/2)}\right). \tag{5.44}$$

Combining results obtained from the analysis of cases $k \geq \delta/\varepsilon$ and $k < \delta/\varepsilon$ in (5.41), (5.43) (5.44) we can finally write

$$\log\left((1+\frac{\delta}{\varepsilon(M+n)})(1-e^{-\varepsilon n})\right)+\mathsf{O}(\delta) \leq (5.40) \leq \log\left((1+\frac{\delta}{\varepsilon(n-1/2)})(1-e^{-\varepsilon n})\right)+\mathsf{O}(\delta).$$

This concludes our proof since the arguments of the logarithms in the left and right-hand side are bounded functions for $\varepsilon \in (0, \log 2)$ and $n \geq 1$. □

For the next lemma we define the quantity

$$\mathcal{A}^{(q)}_{S,X}(\ell_3,\ell_2,\ell_1)=\frac{1}{\Delta_q(\ell_3,\ell_2,\ell_1)}\frac{(q^{S-X};q)_{n_1-n_2}}{(q;q)_{n_1-n_2}}\frac{(q^{S+X};q)_{n_2-n_3}}{(q;q)_{n_2-n_3}}\frac{(q;q)_{n_1-n_3}}{(q^{2S};q)_{n_1-n_3}},$$

where we assumed $1\le\ell_3\le\ell_2\le\ell_1$ and $n_i=\lfloor\log_q(1/\ell_i)\rfloor$. Here Δ_q is defined in (5.21). We think of $\mathcal{A}^{(q)}_{S,X}$ as a q-deformation of $\mathcal{A}_{S,X}$ (5.8).

Lemma 5.1.27. *For any continuous function $f(\ell_2)$ we have*

$$\lim_{q\to1}\int_{\ell_3}^{\ell_1}f(\ell_2)\mathcal{A}^{(q)}_{S,X}(\ell_3,\ell_2,\ell_1)\frac{d\ell_2}{\ell_2}=\int_{\ell_3}^{\ell_1}f(\ell_2)\mathcal{A}_{S,X}(\ell_3,\ell_2,\ell_1)\frac{d\ell_2}{\ell_2},\tag{5.45}$$

uniformly for any $\ell_3\le\ell_1$ bounded away from ∞.

Proof. Fix small positive δ. We will prove our claim distinguishing two cases, based on the distance between ℓ_3 and ℓ_1.

Case 1, $\ell_1-\ell_3>\delta$. The integral in the left-hand side of (5.45) can be decomposed as

$$\int_{\ell_3}^{\ell_1}=\int_{\ell_3+\delta/2}^{\ell_1-\delta/2}+\int_{\ell_3}^{\ell_3+\delta/2}+\int_{\ell_1-\delta/2}^{\ell_1}.$$

When $\ell_3+\delta/2\le\ell_2\le\ell_1-\delta/2$, by virtue of Lemma 5.1.25, we have

$$\int_{\ell_3+\delta/2}^{\ell_1-\delta/2}f(\ell_2)\mathcal{A}^{(q)}_{S,X}(\ell_3,\ell_2,\ell_1)\frac{d\ell_2}{\ell_2}\xrightarrow[q\to1]{}\int_{\ell_3+\delta/2}^{\ell_1-\delta/2}f(\ell_2)\mathcal{A}_{S,X}(\ell_3,\ell_2,\ell_1)\frac{d\ell_2}{\ell_2},$$

uniformly.

On the other hand, when $\ell_3\le\ell_2<\ell_3+\delta/2$ we use estimates

$$\mathcal{A}^{(q)}_{S,X}(\ell_3,\ell_2,\ell_1)\le\begin{cases}C\mathcal{A}_{S,X}(\ell_3,\ell_2,\ell_1) & \text{if } n_3<n_2,\\ \dfrac{C}{\Delta_q(\ell_3,\ell_2,\ell_1)}\left(\dfrac{1-q}{1-\ell_3/\ell_1}\right)^{S+X} & \text{if } n_3=n_2.\end{cases},$$

valid for some constant C independent of q of ℓ_2 and that can be deduced using Lemma 5.1.26 and identity (5.24). This implies that

$$\int_{\ell_3}^{\ell_3+\delta/2}f(\ell_2)\mathcal{A}^{(q)}_{S,X}(\ell_3,\ell_2,\ell_1)\frac{d\ell_2}{\ell_2}=\mathsf{O}(\delta)+\mathsf{O}\left(\frac{1-q}{\delta}\right)^{S+X}.$$

In an analogous fashion one can also show that

$$\int_{\ell_1-\delta/2}^{\ell_1}f(\ell_2)\mathcal{A}^{(q)}_{S,X}(\ell_3,\ell_2,\ell_1)\frac{d\ell_2}{\ell_2}=\mathsf{O}(\delta)+\mathsf{O}\left(\frac{1-q}{\delta}\right)^{S-X}.$$

This concludes the proof of (5.45) when $\ell_1-\ell_3>\delta$.

Case 2, $\ell_1 - \ell_3 \leq \delta$. Assuming δ is very small, for any $\ell_2 \in [\ell_3, \ell_1]$, we can write, by continuity, $f(\ell_2) = f(\ell_1) + \mathsf{o}(1)$, where $\mathsf{o}(1)$ tends to 0 as $\delta \to 0$. Thus, we have

$$\int_{\ell_3}^{\ell_1} f(\ell_2)\mathcal{A}^{(q)}_{S,X}(\ell_3, \ell_2, \ell_1)\frac{d\ell_2}{\ell_2} = \sum_{n_2=n_3}^{n_1} (f(\ell_1) + \mathsf{o}(1))\, q^{-(S+X)(n_1-n_2)}\varphi_{q,q^{S+X},q^{2S}}(n_1 - n_2|n_1 - n_3)$$
$$= f(\ell_1) + \mathsf{o}(1),$$

and by Lemma 5.12 this concludes the analysis of the case $\ell_1 - \ell_3 \leq \delta$.

Since all the estimates we provided are controlled as functions of δ, the convergence in (5.45) is uniform provided that ℓ_1 stays bounded. □

Proof of Proposition 5.1.15. The integral in the left-hand side of (5.25) is equal to

$$\int_{L_{N,N}}^{L_{N,N-1}} \frac{dL_{N-1,N-1}}{L_{N-1,N-1}}\mathcal{A}^{(q)}_{S,X}(L_{N,N}, L_{N-1,N-1}, L_{N,N-1}) \cdots$$
$$\cdots \int_{L_{N,2}}^{L_{N,1}} \frac{dL_{N-1,1}}{L_{N-1,1}}\mathcal{A}^{(q)}_{S,X}(L_{N,2}, L_{N-1,1}, L_{N,1}) \left(\frac{L_{N-1,N-1}\cdots L_{N-1,1}}{L_{N,N}\cdots L_{N,1}}\right)^X f(\underline{L}_{N-1})$$

and we can take the $q \to 1$ limit in each of the $N-1$ integrals using Lemma 5.1.27. This establishes the convergence to the right-hand side of (5.25) as $q \to 1$, uniformly on any compact subset of $\mathcal{W}_N$. □

5.2 Spin Whittaker Processes and beta polymers

In this section define *spin Whittaker processes*, and establish their connection with two beta polymer type models introduced in [BC16a] and [CMP19], respectively.

5.2.1 Spin Whittaker processes

The definition of spin Whittaker processes is a straightforward analogy of the discrete level $\mathfrak{F}/\mathfrak{G}$ processes (Definition 3.1.3). The key role is played by the Cauchy type identities (established for spin Whittaker functions in Section 5.1.7).

Definition 5.2.1. Set $\mathbf{X} = (X_1, \ldots, X_N)$ and $\mathbf{Y} = (Y_1, \ldots, Y_T)$, with $|X_i|, |Y_j| < S$ and $X_i + Y_j > 0$ for all i, j. The (ascending) *spin Whittaker process* is the probability measure on interlacing sequences $\underline{\underline{L}}_N(T) = (L_{k,i}(T))_{1\leq i\leq k\leq N}$ (that is, on the Gelfand-Tsetlin cone $\mathcal{GT}_N$ (5.7)) with the following density with respect to the measure $\frac{d\underline{\underline{L}}_N}{\underline{\underline{L}}_N} = \prod_{1\leq i\leq j\leq N}\frac{dL_{j,i}}{L_{j,i}}$:

$$\mathfrak{P}_{\mathbf{X};\mathbf{Y}}(\underline{\underline{L}}_N) = \frac{\mathfrak{f}_{X_1}(\underline{L}_1)\mathfrak{f}_{X_2}(\underline{L}_1;\underline{L}_2)\cdots\mathfrak{f}_{X_N}(\underline{L}_{N-1};\underline{L}_N)\mathfrak{g}_{\mathbf{Y}}(\underline{L}_N)}{\Pi(\mathbf{X};\mathbf{Y})}. \tag{5.46}$$

The normalizing constant in (5.46) follows from the Cauchy identity of Corollary 5.1.21:

$$\Pi(\mathbf{X};\mathbf{Y}) = \prod_{j=1}^{T}\frac{\Gamma(X_1+Y_j)}{\Gamma(S+X_1)}\left(\prod_{i=2}^{N}\frac{\Gamma(X_i+Y_j)\Gamma(2S)}{\Gamma(S+X_i)\Gamma(S+Y_j)}\right).$$

For the next result we denote the ascending sqW/sqW process, subject to the rescaling (5.19), (5.26), by

$$\mathfrak{P}^{(q)}_{\mathbf{X};\mathbf{Y}}(\underline{\underline{L}}_N) = \frac{\mathfrak{f}^{(q)}_{X_1}(\underline{L}_1)\mathfrak{f}^{(q)}_{X_2}(\underline{L}_1;\underline{L}_2)\cdots\mathfrak{f}^{(q)}_{X_N}(\underline{L}_{N-1};\underline{L}_N)\mathfrak{g}^{(q)}_{\mathbf{Y}}(\underline{L}_N)}{\Pi^{(q)}(\mathbf{X};\mathbf{Y})},$$

where the normalization constant is (cf. (5.32))

$$\Pi^{(q)}(\mathbf{X};\mathbf{Y}) = \prod_{j=1}^{T}\frac{\Gamma_q(X_1+Y_j)}{\Gamma_q(S+X_1)}\left(\prod_{i=2}^{N}\frac{\Gamma_q(X_i+Y_j)\Gamma_q(2S)}{\Gamma_q(S+X_i)\Gamma_q(S+Y_j)}\right).$$

Theorem 5.2.2. *Under the scaling (5.19), (5.26), the ascending sqW/sqW process converges weakly to the spin Whittaker process*

$$\mathfrak{P}^{(q)}_{\mathbf{X};\mathbf{Y}} \xrightarrow[q\to 1]{} \mathfrak{P}_{\mathbf{X};\mathbf{Y}}. \tag{5.47}$$

Proof. For any continuous bounded test function $\phi(\underline{\underline{L}}_N)$ on $\mathcal{GT}_N$ we have

$$\mathbb{E}^{(q)}(\phi) = \frac{1}{\Pi^{(q)}(\mathbf{X};\mathbf{Y})}\int\frac{d\underline{L}_N}{\underline{L}_N}\mathfrak{g}^{(q)}_{\mathbf{Y}}(\underline{L}_N)\int\frac{d\underline{\underline{L}}_{N-1}}{\underline{\underline{L}}_{N-1}}\mathfrak{f}^{(q)}_{X_1}(\underline{L}_1)\mathfrak{f}^{(q)}_{X_2}(\underline{L}_1;\underline{L}_2)\cdots\mathfrak{f}^{(q)}_{X_N}(\underline{L}_{N-1};\underline{L}_N)\phi(\underline{\underline{L}}_N). \tag{5.48}$$

The integral is absolutely convergent and as a consequence of Corollaries 5.1.16 and 5.1.18 it converges to the average $\mathbb{E}(\phi)$ with respect to the spin Whittaker process. □

Remark 5.2.3. Developing the argument sketched in Section 5.1.8 it should be possible to show that the spin Whittaker process of Definition 5.2.1 converges to the α-Whittaker process from [Cor+14], [BC14]. In this case the correct way to rescale the random variables $L_{k,i}(T)$ is

$$L_{k,i}(T) = S^{T+k+1-2i}e^{u_{k,i}(T)}. \tag{5.49}$$

In the limit $S\to\infty$ the process $\{u_{k,i}(T)\colon 1\le i\le k\le N\}$ should be then described by the density

$$\frac{Q^{1\to 0}_{\mathrm{i}X_1}(\underline{u}_1,0)Q^{2\to 1}_{\mathrm{i}X_2}(\underline{u}_2,\underline{u}_1)\cdots Q^{N\to N-1}_{\mathrm{i}X_N}(\underline{u}_N,\underline{u}_{N-1})\theta_{\mathbf{Y}}(\underline{u}_N)}{\prod_{i=1}^{N}\prod_{j=1}^{T}\Gamma(X_i+Y_j)}, \tag{5.50}$$

where $Q^{k+1\to k}$ and $\theta_{\mathbf{Y}}$ are given in (5.2) and (5.4), respectively.

5.2.2 Strict-weak beta polymer model

We will now recall the strict-weak beta polymer introduced in [BC16a].

Definition 5.2.4. Let $B_{i,j}\sim\mathcal{B}(X_i+Y_j,S-Y_j)$ be a family of independent beta random variables. The *strict-weak beta polymer model* partition function $Z(i,j)$, $i\ge 1$, $j\ge 0$, is the random function satisfying the recurrence

$$\begin{cases} Z(i,j) = Z(i,j-1)B_{i,j} + Z(i-1,j-1)(1-B_{i,j}) & \text{for } 1<i\le j;\\ Z(1,j) = Z(1,j-1)B_{1,j} & \text{for } j>0;\\ Z(i,0) = 1 & \text{for } i>0.\end{cases}$$

Note that all the partition functions $Z(i,j)$ belong to $(0,1]$. In particular, the probability distribution of the strict-weak beta polymer is completely determined by the joint moments.

Proposition 5.2.5. *Recall the q-Hahn vertex model height function $\mathcal{H}^{\mathrm{ur}}_{q\text{-Hahn}}$ (Section 3.3.5). Define $Z^{(q)}(i,j) = q^{\mathcal{H}^{\mathrm{ur}}_{q\text{-Hahn}}(i,j)}$. Then, under the scaling (5.19), $Z^{(q)}$ converges weakly to the strict-weak beta polymer partition function:*

$$Z^{(q)}(i,j) \xrightarrow[q\to 1]{} Z(i,j).$$

Proof. This result is equivalent to Proposition 2.1 of [BC16a] in the homogeneous case $X_i = X$, $Y_j = Y$ for all i,j. One can easily check that the proof given there also works in our inhomogeneous setting. □

Theorem 5.2.6. *The marginal process $\{L_{k,k}(T)^{-1}\colon k = 1,\dots N,\, T \geq N\}$ of the spin Whittaker process $\mathfrak{P}_{\mathbf{X},\mathbf{Y}}$ is equivalent in distribution to the strict-weak beta polymer partition functions model $\{Z(k,T)\colon k = 1,\dots,N,\, T\geq N\}$.*

Note that since $L_{k,k}(T) \in \mathbb{R}_{\geq 1}$, we have $L_{k,k}(T)^{-1} \in (0,1]$, which agrees with the range of the beta polymer partition functions.

Proof of Theorem 5.2.6. This is a direct consequence of Theorems 3.3.16 and 5.2.2 and Proposition 5.2.5. Indeed, the last row marginal of the sqW/sqW process is matched to the q-Hahn vertex model height function, and in the limit $q \to 1$ this implies that the last coordinate marginal of the spin Whittaker process is matched to the beta polymer $Z(i,j)$. □

Let us make two remarks on this result.

Remark 5.2.7. A weaker version of Theorem 5.2.6 that matches $L_{k_i,k_i}(T)^{-1}$ and $Z(k_i,T)$ for each single time T can alternatively be proved using moment formulas. Namely, the eigenoperators of Definition 5.1.23 may be used to extract multiple integral formulas for the joint moments of $L_{k_i,k_i}(T)^{-1}$ under the spin Whittaker processes. These formulas can then be matched to the ones for the joint moments of the beta polymer. The latter in the homogeneous case are obtained in [BC16a, Proposition 3.4], and their inhomogeneous generalization is rather straightforward, cf. [Pet19, Proposition 6.1].

Remark 5.2.8. It was noticed in [BC16a, Remark 1.5] that under the scaling $Z(i,T) = S^{T-i+1}z(i,T)$ the process $z(i,T)$ converges, when $S \to \infty$, to the strict-weak gamma polymer model introduced by Seppäläinen in an unpublished note and studied in [OO15], [CSS15]. This scaling of polymers corresponds to the scaling (5.49) for the full spin Whittaker process. As S goes to infinity, Theorem 5.2.6 turns into the matching between strict weak gamma polymer model and α-Whittaker process that was originally discovered in [OO15]. This observation is another piece of evidence supporting the formal $S \to +\infty$ scaling described in Section 5.1.8.

5.2.3 Another beta polymer type model

Let us now recall the beta polymer type model which was introduced in [CMP19]. We employ notation from Chapter A.

Definition 5.2.9. The random function $\widetilde{Z}(i,j)$, for $i,j \in \mathbb{Z}_{\geq 0}$ is defined by the recurrence

$$\widetilde{Z}(i,j) = \begin{cases} 1 & \text{for } j=0, \\ \widetilde{Z}(1,j-1)\widetilde{B}_{1,j} & \text{for } i=1, \\ W^{>}_{i,j}\widetilde{Z}(i,j-1) + (1-W^{>}_{i,j})\widetilde{Z}(i-1,j) & \text{if } \widetilde{Z}(i,j-1) > \widetilde{Z}(i-1,j), \\ (1-W^{<}_{i,j})\widetilde{Z}(i,j-1) + W^{<}_{i,j}\widetilde{Z}(i-1,j) & \text{if } \widetilde{Z}(i,j-1) < \widetilde{Z}(i-1,j), \end{cases} \tag{5.51}$$

where $\widetilde{B}_{1,j} \sim \mathscr{B}^{-1}(X_1+Y_j, S-Y_j)$ are independent inverse beta random variables, and

$$\begin{aligned} W^{>}_{i,j} &\sim \mathscr{NBB}^{-1}\left(2S-1, \frac{\widetilde{Z}(i-1,j)-\widetilde{Z}(i-1,j-1)}{\widetilde{Z}(i,j-1)-\widetilde{Z}(i-1,j-1)}, X_i+Y_j, S-Y_j\right), \\ W^{<}_{i,j} &\sim \mathscr{NBB}^{-1}\left(2S-1, \frac{\widetilde{Z}(i,j-1)-\widetilde{Z}(i-1,j-1)}{\widetilde{Z}(i-1,j)-\widetilde{Z}(i-1,j-1)}, X_i+Y_j, S-X_i\right). \end{aligned} \tag{5.52}$$

For $i>1$, $j>0$, we have $\widetilde{Z}(i,j-1) \neq \widetilde{Z}(i-1,j)$ with probability one.

Proposition 5.2.10. *Recall the ${}_4\phi_3$ vertex model height function $\mathcal{H}^{\mathrm{ul}}_{\phi}(i,j)$ (Section 3.3.6). Define $\widetilde{Z}^{(q)}(i,j) = q^{-\mathcal{H}^{\mathrm{ul}}_{\phi}(i,j)}$. Then, under the scaling (5.19), $Z^{(q)}$ converges weakly to the process $\widetilde{Z}$:*

$$\widetilde{Z}^{(q)}(i,j) \xrightarrow[q\to 1]{} \widetilde{Z}(i,j).$$

Proof. In the homogeneous case $X_i = 0$, $Y_j = Y$ for all i,j, this was proven in [CMP19]. The same argument also essentially applies to the inhomogeneous case, and we will not repeat the computations here. The non-trivial part of the proof is to understand how the X_i parameters appear in the definition of $W^{<}_{i,j}, W^{>}_{i,j}$. The interested reader can check the validity of our statements starting from (3.33) and reproducing the computations of Section 4.3 of [CMP19]. □

Theorem 5.2.11. *The marginal process $\{L_{k,1}(T) \colon k = 1\dots N,\ T \geq N\}$ of the spin Whittaker process $\mathfrak{P}_{\mathbf{X},\mathbf{Y}}$ is equivalent in distribution to the process $\{\widetilde{Z}(k,T) \colon k=1,\dots N,\ T \geq N\}$.*

Proof. This is established similarly to Theorem 5.2.6 by combining the matching of Theorem 3.3.20 with the $q \to 1$ scaling limits. □

5.2.4 Reduction to log-gamma polymer

Here we show that the model $\widetilde{Z}(i,j)$ of Definition 5.2.9 reduces, as $S \to +\infty$, to the well-known log-gamma polymer model introduced in [Sep12]. This proof is more involved than the rather straightforward observation for the strict-weak beta polymer (Remark 5.2.8).

Definition 5.2.12 (Log-gamma polymer)**.** Let $\{g_{i,j} \colon i,j \in \mathbb{Z}_{\geq 1}\}$ be a sequence of independent inverse gamma random variables, $g_{i,j} \sim \mathrm{Gamma}^{-1}(X_i + Y_j)$ with density (A.22). The random function $\widetilde{z}$ defined by the recurrence

$$\widetilde{z}(i,j) = \begin{cases} g_{i,j}\left(\widetilde{z}(i-1,j) + \widetilde{z}(i,j-1)\right) & \text{if } i,j \geq 1 \text{ and } i+j \geq 3; \\ g_{1,1} & \text{if } i=j=1; \\ 0 & \text{else,} \end{cases} \tag{5.53}$$

is the *point-to-point log-gamma polymer partition function.*

The log-gamma polymer model was introduced (with a proof of its exact solvability) by Seppäläinen in [Sep12]. One can view $\widetilde{z}(i,j)$ as a partition function of up-right directed paths from $(1,1)$ to (i,j), where the weight of each path equals the product of the quantities $g_{i',j'}$ along the path. In [Cor+14] the log-gamma polymer model was given a powerful combinatorial interpretation using Kirillov's geometric RSK (Robinson-Schensted-Knuth) algorithm. This showed the distributional matching of the log-gamma polymer with a marginal of the Whittaker process (5.50).

The next statement shows that the log-gamma polymer model can be obtained in a $S \to +\infty$ scaling limit from the beta polymer like model of Definition 5.2.9. Modulo Remark 5.2.3, this together with Theorem 5.2.11 produces an alternative derivation of the results of [Cor+14].

Proposition 5.2.13. *Consider the scaling $\widetilde{Z}(i,j) = S^{j+i-1}\widetilde{\mathscr{z}}^{(S)}(i,j)$ of the process from Definition 5.2.9. Then the rescaled process $\widetilde{\mathscr{z}}^{(S)}$ converges weakly to the log-gamma polymer:*

$$\widetilde{\mathscr{z}}^{(S)}(i,j) \xrightarrow[S\to\infty]{} \widetilde{z}(i,j).$$

Proof. We argue by induction. When $i=j=1$, then $\widetilde{\mathscr{z}}^{(S)}(1,1) = S^{-1}\mathscr{B}^{-1}(X_1+Y_1, S-Y_1)$. In the large S limit this converges to $\mathrm{Gamma}^{-1}(X_1+Y_1)$, which is precisely $\widetilde{z}(1,1)$.

Fix i,j and assume that for all i',j' such that $i'+j' < i+j$ the convergence $\widetilde{\mathscr{z}}^{(S)}(i',j') \to \widetilde{z}(i',j')$ holds. Let us compute the densities of random variables $S^{-1}W^{>}_{i,j}$ and $S^{-1}W^{<}_{i,j}$, that are rescalings of (5.52), in the large S limit. We show the computations only for $W^{>}_{i,j}$ since the other case is very similar. The density of $S^{-1}W^{>}_{i,j}$ (depending on the variable $x \in (0,1)$) is, from (5.52) and (A.23), equal to

$$\begin{aligned}\frac{\left(\frac{1}{x}\right)^{X_i+Y_j+1}\left(1-\frac{1}{Sx}\right)^{S-Y_j-1}}{\Gamma(X_i+Y_j)}\frac{\Gamma(S+X_i)}{S^{X_i+Y_j}\Gamma(S-Y_j)}\\ \times (1-p_S)^{2S-1}{}_2F_1\left(\begin{matrix}2S-1, & S+X_i \\ S-Y_j & -\end{matrix}\middle|\, p_S\left(1-\frac{1}{Sx}\right)\right),\end{aligned} \tag{5.54}$$

where

$$p_S = \frac{\widetilde{Z}(i-1,j) - \widetilde{Z}(i-1,j-1)}{\widetilde{Z}(i,j-1) - \widetilde{Z}(i-1,j-1)} = \frac{S\widetilde{\mathscr{z}}^{(S)}(i-1,j) - \widetilde{\mathscr{z}}^{(S)}(i-1,j-1)}{S\widetilde{\mathscr{z}}^{(S)}(i,j-1) - \widetilde{\mathscr{z}}^{(S)}(i-1,j-1)} \sim p := \frac{\widetilde{z}(i-1,j)}{\widetilde{z}(i,j-1)}$$

is smaller than 1.

The limit of the first few factors in (5.54) is straightforward:

$$\frac{\left(\frac{1}{x}\right)^{X_i+Y_j+1}\left(1-\frac{1}{Sx}\right)^{S-Y_j-1}}{\Gamma(X_i+Y_j)}\frac{\Gamma(S+X_i)}{S^{X_i+Y_j}\Gamma(S-Y_j)}\xrightarrow[S\to\infty]{}\frac{\left(\frac{1}{x}\right)^{X_i+Y_j+1}e^{-\frac{1}{x}}}{\Gamma(X_i+Y_j)}.$$

To compute the limit of the Gaussian hypergeometric function, we use the Euler transformation

$${}_2F_1\left(\begin{matrix}a, & b\\ c, & -\end{matrix}\middle| z\right)=(1-z)^{c-a-b}{}_2F_1\left(\begin{matrix}c-a, & c-b\\ c & -\end{matrix}\middle| z\right),$$

so that the remaining terms in (5.54) become

$$\left(\frac{1-p_S}{1-p_S+\frac{p_S}{Sx}}\right)^{2S-1}\left(1-p_S+\frac{p_S}{Sx}\right)^{-X_i-Y_j}{}_2F_1\left(\begin{matrix}-S-Y_j+1, & -X_i-Y_j\\ S-Y_j, & -\end{matrix}\middle| p_S\left(1-\frac{1}{Sx}\right)\right).$$

We have

$$\left(\frac{1-p_S}{1-p_S+\frac{p_S}{Sx}}\right)^{2S-1}\left(1-p_S+\frac{p_S}{Sx}\right)^{-X_i-Y_j}\xrightarrow[S\to\infty]{}e^{-\frac{2p}{(1-p)x}}(1-p)^{-X_i-Y_j},$$

whereas

$${}_2F_1\left(\begin{matrix}-S-Y_j+1, & -X_i-Y_j\\ S-Y_j, & -\end{matrix}\middle| p_S\left(1-\frac{1}{Sx}\right)\right)\xrightarrow[S\to\infty]{}{}_1F_0\left(\begin{matrix}-X_i-Y_j\\ -\end{matrix}\middle| -p\right)=(1+p)^{X_i+Y_j}.$$

Our computations imply that

$$S^{-1}W^{>}_{i,j}\xrightarrow[S\to\infty]{}\frac{\widetilde{z}(i-1,j)+\widetilde{z}(i,j-1)}{\widetilde{z}(i,j-1)-\widetilde{z}(i-1,j)}\,\mathrm{Gamma}^{-1}(X_i+Y_j).$$

Essentially repeating the computations for $S^{-1}W^{<}_{i,j}$, we obtain

$$S^{-1}W^{<}_{i,j}\xrightarrow[S\to\infty]{}\frac{\widetilde{z}(i-1,j)+\widetilde{z}(i,j-1)}{\widetilde{z}(i-1,j)-\widetilde{z}(i,j-1)}\,\mathrm{Gamma}^{-1}(X_i+Y_j).$$

Thus, we see that in the scaling limit as $S\to+\infty$, the beta polymer like model recurrence relation (5.51) becomes (5.53), the recurrence for the log-gamma polymer partition functions. This completes the proof. □

5.3 Deformed quantum Toda system

In this section we consider the scaling limit of the Pieri rule (2.36) which states that the spin q-Whittaker polynomials $\mathbb{F}_\lambda(x_1,\ldots,x_N)$ are eigenfunctions of an operator acting on the *label* λ. This scaling limit leads to an eigenoperator for the spin Whittaker functions. This operator acts as a second order differential operator in the (additive versions of the) variables $\underline{L}_N$. We call is the *S-deformed quantum Toda Hamiltonian*. Our scaling of the Pieri rules are inspired by [GLO12] where the Pieri rule for the q-Whittaker polynomials was understood as a discretization of the (undeformed) quantum Toda Hamiltonian.

5.3.1 Refined Pieri operators

We start by refining the Pieri operator $(\mathfrak{H}^{\mathrm{sHL}} f)(\mu) = \sum_\lambda f(\lambda)\, \mathsf{F}^*_{\lambda'/\mu'}(v)$ introduced in (2.37), by considering its expansion in powers of v. Recall identity (2.36) which states that

$$(\mathfrak{H}^{\mathrm{sHL}} f)(\lambda) = \left(\left(\frac{1}{1-sv} \right)^{N-1} \prod_{i=i}^{N} (1+x_i v) \right) f(\lambda), \qquad f(\lambda) = \mathbb{F}_\lambda(x_1,\dots,x_N).$$

Defining $\mathfrak{H}_k$ by

$$(1-vs)^{N-1}\mathfrak{H}^{\mathrm{sHL}} = \sum_{k=0}^{N} v^k \mathfrak{H}_k, \tag{5.55}$$

we see that

$$\mathfrak{H}_k \mathbb{F}_\lambda = e_k(x_1,\dots,x_N)\mathbb{F}_\lambda. \tag{5.56}$$

The action of the $\mathfrak{H}_k$'s on functions $f(\lambda)$ can in principle be recovered using the vertex weights w^* in fig. 2.5 (without the denominator $1-vs$) which compose the sHL functions $(1-vs)^{N-1}\mathsf{F}^*_{\lambda'/\mu'}$. In the simplest cases $k=0$ or N one can verify that

$$\mathfrak{H}_0 = \mathrm{Id}, \qquad \mathfrak{H}_N = \mathcal{T}_{\mu_1}\cdots\mathcal{T}_{\mu_N},$$

where $\mathcal{T}$ is the shift operator

$$(\mathcal{T}_{\mu_i} f)(\mu) = \begin{cases} f(\mu+\mathrm{e}_i), & \text{if } \mu_i < \mu_{i-1} \text{ or } i=1; \\ 0, & \text{otherwise.} \end{cases}$$

Indeed, $\mathfrak{H}_0$ requires no vertical arrows to change from μ to λ, and $\mathfrak{H}_N$ corresponds to adding a full horizontal path starting at zero and ending at N, so that the arrow configuration corresponding to λ is obtained from the one for μ by adding one vertical arrow at location N.

When $1 \le k \le N-1$, explicit formulas for $\mathfrak{H}_k$ look significantly more involved. We need only the one for $k=1$, and will not discuss the other operators $\mathfrak{H}_k$.[2] In the next statement, by agreement, we set $\mu_0 = +\infty$, $\mu_{N+1} = -\infty$.

Proposition 5.3.1. *We have*

$$\mathfrak{H}_1 = h_{0,0}\,\mathrm{Id} + \sum_{0\le k<\ell\le N} h_{k,\ell}\mathcal{T}_{\mu_{k+1}}\cdots\mathcal{T}_{\mu_\ell},$$

with

$$h_{0,0} = -s\sum_{j=1}^{N-1} q^{\mu_j-\mu_{j+1}},$$
$$h_{k,\ell} = (1-q^{\mu_k-\mu_{k+1}})(-s)^{\ell-k-1} q^{\mu_{k+1}-\mu_\ell}(1-s^2 q^{\mu_\ell-\mu_{\ell+1}}).$$

[2] Appropriate scaling limits of the higher operators $\mathfrak{H}_k$ could potentially lead to higher order differential operators commuting with the deformed quantum Toda Hamiltonian $\mathcal{H}_2$ introduced below in this section. We leave this investigation to a future work.

Proof. Express the action of $\mathfrak{H}_1$ as

$$\mathfrak{H}_1 f(\mu) = \sum_{\mu \prec \lambda} H(\mu; \lambda) f(\lambda),$$

where the term $H(\mu; \lambda)$ corresponds to the weight of a row of vertices having a configuration λ at the top and μ at the bottom. Recall that we are using down-right directed paths as in fig. 2.5, and all the individual vertex weights are multiplied by $(1 - vs)$.

Observe that each vertex 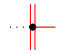 somewhere in the bulk comes with the weight $v(1 - q^{\mu_i - \mu_{i+1}})$. Therefore, terms proportional to v can only come from configurations with no horizontal arrows 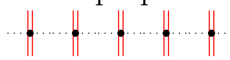 or with a single sequence of horizontal arrows 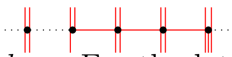. The first case, corresponding to $\lambda = \mu$, provides us with the term $h_{0,0}$. For the latter case, let k be the column of the leftmost vertex emanating an horizontal arrow, and let ℓ be the column where the single horizontal path stops. Such configuration corresponds to a partition $\lambda = \mu + \mathbf{e}_{k+1} + \cdots + \mathbf{e}_\ell$. Isolating the coefficient of v in the expansion of product of vertex weights, we recover $h_{k,\ell}$. $\square$

5.3.2 Scaling of the Pieri operators

Introduce the differential operators acting in the variables $u_1, \ldots, u_N$:

$$\mathcal{H}_1 \coloneqq \sum_{i=1}^{N} \partial_{u_i}; \tag{5.57}$$

$$\mathcal{H}_2 \coloneqq -\frac{1}{2} \sum_{i=1}^{N} \partial_{u_i}^2 + \sum_{1 \le i < j \le N} S^{-2(j-i)} e^{u_j - u_i} (S - \partial_{u_i})(S + \partial_{u_j}). \tag{5.58}$$

In the second operator, the product is understood in the usual way as

$$(S - \partial_{u_i})(S + \partial_{u_j}) = S^2 \,\mathrm{Id} + S(\partial_{u_j} - \partial_{u_i}) - \partial_{u_i}\partial_{u_j}.$$

For the next result we define the rescaling

$$q = e^{-\varepsilon}, \qquad q^{\lambda_i} = \frac{e^{-u_i}}{S^{N+1-2i}}, \qquad s = -e^{-\varepsilon S}. \tag{5.59}$$

Proposition 5.3.2. *Under the scaling (5.59), we have*

$$\mathcal{H}_1 = \lim_{\varepsilon \to 0} \frac{1}{\varepsilon} \left(\mathfrak{H}_1 - N \right),$$

$$\mathcal{H}_2 = -\lim_{\varepsilon \to 0} \frac{1}{\varepsilon^2} \left(\mathfrak{H}_1 - N + \frac{1}{2} \mathfrak{H}_N^2 - 2\, \mathfrak{H}_N + \frac{3}{2} \right).$$

We remark that the combinations of the refined Pieri operators leading to $\mathcal{H}_1$ and $\mathcal{H}_2$ are the same as in the q-Whittaker case [GLO12, Proposition 2.1], and correspond to the scaling of eigenvalues in the proof of Theorem 5.3.3 below. The scaling (5.59) of the variables, however, is different.

Proof of Proposition 5.3.2. First, expand the shift operator as $\varepsilon \to 0$. From (5.59) we see that the increment by 1 in μ_i corresponds to the increment by $\log(q^{-1}) = \varepsilon$ in the scaled variable u_i. Therefore,

$$\mathcal{T}_{\mu_k} = \mathrm{Id} + \varepsilon \partial_{u_k} + \frac{\varepsilon^2}{2} \partial_{u_k}^2 + \mathsf{o}(\varepsilon^2),$$

and hence

$$\mathcal{T}_{\mu_{k+1}} \cdots \mathcal{T}_{\mu_\ell} = \mathrm{Id} + \varepsilon \sum_{\alpha=k+1}^{\ell} \partial_{u_\alpha} + \frac{\varepsilon^2}{2} \sum_{k+1 \le \alpha, \beta \le \ell} \partial_{u_\alpha, u_\beta} + \mathsf{o}(\varepsilon^2).$$

This implies that

$$\frac{1}{2}\mathfrak{H}_N^2 - 2\mathfrak{H}_N + \frac{3}{2} = -\varepsilon \sum_{i=1}^{N} \partial_{u_i} + \mathsf{o}(\varepsilon^2). \tag{5.60}$$

Next we address the scaling of $\mathfrak{H}_1$. Set

$$a_{k,\ell} = \begin{cases} S^{-2(\ell-k)} e^{u_\ell - u_k} & \text{if } 1 \le k \le \ell \le N, \\ 0 & \text{else.} \end{cases}$$

Expanding the coefficients $h_{k,\ell}$, we have

$$h_{0,0} = \left(1 - \varepsilon S + \frac{\varepsilon^2}{2} S^2\right) \sum_{j=1}^{N-1} a_{j,j+1} + \mathsf{o}(\varepsilon^2),$$

and (recall that we assume $k < \ell$)

$$\begin{aligned} h_{k,\ell} =& (a_{k+1,\ell} - a_{k,\ell} - a_{k+1,\ell+1} + a_{k,\ell+1}) \\ &+ \varepsilon S \Big\{ -(\ell-k-1)(a_{k+1,\ell} - a_{k,\ell}) + (\ell-k+1)(a_{k+1,\ell+1} - a_{k,\ell+1}) \Big\} \\ &+ \frac{\varepsilon^2}{2} S^2 \Big\{ (\ell-k-1)^2 (a_{k+1,\ell} - a_{k,\ell}) - (\ell-k+1)^2 (a_{k+1,\ell+1} - a_{k,\ell+1}) \Big\} + \mathsf{o}(\varepsilon^2). \end{aligned}$$

Together with the action of the shifts $\mathcal{T}$, we see that $h_{k,\ell}\mathcal{T}_{k+1} \cdots \mathcal{T}_\ell$ expands as

$$\begin{aligned} &(a_{k+1,\ell} - a_{k,\ell} - a_{k+1,\ell+1} + a_{k,\ell+1})\,\mathrm{Id} \\ &+ \varepsilon \Big\{ - S(\ell-k-1)(a_{k+1,\ell} - a_{k,\ell})\,\mathrm{Id} + S(\ell-k+1)(a_{k+1,\ell+1} - a_{k,\ell+1})\,\mathrm{Id} \\ &\qquad + (a_{k+1,\ell} - a_{k,\ell} - a_{k+1,\ell+1} + a_{k,\ell+1}) \sum_{\alpha=k+1}^{\ell} \partial_{u_\alpha} \Big\} \\ &+ \frac{\varepsilon^2}{2} \Big\{ S^2 (\ell-k-1)^2 (a_{k+1,\ell} - a_{k,\ell})\,\mathrm{Id} - S^2 (\ell-k+1)^2 (a_{k+1,\ell+1} - a_{k,\ell+1})\,\mathrm{Id} \\ &\qquad + (a_{k+1,\ell} - a_{k,\ell} - a_{k+1,\ell+1} + a_{k,\ell+1}) \sum_{k+1 \le \alpha, \beta \le \ell} \partial^2_{u_\alpha, u_\beta} \\ &\qquad + 2S\big(-(\ell-k-1)(a_{k+1,\ell} - a_{k,\ell}) + (\ell-k+1)(a_{k+1,\ell+1} - a_{k,\ell+1}) \big) \sum_{\alpha=k+1}^{\ell} \partial_{u_\alpha} \Big\} + \mathsf{o}(\varepsilon^2). \end{aligned}$$

To evaluate the summation $\sum_{0\le k<\ell\le N} h_{k,\ell}\mathcal{T}_{\mu_{k+1}}\cdots\mathcal{T}_{\mu_\ell}$, we use the identities in Proposition C.3.1. We obtain

$$h_{0,0}+\sum_{0\le k<\ell\le N} h_{k,\ell}\mathcal{T}_{\mu_{k+1}}\cdots\mathcal{T}_{\mu_\ell}$$
$$=N+\varepsilon\sum_{i=1}^{N}\partial_{u_i}+\varepsilon^2\left\{\frac{1}{2}\sum_{i=1}^{N}\partial_{u_i}^2-\sum_{1\le i<j\le N}S^{2(i-j)}e^{u_j-u_i}\left(S-\partial_{u_i}\right)\left(S+\partial_{u_j}\right)\right\}+\mathsf{o}(\varepsilon^2).$$

Together with (5.60) this yields the proof. □

For the next result we employ the spin Whittaker functions in the *additive parameters* u_i, where the multiplicative parameters $\underline{L}_N=(L_{N,N},\ldots,L_{N,1})$ are expressed through the u_i's as

$$L_{N,i}=S^{N+1-2i}e^{u_i}. \tag{5.61}$$

Denote the spin Whittaker function $\mathfrak{f}_{\underline{X}}(\underline{L}_N)$ in the additive parameters by $\mathfrak{f}^{add}_{\underline{X}}(u_1,\ldots,u_N)$. Here $\underline{X}=(X_1,\ldots,X_N)$ are such that $|X_i|<S$ for all i.

Theorem 5.3.3. *The spin Whittaker functions $\mathfrak{f}^{add}_{\underline{X}}(u_1,\ldots,u_N)$ in the additive variables (5.61) are eigenfunctions of the differential operators $\mathcal{H}_1$ (5.57) and $\mathcal{H}_2$ (5.58). In particular, we have*

$$\mathcal{H}_1\mathfrak{f}^{add}_{\underline{X}}(u_1,\ldots,u_N)=-\left(X_1+\cdots+X_N\right)\mathfrak{f}^{add}_{\underline{X}}(u_1,\ldots,u_N),$$
$$\mathcal{H}_2\mathfrak{f}^{add}_{\underline{X}}(u_1,\ldots,u_N)=-\frac{1}{2}\left(X_1^2+\cdots+X_N^2\right)\mathfrak{f}^{add}_{\underline{X}}(u_1,\ldots,u_N).$$

Proof. This result is a combination of the refined Pieri rules (5.56) viewed as eigenrelations for the spin q-Whittaker functions, and the convergence of the functions (Theorem 5.1.14) and the operators (Proposition 5.3.2). More precisely, under the scaling $x_i=e^{-\varepsilon X_i}$ for the eigenvalues $e_k(x_1,\ldots,x_N)$ we have

$$\frac{1}{\varepsilon}\left(e_1(x_1,\ldots,x_N)-N\right)\xrightarrow[\varepsilon\to 0]{}-X_1-\cdots-X_N,$$

and

$$\frac{1}{\varepsilon^2}\left(e_1(x_1,\ldots,x_N)-N+\frac{1}{2}e_N(x_1,\ldots,x_N)^2-2e_N(x_1,\ldots,x_N)+\frac{3}{2}\right)\xrightarrow[\varepsilon\to 0]{}\frac{1}{2}(X_1^2+\cdots X_N^2).$$

This leads to the desired results. □

5.3.3 Reduction to the quantum Toda Hamiltonian

It is natural to call the second order differential operator $\mathcal{H}_2$ (5.58) the *deformed quantum Toda Hamiltonian*. Namely, it is diagonal in the spin Whittaker functions which (formally) reduce, as $S\to+\infty$, to the classical $\mathfrak{gl}_n$ Whittaker functions (Section 5.1.8). Further justification to this name comes from the fact that the operator $\mathcal{H}_2$ itself degenerates as $S \to +\infty$ to the usual quantum Toda Hamiltonian

$$\mathcal{H}_2^{\mathrm{Toda}} := -\frac{1}{2}\sum_{i=1}^{N} \partial_{u_i}^2 + \sum_{i=1}^{N-1} e^{u_{i+1}-u_i}. \tag{5.62}$$

Proposition 5.3.4. *As $S \to +\infty$, the operator $\mathcal{H}_2$ (5.58) converges to the quantum Toda Hamiltonian $\mathcal{H}_2^{\mathrm{Toda}}$ (5.62).*

Proof. The factors $S^{-2(j-i)}$, $1 \le i \le j \le N$, in the sum in (5.58) decay at least as fast as S^{-2} as $S \to +\infty$. Therefore, the only surviving contribution in the limit $S \to +\infty$ comes from the terms with $j = i+1$, for which we have

$$S^{-2} e^{u_{i+1}-u_i}(S - \partial_{u_i})(S + \partial_{u_{i+1}}) \to e^{u_{i+1}-u_i}, \qquad S \to +\infty.$$

This completes the proof. □

Appendix A

Special functions

A.1 q-deformed quantities

Along the course of the thesis we largely made use of q-deformed quantities, such as q-Pochhammer symbols and q-hypergeometric series. The reader might consider these as fairly common and established notions, but, for the sake of completeness, we still like to dedicate this appendix to recall their definitions.

Assuming q is a parameter in the interval $[0,1)$, we define the q-Pochhammer symbol

$$(z;q)_n = \begin{cases} (1-z)(1-zq)\cdots(1-zq^{n-1}), & \text{if } n \in \mathbb{Z}_{>0}, \\ 1, & \text{if } n = 0, \\ (1-zq^n)^{-1}(1-zq^{n-1})^{-1}\cdots(1-zq)^{-1}, & \text{if } n \in \mathbb{Z}_{<0}, \end{cases} \tag{A.1}$$

for every meaningful $z \in \mathbb{C}$. We also denote the product of multiple q-Pochhammer symbols of the same order in the compact notation

$$(z_1;q)_n \cdots (z_k;q)_n = (z_1,\dots,z_k;q)_n. \tag{A.2}$$

When n is positive, the q-Pochhammer symbol (A.1) is a polynomial in z and it admits the expansion

$$(z;q)_n = \sum_{k=0}^{n} (-z)^k q^{\binom{k}{2}} \binom{n}{k}_q, \tag{A.3}$$

where we introduced the q-binomial

$$\binom{n}{k}_q = \frac{(q;q)_n}{(q;q)_k (q;q)_{n-k}}. \tag{A.4}$$

The q-binomial admits the combinatorial expansion

$$\binom{n}{k}_q = \sum_{\substack{I \subset \{1,\dots,n\} \\ |I| = k}} q^{\|I\| - \binom{k+1}{2}}, \tag{A.5}$$

with $I = \{i_1, \ldots, i_k\}$ and $\|I\| = i_1 + \cdots + i_k$.

When we let the integer n grow to $+\infty$, we see that the product in the left hand side of (A.1) is convergent and hence we can define

$$(z; q)_\infty = \prod_{j \geq 0} (1 - zq^j). \tag{A.6}$$

An important result concerning q-Pochhammer symbols is the summation identity

$$\sum_{k \geq 0} \frac{(a; q)_k}{(q; q)_k} z^k = \frac{(za; q)_\infty}{(z; q)_\infty} \qquad \text{for } a \in \mathbb{C}, |z| < 1, \tag{A.7}$$

which can be found in [Ism05], Theorem 12.2.5. and it is usually called q-binomial theorem. A slightly more general version of summation (A.7) is the so called q-Gauss summation ([Ism05], Theorem 12.2.4)

$$\sum_{n \geq 0} \left(\frac{c}{ab}\right)^n \frac{(a, b; q)_n}{(c, q; q)_n} = \frac{(c/a, c/b; q)_\infty}{(c, c/(ab); q)_\infty}, \qquad \text{for } |c/(ab)| < 1, \qquad \text{or } b \in q^{\mathbb{Z}_{<0}}. \tag{A.8}$$

The q-hypergeometric series

$${}_{r+1}\phi_r \left(\begin{matrix} a_1, a_2, \ldots, a_{r+1} \\ b_1, b_2, \cdots, \ b_r \end{matrix} \middle| q, z \right) = \sum_{k \geq 0} \frac{(a_1, \ldots, a_{r+1}; q)_k}{(b_1, \ldots, b_r, q; q)_k} z^k, \tag{A.9}$$

is defined for generic parameters $a_1, \ldots, a_{r+1} \in \mathbb{C}$, $b_1, \ldots, b_r \in \mathbb{C} \setminus q^{\mathbb{Z}_{<0}}$ and $|z| < 1$. In the case when at least one of the a_j is of the form q^{-k}, for some non-negative integer k, the q-hypergeometric series (A.9) becomes a finite sum and its definition holds also for more general complex numbers z. The regularized terminating q-hypergeometric function is also defined as

$${}_{r+1}\bar{\phi}_r \left(\begin{matrix} q^{-n}, a_1, \ldots, a_r \\ b_1, \ b_2, \cdots, b_r \end{matrix} \middle| q, z \right) = \sum_{k=0}^{n} z^k \frac{(q^{-n}; q)_k}{(q; q)_k} \prod_{j=1}^{r} (a_j; q)_k (q^k b_j; q)_{n-k}. \tag{A.10}$$

In the thesis we also made use of functions $\boldsymbol{\upsilon}_j$, defined as

$$\boldsymbol{\upsilon}_j(z) = \sum_{k \geq 1} \frac{k^j z^k}{1 - q^k}. \tag{A.11}$$

They are related to the more classical q-polygamma function [Wei]

$$\boldsymbol{\psi}_q(\theta) = -\log(1 - q) + \log(q) \sum_{n \geq 0} \frac{q^{n+\theta}}{1 - q^{n+\theta}},$$

since

$$\boldsymbol{\upsilon}_0(z) = \frac{1}{\log(q)} \left[\log(1 - q) + \boldsymbol{\psi}_q\left(\frac{\log(z)}{\log(q)}\right) \right] \tag{A.12}$$

and

$$\frac{d}{dz}\boldsymbol{\upsilon}_j(z) = \frac{1}{z}\boldsymbol{\upsilon}_{j+1}(z). \tag{A.13}$$

The inverse of the infinite q-Pochhammer symbol (A.6) is often called q-exponential and through it one can define a q-deformed notion of the common Laplace transform. For a given $f \in \ell^1(\mathbb{Z})$ the function

$$\widetilde{f}(\zeta) = \sum_{n\in\mathbb{Z}} \frac{f(n)}{(q^n\zeta;q)_\infty} \qquad \text{for } \zeta \in \mathbb{C}\setminus q^{\mathbb{Z}} \tag{A.14}$$

is the q-Laplace transform of f. As for the usual Laplace transform, the operation $f \mapsto \widetilde{f}$ admits an inverse. This is discussed, for example, in [IS19] and we do not report the exact form of the inverse q-Laplace transform as we do not explicitly make use of it during this thesis.

The q-gamma and the q-beta functions are

$$\Gamma_q(X) = \frac{(q;q)_\infty}{(q^X;q)_\infty}(1-q)^{1-X}, \qquad \mathrm{B}_q(X,Y) = \frac{\Gamma_q(X)\Gamma_q(Y)}{\Gamma_q(X+Y)}, \qquad \text{for } X,Y>0. \tag{A.15}$$

A.1.1 q-beta binomial distribution

Recall the definition of the q-deformed beta-binomial distribution $\varphi_{q,\mu,\nu}$ from [Pov13], [Cor14].

Definition A.1.1. For $m \in \mathbb{Z}_{\geq 0}$, consider the following distribution on $\{0,1,\dots,m\}$:

$$\varphi_{q,\mu,\nu}(j \mid m) = \mu^j \, \frac{(\nu/\mu;q)_j(\mu;q)_{m-j}}{(\nu;q)_m} \frac{(q;q)_m}{(q;q)_j(q;q)_{m-j}}, \qquad 0 \leq j \leq m. \tag{A.16}$$

When $m = +\infty$, extend the definition as

$$\varphi_{q,\mu,\nu}(j \mid \infty) = \mu^j \frac{(\nu/\mu;q)_j}{(q;q)_j}\frac{(\mu;q)_\infty}{(\nu;q)_\infty}, \qquad j \in \mathbb{Z}_{\geq 0}. \tag{A.17}$$

The distribution depends on q and two other parameters μ,ν.

When $0 \leq \mu \leq 1$ and $\nu \leq \mu$, the weights $\varphi_{q,\mu,\nu}(j \mid m)$ are nonnegative.[1] They also sum to one:

$$\sum_{j=0}^{m} \varphi_{q,\mu,\nu}(j \mid m) = 1, \qquad m \in \{0,1,\dots\} \cup \{+\infty\}.$$

Particular cases of the q-deformed beta-binomial are the q-negative binomial distribution defined as

$$X \sim q\mathrm{NB}(b,p) \qquad \Longrightarrow \qquad \mathbb{P}(X=n) = p^n \frac{(b;q)_n}{(q;q)_n}\frac{(p;q)_\infty}{(pb;q)_\infty}, \qquad \text{for all } n \in \mathbb{Z}_{\geq 0} \tag{A.18}$$

[1] These conditions do not exhaust the full range of (q,μ,ν) for which the weights are nonnegative. See, e.g., [BP18a, Section 6.6.1] for additional families of parameters leading to nonnegative weights.

and the q-Poisson distribution

$$X \sim q\text{-Poi}(p) \qquad \Longrightarrow \qquad \mathbb{P}(X = n) = \frac{p^n}{(q;q)_n}(p;q)_\infty, \qquad \text{for all } n \in \mathbb{Z}_{\geq 0} \tag{A.19}$$

The q-hypergeometric distribution is

$$\psi_{q,a,b,c}(n) = \left(\frac{c}{ab}\right)^n \frac{(a,b;q)_n}{(c,q;q)_n} \frac{(c,c/(ab);q)_\infty}{(c/a,c/b;q)_\infty}. \tag{A.20}$$

The fact that the weights (A.20) sum to one over $n \in \mathbb{Z}_{\geq 0}$ follows from the q-Gauss sum (A.8).

A.2 Classical special functions

It is well-known that $\Gamma_q(X)$ converges to $\Gamma(X)$ as $q \to 1$ uniformly for $X > 0$, where Γ is the usual gamma function $\Gamma(z) = \int_0^\infty e^{-t}t^{z-1}dt$, $z > 0$ (e.g., see [And86]). Hence $\mathrm{B}_q(X,Y) \to \mathrm{B}(X,Y)$ uniformly for $X, Y > 0$, where B is the beta function

$$\mathrm{B}(x,y) = \frac{\Gamma(x)\Gamma(y)}{\Gamma(x+y)} = \int_0^1 t^{x-1}(1-t)^{y-1}dt, \qquad x,y > 0. \tag{A.21}$$

The *inverse gamma distribution* $\Gamma^{-1}(\alpha)$ on $(0,+\infty)$ with a parameter $\alpha > 0$ is

$$\Gamma^{-1}(\alpha)[x] = \frac{x^{-1-\alpha}e^{-1/x}}{\Gamma(\alpha)}. \tag{A.22}$$

The *beta distribution* on $(0,1)$ with (real) parameters $m,n > 0$ has density

$$\mathcal{B}(m,n)[x] = \frac{x^{m-1}(1-x)^{n-1}}{\mathrm{B}(n,m)} \qquad \text{for } x \in (0,1).$$

We also recall that a random variable with *negative binomial* distribution has probability mass function

$$\mathcal{NB}(r,p)[k] = p^k(1-p)^r\binom{k+r-1}{k}, \qquad \text{for } k \in \mathbb{Z}_{\geq 0}$$

and $r > 0$, $0 \leq p \leq 1$. Sampling x in the interval $(0,1)$ with $\mathcal{B}(m,n+k)$ law, where k is a $\mathcal{NB}(r,p)$ independent random variable generates the *negative beta binomial* distribution on $(0,1)$. It has the probability density

$$\mathcal{NBB}(r,p,m,n)[x] = \frac{(1-p)^r x^{m-1}(1-x)^{n-1}}{\mathrm{B}(n,m)}\, {}_2F_1\left(\begin{matrix} r, & n+m \\ n & - \end{matrix}\,\middle|\, p(1-x)\right), \tag{A.23}$$

where we used the Gauss hypergeometric function

$${}_2F_1\left(\begin{matrix} a, & b \\ c & - \end{matrix}\,\middle|\, z\right) = \sum_{k\geq 0} \frac{(a)_k(b)_k}{(c)_k}\frac{z^k}{k!}, \tag{A.24}$$

and $(r)_k = r(r+1)\cdots(r+k-1)$ is the Pochhammer symbol. Note that the inverse gamma, beta, and the negative beta binomial are continuous distributions, while the negative binomial is a discrete distribution.

Appendix B

Yang-Baxter equations

Here we review the Yang-Baxter equations used throughout the thesis.

B.1 $U_q(\widehat{\mathfrak{sl}}_2)$ R-matrices

B.1.1 Basic cases

Most of the Yang-Baxter equations we use can be traced to the following basic one:

Proposition B.1.1. *Consider the vertex weights w, r defined respectively in Figure 2.3 and Figure B.1. Then we have*

$$\begin{aligned}\sum_{k_1,k_2,k_3} r_{u/v}(i_2,i_1;k_2,k_1)\, w_{v,s}(i_3,k_1;k_3,j_1)\, w_{u,s}(k_3,k_2;j_3,j_2)\\ = \sum_{k_1',k_2',k_3'} w_{v,s}(k_3',i_1;j_3,k_1')\, w_{u,s}(i_3,i_2;k_3',k_2')\, r_{u/v}(k_2',k_1';j_2,j_1)\end{aligned} \tag{B.1}$$

for all $i_1, i_2, j_1, j_2 \in \{0,1\}$ and $i_3, j_3 \in \mathbb{Z}_{\geq 0}$. A visual representation of this equation is given in Figure B.2.

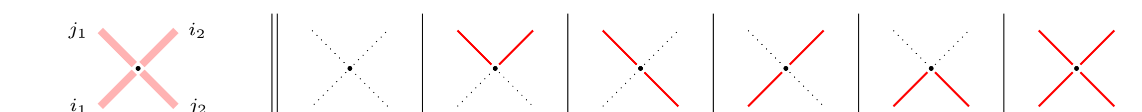

$r_z(i_1,j_1;i_2,j_2)$	1	$\frac{z(1-q)}{1-qz}$	$\frac{1-z}{1-qz}$	$\frac{q(1-z)}{1-qz}$	$\frac{1-q}{1-qz}$	1

Figure B.1: In the top row we see all acceptable configurations of paths entering and exiting a vertex; below we reported the corresponding vertex weights $r_z(i_1, j_1; i_2, j_2)$.

Proof of Proposition B.1.1. This is established by a straightforward verification. Equation (B.1) appeared in several other works, including [Man14], [Bor17], [BW17]. □

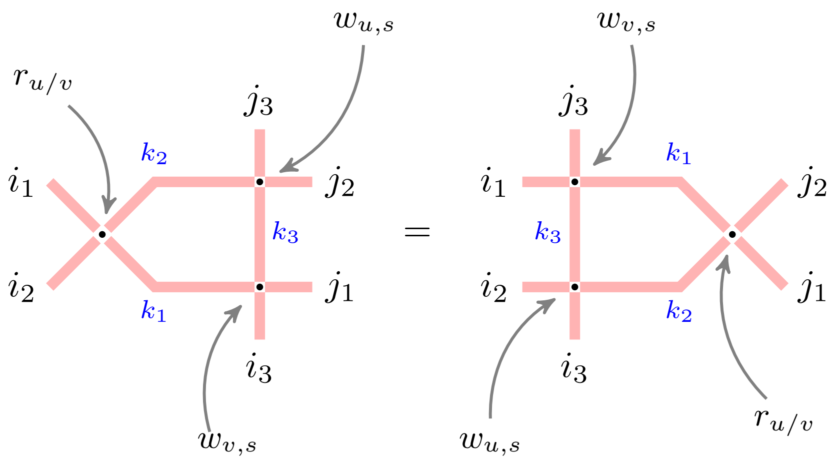

Figure B.2: A schematic representation of the Yang-Baxter equation (B.1).

As explained in Section 2.2.2, from vertex weights $w_{u,s}$ one can define the dual weights $w^*_{v,s}$ by changing u to $1/v$, swapping the value of horizontal occupation numbers $0 \leftrightarrow 1$, and multiplying by $(s-v)/(1-sv)$ in order to assign weight 1 to the empty configuration. These manipulations clearly preserve the structure of the Yang-Baxter equation, provided that the same swapping of the occupation numbers is applied to the cross weight r_z. This leads to the definition of the cross weight R_z, see Figure B.3, also normalized so that the empty configuration has weight 1.

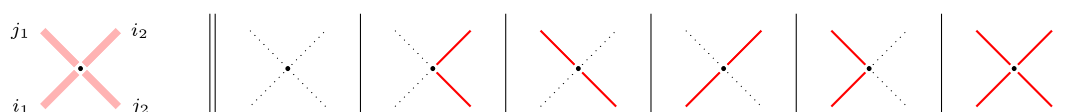

$R_z(i_1, j_1; i_2, j_2)$	1	$\frac{(1-q)z}{1-z}$	$\frac{1-qz}{1-z}$	$\frac{1-qz}{1-z}$	$\frac{1-q}{1-z}$	q

Figure B.3: The cross vertex weights $R_z(i_1, j_1; i_2, j_2)$.

Proposition B.1.2. *Consider the vertex weights w, w^* and R, defined respectively in Figures 2.3 and 2.5, and Figure B.3. Then we have*

$$\begin{aligned}&\sum_{k_1,k_2,k_3} R_{uv}(i_2, i_1; k_2, k_1)\, w^*_{v,s}(i_3, k_1; k_3, j_1)\, w_{u,s}(k_3, k_2; j_3, j_2)\\ &\qquad = \sum_{k'_1,k'_2,k'_3} w^*_{v,s}(k'_3, i_1; j_3, k'_1)\, w_{u,s}(i_3, i_2; k'_3, k'_2)\, R_{uv}(k'_2, k'_1; j_2, j_1)\end{aligned} \tag{B.2}$$

for all $i_1, i_2, j_1, j_2 \in \{0, 1\}$ and $i_3, j_3 \in \mathbb{Z}_{\geq 0}$.

B.1.2 Fusion

Through a fusion procedure we generalize vertex weights $w_{u,s}$ and allow configurations with multiple paths crossing a vertex in the horizontal direction. This technique of generalizing solutions to the Yang-Baxter equation was originally introduced in [KRS81] and consist in collapsing together a series of vertically attached vertices with spectral parameters forming a geometric progression of ratio q. The fusion of vertex weights also admits a probabilistic interpretation [CP16], [BP18a], [BW17].

Define the fused vertex weight

$$\begin{aligned} w^{(J)}_{u,s}(i_1,j_1;i_2,j_2) = \mathbf{1}_{i_1+j_1=i_2+j_2} \, & \frac{(-1)^{i_1+j_2} q^{\frac{1}{2}i_1(i_1-1+2j_1)} s^{j_2-i_1} u^{i_1} (u/s;q)_{j_1-i_2} (q;q)_{j_1}}{(q;q)_{i_1}(q;q)_{j_2}(su;q)_{j_1+i_1}} \\ & \times {}_4\overline{\phi}_3 \left(\begin{matrix} q^{-i_1}; q^{-i_2}, suq^J, qs/u \\ s^2, q^{1+j_2-i_1}, q^{1-i_2-j_2+J} \end{matrix} \,\middle|\, q,q \right), \end{aligned} \tag{B.3}$$

where ${}_4\overline{\phi}_3$ is the regularized q-hypergeometric series (A.9). Here J is originally a positive integer representing the number of vertices which were fused together. However, it is easy to see that $w^{(J)}$ depends on q^J in a rational way, thus q^J can be regarded as the fourth independent parameter in (B.3) (along with u, s, and q). Since the regularized series ${}_4\overline{\phi}_3$ terminates, (B.3) depends on all these parameters in a rational way. Moreover, in case $i_1, i_2 \to \infty$, the weight w loses its dependence of j_1 and we have

$$\lim_{n\to\infty} w^{(J)}_{u,s}(n,j_1;n+j_1-j_2,j_2) = (-uq^J)^{j_2} \frac{(q^{-J};q)_{j_2}}{(q;q)_{j_2}} \frac{(suq^J;q)_\infty}{(su;q)_\infty}. \tag{B.4}$$

Just as in the $J=1$ case, the fused boundary weight is obtained removing the normalization factor from (B.4), and we define

$$w^{(J)}_{u,s}\left(\begin{matrix} \infty \\ \cdot\!\!\equiv\; k \\ \infty \end{matrix} \right) = (-uq^J)^k \frac{(q^{-J};q)_k}{(q;q)_k}. \tag{B.5}$$

This normalization is needed to assign weight 1 to the empty configuration of paths in the grid. The fused analog of the dual weights w is defined similarly to (2.9):

$$w^{*,(I)}_{v,s}(i_1,j_1;i_2,j_2) = \frac{(s^2;q)_{i_1}(q;q)_{i_2}}{(q;q)_{i_1}(s^2;q)_{i_2}} w^{(I)}_{v,s}(i_2,j_1;i_1;j_2). \tag{B.6}$$

These quantities also depend on v, s, q, and q^I in a rational way.

What makes the fused weights remarkable is that they satisfy a general version of the Yang-Baxter equation (previously in Section B.1.1 the horizontal occupation numbers had to be either 0 or 1). In order to state this equation we need to consider the fusion of the cross weights R_z leading to

$$\begin{aligned} R^{(I,J)}_z(i_1,j_1;i_2,j_2) := \mathbf{1}_{i_2+j_1=i_1+j_2} \, & \frac{q^{i_2 i_1+\frac{1}{2}j_2(j_2-1)+j_2 J}(-z)^{j_2}(q;q)_{j_1}}{(z;q)_{j_1+i_2}(q;q)_{j_2}(q;q)_{i_2}(q^{1-J}/z;q)_{i_1-j_1}} \\ & \times {}_4\overline{\phi}_3 \left(\begin{matrix} q^{-i_2}; q^{-i_1}, zq^I, q^{1-J}/z \\ q^{-J}, q^{1+j_2-i_2}, q^{1-i_1-j_2+I} \end{matrix} \,\middle|\, q,q \right). \end{aligned} \tag{B.7}$$

Proposition B.1.3. *Consider the weights $w^{(J)}, w^{*,(I)}$ and $R^{(I,J)}$ defined in (B.3), (B.6), (B.7). Then we have*

$$\begin{aligned}\sum_{k_1,k_2,k_3} R^{(I,J)}_{uv}(i_2,i_1;k_2,k_1)\, w^{*,(I)}_{v,s}(i_3,k_1;k_3,j_1)\, w^{(J)}_{u,s}(k_3,k_2;j_3,j_2)\\ = \sum_{k_1',k_2',k_3'} w^{*,(I)}_{v,s}(k_3',i_1;j_3,k_1')\, w^{(J)}_{u,s}(i_3,i_2;k_3',k_2')\, R^{(I,J)}_{uv}(k_2',k_1';j_2,j_1),\end{aligned} \tag{B.8}$$

for all admissible values of i_1, i_2, j_1, j_2 (that is, $i_1, j_1 \in \{0, 1, \ldots, I-1\}$ for I a positive integer, or $i_1, j_1 \in \mathbb{Z}_{\geq 0}$ if q^I is generic, and similarly for i_2, j_2), and $i_3, j_3 \in \mathbb{Z}_{\geq 0}$.

Note that in (B.8) (and in all other Yang-Baxter equations in this Appendix) for fixed boundary occupation numbers $i_1, i_2, i_3, j_1, j_2, j_3$ the sums over k and k' indeces in both sides are finite due to arrow preservation, so there are no convergence issues when i_3 and j_3 are finite.

Remark B.1.4. The fused cross weights $R^{(I,J)}$ inherit symmetries of the unfused weight R of Figure B.3. One of these is given by the identity

$$R^{(I,J)}_z(i_1,j_1;i_2,j_2) = R^{(J,I)}_z(j_1,i_1;j_2,i_2) \tag{B.9}$$

for all $i_1, j_1, i_2, j_2 \in \mathbb{Z}_{\geq 0}$.

Proposition B.1.5. *Consider the vertex weight $R^{(I,J)}_z$ defined in (B.7). Then we have*

$$\sum_{k_1,k_2} R^{(I,J)}_z(a_2,a_1;k_1,k_2) = R^{(I,J)}_z(0,I;0,I) = R^{(I,J)}_z(J,0;J,0) = \frac{(zq^I;q)_\infty (zq^J;q)_\infty}{(z;q)_\infty (zq^{I+J};q)_\infty} \tag{B.10}$$

for all $a_1, a_2 \in \mathbb{Z}_{\geq 0}$.

Proof. The second and the third equalities in (B.10) follow, after algebraic manipulations, from the definition of the fused cross weight $R^{(I,J)}_z$ given in (B.7).

The first equality in (B.10) is a trivial check in the case when $I = J = 1$, using the definition of R_z of Figure B.3. It lifts to more general I, J as the fusion procedure does not affect the structure of the identity. □

B.1.3 Spin q-Whittaker specialization

The spin q-Whittaker specialization of the general fused weights (B.3), (B.6) is obtained by setting $u = s$ and $q^J = -x/s$ (recall that one can regard q^J as a generic parameter). After this specialization the complicated expression $w^{(J)}_{u,s}(i_1,j_1;i_2,j_2)$ (B.3) factorizes and becomes $W_{x,s}(i_1,j_1;i_2,j_2)$ given by (2.13). Analogously, the dual fused weight $w^{*,(I)}_{v,s}(i_1,j_1;i_2,j_2)$ (B.6) turns into $W^*_{y,s}(i_1,j_1;i_2,j_2)$ (2.29) after setting $v = s$ and $q^I = -y/s$.

The most general Yang Baxter equation (B.8) specializes to Yang-Baxter equations involving $W_{x,s}$ and $W^*_{y,s}$ as long as the corresponding specializations are applied to the cross weight $R^{(I,J)}_{uv}$, too. Let us record the resulting identities:

Proposition B.1.6. *We have the following Yang-Baxter equations:*

$$\begin{aligned}\sum_{k_1,k_2,k_3} \mathcal{R}_{x,v,s}(i_2,i_1;k_2,k_1)\, w^*_{v,s}(i_3,k_1;k_3,j_1)\, W_{x,s}(k_3,k_2;j_3,j_2)\\ = \sum_{k'_1,k'_2,k'_3} w^*_{v,s}(k'_3,i_1;j_3,k'_1)\, W_{x,s}(i_3,i_2;k'_3,k'_2)\, \mathcal{R}_{x,v,s}(k'_2,k'_1;j_2,j_1);\end{aligned} \tag{B.11}$$

$$\begin{aligned}\sum_{k_1,k_2,k_3} \mathbb{R}_{x,y,s}(i_2,i_1;k_2,k_1)\, W^*_{y,s}(i_3,k_1;k_3,j_1)\, W_{x,s}(k_3,k_2;j_3,j_2)\\ = \sum_{k'_1,k'_2,k'_3} W^*_{y,s}(k'_3,i_1;j_3,k'_1)\, W_{x,s}(i_3,i_2;k'_3,k'_2)\, \mathbb{R}_{x,y,s}(k'_2,k'_1;j_2,j_1).\end{aligned} \tag{B.12}$$

The cross vertex weights in (B.11) *are given in Figure B.4. In the third identity* (B.12) *the cross vertex weights do not factorize (here $i_1,i_2,j_1,j_2 \in \mathbb{Z}_{\geq 0}$):*

$$\begin{aligned}\mathbb{R}_{x,y,s}(i_1,j_1;i_2,j_2) = \mathbf{1}_{i_2+j_1=i_1+j_2} \frac{q^{i_2 i_1+\frac{1}{2}j_2(j_2-1)}(sx)^{j_2}(q;q)_{j_1}}{(s^2;q)_{j_1+i_2}(q;q)_{j_2}(q;q)_{i_2}(-q/(sx);q)_{i_1-j_1}}\\ \times {}_4\overline{\phi}_3\left(\begin{matrix} q^{-i_2};q^{-i_1},-sy,-q/(sx)\\ -s/x,q^{1+j_2-i_2},-yq^{1-i_1-j_2}/s\end{matrix}\,\middle|\, q,q\right).\end{aligned} \tag{B.13}$$

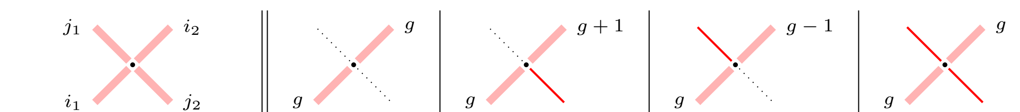

$\mathcal{R}_{\xi,v,s}(i_1,j_1;i_2,j_2)$	$\frac{1-q^g sv}{1-sv}$	$\frac{\xi v+q^g sv}{1-sv}$	$\frac{1-q^g}{1-sv}$	$\frac{q^g+v\xi}{1-sv}$

Figure B.4: The cross vertex weights $\mathcal{R}_{x,v,s}(i_1,j_1;i_2,j_2)$, $j_1,j_2\in\{0,1\}$, $i_1,i_2\in\mathbb{Z}_{\geq 0}$.

So far we have listed Yang-Baxter relations between weights W and their dual form W^*. Nevertheless eq. (B.1) extends, after fusion also to a Yang-Baxter equation for pairs of W weights. Let us introduce the cross vertex weight

$$\bar{r}_{x,y}(i_1,j_1;i_2,j_2) := \mathbf{1}_{i_1+j_1=i_2+j_2}\,\mathbf{1}_{i_1\geq j_2}\,(y/x)^{j_2}\,\frac{(-s/y;q)_{j_2}(y/x;q)_{i_1-j_2}(q;q)_{i_1}}{(q;q)_{j_2}(q;q)_{i_1-j_2}(-s/x;q)_{i_1}}. \tag{B.14}$$

Proposition B.1.7. *For any $i_1,i_2,i_3,j_1,j_2,j_3\in\mathbb{Z}_{\geq 0}$, we have*

$$\begin{aligned}\sum_{k_1,k_2,k_3\geq 0} \bar{r}_{x,y}(i_2,i_1;k_2,k_1)W_{y,s}(i_3,k_1;k_3,j_1)W_{x,s}(k_3,k_2;j_3,j_2)\\ = \sum_{k'_1,k'_2,k'_3\geq 0} W_{x,s}(i_3,i_2;k'_3,k'_2)W_{y,s}(k'_3,i_1;j_3,k'_1)\bar{r}_{x,y}(k'_2,k'_1;j_2,j_1),\end{aligned} \tag{B.15}$$

where $W^{\bullet}$ are the bulk weights defined by (2.13)*. See Figure B.2 for a graphical interpretation.*

Proof. This is obtained in [BW17, Corollary 4.3] via fusion from the elementary Yang–Baxter equation for the higher spin $\mathfrak{sl}_2$ vertex model. Note that the claim of [BW17, Corollary 4.3] contains a typo: the spectral parameters x, y in the definition of the cross vertex weight should be swapped. This is corrected here by defining $R_{x,y}$ in (B.14) with parameters already swapped. ☐

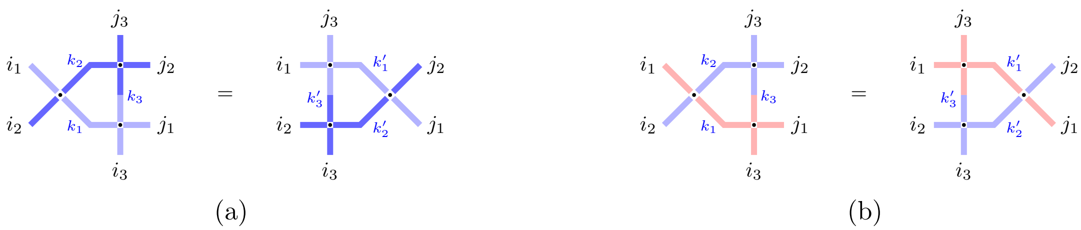

Figure B.5: Graphical representation of the Yang–Baxter equations with non-dual weights and dual weights resp. (a) and (b).

B.1.4 Scaled geometric specialization

The scaled geometric specialization of the general fused weight $w^{(J)}_{u,s}$ is given by setting $u = -\epsilon\alpha$, $q^J = 1/\epsilon$ and taking the limit $\epsilon \to 0$. Analogously we can specialize the dual weight $w^{*,(I)}_{v,s}$ taking $v = -\beta\epsilon$, $q^I = 1/\epsilon$ and again $\epsilon \to 0$. In this case the expessions (B.3), (B.5) simplify:

$$\breve{w}_{\alpha,s}(i_1, j_1; i_2, j_2) = \mathbf{1}_{i_1+j_1=i_2+j_2} \frac{(-\alpha/s)^{i_1}(-s)^{j_2}(q;q)_{j_1}}{(q;q)_{i_1}(q;q)_{j_2}} \, {}_3\bar{\phi}_2 \left(\begin{matrix} q^{-i_1}; q^{-i_2}, -s\alpha \\ s^2, q^{1+j_2-i_1} \end{matrix} \middle| \, q, -\frac{sq^{1+i_2+j_2}}{\alpha} \right), \tag{B.16}$$

and

$$\breve{w}_{\alpha,s}\left(\begin{matrix} \infty \\ \cdot\!\equiv k \\ \infty \end{matrix} \right) = \frac{\alpha^k}{(q;q)_k}. \tag{B.17}$$

The dual weights $\breve{w}^*_{\beta,s}$ are defined in the usual way as in (2.9).

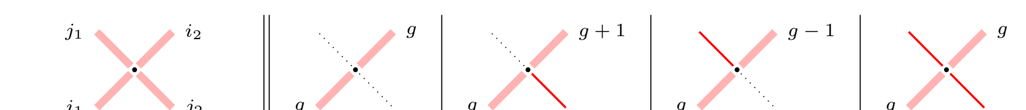

$R^{(\mathrm{sHL,sg})}_{\alpha,v}(i_1, j_1; i_2, j_2)$	1	αv	$1 - q^g$	$q^g + v\alpha$

Figure B.6: The cross vertex weight $R^{(\mathrm{sHL,sg})}_{\alpha,v}(i_1, j_1; i_2, j_2)$, $j_1, j_2 \in \{0, 1\}$, $i_1, i_2 \in \mathbb{Z}_{\geq 0}$.

We also consider the scaled geometric specialization of the fused cross weight $R^{(I,J)}$, in this case in the parameters v, q^I, defining

$$R^{(\mathrm{sg},J)}_{u,\beta}(i_1,j_1;i_2,j_2) = \mathbf{1}_{i_2+j_1=i_1+j_2} \frac{(-uq^J\beta)^{i_2}(q^{-J};q)_{i_2}}{(q;q)_{i_2}(q^{-J};q)_{i_1}} \, {}_3\overline{\phi}_2 \left(\begin{matrix} q^{-i_1}; q^{-i_2}, -u\beta \\ q^{-J}, q^{1+j_2-i_2} \end{matrix} \middle| \, q, -\frac{q^{1+i_1+j_2}}{uq^J\beta} \right). \tag{B.18}$$

The scaled geometric specialization of $R^{(I,J)}$ in the parameters u, q^J can be derived from (B.18) using the symmetry (B.9) and it is

$$R^{(I,\mathrm{sg})}_{\alpha,v}(i_1,j_1;i_2,j_2) = R^{(\mathrm{sg},I)}_{v,\alpha}(j_1,i_1;j_2,i_2). \tag{B.19}$$

Further degenerations of $R^{(I,\mathrm{sg})}_{\alpha,v}$ involve specializations of parameters v, q^I in one of the three cases, sHL(v) (which is simply $I=1$), sqW(y), or sg(β). These cross vertex weights are given, respectively, in Figure B.6 and below:

$$R^{(\mathrm{sqW},\mathrm{sg})}_{\alpha,y}(i_1,j_1;i_2,j_2) = \mathbf{1}_{i_2+j_1=i_1+j_2} \frac{(\alpha y)^{j_2}(-s/y;q)_{j_2}}{(q;q)_{j_2}(-s/y;q)_{j_1}} \, {}_3\overline{\phi}_2 \left(\begin{matrix} q^{-j_1}; q^{-j_2}, -s\alpha \\ -s/y, q^{1+i_1-j_1} \end{matrix} \middle| \, q, \frac{q^{1+j_1+i_2}}{\alpha y} \right), \tag{B.20}$$

$$R^{(\mathrm{sg},\mathrm{sg})}_{\alpha,\beta}(i_1,j_1;i_2,j_2) = \mathbf{1}_{i_2+j_1=i_1+j_2} \frac{(\alpha\beta)^{j_2}}{(q;q)_{j_2}} \, {}_2\overline{\phi}_1 \left(\begin{matrix} q^{-j_1}; q^{-j_2} \\ q^{1+i_1-j_1} \end{matrix} \middle| \, q, \frac{q^{1+j_1+i_2}}{\alpha\beta} \right). \tag{B.21}$$

These cross vertex weights enter a number of Yang-Baxter equations which are specializations of the general fused one (B.8):

Proposition B.1.8. *We have the following Yang-Baxter equations:*

$$\begin{aligned}\sum_{k_1,k_2,k_3} & R^{(\mathrm{sHL},\mathrm{sg})}_{\alpha,v}(i_2,i_1;k_2,k_1)\, w^*_{v,s}(i_3,k_1;k_3,j_1)\, \breve{w}_{\alpha,s}(k_3,k_2;j_3,j_2) \\ &= \sum_{k_1',k_2',k_3'} w^*_{v,s}(k_3',i_1;j_3,k_1')\, \breve{w}_{\alpha,s}(i_3,i_2;k_3',k_2')\, R^{(\mathrm{sHL},\mathrm{sg})}_{\alpha,v}(k_2',k_1';j_2,j_1);\end{aligned} \tag{B.22}$$

$$\begin{aligned}\sum_{k_1,k_2,k_3} & R^{(\mathrm{sqW},\mathrm{sg})}_{\alpha,y}(i_2,i_1;k_2,k_1)\, W^*_{y,s}(i_3,k_1;k_3,j_1)\, \breve{w}_{\alpha,s}(k_3,k_2;j_3,j_2) \\ &= \sum_{k_1',k_2',k_3'} W^*_{y,s}(k_3',i_1;j_3,k_1')\, \breve{w}_{\alpha,s}(i_3,i_2;k_3',k_2')\, R^{(\mathrm{sqW},\mathrm{sg})}_{\alpha,y}(k_2',k_1';j_2,j_1);\end{aligned} \tag{B.23}$$

$$\begin{aligned}\sum_{k_1,k_2,k_3} & R^{(\mathrm{sg},\mathrm{sg})}_{\alpha,\beta}(i_2,i_1;k_2,k_1)\, \breve{w}^*_{\beta,s}(i_3,k_1;k_3,j_1)\, \breve{w}_{\alpha,s}(k_3,k_2;j_3,j_2) \\ &= \sum_{k_1',k_2',k_3'} \breve{w}^*_{\beta,s}(k_3',i_1;j_3,k_1')\, \breve{w}_{\alpha,s}(i_3,i_2;k_3',k_2')\, R^{(\mathrm{sg},\mathrm{sg})}_{\alpha,\beta}(k_2',k_1';j_2,j_1).\end{aligned} \tag{B.24}$$

Dual cases of (B.22),(B.23),(B.24) *obtained swapping the specializations are easily derived making use of the symmetry of the cross weight* (B.19).

In Chapter 2, Cauchy Identities for spin Hall-Littlewood and spin q-Whittaker functions were stated as corollaries of the Yang-Baxter equations given in this appendix. In particular, the emergence of the prefactors in the right-hand sides of all the skew Cauchy identities can be traced to Proposition B.1.5.

B.2 Corner R-matrices

In this section we list the Yang–Baxter equations involving the class of vertex weight $W^{\lrcorner}$.

B.2.1 Non dual sqW/sqW Yang–Baxter equation

Proposition B.2.1. *For any $i_1, i_2, j_1, j_2 \in \mathbb{Z}_{\geq 0}$, we have*

$$\sum_{k_1,k_2\geq 0} \bar{r}_{x,y}(i_2, i_1; k_2, k_1) W^{\lrcorner}_{y,s}(k_1) W_{x,s}(k_1, k_2; j_2, j_1) W^{\lrcorner}_{x,s}(j_1) \\ = W^{\lrcorner}_{x,s}(i_2) W_{y,s}(i_2, i_1; j_2, j_1) W^{\lrcorner}_{y,s}(j_1), \tag{B.25}$$

where $W^{\lrcorner}$ are the right corner weight defined by (2.14). See Figure B.5 (a) *for an illustration.*

Proof. Expanding both right and left-hand side of (B.25) and simplifying common factors we end up with the identity

$$\sum_{k=j_1}^{i_2} (y/x)^{k-j_1} \frac{(y/x;q)_{i_2-k}}{(q;q)_{i_2-k}} \frac{(-sx;q)_{k-j_1}}{(q;q)_{k-j_1}} = \frac{(-sy;q)_{i_2-j_1}}{(q;q)_{i_2-j_1}},$$

which follows from the q-Gauss summation (A.8). □

B.2.2 Yang–Baxter equations with dual weights

Our additional Yang–Baxter equations involve the dual sHL weights $w^*_{v,s}$ which are given in (2.9) in the text and the dual sqW weights (2.28)–(2.30). We use the cross vertex weights $\mathcal{R}_{x,v,s}$ given in Figure B.4 and the cross vertex weights (B.13).

Proposition B.2.2. *For any $i_1 \in \{0,1\}$ and $i_2, i_3, j_2, j_3 \in \mathbb{Z}_{\geq 0}$, we have*

$$\sum_{k_1,k_2,k_3\geq 0} \mathcal{R}_{x,v,s}(i_2, i_1; k_2, k_1)\, W^{*,\urcorner}(i_3, k_1; k_3)\, W_{x,s}(k_3, k_2; j_3, j_2)\, W^{\lrcorner}_{x,s}(j_2) \\ = \sum_{k'_1,k'_2,k'_3\geq 0} W_{x,s}(i_3, i_2; k'_3, k'_2)\, W^{\lrcorner}_{x,s}(k'_2)\, w^*_{v,s}(k'_3, i_1; j_3, k'_1)\, W^{*,\urcorner}(k'_2, k'_1; j_2). \tag{B.26}$$

See Figure B.5 (b) *for a graphical interpretation.*

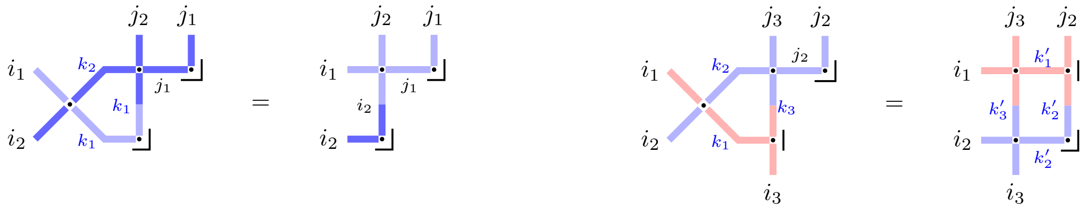

Figure B.7: Graphical representation of the Yang–Baxter equations with corner R-matrices.

Proof. Consider separately the cases $i_1 = 0$ and $i_1 = 1$. Start with $i_1 = 0$. We see that (B.26) is nontrivial only when $i_2 + i_3 = j_2 + j_3$ (say $j_2 = i_2 + i_3 - j_3$) and $j_3 \geq i_2$. Under these conditions we have

$$\begin{aligned}
&\mathcal{R}_{x,v,s}(i_2, 0; i_2, 0) W_{x,s}(i_3, i_2; j_3, i_2 + i_3 - j_3) W^{\lrcorner}_{x,s}(i_2 + i_3 - j_3) \\
&\qquad + \mathcal{R}_{x,v,s}(i_2, 0; i_2 + 1, 1) W_{x,s}(i_3 - 1, i_2 + 1; j_3, i_2 + i_3 - j_3) W^{\lrcorner}_{x,s}(i_2 + i_3 - j_3) \\
&= w^*_{v,s}(j_3, 0; j_3, 0) W_{x,s}(i_3, i_2; j_3, i_2 + i_3 - j_3) W^{\lrcorner}_{x,s}(i_2 + i_3 - j_3) \\
&\qquad + w^*_{v,s}(j_3 - 1, 0; j_3, 1) W_{x,s}(i_3, i_2; j_3 - 1, i_2 + i_3 - j_3 + 1) W^{\lrcorner}_{x,s}(i_2 + i_3 - j_3 + 1).
\end{aligned}$$

After the required simplifications, the previous relation reduces to

$$\begin{aligned}
&(1 - q^{i_2} sv)(1 + sxq^{j_3 - i_2 - 1}) + (xv + svq^{i_2})(1 - q^{j_3 - i_2}) \\
&\qquad = (1 - svq^{j_3})(1 + sxq^{j_3 - i_2 - 1}) + xv(1 - q^{j_3 - i_2})(1 - s^2 q^{j_3 - 1}),
\end{aligned}$$

that can be checked directly.

When $i_1 = 1$, as in the $i_1 = 0$ case, (B.26) is an equality between sums of at most two terms that after simplification reduces to

$$\begin{aligned}
&(1 - q^{i_2})(1 + sxq^{j_3 - i_2}) + (q^{i_2} + xv)(1 - q^{j_3 - i_2 + 1}) \\
&\qquad = (1 - q^{j_3 + 1})(1 + sxq^{j_3 - i_2}) + x(1 - q^{j_3 - i_2 + 1})(v - sq^{j_3}),
\end{aligned}$$

which is again checked directly. □

Proposition B.2.3. *For any $i_1, i_2, i_3, j_1, j_2, j_3 \in \mathbb{Z}_{\geq 0}$, we have*

$$\begin{aligned}
&\sum_{k_1, k_2, k_3 \geq 0} \mathbb{R}_{x,y,s}(i_2, i_1; k_2, k_1) W^{*,\urcorner}(i_3, k_1; k_3) W_{x,s}(k_3, k_2; j_3, j_2) W^{\lrcorner}_{x,s}(j_2) \\
&\qquad = \frac{(-sy; q)_\infty}{(s^2; q)_\infty} \sum_{k'_1, k'_2, k'_3 \geq 0} W_{x,s}(i_3, i_2; k'_3, k'_2) W^{\lrcorner}_{x,s}(k'_2) W^*_{y,s}(k'_3, i_1; j_3, k'_1) W^{*,\urcorner}(k'_2, k'_1; j_2).
\end{aligned} \tag{B.27}$$

Proof. This follows from the analogous relation (B.26). In fact both the R-matrix $\mathbb{R}$ and the vertex weight W^* can be constructed respectively from $\mathcal{R}$ and w^* via fusion with respect to the spectral parameter v (see [BW17], [BMP19] for details). The coefficient $\frac{(-sy;q)_\infty}{(s^2;q)_\infty}$ arises from fusion of w^* and does not simplify since in the left hand side of (B.26) the bulk weight w^* is missing. One can check that the fusion procedure preserves identity (B.26) and hence (B.27) holds. □

B.3 Nonnegativity of terms in the Yang-Baxter equations

Here we list conditions which are sufficient for the nonnegativity of all terms in both sides of the Yang-Baxter equations described in the previous parts of this Appendix. We will not discuss which of these assumptions are necessary. If the terms are nonnegative, then a stochastic bijectivization of the Yang-Baxter equation exists. We assume that $s \in (-1, 0)$ and $q \in (0, 1)$ throughout the rest of the subsection.

First, the weights $w_{u,s}$ and $w^*_{v,s}$ given in Figure 2.3 and Figure 2.5 are nonnegative for $u, v \in [0, 1]$. The cross vertex weights $r_{u/v}$ from Figure B.1 are nonnegative when in addition $u < v$. Thus,

> All summands in both sides of the Yang-Baxter equation (B.1) containing the weights $w_{u,s}, w_{v,s}$, and $r_{u/v}$ are nonnegative if $0 \leq u < v \leq 1$.

Next, the cross vertex weights R_{uv} from Figure B.3 are nonnegative when $0 \leq uv < 1$. Therefore,

> All summands in both sides of the Yang-Baxter equation (B.2) containing the weights $w_{u,s}, w^*_{v,s}$, and R_{uv} are nonnegative if $u, v \in [0, 1)$. This in fact implies that $(u, v) \in \mathsf{Adm}$ for the sHL/sHL skew Cauchy structure (definition 3.1.4).

Let us now turn to the spin q-Whittaker weights. The weights $W_{x,s}$ and $W^*_{y,s}$ are nonnegative when $x, y \in [-s, -s^{-1}]$. The weights $\mathcal{R}_{x,v,s}$ from Figure B.4 are nonnegative when $v \in [0, 1)$ and $x \in [-s, s^{-1}]$. Thus, we have

> All summands in both sides of the Yang-Baxter equation (B.11) containing the weights $W_{x,s}, w^*_{v,s}$, and $\mathcal{R}_{x,v,s}$ are nonnegative if $v \in [0, 1)$ and $x \in [-s, -s^{-1}]$.

Further, let us consider (B.12) containing $W_{x,s}$, $W^*_{y,s}$, and the non-factorized weights $\mathbb{R}_{x,y,s}$ (B.13). Their nonnegativity is not as straightforward, and requires an additional restriction on the parameters s and q:

Proposition B.3.1. *For $x, y \in [-s, -s^{-1}]$, $q \in (0, 1)$ and $s \in [-\sqrt{q}, 0)$, we have*

$$\mathbb{R}_{x,y,s}(i_1, j_1; i_2, j_2) \geq 0 \qquad \text{for all } i_1, j_1, i_2, j_2 \in \mathbb{Z}_{\geq 0}.$$

The proof of this proposition is similar to [CMP19, Proposition 3.1], with an additional simplification in the second case due to a symmetry of $\mathbb{R}_{x,y,s}$.

Proof of Proposition B.3.1. Throughout the proof we will assume that $i_2 + j_1 = i_1 + j_2$. We need to show that

$$\frac{s^{j_2}(-yq^{1-i_1-j_2}/s;q)_{i_2}}{(-q/(sx);q)_{i_1-j_1}}\,{}_4\phi_3\left(\left.\begin{matrix} q^{-i_2}, -\frac{q}{sx}, -sy, q^{-i_1} \\ -\frac{y}{s}q^{1-i_1-j_2}, -\frac{s}{x}, q^{1+j_2-i_2} \end{matrix}\right| q, q\right) \geq 0. \tag{B.28}$$

Here we used (A.9) to get to the usual q-hypergeometric function, and also the fact that the remaining prefactor in $\mathbb{R}_{x,y,s}$ having the form

$$\frac{q^{i_2 i_1+\frac{1}{2}j_2(j_2-1)}x^{j_2}(q;q)_{j_1}(-s/x;q)_{i_2}(q^{1+j_2-i_2};q)_{i_2}}{(s^2;q)_{j_1+i_2}(q;q)_{j_2}(q;q)_{i_2}}$$

is nonnegative under our parameter restrictions in a straightforward way.

We will use Watson's transformation formula [GR04, (III.19)]

$${}_4\phi_3\left(\left.\begin{matrix} q^{-n}, & a, & b, & c \\ d, & e, & f & - \end{matrix}\right| q, q\right) = \frac{(d/b;q)_n(d/c;q)_n}{(d;q)_n(d/(bc);q)_n}\,{}_8\phi_7\left(\left.\begin{matrix} q^{-n}, \sigma, q\sigma^{1/2}, -q\sigma^{1/2}, \frac{f}{a}, \frac{e}{a}, b, c \\ \sigma^{1/2}, -\sigma^{1/2}, e, f, \frac{ef}{ab}, \frac{ef}{ac}, \frac{efq^n}{a} \end{matrix}\right| q, \frac{efq^n}{bc}\right), \tag{B.29}$$

where $def = abcq^{1-n}$ and $\sigma = ef/aq$.

Case 1. When $i_2 \leq j_2$, we apply (B.29) to (B.28) with $n = i_2$. The prefactor in (B.29) combined with the one from (B.28) becomes

$$\frac{s^{j_2}}{(-q/(sx);q)_{i_1-j_1}}\frac{(q^{1-i_1-j_2}/s^2;q)_{i_2}(-yq^{1-j_2}/s;q)_{i_2}}{(q^{1-j_2}/s^2;q)_{i_2}}.$$

We have

$$\frac{(q^{1-i_1-j_2}/s^2;q)_{i_2}}{(q^{1-j_2}/s^2;q)_{i_2}} = \prod_{m=1}^{i_2}\frac{q^{m-j_2}q^{-i_1}-s^2}{q^{m-j_2}-s^2} \geq 0,$$

since $m - j_2 \leq 0$ in the product. We also have

$$\frac{s^{j_2}(-yq^{1-j_2}/s;q)_{i_2}}{(-q/(sx);q)_{i_1-j_1}} = s^{j_2}\prod_{k=1}^{i_2}\left(1+\frac{y}{s}\,q^{k-j_2}\right)\prod_{m=1}^{j_2-i_2}\left(1+\frac{q^{1-m}}{sx}\right) \geq 0,$$

since all factors above (including s^{j_2}) are nonpositive, and there is a total of $2j_2$ of them.

The q-hypergeometric function after applying (B.29) to (B.28) takes the form

$${}_8\phi_7\left(\left.\begin{matrix} q^{-i_2}, \sigma, q\sigma^{1/2}, -q\sigma^{1/2}, -sxq^{j_2-i_2}, \frac{s^2}{q}, -sy, q^{-i_1} \\ \sigma^{1/2}, -\sigma^{1/2}, -\frac{s}{x}, q^{1+j_2-i_2}, -\frac{s}{y}q^{j_2-i_2}, s^2q^{j_1}, s^2q^{j_2} \end{matrix}\right| q, \frac{q^{i_1+j_2+1}}{xy}\right),$$

with $\sigma = s^2q^{j_2-i_2-1} \in (0,1)$ because $s^2 \leq q$. One readily sees that each summand in this (terminating) q-hypergeometric series is nonnegative. Indeed, the only negative signs may come from $(q^{-i_2};q)_k$, $(q^{-i_1};q)_k$, and $(s^2q^{-1};q)_k$. However, the product of the former two factors is always nonnegative, and $(s^2q^{-1};q)_k \geq 0$ also due to our additional parameter restriction $s^2 \leq q$. This implies the nonnegativity of $\mathbb{R}_{x,y,s}(i_1,j_1;i_2,j_2)$ when $i_2 \leq j_2$.

Case 2. When $i_2 > j_2$, the claim follows due to the symmetry of $\mathbb{R}_{x,y,s}$. Namely, by means of Remark B.1.4, we have

$$\mathbb{R}_{x,y,s}(i_1, j_1; i_2, j_2) = \mathbb{R}_{y,x,s}(j_1, i_1; j_2, i_2)$$

for all $i_1, j_1, i_2, j_2 \in \mathbb{Z}_{\geq 0}$. This completes the proof. □

Proposition B.3.1 implies that

> All summands in both sides of the Yang-Baxter equation (B.12) containing the weights $W_{x,s}, W^*_{y,s}$, and $\mathbb{R}_{x,y,s}$ are nonnegative if $x, y \in [-s, -s^{-1}]$, $q \in (0, 1)$, and $s \in [-\sqrt{q}, 0)$.

Finally, we address the nonnegativity of terms of the Yang-Baxter equations involving scaled geometric specializations from Proposition B.1.8.

Proposition B.3.2. *For $\alpha \in [0, -s^{-1}]$, $q \in (0, 1)$ and $s \in (-1, 0)$ we have*

$$\breve{w}_{\alpha,s}(i_1, j_1; i_2, j_2) \geq 0 \qquad \text{for all } i_1, j_1, i_2, j_2 \in \mathbb{Z}_{\geq 0}.$$

Proof. Under our assumptions the prefactor

$$\frac{(-\alpha/s)^{i_1}(-s)^{j_2}(q;q)_{j_1}}{(q;q)_{i_1}(q;q)_{j_2}}$$

is nonnegative. To check the remaining term, we write down the generic summand of the terminating q-hypergeometric series as (cf. (A.9)):

$$\left(\frac{-sq^{1+j_2+i_2}}{\alpha}\right)^k \frac{(q^{-i_1};q)_k}{(q;q)_k}(q^{-i_2};q)_k(-s\alpha;q)_k(s^2q^k;q)_{i_1-k}(q^{1+j_2-i_1+k};q)_{i_1-k},$$

where $k = 0, \ldots, i_1$. The leading monomial term, along with $(s^2q^k;q)_{i_1-k}$ and $(q;q)_k$ are always nonnegative. The q-Pochhammer symbols of q^{-i_1} and q^{-i_2} either vanish, or they both carry a sign $(-1)^k$, so that their contribution is nonnegative too. Next, $(q^{1+j_2-i_1+k};q)_{i_1-k}$ is either nonnegative if $1 + j_2 - i_1 + k > 0$, or vanishes if $1 + j_2 - i_1 + k \leq 0$ (in the latter case, the last term of the product has power $j_2 \geq 0$, which means that that product passes through $1 - q^0 = 0$). Finally, $(-s\alpha;q)_k \geq 0$ because $\alpha \leq -s^{-1}$. □

Proposition B.3.2 and the explicit form of $R^{(\mathrm{sHL,sg})}_{\alpha,v}$ (Figure B.6) implies that

> All summands in both sides of the Yang-Baxter equation (B.22) containing the weights $\breve{w}_{\alpha,s}$, $w^*_{v,s}$, and $R^{(\mathrm{sHL,sg})}_{\alpha,v}$ are nonnegative if $\alpha \in [0, -s^{-1}]$, $v \in [0, 1)$.

In order to demonstrate the nonnegativity of (B.23) we consider the corresponding cross vertex weight:

Proposition B.3.3. *For $\alpha \in [0, -s^{-1}]$ and $y \in [-s, -s^{-1}]$, we have*

$$R^{(\mathrm{sqW,sg})}_{\alpha,y}(i_1, j_1; i_2, j_2) \geq 0 \qquad \text{for all } i_1, j_1, i_2, j_2 \in \mathbb{Z}_{\geq 0}.$$

Proof. Assume first that $y > -s$. In (B.20), the factors outside ${}_3\overline{\phi}_2$ are nonnegative. In the expansion of ${}_3\overline{\phi}_2$ using (A.9), one readily sees that all terms are nonnegative similarly to the proof of Proposition B.3.2 above (here we use the fact that $-s\alpha$ and $-s/y$ are less than 1 because of our assumptions).

We can now take the limit $y \to -s$ and show that the weight $R^{(\text{sqW},\text{sg})}$ survives this transition. To do so, expand ${}_3\overline{\phi}_2$ using (A.9), and collect terms containing $-s/y$:

$$\frac{(-s/y;q)_{j_2}(-q^k s/y;q)_{j_1-k}}{(-s/y;q)_{j_1}} = (-q^k s/y;q)_{j_2-k},$$

with $k = 0, \ldots, \min(j_1, j_2)$. The last expression is nonsingular at $y = -s$, and is nonnegative. □

Therefore,

> All summands in both sides of the Yang-Baxter equation (B.23) containing $\breve{w}_{\alpha,s}, W^*_{y,s}$, and $R^{(\text{sqW},\text{sg})}_{\alpha,y}$ are nonnegative if $\alpha \in [0, -s^{-1}]$, $y \in [-s, -s^{-1}]$.

We come now to the last Yang-Baxter equation we stated (B.24), in which one readily sees (similarly to Propositions B.3.2 and B.3.3 above) that $R^{(\text{sg},\text{sg})}_{\alpha,\beta}$ is nonnegative when $0 \le \alpha, \beta \le -s^{-1}$. Therefore,

> All summands in both sides of the Yang-Baxter equation (B.24) containing $\breve{w}_{\alpha,s}, \breve{w}^*_{\beta,s}$, and $R^{(\text{sg},\text{sg})}_{\alpha,\beta}$ are nonnegative if $\alpha, \beta \in [0, -s^{-1}]$.

Appendix C

Extras

C.1 Bounds for $\phi_l, \psi_l, \Phi_x, \Psi_x$

We collect here some useful bounds for the quantities $\phi_l, \psi_l, \Phi_x, \Psi_x$ defined in eqs. (4.8) to (4.11). Terms Φ_x, Ψ_x can be further decomposed as

$$\Phi_x(n) = \Phi_x^{(1)}(n) + \Phi_x^{(2)}(n),$$
$$\Psi_x(n) = \Psi_x^{(1)}(n) + \Psi_x^{(2)}(n),$$

obtained separating from the integration (4.10) (resp. (4.11)) the contribution of pole $w = \text{đ}$ (resp. $z = v$) from that of other poles. Their exact expression was given in eqs. (4.22) to (4.25).

Proposition C.1.1. *Let $v < \text{đ}$. Then, for all fixed x, there exist constants $\Gamma_1, \Gamma_2, \Gamma_3, \Gamma_4 > 0$, such that*

$$|\phi_l(n)|, |\psi_l(n)|, |\Phi_x(n)|, |\Phi_x^{(2)}(n)| < \Gamma_1 e^{-\Gamma_2 |n|} \qquad \text{for all } n \in \mathbb{Z} \tag{C.1}$$

and

$$|\Psi_x(n)| < \begin{cases} \Gamma_1 e^{-\Gamma_2 |n|} & \text{if } n \in \mathbb{Z}_{<0} \\ \Gamma_3 e^{-\Gamma_4 |n|} & \text{if } n \in \mathbb{Z}_{\geq 0}. \end{cases} \tag{C.2}$$

Moreover Γ_1, Γ_2 can be chosen so that their relative bounds also hold for $v, \text{đ}$ in the region (4.16) (in this case the parameter b appearing in the definition of τ (4.12) satisfies $qv < b < \text{đ}$).

Proof. We start with the terms $\phi_l, \Phi_x(n), \Phi_x^{(2)}$. Evaluating the complex integrals as sums of residues it is straightforward to get the inequalities

$$|\phi_l(n)|, |\Phi_x(n)|, |\Phi_x^{(2)}(n)| \leq \text{const.}\tau(n) \left(\frac{\mathbb{1}_{n\geq 0}}{|\text{đ}|^{|n|}} + \mathbb{1}_{n<0} \max_{i\geq 2}(|\xi_i s_i|)^{|n|} \right) \leq \Gamma_1 e^{-\Gamma_2 |n|},$$

for some constants Γ_1, Γ_2 depending on the integrand functions but not on n.

To obtain a similar bound for the term $\psi_l(n)$ we distinguish two cases. When n is positive we take the contour C to be a circle of radius r_+ so that $qv < r_+ < b$. On the other hand, when n is negative we take C to be a circle of radius r_- strictly bigger than c, not containing any of the numbers ξ_i/s_i (we remark that the definition itself of $\tau(n)$ and of numbers b, c is tailor-made for these conditions to be possible). With this choices we easily get

$$|\psi_l(n)| \leq \text{const.}\frac{1}{\tau(n)}\left(\mathbb{1}_{n\geq 0} r_+^{|n|} + \mathbb{1}_{n<0}\frac{1}{r_-^{|n|}}\right) \leq \Gamma_1 e^{-\Gamma_2|n|}.$$

An argument equivalent to that used for ψ_l can be carried to show (C.2). The only difference here is that the radius r_+ has to be chosen so that $v < r_+ < b$ and hence we cannot extend this bound to the region $qv < b \leq v$. □

Proposition C.1.2. *Let v satisfy (4.4) and $v < d$ or possibly (4.16). Then, for each x, there exist constants $\Gamma_1, \Gamma_2 > 0$ such that*

$$|\phi_l(n)\Psi_x(n)|, |\Phi_x^{(2)}(n)\Psi_x(n)| < \Gamma_1 e^{-\Gamma_2|n|}. \tag{C.3}$$

Proof. From Proposition C.1.1 we see that we only have to prove (C.3) for positive n's. When this is the case we see directly from the integral expression (4.11) and (4.8) that we can bound both $|\phi_l(n)\Psi_x(n)|$ and $|\Phi_x^{(2)}(n)\Psi_x(n)|$ with some quantity proportional to

$$\frac{|v+\epsilon|^n}{\min_{k\geq 2}|\xi_k s_k|^n}, \tag{C.4}$$

by simply taking the C contour as a circle of radius $v+\epsilon$, for ϵ being sufficiently small. Due to the condition

$$v < \min_{k\geq 2}|\xi_k s_k|,$$

we see that ϵ can be chosen so that (C.4) decays to zero and this completes the proof. □

Proposition C.1.3. *Let v, d satisfy (4.16). Then, for each fixed x, there exist constants $\Gamma_1, \Gamma_2 > 0$ such that*

$$|f(n)\Phi_x^{(1)}(n)\Psi_x^{(2)}(n)| < \Gamma_1 e^{-\Gamma_2|n|}.$$

Proof. We use the integral expression (4.25). When n is positive we take the integration contour C_1 to be a circle of radius $qv+\epsilon$. A bound we can easily obtain is

$$|f(n)\Phi_x^{(1)}(n)\Psi_x^{(2)}(n)| < \text{const.}\frac{(qv+\epsilon)^n}{d^n} \qquad \text{for } n \geq 0.$$

On the other hand, when n is negative we chose the contour C_1 as a circle of radius $v-\epsilon$ to get a bound like

$$|f(n)\Phi_x^{(1)}(n)\Psi_x^{(2)}(n)| < \text{const.}\frac{1}{1-q^n/\zeta}\frac{(v-\epsilon)^n}{d^n} \qquad \text{for } n < 0.$$

In both cases condition (4.16) allows us to select ϵ small enough to guarantee exponential decay in $|n|$. □

C.2 Construction of contours

Here we discuss the construction of the steep descent contour C and that of the steep ascent contour D which were used in the asymptotic analysis of the stationary higher spin vertex model in section 4.2.

Proposition C.2.1. *Consider fixed real numbers*

$$0 < \upsilon < \varsigma, \qquad 0 < q < 1$$

and assume that

$$\varsigma < \inf_{k\geq 2}\{\xi_k s_k\} \leq \sup_{k\geq 2}\{\xi_k s_k\} < \infty \qquad \textit{and} \qquad 0 \leq s_k^2 < 1, \qquad \textit{for all } k \geq 2.$$

Take also a number $\rho < \varsigma$ and define the contour

$$C_\rho = \{\rho e^{\mathrm{i}\vartheta} | \vartheta \in [0, 2\pi)\}.$$

Then, for ρ sufficiently close to ς we have

$$\frac{d}{d\vartheta}\mathfrak{Re}\{g(\rho e^{\mathrm{i}\vartheta})\} < 0 \qquad \textit{for } 0 < \vartheta < \pi, \tag{C.5}$$

where g is given in (4.80).

Remark C.2.2. The result of Proposition C.2.1 implies that C_ρ is a steep descent contour for $\mathfrak{Re}(g)$ and in particular

1. $\max_{z\in C_\rho} \mathfrak{Re}\{g(z)\} = g(\rho)$;
2. $\max_{z\in C_\rho} |z| = \rho$.

This easily follows from (C.5) and from the fact that $g(\overline{z}) = \overline{g(z)}$, which implies that $\mathfrak{Re}(g)$ is symmetric with respect to the real axis.

Proof. Evaluating the derivative we have

$$\begin{aligned}\frac{d}{d\vartheta}\mathfrak{Re}\{g(\rho e^{\mathrm{i}\vartheta})\} =& \sin\vartheta\,\kappa\left(\sum_{i=0}^{J-1}\frac{q^i u\rho}{1+q^{2i}u^2\rho^2-2q^iu\rho\cos\vartheta}\right)\\ &+\sin\vartheta\frac{1}{x}\sum_{k=2}^{x}\sum_{j\geq 0}\left(\frac{\frac{q^j\rho}{\xi_k s_k}}{1+\left(\frac{q^j\rho}{\xi_k s_k}\right)^2-2\frac{q^j\rho}{\xi_k s_k}\cos\vartheta}-\frac{\frac{q^j s_k^2\rho}{\xi_k s_k}}{1+\left(\frac{q^j s_k^2\rho}{\xi_k s_k}\right)^2-2\frac{q^j s_k^2\rho}{\xi_k s_k}\cos\vartheta}\right).\end{aligned} \tag{C.6}$$

Each term

$$\frac{q^i u\rho}{1+q^{2i}u^2\rho^2-2q^iu\rho\cos\vartheta},$$

has a maximum in $\vartheta = 0$ due to the fact that u and ρ have opposite sign, and so does each single one of the summands in the double summation in (C.6), since the generic function

$$\frac{a}{1 + a^2 - 2a\cos\vartheta} - \frac{a\sigma}{1 + a^2\sigma^2 - 2a\sigma\cos\vartheta}$$

is decreasing in $0 < \vartheta < \pi$, provided that $0 < a, \sigma < 1$. Now, if ρ is taken sufficiently close to the critical point ς, in a neighborhood of $\vartheta = 0$, the derivative of $\mathfrak{Re}\{g(\rho e^{i\vartheta})\}$ is negative by construction and, thanks to considerations we just made, it stays negative along the whole half circle. $\square$

The construction of an explicit steepest descent contour D for a general choice of parameters $q, \Xi, \mathbf{S}$ becomes more complicated. Therefore we use the next Proposition both to exhibit a contour in a rather simple setting and to implicitly deduce conditions on $q, \Xi, \mathbf{S}$ under which our arguments of Section 4.2 are perfectly well posed.

Proposition C.2.3. *For each choice of*

$$0 < \varsigma < a, \qquad u < 0, \qquad 0 < \sigma < 1,$$

there exist constants $R_a, R_\sigma, R_q > 0$, such that for each choice of parameters $\{\xi_k\}_{k\geq 2}, \{s_k\}_{k\geq 2}$, q satisfying

$$\varsigma < \inf_{k\geq 2}\{\xi_k s_k\}, \qquad |\xi_k s_k - a| < R_a, \qquad |s_k^2 - \sigma| < R_\sigma, \qquad q < R_q,$$

we are able to construct a complex contour D encircling the set $\{\xi_k s_k\}_{k\geq 2}$, for which

1. $\min_{z\in D} \mathfrak{Re}\{g(z)\} = g(\varsigma)$;
2. $\min_{z\in D} |z| = \varsigma$,

where g is given in (4.80).

Proof. To show this result we essentially make use of a continuity argument. We start studying the case when

$$q = 0, \qquad \xi_k, s_k = a \qquad s_k^2 = \sigma \qquad \text{for all } k \geq 2.$$

With this choice of parameters the function g becomes

$$g(z) = -\eta\log(z) + \kappa\log(1 - uz) + \log\left(\frac{a - z}{a - \sigma z}\right) + \mathcal{O}(x^{-1}), \tag{C.7}$$

where we can neglect the contribution of the $\mathcal{O}(x^{-1})$ term as we are interested in this result only in the limiting case of $x \to \infty$. We define the contour D to be the level curve

$$D = \left\{z : \ \mathfrak{Re}\left\{\log\left(\frac{a - z}{a - \sigma z}\right)\right\} = \log\left(\frac{a - \varsigma}{a - \sigma\varsigma}\right)\right\},$$

which is a circle and admit the parametrization

$$\left\{\varsigma+\rho+\rho e^{\mathrm{i}\vartheta} \middle|\ \vartheta\in[0,2\pi)\right\},$$

with the radius ρ being

$$\rho=\frac{a^2-a\varsigma-a\varsigma\sigma+\varsigma^2\sigma}{a+a\sigma-2\varsigma\sigma}.$$

We also report that the leftmost and rightmost extremes of the contour D are respectively ς and $\varsigma+2\rho$ and one can easily find that the latter satisfies the inequality

$$\varsigma+2\rho\leq\frac{2a}{1+\sigma}. \tag{C.8}$$

Along the curve D we are able to calculate

$$\frac{d}{d\vartheta}\mathfrak{Re}\left\{g(\varsigma+\rho+\rho e^{\mathrm{i}\vartheta})\right\}$$

and to analytically show that its only critical points are $\theta\in\mathbb{Z}\pi$. More specifically, substituting in (C.7) the correct expressions of coefficients η,κ given in (4.35)

$$\eta=\frac{a\varsigma^2(1-\sigma)(a-a^2u+a\sigma-2\varsigma\sigma+\varsigma^2u\sigma)}{(a-\varsigma)^2(a-\varsigma\sigma)^2}, \tag{C.9}$$

$$\kappa=-\frac{a(1-\varsigma u)^2(1-\sigma)(a^2-\varsigma^2\sigma)}{u(a-\varsigma)^2(a-\varsigma\sigma)^2}, \tag{C.10}$$

we get

$$\frac{d}{d\vartheta}\mathfrak{Re}\left\{g(\varsigma+\rho+\rho e^{\mathrm{i}\vartheta})\right\}=\sin\vartheta(1+\cos\vartheta)\frac{1}{P(\cos\vartheta)}.$$

In the last expression P is a polynomial of degree two in the argument and we see that zeros are only achieved on the real axis for $\theta=k\pi$ for $k\in\mathbb{Z}$. We can at this point readily verify that, along D the real part of g assumes a minimum at $z=\varsigma$ and a maximum at $z=\varsigma+2\rho$ as the function

$$-\eta\log(y)+\kappa\log(1-uy)$$

is increasing for $y>\varsigma$, and one can check this by direct inspection of its first derivative, by making use of expressions (4.35) for η and κ.

We can now use the fact that g is continuous in the parameters $\Xi,\mathbf{S},q$ for z belonging to D and the fact that, by construction, it will always have a critical point in $z=\varsigma$, to state the existence of neighborhoods respectively of a,σ and 0 in which every choice of $\xi_k s_k, s_k^2$ and q will preserve the steepest descent properties 1 and 2. □

C.3 Triangular Sums

Here we write down a number of identities of summations of certain symbols $a_{k,\ell},b_\alpha$ used in the proof of Proposition 5.3.2. Fix a positive integer N, and assume that the symbols

b_α, $\alpha = 1, \ldots, N$ commute with each other. Let $a_{k,\ell}$ be

$$a_{k,\ell} = \begin{cases} 0 & \text{if } 0 = k, \text{ or } \ell = N+1; \\ 1 & \text{if } 0 \le k = \ell \le N; \\ \in \mathbb{R} & \text{else.} \end{cases}$$

Proposition C.3.1. *For any $N \geq 1$, the following identities hold*

$$\sum_{0\le k<\ell\le N} a_{k+1,\ell} - a_{k,\ell} - a_{k+1,\ell+1} + a_{k,\ell+1} = N - \sum_{j=1}^{N-1} a_{j,j+1};$$

$$\sum_{0\le k<\ell\le N} (\ell-k+1)(a_{k+1,\ell+1} - a_{k,\ell+1}) - (\ell-k-1)(a_{k+1,\ell} - a_{k,\ell}) = \sum_{j=1}^{N-1} a_{j,j+1};$$

$$\sum_{0\le k<\ell\le N} (a_{k+1,\ell} - a_{k,\ell} - a_{k+1,\ell+1} + a_{k,\ell+1}) \sum_{\alpha=k+1}^{\ell} b_\alpha = \sum_{\alpha=1}^{N} b_\alpha;$$

$$\sum_{0\le k<\ell\le N} (\ell-k-1)^2(a_{k+1,\ell} - a_{k,\ell}) - (\ell-k+1)^2(a_{k+1,\ell+1} - a_{k,\ell+1})$$
$$= -\sum_{j=1}^{N-1} a_{j,j+1} - 2\sum_{1\le k<\ell\le N} a_{k,\ell};$$

$$\sum_{0\le k<\ell\le N} (a_{k+1,\ell} - a_{k,\ell} - a_{k+1,\ell+1} + a_{k,\ell+1}) \sum_{k+1\le\alpha,\beta\le l} b_\alpha b_\beta = \sum_{\alpha=1}^{N} b_\alpha^2 + 2\sum_{1\le k<\ell\le N} a_{k,\ell} b_k b_\ell;$$

$$\sum_{0\le k<\ell\le N} \Big((\ell-k+1)(a_{k+1,\ell+1} - a_{k,\ell+1}) - (\ell-k-1)(a_{k+1,\ell} - a_{k,\ell})\Big) \sum_{\alpha=k+1}^{\ell} b_\alpha$$
$$= \sum_{1\le k<\ell\le N}^{N} a_{k,\ell}(b_k - b_\ell).$$

Proof. All these identities are elementary and can be proven by induction in a straightforward way. □

Bibliography

[Dys62] F.J. Dyson. "A Brownian motion model for the eigenvalues of a random matrix". In: *Journal of Mathematical Physics* 3.6 (1962), pp. 1191–1198.

[Jac67] H. Jacquet. "Fonctions de Whittaker associées aux groupes de Chevalley". fr. In: *Bulletin de la Société Mathématique de France* 95 (1967), pp. 243–309.

[Knu70] D. Knuth. "Permutations, matrices, and generalized Young tableaux". In: *Pacific J. Math.* 34.3 (1970), pp. 709–727.

[Kos78] B. Kostant. "On Whittaker vectors and representation theory". In: *Inventiones mathematicae* 48.2 (1978), pp. 101–184.

[Kos80] B. Kostant. "Quantization and representation theory". In: *Representation Theory of Lie Groups*. Vol. 34. LMS Lecture Notes. Cambridge Univ. Press, 1980, pp. 287–316.

[KRS81] P. Kulish, N. Reshetikhin, and E. Sklyanin. "Yang-Baxter equation and representation theory: I". In: *Letters in Mathematical Physics* 5.5 (1981), pp. 393–403.

[Ros81] H. Rost. "Nonequilibrium behaviour of a many particle process: density profile and local equilibria". In: *Z. Wahrsch. Verw. Gebiete* 58.1 (1981), pp. 41–53.

[HH85] D. Huse and C. Henley. "Pinning and roughening of domain wall in Ising systems due to random impurities". In: *Phys. Rev. Lett* 54.25 (1985), p. 2708.

[And86] G. Andrews. *q-Series: Their Development and Application in Analysis, Number Theory, Combinatorics, Physics and Computer Algebra*. 66. AMS, 1986.

[KPZ86] M. Kardar, G. Parisi, and Y. Zhang. "Dynamic scaling of growing interfaces". In: *Physical Review Letters* 56.9 (1986), p. 889.

[Bum89] D. Bump. "The Rankin-Selberg method: a Survey". In: *Number Theory, Trace Formulas, and Discrete Groups*. Ed. by K.E. Aubert, E. Bombieri, and D. Goldfeld. Academic Press, 1989.

[DF90] P. Diaconis and J.A. Fill. "Strong Stationary Times via a New Form of Duality". In: *Ann. Probab.* 18 (1990), pp. 1483–1522.

[GS92] L.-H. Gwa and H. Spohn. "Six-vertex model, roughened surfaces, and an asymmetric spin Hamiltonian". In: *Phys. Rev. Lett.* 68.6 (1992), pp. 725–728.

[FF94] P. A. Ferrari and L. R. G. Fontes. "Current Fluctuations for the Asymmetric Simple Exclusion Process". In: *Ann. Probab.* 22.2 (Apr. 1994), pp. 820–832.

[TW94] C. Tracy and H. Widom. "Level-spacing distributions and the Airy kernel". In: *Commun. Math. Phys.* 159.1 (1994). arXiv:hep-th/9211141, pp. 151–174.

[Fom95] S. Fomin. "Schensted algorithms for dual graded graphs". In: *J. Algebr. Comb.* 4.1 (1995), pp. 5–45.

[KB95] A.N. Kirillov and A.D. Berenstein. "Groups generated by involutions, Gelfand–Tsetlin patterns, and combinatorics of Young tableaux". In: *Algebra i Analiz* 7.1 (1995), pp. 92–152.

[Mac95] I.G. Macdonald. *Symmetric functions and Hall polynomials.* 2nd. Oxford University Press, 1995.

[Ful97] W. Fulton. *Young Tableaux with Applications to Representation Theory and Geometry.* Cambridge University Press, 1997.

[Giv97] A. Givental. "Stationary phase integrals, quantum Toda lattices, flag manifolds and the mirror conjecture". In: *Topics in singularity theory.* American Mathematical Society Translations Ser 2. arXiv:alg-geom/9612001. AMS, 1997.

[Wak+97] J. Wakita et al. "Self-Affinity for the Growing Interface of Bacterial Colonies". In: *Journal of the Physical Society of Japan* 66.1 (1997), pp. 67–72.

[SW98] T. Sasamoto and M. Wadati. "Exact results for one-dimensional totally asymmetric diffusion models". In: *J. Phys. A* 31 (1998), pp. 6057–6071.

[BDJ99] J. Baik, P. Deift, and K. Johansson. "On the distribution of the length of the longest increasing subsequence of random permutations". In: *Jour. AMS* 12.4 (1999). arXiv:math/9810105 [math.CO], pp. 1119–1178.

[Eti99] P. Etingof. "Whittaker functions on quantum groups and q-deformed Toda operators". In: *Amer. Math. Soc. Transl. Ser. 2* 194 (1999). arXiv:math/9901053 [math.QA], pp. 9–25.

[BR00] J. Baik and E. M. Rains. "Limiting Distributions for a Polynuclear Growth Model with External Sources". In: *Journal of Statistical Physics* 100.3 (Aug. 2000), pp. 523–541.

[Joh00] K. Johansson. "Shape fluctuations and random matrices". In: *Commun. Math. Phys.* 209.2 (2000). arXiv:math/9903134 [math.CO], pp. 437–476.

[PS00] M. Prähofer and H. Spohn. "Universal Distributions for Growth Processes in 1+1 Dimensions and Random Matrices". In: *Physical Review Letters* 84 (2000). arXiv:cond-mat/9912264 [cond-mat.stat-mech].

[BR01] J. Baik and E.M. Rains. "Symmetrized random permutations". In: *Random matrix models and their applications* (2001). arXiv:math/9910019 [math.CO], pp. 1–29.

[KL01] S. Kharchev and D. Lebedev. “Integral representations for the eigenfunctions of quantum open and periodic Toda chains from the QISM formalism”. In: *Journal of Physics A: Mathematical and General* 34.11 (Mar. 2001), pp. 2247–2258.

[Myl+01] M. Myllys et al. “Kinetic roughening in slow combustion of paper”. In: *Phys. Rev. E* 64 (3 Aug. 2001).

[OY01] N. O’Connell and M. Yor. “Brownian analogues of Burke’s theorem”. In: *Stochastic Processes and their Applications* 96.2 (2001), pp. 285–304.

[Oko01] A. Okounkov. “Infinite wedge and random partitions”. In: *Selecta Math.* 7.1 (2001). arXiv:math/9907127 [math.RT], pp. 57–81.

[Pak01] I. Pak. “Hook length formula and geometric combinatorics”. In: *Sém. Lothar. Combin* 46.B46f (2001), p. 13.

[Sag01] B.E. Sagan. *The symmetric group: representations, combinatorial algorithms, and symmetric functions*. Springer Verlag, 2001.

[Sta01] R. Stanley. *Enumerative Combinatorics. Vol. 2*. With a foreword by Gian-Carlo Rota and appendix 1 by Sergey Fomin. Cambridge: Cambridge University Press, 2001.

[PS02] M. Prähofer and H. Spohn. “Scale invariance of the PNG droplet and the Airy process”. In: *J. Stat. Phys.* 108 (2002). arXiv:math.PR/0105240, pp. 1071–1106.

[Sta02] E. Stade. “Archimedean L-factors on $GL(n) \times GL(n)$ and generalized Barnes integrals”. In: *Israel J. Math.* 127 (2002), pp. 201–219.

[KN03] Y. Kajihara and M. Noumi. “Multiple elliptic hypergeometric series. An approach from the Cauchy determinant”. In: *Indagationes Mathematicae* 14.3 (2003). Proceedings of the Koninklijke Nederlandse Akademie van Wetenschappen, Series A, Mathematical Sciences, pp. 395–421.

[OR03] A. Okounkov and N. Reshetikhin. “Correlation function of Schur process with application to local geometry of a random 3-dimensional Young diagram”. In: *Jour. AMS* 16.3 (2003). arXiv:math/0107056 [math.CO], pp. 581–603.

[Fer04] P. Ferrari. “Polynuclear growth on a flat substrate and edge scaling of GOE eigenvalues”. In: *Commun. Math. Phys.* 252.1 (2004). arXiv:math-ph/0402053, pp. 77–109.

[GR04] G. Gasper and M. Rahman. *Basic hypergeometric series*. Cambridge University Press, 2004.

[Ism05] M.E.H. Ismail. *Classical and Quantum Orthogonal Polynomials in One Variable*. Cambridge University Press, 2005.

[Sas05] T. Sasamoto. “Spatial correlations of the 1D KPZ surface on a flat substrate”. In: *Journal of Physics A: Mathematical and General* 38.33 (2005).

[FS06] P. L. Ferrari and H. Spohn. “Scaling Limit for the Space-Time Covariance of the Stationary Totally Asymmetric Simple Exclusion Process”. In: *Communications in Mathematical Physics* 265.1 (July 2006), pp. 45–46.

[Ger+06] A. Gerasimov et al. “On a Gauss-Givental representation of quantum Toda chain wave function”. In: *International Mathematics Research Notices* 2006 (Jan. 2006).

[BFS08] A. Borodin, Patrik L. Ferrari, and T. Sasamoto. “Transition between Airy1 and Airy2 processes and TASEP fluctuations”. In: *Communications on Pure and Applied Mathematics* 61.11 (2008), pp. 1603–1629.

[GLO08] A. Gerasimov, D. Lebedev, and S. Oblezin. “Baxter operator and Archimedean Hecke algebra”. In: *Commun. Math. Phys.* 284.3 (2008). arXiv:0706.3476 [math.RT], p. 867.

[Fei+09] B. Feigin et al. “A commutative algebra on degenerate CP1 and Macdonald polynomials”. In: *Journal of Mathematical Physics* 50.9 (2009). arXiv:0904.2291 [math.CO].

[FW09] O. Foda and M. Wheeler. “Hall-Littlewood Plane Partitions and KP”. In: *Int. Math. Res. Notices* 2009.14 (2009). arXiv:0809.2138 [math-ph].

[Sep09] T. Seppäläinen. “Lecture notes on the corner growth model”. In: *Unpublished lecture notes* (2009).

[BFP10] J. Baik, P. L. Ferrari, and S. Péché. “Limit process of stationary TASEP near the characteristic line”. In: *Communications on Pure and Applied Mathematics* 63.8 (2010), pp. 1017–1070.

[Bor10] F. Bornemann. “On the numerical evaluation of Fredholm determinants”. In: *Math. Comp.* 79.270 (2010). arXiv:0804.2543 [math.NA], pp. 871–915.

[CLR10] P. Calabrese, P. Le Doussal, and A. Rosso. “Free-energy distribution of the directed polymer at high temperature”. In: *Euro. Phys. Lett.* 90.2 (2010).

[Hue+10] M. A. C. Huergo et al. “Morphology and dynamic scaling analysis of cell colonies with linear growth fronts”. In: *Phys. Rev. E* 82 (3 Sept. 2010).

[SS10] T. Sasamoto and H. Spohn. “Exact height distributions for the KPZ equation with narrow wedge initial condition”. In: *Nuclear Physics B* 834.3 (2010). arXiv:1002.1879 [cond-mat.stat-mech], pp. 523–542.

[TS10] K. Takeuchi and M. Sano. “Universal fluctuations of growing interfaces: evidence in turbulent liquid crystals”. In: *Phys. Rev. Lett.* 104.23 (2010). arXiv:1001.5121 [cond-mat.stat-mech].

[ACQ11] G. Amir, I. Corwin, and J. Quastel. “Probability distribution of the free energy of the continuum directed random polymer in 1+ 1 dimensions”. In: *Comm. Pure Appl. Math.* 64.4 (2011). arXiv:1003.0443 [math.PR], pp. 466–537.

[Dot11] V. Dotsenko. "Universal randomness". In: *Physics Uspekhi* 54.3 (2011). arXiv:1009.3116 [cond-mat.stat-mech], pp. 259–280.

[Yun+11] P. J. Yunker et al. "Suppression of the coffee-ring effect by shape-dependent capillary interactions". In: *Nature* 476 (7360 Aug. 2011), pp. 308–311.

[Cor12] I. Corwin. "The Kardar-Parisi-Zhang equation and universality class". In: *Random Matrices Theory Appl.* 1 (2012). arXiv:1106.1596 [math.PR].

[GLO12] A. Gerasimov, D. Lebedev, and S. Oblezin. "On a classical limit of q-deformed Whittaker functions". In: *Letters in Mathematical Physics* 100.3 (2012). arXiv:1101.4567 [math.AG], pp. 279–290.

[Hue+12] M. A. C. Huergo et al. "Growth dynamics of cancer cell colonies and their comparison with noncancerous cells". In: *Phys. Rev. E* 85 (1 Jan. 2012).

[LC12] P. Le Doussal and P. Calabrese. "The KPZ equation with flat initial condition and the directed polymer with one free end". In: *Journal of Statistical Mechanics: Theory and Experiment* 2012.06 (June 2012).

[OCo12] N. O'Connell. "Directed polymers and the quantum Toda lattice". In: *Ann. Probab.* 40.2 (2012). arXiv:0910.0069 [math.PR], pp. 437–458.

[Sep12] T. Seppäläinen. "Scaling for a one-dimensional directed polymer with boundary conditions". In: *Ann. Probab.* 40(1) (2012). arXiv:0911.2446 [math.PR], pp. 19–73.

[Spo12] H. Spohn. "KPZ Scaling Theory and the Semi-discrete Directed Polymer Model". In: *arXiv preprint* (2012). arXiv:1201.0645 [cond-mat.stat-mech].

[TS12] K. Takeuchi and M. Sano. "Evidence for geometry-dependent universal fluctuations of the Kardar-Parisi-Zhang interfaces in liquid-crystal turbulence". In: *Journal of Statistical Physics* 147 (2012). arXiv:1203.2530 [cond-mat.stat-mech], pp. 853–890.

[IS13] T. Imamura and T. Sasamoto. "Stationary Correlations for the 1D KPZ Equation". In: *Journal of Statistical Physics* 150 (5 Mar. 2013), pp. 908–939.

[OP13] N. O'Connell and Y. Pei. "A q-weighted version of the Robinson-Schensted algorithm". In: *Electron. J. Probab.* 18.95 (2013). arXiv:1212.6716 [math.CO], pp. 1–25.

[Pov13] A. Povolotsky. "On integrability of zero-range chipping models with factorized steady state". In: *J. Phys. A* 46 (2013). arXiv:1308.3250 [math-ph].

[Yun+13] P. J. Yunker et al. "Effects of Particle Shape on Growth Dynamics at Edges of Evaporating Drops of Colloidal Suspensions". In: *Phys. Rev. Lett.* 110 (3 Jan. 2013).

[BSS14] R. Basu, V. Sidoravicius, and A. Sly. "Last Passage Percolation with a Defect Line and the Solution of the Slow Bond Problem". In: *arXiv preprint* (2014). arXiv:1408.3464 [math.PR].

[BC14] A. Borodin and I. Corwin. "Macdonald processes". In: *Probab. Theory Relat. Fields* 158 (2014). arXiv:1111.4408 [math.PR], pp. 225–400.

[BCS14] A. Borodin, I. Corwin, and T. Sasamoto. "From duality to determinants for q-TASEP and ASEP". In: *Ann. Probab.* 42.6 (2014). arXiv:1207.5035 [math.PR], pp. 2314–2382.

[BF14] A. Borodin and P. Ferrari. "Anisotropic growth of random surfaces in 2+1 dimensions". In: *Commun. Math. Phys.* 325 (2014). arXiv:0804.3035 [math-ph], pp. 603–684.

[Cor14] I. Corwin. "The q-Hahn Boson process and q-Hahn TASEP". In: *Int. Math. Res. Notices* rnu094 (2014). arXiv:1401.3321 [math.PR].

[CH14] I. Corwin and A. Hammond. "Brownian Gibbs property for Airy line ensembles". In: *Inventiones mathematicae* 195.2 (2014). arXiv:1108.2291 [math.PR], pp. 441–508.

[Cor+14] I. Corwin et al. "Tropical Combinatorics and Whittaker functions". In: *Duke J. Math.* 163.3 (2014). arXiv:1110.3489 [math.PR], pp. 513–563.

[Hop14] S. Hopkins. "RSK via local transformations". In: *Unpublished notes* (2014). http://www-users.math.umn.edu/~shopkins/docs/rsk.pdf.

[Man14] V. Mangazeev. "On the Yang–Baxter equation for the six-vertex model". In: *Nuclear Physics B* 882 (2014). arXiv:1401.6494 [math-ph], pp. 70–96.

[OSZ14] N. O'Connell, T. Seppäläinen, and N. Zygouras. "Geometric RSK correspondence, Whittaker functions and symmetrized random polymers". In: *Invent. Math.* 197 (2014). arXiv:1110.3489 [math.PR], pp. 361–416.

[Tak14] K. Takeuchi. "Experimental approaches to universal out-of-equilibrium scaling laws: turbulent liquid crystal and other developments". In: *Journal of Statistical Mechanics: Theory and Experiment* 2014.1 (Jan. 2014).

[Agg15] A. Aggarwal. "Correlation functions of the Schur process through Macdonald difference operators". In: *Journal of Combinatorial Theory, Series A* 131 (2015). arXiv:1401.6979 [math.CO], pp. 88–118.

[Bor+15a] A. Borodin et al. "Height fluctuations for the stationary KPZ equation". In: *Mathematical Physics, Analysis and Geometry* 18.1 (2015). arXiv:1407.6977 [math.PR], pp. 1–95.

[Bor+15b] A. Borodin et al. "Spectral theory for interacting particle systems solvable by coordinate Bethe ansatz". In: *Commun. Math. Phys.* 339.3 (2015). Updated version including erratum. Available at https://arxiv.org/abs/1407.8534v4, pp. 1167–1245.

[Bor+15c] A. Borodin et al. "Spectral theory for the q-Boson particle system". In: *Compos. Math.* 151.1 (2015). arXiv:1308.3475 [math-ph], pp. 1–67.

[CSS15] I. Corwin, T. Seppäläinen, and H. Shen. "The strict-weak lattice polymer". In: *J. Stat. Phys* 160.4 (2015). arXiv:1409.1794 [math.PR], pp. 1027–1053.

[FV15] P. Ferrari and B. Veto. “Tracy-Widom asymptotics for q-TASEP”. In: *Ann. Inst. H. Poincaré, Probabilités et Statistiques* 51.4 (2015). arXiv:1310.2515 [math.PR], pp. 1465–1485.

[OO15] N. O’Connell and J. Ortmann. “Tracy-Widom asymptotics for a random polymer model with gamma-distributed weights.” In: *Electron. J. Probab.* 20.25 (2015). arXiv:1408.5326 [math.PR], pp. 1–18.

[QS15] J. Quastel and H. Spohn. “The one-dimensional KPZ equation and its universality class”. In: *J. Stat. Phys* 160.4 (2015). arXiv:1503.06185 [math-ph], pp. 965–984.

[BC16a] G. Barraquand and I. Corwin. “Random-walk in Beta-distributed random environment”. In: *Probab. Theory Relat. Fields* 167.3-4 (2016). arXiv:1503.04117 [math.PR], pp. 1057–1116.

[BC16b] G. Barraquand and I. Corwin. “The q-Hahn asymmetric exclusion process”. In: *Annals of Applied Probability* 26.4 (2016). arXiv:1501.03445 [math.PR], pp. 2304–2356.

[BCG16] A. Borodin, I. Corwin, and V. Gorin. “Stochastic six-vertex model”. In: *Duke J. Math.* 165.3 (2016). arXiv:1407.6729 [math.PR], pp. 563–624.

[BP16] A. Borodin and L. Petrov. “Nearest neighbor Markov dynamics on Macdonald processes”. In: *Adv. Math.* 300 (2016). arXiv:1305.5501 [math.PR], pp. 71–155.

[Bor+16] A. Borodin et al. “Observables of Macdonald processes”. In: *Trans. AMS* 368.3 (2016). arXiv:1306.0659 [math.PR], pp. 1517–1558.

[CP16] I. Corwin and L. Petrov. “Stochastic higher spin vertex models on the line”. In: *Commun. Math. Phys.* 343.2 (2016). arXiv:1502.07374 [math.PR], pp. 651–700.

[BSS17] R. Basu, S. Sarkar, and A. Sly. “Invariant Measures for TASEP with a Slow Bond”. In: *arXiv preprint* (2017). arXiv:1704.07799.

[Bor17] A. Borodin. “On a family of symmetric rational functions”. In: *Adv. Math.* 306 (2017). arXiv:1410.0976 [math.CO], pp. 973–1018.

[BW17] A. Borodin and M. Wheeler. “Spin q-Whittaker polynomials”. In: *arXiv preprint* (2017). arXiv:1701.06292 [math.CO].

[MQR17] K. Matetski, J. Quastel, and D. Remenik. “The KPZ fixed point”. In: *arXiv preprint* (2017). arXiv:1701.00018 [math.PR].

[MP17] K. Matveev and L. Petrov. “q-randomized Robinson–Schensted–Knuth correspondences and random polymers”. In: *Annales de l’IHP D* 4.1 (2017). arXiv:1504.00666 [math.PR], pp. 1–123.

[OP17] D. Orr and L. Petrov. “Stochastic Higher Spin Six Vertex Model and q-TASEPs”. In: *Adv. Math.* 317 (2017), pp. 473–525.

[Agg18] A. Aggarwal. “Current Fluctuations of the Stationary ASEP and Six-Vertex Model”. In: *Duke Math J.* 167.2 (2018). arXiv:1608.04726 [math.PR], pp. 269–384.

[Bar+18] G. Barraquand et al. “Stochastic six-vertex model in a half-quadrant and half-line open asymmetric simple exclusion process”. In: *Duke Math. J.* 167.13 (Sept. 2018), pp. 2457–2529.

[BBW18] A. Borodin, A. Bufetov, and M. Wheeler. “Between the stochastic six vertex model and Hall-Littlewood processes”. In: *Duke Math. J.* 167.13 (2018). arXiv:1611.09486 [math.PR], pp. 2457–2529.

[BP18a] A. Borodin and L. Petrov. “Higher spin six vertex model and symmetric rational functions”. In: *Selecta Math.* 24.2 (2018). arXiv:1601.05770 [math.PR], pp. 751–874.

[BP18b] A. Borodin and L. Petrov. “Inhomogeneous exponential jump model”. In: *Probab. Theory Relat. Fields* 172 (2018). arXiv:1703.03857 [math.PR], pp. 323–385.

[BM18] A. Bufetov and K. Matveev. “Hall-Littlewood RSK field”. In: *Selecta Math.* 24.5 (2018). arXiv:1705.07169 [math.PR], pp. 4839–4884.

[Dim18] E. Dimitrov. “Six-vertex Models and the GUE-corners Process”. In: *Intern. Math. Research Notices* (2018). arXiv:1610.06893 [math.PR], rny072.

[BRS19] Márton Balázs, Firas Rassoul-Agha, and Timo Seppäläinen. “Large deviations and wandering exponent for random walk in a dynamic beta environment”. In: *Ann. Probab.* 47.4 (July 2019), pp. 2186–2229.

[BZ19] E. Bisi and N. Zygouras. “Point-to-line polymers and orthogonal Whittaker functions”. In: *Trans. Amer. Math. Soc.* 371 (2019), pp. 8339–8379.

[BGW19] A. Borodin, V. Gorin, and M. Wheeler. “Shift-invariance for vertex models and polymers”. In: *arXiv preprint* (2019). arXiv:1912.02957 [math.PR].

[BMP19] A. Bufetov, M. Mucciconi, and L. Petrov. “Yang-Baxter random fields and stochastic vertex models”. In: *arXiv preprint* (2019). arXiv:1905.06815 [math.PR]. To appear in Adv. Math.

[BP19] A. Bufetov and L. Petrov. “Yang-Baxter field for spin Hall-Littlewood symmetric functions”. In: *Forum Math. Sigma* 7 (2019). arXiv:1712.04584 [math.PR].

[CMP19] I. Corwin, K. Matveev, and L. Petrov. “The q-Hahn PushTASEP”. In: *Intern. Math. Research Notices* rnz106 (2019). arXiv:1811.06475 [math.PR].

[IS19] T. Imamura and T. Sasamoto. “Fluctuations for stationary q-TASEP”. In: *Probab. Theory Relat. Fields* 174 (2019). arXiv:1701.05991 [math-ph], pp. 647–730.

[Kos19] S Koshida. “Free field approach to the Macdonald Processes”. In: *arXiv preprint* (2019). arXiv:1905.07087v2 [math-QA].

[LŽP19] M. Ljubotina, M. Žnidarič, and T. Prosen. “Kardar-Parisi-Zhang Physics in the Quantum Heisenberg Magnet”. In: *Phys. Rev. Lett.* 122 (21 May 2019).

[Pet19] L. Petrov. “Parameter permutation symmetry in particle systems and random polymers”. In: *arXiv preprint* (2019). arXiv:1912.06067 [math.PR].

[Dim20] E. Dimitrov. “Two-point convergence of the stochastic six-vertex model to the Airy process”. In: (2020). arXiv:2006.15934 [math.PR].

[IMS20] T. Imamura, M. Mucciconi, and T. Sasamoto. “Stationary Higher Spin Six Vertex Model and q-Whittaker measure”. In: *Probability Theory and Related Fields* (Mar. 2020).

[IFT20] T. Iwatsuka, Y. Fukai, and K. Takeuchi. “Direct Evidence for Universal Statistics of Stationary Kardar-Parisi-Zhang Interfaces”. In: *arXiv preprint* (2020). arXiv:2004.11652 [cond-mat.stat-mech].

[MP20] M. Mucciconi and L. Petrov. “Spin q-Whitaker polynomials and deformed quantum Toda”. In: *arXiv preprint* (2020). arXiv:2003.14260 [math.PR].

[Spo20] Herbert Spohn. “The (1+1) dimensional Kardar-Parisi-Zhang equation: more surprises”. In: *Journal of Statistical Mechanics: Theory and Experiment* 2020.4 (Apr. 2020).

[Wei] E. W. Weisstein. *q-Polygamma Function. From MathWorld—A Wolfram Web Resource.*